

Enhanced Protein Functionalities

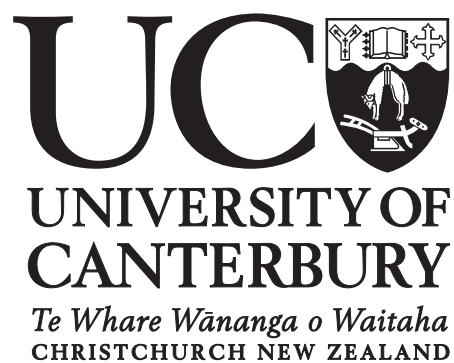
A thesis submitted in partial fulfilment of the
requirements for the degree of

Doctor of Philosophy in Biochemistry

in the School of Biological Sciences

by Xiaoli Sun

University of Canterbury



March 2016

Abstract

Bovine milk has been processed into a variety of dairy products that provide different nutritional and functional properties. The physicochemical properties of milk protein play an important role in dairy products, impacting on viscosity, emulsifying properties, solubility, texture and heat stability. Understanding the impact of milk protein interactions on the functional properties of the milk proteins can be beneficial to tailoring the properties of dairy foods. This project aimed to investigate the impact of protein modifications on the physicochemical and functional properties of dairy proteins.

Experiments involved three protein modification approaches: dephosphorylation, succinylation and transglutaminase-modified protein. α_{s1} -Casein as a key ingredient in dairy products was chosen for the experimental material. The level of modifications was controlled, and the physicochemical and functional properties of the modified proteins were investigated. This study investigated how the changes in the physicochemical properties affected the functionalities of α_{s1} -protein. In addition, the relationship between different measurement methods was studied.

Results demonstrated that the physicochemical and functional properties of α_{s1} -casein can be manipulated by controlling the level of modification. The correlation between the physicochemical properties and functionalities of α_{s1} -casein was established. It was shown that dephosphorylation decreased net charge and increased surface hydrophobicity of α_{s1} -casein, whereas, succinylation increased net charge and decreased surface hydrophobicity α_{s1} -casein. Succinylation had a significant effect on the secondary structure of α_{s1} -casein; it also decreased the self-association behaviour. However, dephosphorylation did not change the secondary structure of α_{s1} -casein, but enhanced the self-association behaviour of α_{s1} -casein.

The surface tension of protein solutions was affected by the net charge and surface hydrophobicity of α_{s1} -casein. The water binding capacity of α_{s1} -casein was influenced by the

amino acid groups on the proteins. The foam stabilising ability of α_{s1} -casein was affected by the combined effect of net charge and surface hydrophobicity, whereas, the emulsion stability was mainly dependent on the net charge of the protein. On the other hand, molecular weight was found to have a significant effect on the surface tension and emulsion stability of α_{s1} -casein. The findings reported in this study could be tested in model food systems, which may inform the development of dairy products by manipulating the functional properties of dairy products. Moreover, the understanding of protein interactions and the ability to control the physicochemical parameters of proteins may advise an optimised process design for dairy products.

Acknowledgements

I would like to thank my supervisors: Dr Juliet Gerrard, Dr Skelte Anema and Dr Christina Coker for all the encouragement and guidance through my PhD.

Thank you to Bert Fong and Kevin Ma for your support on Mass spectrometry, Jason Hindmarsh for your support on NMR, Mita Lad for your training on Pendant drop, and Ren Dobson and Ali Nazmi for your support on AUC. A special thank to Justine Cottam who has helped and mentored me along the way, and thank you for the proof reading. I would like to thank Susie Meade for assistance with travel arrangements and paperwork. To everyone at FRDC food science lab and BIC lab who has helped me during my PhD study, your name is not here but in my mind, I am grateful to you. Thanks you to the expert panel members of the food structure design group for the help in assessing my work and discussion with them.

I would like to acknowledge Fonterra and the Ministry for Primary Industries for the financial support via the Primary Growth Partnership Transforming the Dairy Value Chain – Food Structure Design.

Table of contents

Chapter 1	Introduction and literature review	1
1.1	Milk composition	2
1.1.1	Proteins in milk	3
1.1.2	Whey proteins	4
1.1.3	Casein proteins	9
1.2	Minerals and other components in milk	13
1.2.1	Casein micelles	16
1.3	Protein modifications	23
1.4	Protein modifications catalysed by phosphatases.....	23
1.4.1	Phosphatases.....	24
1.4.2	Dephosphorylation of protein fractions	26
1.4.3	Emulsion properties of dephosphorylated caseins	29
1.4.4	Phosphorylation	32
1.5	Protein modifications catalysed by transglutaminase	33
1.5.1	Transglutaminase	33
1.5.2	Transglutaminase-catalysed reactions	34
1.5.3	Transglutaminase in whey proteins.....	34
1.5.4	Transglutaminase in casein proteins	36
1.6	Succinylation.....	38
1.6.1	Succinylation of whey proteins and other food proteins	38
1.6.2	Succinylation of casein proteins	40
1.7	Other protein modifications	41
1.7.1	Acetylation.....	41
1.7.2	Reductive alkylation	42
1.7.3	Genetic variation	43
1.7.4	Conclusions.....	43
1.8	Thesis aims.....	44
Chapter 2	Experimental	46
2.1	Materials.....	46
2.1.1	Proteins and protein solutions	46
2.1.2	Chemicals.....	46
2.2	Methods	47
2.2.1	Dephosphorylation of α_{s1} -casein	47
2.2.2	Succinylation of α_{s1} -casein.....	48
2.2.3	Crosslinking of α_{s1} -casein.....	49

2.2.4	Ultraviolet – spectrophotometry.....	50
2.2.5	Sodium dodecyl sulphate and alkaline urea polyacrylamide gel electrophoresis	52
2.2.6	Isoelectric focusing electrophoresis	55
2.2.7	<i>o</i> -Phthaldialdehyde colorimetric assay.....	56
2.2.8	Mass spectrometry	57
2.2.9	Zeta potential measurements	58
2.2.10	1-Anilinonaphthalene-8-sulfonic acid fluorescence probe	58
2.2.11	Sodium dodecyl sulphate (SDS) binding	59
2.2.12	Calcium ion activity.....	60
2.2.13	Circular dichroism.....	60
2.2.14	Analytical ultracentrifugation	61
2.2.15	Nuclear magnetic resonance spectroscopy	62
2.2.16	Viscosity measurements of modified α_{s1} -casein.....	62
2.2.17	Surface tension (air-water) measurement - Wilhelmy plate method	63
2.2.18	Interfacial tension (oil-water) measurement – the pendant drop method.....	64
2.2.19	Foaming property measurements	64
2.2.20	Particle size measurement using laser light scattering.....	65
2.2.21	Emulsion preparation	65
2.2.22	Protein-coated latex samples preparation and measurement.....	65
2.3	Statistical analysis	67
Chapter 3	Characterization of dephosphorylated α_{s1}-casein	68
3.1	Introduction	68
3.2	Results and discussion.....	69
3.2.1	Determination of dephosphorylation of α_{s1} -casein	69
3.2.2	Discussion of the dephosphorylation of α_{s1} -casein	78
3.2.3	Isoelectric point of dephosphorylated α_{s1} -casein.....	82
3.2.4	Hydrophobicity of dephosphorylated α_{s1} -casein.....	93
3.2.5	Secondary structure of dephosphorylated α_{s1} -casein	99
3.2.6	Self-association behaviour of dephosphorylated α_{s1} -casein	104
3.3	Conclusions	110
Chapter 4	Functional properties of dephosphorylated α_{s1}-casein	112
4.1	Introduction	112
4.2	Results and discussion.....	112
4.2.1	Calcium ion binding of dephosphorylated α_{s1} -casein	112
4.2.2	Viscosity of dephosphorylated α_{s1} -casein.....	122
4.2.3	Water binding properties of dephosphorylated α_{s1} -casein	125

4.2.4	Surface tension of air-water interfaces of dephosphorylated α_{s1} -casein	129
4.2.5	Surface tension of oil-water interfaces of dephosphorylated α_{s1} -casein	133
4.2.6	Emulsifying properties of α_{s1} -casein	136
4.2.7	Foaming properties of dephosphorylated α_{s1} -casein	140
4.3	Conclusions	144
Chapter 5	Characterizations of succinylated α_{s1}-casein	146
5.1	Introduction	146
5.2	Results and discussion.....	147
5.2.1	Determination of succinylation of α_{s1} -casein	147
5.2.2	Isoelectric point of succinylated α_{s1} -casein	155
5.2.3	Hydrophobicity of succinylated α_{s1} -casein	165
5.2.4	Secondary structure of succinylated α_{s1} -casein.....	167
5.2.5	Self-association behaviour of succinylated α_{s1} -casein	170
5.3	Conclusions	172
Chapter 6	Functional properties of succinylated α_{s1}-casein	174
6.1	Introduction	174
6.2	Results and discussion.....	174
6.2.1	Viscosity of succinylated α_{s1} -casein	174
6.2.2	Water binding properties of succinylated α_{s1} -casein.....	176
6.2.3	Surface tension of air-water interfaces of succinylated α_{s1} -casein	178
6.2.4	Surface tension of oil-water interfaces of succinylated α_{s1} -casein.....	179
6.2.5	Emulsifying properties of succinylated α_{s1} -casein	181
6.2.6	Foaming properties of succinylated α_{s1} -casein.....	183
6.3	Conclusions	186
Chapter 7	Characterization of transglutaminase-modified α_{s1}-casein	188
7.1	Introduction	188
7.2	Results and discussion.....	189
7.2.1	Determination of cross-linking for α_{s1} -casein	189
7.2.2	Isoelectric point of TGA-treated α_{s1} -casein	198
7.2.3	Hydrophobicity of TGA-treated α_{s1} -casein	204
7.2.4	Secondary structure of TGA-modified α_{s1} -casein	207
7.3	Succinylated α_{s1}-casein with TGA treatment.....	209
7.4	Conclusions	212
Chapter 8	Functional properties of transglutaminase-modified α_{s1}-casein	213
8.1	Introduction	213

8.2 Results and discussion.....	213
8.2.1 Viscosity of TGA-treated α_{s1} -casein	213
8.2.2 Water binding properties of TGA-treated α_{s1} -casein.....	215
8.2.3 Surface tension of air-water interfaces of TGA-treated α_{s1} -casein.....	217
8.2.4 Surface tension of oil-water interfaces of TGA-treated α_{s1} -casein.....	219
8.2.5 Emulsifying properties of TGA-treated α_{s1} -casein	221
8.2.6 Foaming properties of TGA-treated α_{s1} -casein.....	224
8.3 Conclusions	227
Chapter 9 The effect of charge on the surface structure of α_{s1}-casein-coated polystyrene latex particles.....	228
9.1 Introduction	228
9.2 Results and discussion.....	229
9.2.1 Native casein-coated latex particles	229
9.2.2 Fully dephosphorylated α_{s1} -casein-coated latex	231
9.2.3 Dephosphorylation of casein-coated latex particles	234
9.2.4 Fully succinylated α_{s1} -casein-coated latex.....	237
9.2.5 Succinylation of α_{s1} -casein-coated latex.....	240
9.3 Conclusions	242
Chapter 10 General discussion and conclusions	244
10.1 Effect of physicochemical properties of α_{s1} -casein on the viscosity, water binding capacity and surface tension of α_{s1} -casein.....	248
10.2 Effect of physicochemical properties of α_{s1} -casein on the emulsifying properties	253
10.3 Effect of physicochemical properties of α_{s1} -casein on the foaming properties	254
10.4 Recommendations	257
References.....	259
Appendices.....	292

List of figures

Figure 1.1 Milk composition.	3
Figure 1.2 The self-association behaviour of β -lg as a function of pH and temperature	6
Figure 1.3 The structure of a monomer of bovine β -lg	6
Figure 1.4 The structure of a dimeric form of β -lg.	7
Figure 1.5 The structure of α -lac showing the Ca^{2+} binding site	8
Figure 1.6 Immunoglobulin monomer showing intermolecular and intramolecular disulphide bonds.....	8
Figure 1.7 (a) The distribution of hydrophobic residues and charge along the α_{s1} -casein protein chain, hydrophobic residues at the N-terminus and C-terminus.....	10
Figure 1.8 The distribution of hydrophobic residues and charge along the α_{s2} -casein protein chain, hydrophobic residues at N-terminus and at C-terminus	11
Figure 1.9 (a) The distribution of hydrophobic residues and charge along the β -casein protein chain, hydrophobic residues at N-terminus and at C-terminus.....	12
Figure 1.10 The distribution of hydrophobic residues and charge along the κ -casein protein chain, hydrophobic residues at N-terminus and C-terminus.....	13
Figure 1.11 Structural formula of α -lactose.	15
Figure 1.12 Structure of fat globules in milk	15
Figure 1.13 Casein sub-micelle structure. A. A sub-micelle with the hydrophobic core; B. Casein micelle consisting of numerous sub-micelles.....	17
Figure 1.14 Hairy casein sub-micelle structure	18
Figure 1.15 Modified hairy casein sub-micelle structure	19
Figure 1.16 Casein nanocluster structure.....	20
Figure 1.17 Casein dual-binding structure.....	21
Figure 1.18 Schematic structure of the casein micelle, incorporating calcium phosphate nanoclusters	22
Figure 1.19 Reduced SDS-PAGE profiles of sodium caseinate and its different biopolymers induced by TGA.	37
Figure 1.20 Schematic diagram of the acetylation reaction.....	41
Figure 1.21. Schematic diagram of the reductive methylation	43
Figure 2.1 Standard curve of absorbance ($A_{280}-A_{320}\times 1.7$) against protein concentration. Error bars represent the standard deviation of the mean of three replicates.....	51
Figure 3.1 Dephosphorylation of the serine phosphate residues with alkaline phosphatase	69

Figure 3.2 Abbreviated sequence of α_{s1} -casein: Asn ₃₈ -Glu ₅₀ , Glu ₆₁ -Glu ₇₇ , Pro ₁₁₃ -Arg ₁₁₉ , highlighting the eight common phosphoserine residues	69
Figure 3.3: AU-PAGE for dephosphorylation of α_{s1} -casein at different incubation times with alkaline phosphatase.....	71
Figure 3.4 SDS-PAGE for dephosphorylation of α_{s1} -casein at different incubation times with alkaline phosphatase.....	72
Figure 3.5 Schematic layout of the LTQ Orbitrap mass spectrometer.	74
Figure 3.6 HPLC peptide maps, parent mass spectrum (A) and mass spectrum of fragmented peptide Gln ₅₉ -Lys ₇₉ (B) from trypsin-digested native α_{s1} -casein	76
Figure 3.7 Dephosphorylated serine residues at incubation times of: 20 min, 90 min and 180 min, monitored by AU-PAGE (left PAGE pattern) and mass spectrometry (right) ..	78
Figure 3.8 The effect of concentration of theophylline, arsenate and PO_4^{3-} on the inhibition of calf intestinal alkaline phosphatase at pH 9.8.....	81
Figure 3.9 A. The calculated charge of α_{s1} -casein with different numbers of phosphate groups (zero to nine) at pH range of 3.0 to 7.0. B. The calculated charge of α_{s1} -casein with different numbers of phosphate groups (zero to nine) at pH over the range of 4.2 to 5.2.	83
Figure 3.10 The isoionic pH of α_{s1} -casein with different numbers of phosphate groups attached.	83
Figure 3.11 Schematic representation of the zeta potential of a particle.....	84
Figure 3.12 Zeta potentials of the native and dephosphorylated α_{s1} -casein at different incubation times.....	85
Figure 3.13 The isoelectric point of dephosphorylated α_{s1} -casein at different incubation times.....	86
Figure 3.14 Separation of protein molecules by isoelectric focusing.....	87
Figure 3.15 IEF-PAGE for the dephosphorylation of α_{s1} -casein at different incubation times.	88
Figure 3.16 The isoelectric point of dephosphorylated α_{s1} -casein at different incubation times.....	89
Figure 3.17 The relationship between charge calculation and IEF gel method (A), or charge calculation and zeta potential method (B) for measuring the pI of native and dephosphorylated α_{s1} -casein.	90
Figure 3.18 The relationship between zeta potential and IEF gel methods for measuring the pI of native and dephosphorylated α_{s1} -casein.	91
Figure 3.19 A. The charge of β -casein with different numbers of phosphate groups (0-4) over the pH range of 3.0 to 7.0. B. The charge of β -casein with different numbers of phosphate groups (0-4) over the pH range of 4.6 to 5.4.....	92
Figure 3.20 Amount of SDS (μg) bound per mg of α_{s1} -casein for native α_{s1} -casein and α_{s1} -casein dephosphorylated for different times.	94

Figure 3.21 Relative fluorescence intensity of α_{s1} -casein	96
Figure 3.22 Initial slope (S_0) of the relative fluorescence intensity versus dephosphorylation incubation time of α_{s1} -casein.	97
Figure 3.23 The relationship between SDS binding and ANS probe methods for measuring the apparently hydrophobicity of native and dephosphorylated α_{s1} -casein.	98
Figure 3.24 Origin of the CD effect. (A) The left (L) and right (R) circularly polarised radiation: (1) the two components have the same amplitude and when combined generate plane polarised radiation; (2) the components are of different magnitude and the resultant (dashed line) is elliptically polarised. (B) The relationship between absorption and CD spectra.	100
Figure 3.25 Far UV CD spectra associated with various types of secondary structure: α -helix, β -sheet, random coil and turn structure	101
Figure 3.26 Effect of dephosphorylation levels on the far-UV CD mean residue ellipticity [θ] of α_{s1} -casein expressed in degree cm ² /dmol.....	102
Figure 3.27 Schematic diagram of the optical system of the analytical ultracentrifuge	104
Figure 3.28 Double-sector centrepiece. The sample solution is placed in one sector, and sample of the solvent is placed in the reference sector.....	106
Figure 3.29 An example of an AUC experiment: movement of the boundary in a sedimentation velocity experiment with a recombinant malaria antigen protein.	106
Figure 3.30 Sedimentation coefficient distribution of native and dephosphorylated α_{s1} -casein in 10 mM phosphate buffer (containing 2.7 mM KCl and 137 mM NaCl, pH 7.4) at protein concentrations of: A: 1 mg/mL, B: 2 mg/mL and C: 3 mg/mL.	108
Figure 4.1 Schematic representation of the ion-selective electrode	113
Figure 4.2 Electrical potential of dephosphorylated α_{s1} -casein containing different levels of calcium chloride measured using the ion-selective electrode. A. Potential of free calcium ions of α_{s1} -casein with the calcium ion concentration range of 0.14 mM – 4 mM. B. Potential of free calcium ions of α_{s1} -casein with the calcium ion concentration from 0.14 to 0.16 mM.....	115
Figure 4.3 Calcium ion levels in the serum phase of standard CaCl ₂ solution (solid line), standard-native α_{s1} -casein (◆), control-native α_{s1} -casein with heat treatment at 85°C for 5 min (■), α_{s1} -casein incubated with phosphatase for 5 min.....	116
Figure 4.4 Bound calcium ion levels in standard-native α_{s1} -casein (◆), control-native α_{s1} -casein with heat treatment at 85°C for 5 min (■), α_{s1} -casein incubated with phosphatase for 5 min.....	117
Figure 4.5 Isotherms of calcium ions bound to α_{s1} -casein and the fitted Langmuir model curves (solid line). Standard-native α_{s1} -casein (◆), control-native α_{s1} -casein with heat treatment at 85°C for 5 min (■), dephosphorylated α_{s1} -casein at incubation times of 5 min.....	119
Figure 4.6 Bound calcium ions on α_{s1} -casein at different pI values of dephosphorylated α_{s1} -casein.....	121

Figure 4.7 The relationship between predicted calcium ion binding and experimental calcium ion binding.....	122
Figure 4.8 Viscosity of dephosphorylated α_{s1} -casein solutions incubated with phosphatase for different times (A). Viscosity of dephosphorylated α_{s1} -casein that bound to different numbers of calcium ions (B).	123
Figure 4.9 The basis of NMR.....	125
Figure 4.10 T2 relaxation constant time for α_{s1} -casein incubated with phosphatase for different times.....	127
Figure 4.11 Schematic diagram of the Wilhelmy plate method	129
Figure 4.12 Surface tension (air-water) of dephosphorylated α_{s1} -casein solutions measured using the Wilhelmy plate method.	131
Figure 4.13 A pendant drop showing the characteristic dimension.....	134
Figure 4.14 Interfacial tension (oil-water) of dephosphorylated α_{s1} -casein measured using a pendant drop tensiometer.	135
Figure 4.15 A schematic diagram of the light scattering of a particle	136
Figure 4.16 Particle size $d_{(3,2)}$ of canola oil droplet in emulsions made with α_{s1} -casein.	137
Figure 4.17 The proposed mechanisms of emulsion coalescence.....	140
Figure 4.18 Protein serum separation time for samples incubated with phosphatase for different times.....	142
Figure 4.19 The diagram illustrates proposed electrostatic repulsion between air bubbles coated with A. native α_{s1} -casein and B. dephosphorylated α_{s1} -casein in a foam system.	144
Figure 5.1 The capping of lysine residues with succinic anhydride	146
Figure 5.2 Reaction of OPA with amine and 2-mercaptoethanol.....	147
Figure 5.3 α_{s1} -Casein solutions with the addition of different amounts of succinic anhydride	148
Figure 5.4 Reduced SDS-PAGE of α_{s1} -casein with different levels of succinylation.....	149
Figure 5.5 The band intensity of α_{s1} -casein with the addition of different amounts of succinic anhydride on SDS gel.....	150
Figure 5.6 The relationship between SDS gel and OPA methods.	151
Figure 5.7 HPLC peptide maps, parent mass spectrum (A) and mass spectrum of fragmented peptide Lys ₁₂₃ -Lys ₁₄₄ (B) from the trypsin-digested native α_{s1} -casein	152
Figure 5.8 α_{s1} -Casein with different levels of succinylation monitored by reduced SDS-PAGE and mass spectrometry.	154
Figure 5.9. The calculated charge of α_{s1} -casein with eight phosphoserine residues and different numbers of succinylated lysine residues (0-13) at pH over the range of 3.0 to 5.0 (A) and at pH over the range of 3.5 to 4.5 (B).	156

Figure 5.10 The calculated isoionic point of α_{s1} -casein with different numbers of succinylated lysine residues.	157
Figure 5.11 The zeta potentials of native and succinylated α_{s1} -casein at different pH values	158
Figure 5.12 The isoelectric point of α_{s1} -casein, as determined from zeta potential measurements, for samples with different levels of succinylation.....	159
Figure 5.13 IEF-PAGE of α_{s1} -casein with different levels of succinylation.....	160
Figure 5.14 The isoelectric point of succinylated α_{s1} -casein with different level of succinylation.....	161
Figure 5.15 The relationship between charge calculation and zeta potential methods (A), The relationship between charge calculation and IEF gel methods for measuring the pl of native and succinylated α_{s1} -casein (B).	163
Figure 5.16 The relationship between zeta potential and IEF gel methods for measuring the pl of native and succinylated α_{s1} -casein.....	164
Figure 5.17 Relative fluorescence intensity of α_{s1} -casein.....	165
Figure 5.18 Initial slope (S_0) of the relative fluorescence intensity of the α_{s1} -caseins with different levels of succinylated lysine residues.	166
Figure 5.19 Effect of succinylation levels on the far-UV CD mean residue ellipticity $[\theta]$ of α_{s1} -casein expressed in degree cm^2/dmol	168
Figure 5.20 Sedimentation coefficient distribution of native and succinylated α_{s1} -casein in 10 mM phosphate buffer (containing 2.7 mM KCl and 137 mM NaCl, pH 7.4) at protein concentrations of A: 1 mg/mL, B: 2 mg/mL and C: 3 mg/mL.	171
Figure 6.1 Viscosity of α_{s1} -casein with different levels of succinylation.....	175
Figure 6.2 T2 relaxation constant time of succinylated α_{s1} -casein measured using NMR. ..	176
Figure 6.3 Surface tension (air-water) of succinylated α_{s1} -casein measured using the Wilhelmy plate method.....	178
Figure 6.4 Interfacial tension (oil-water) of succinylated α_{s1} -casein measured using a pendant drop tensiometer.	180
Figure 6.5 Particle size $d_{(3,2)}$ of canola oil droplet in emulsions made with α_{s1} -casein.	181
Figure 6.6 Protein serum separation time. α_{s1} -Casein with different levels of succinylation.	183
Figure 6.7 The proposed correlation model of hydrophobicity and net charge vs foam stability of α_{s1} -casein.	186
Figure 7.1 The transglutaminase induced reactions: A. deamidation B. amino incorporation C. cross-linking.....	189
Figure 7.2 SDS-PAGE of cross-linked α_{s1} -casein at different incubation times.....	190
Figure 7.3 Full sequence of native α_{s1} -casein, highlighting the potential residues for cross linking (green and blue) and deamidation (red and blue) in the sequence	192

Figure 7.4 HPLC peptide maps, parent mass spectrum (A) and mass spectrum of fragmented peptide Lys ₇ -Arg ₂₂ (B) from the trypsin-digested native α_{s1} -casein (1) and α_{s1} -casein incubated with TGA at 120 min (2).....	194
Figure 7.5 α_{s1} -Casein incubated with TGA at incubation time: 0 min (Sd = standard – native α_{s1} -casein and control – native α_{s1} -casein with heat treatment of 85°C for 5 min), 5 min and 120 min, monitored by mass spectrometry. Q (black): glutamine residues, Q (red): partially deamidated glutamine residues, which were identified by the database mapping.	197
Figure 7.6 The zeta potentials of native and TGA-treated α_{s1} -casein at different pH values	199
Figure 7.7 The isoelectric point of TGA-modified α_{s1} -casein at different incubation times.	200
Figure 7.8 IEF-PAGE for the cross-linked α_{s1} -casein at different incubation times.	201
Figure 7.9 The isoelectric point of TGA-modified α_{s1} -casein at different incubation times, which were determined using an IEF gel.....	202
Figure 7.10 The relationship between zeta potential and IEF gel methods for measuring the pl of native and TGA-modified α_{s1} -casein.....	204
Figure 7.11 Relative fluorescence intensity of α_{s1} -casein	205
Figure 7.12 Initial slope (S_0) of the relative fluorescence intensity versus TGA incubation time of α_{s1} -casein.....	205
Figure 7.13 Effect of TGA incubation time on the far-UV CD mean residue ellipticity $[\theta]$ of α_{s1} -casein expressed in degree cm ² /dmol.....	207
Figure 7.14 Reduced SDS-PAGE of succinylated α_{s1} -casein incubated with TGA for 120 min.	210
Figure 7.15 Succinylated α_{s1} -casein (99%) incubated with TGA at incubation time 120 min monitored by mass spectrometry. Q (black): glutamine residues, Q (red): partially deamidated glutamine residues, which were identified by the database mapping (more data is stated in Appendix C).	211
Figure 8.1 Viscosity of TGA-treated α_{s1} -casein.	214
Figure 8.2 T ₂ relaxation constant time of TGA-treated α_{s1} -casein measured using NMR....	215
Figure 8.3 Surface tension (air-water) of TGA-treated α_{s1} -casein solutions measured using the Wilhelmy plate method.	218
Figure 8.4 Interfacial tension (oil-water) of TGA-treated α_{s1} -casein measured using pendant drop tensiometer.	220
Figure 8.5 Particle size $d_{(3,2)}$ of canola oil droplet in emulsions made with α_{s1} -casein.	222
Figure 8.6 Protein serum separation time.....	225
Figure 9.1 The method for coating latex particles with modified α_{s1} -casein and for modification of α_{s1} -casein-coated latex particles.....	228
Figure 9.2 The changes in the diameters of native β -casein (▲), κ -casein (◆) and α_{s1} -casein (■) -coated 60 nm (A) and 100 nm (B) latex particles.....	230

Figure 9.3 The changes in the diameters of native α_{s1} -casein (◆) and fully dephosphorylated α_{s1} -casein (▲)-coated 60 nm (A) and 100 nm (B) latex particles.....	231
Figure 9.4 The proposed structure of native and dephosphorylated α_{s1} -casein on a latex particle.....	232
Figure 9.5 The zeta potential of native α_{s1} -casein (◆) and fully dephosphorylated α_{s1} -casein (▲)-coated 60 nm (A) and 100 nm (B) latex particles.....	233
Figure 9.6 The changes in the diameters of native α_{s1} -casein-coated 60 nm (A) and 100 nm (B) latex particles incubated with 0.5 μ L (◆), 3 μ L (▲) and 6 μ L (×) of phosphatase for different times.	234
Figure 9.7 The changes in diameters of native κ -casein (◆), β -casein (▲) and α_{s1} -casein (■)-coated 60 nm (A) and 100 nm (B) latex particles incubated with 6 μ L of phosphatase at different times.	236
Figure 9.8 The changes in diameters of native α_{s1} -casein (◆) and fully succinylated α_{s1} -casein (▲)-coated 60 nm (A) and 100 nm (B) latex particles.....	237
Figure 9.9 Train and loop model of primary structure of α_{s1} -casein	238
Figure 9.10 The changes in diameters of native α_{s1} -casein (◆)-coated 60 nm and 100 nm latex particles, and the effect of succinylation (■) on the changes in diameters. Each data point is an average of two replicates.....	240
Figure 9.11 The proposed structure of succinylation on the native α_{s1} -casein-coated latex particles.	241
Figure 10.1 The relationship between net charge and surface hydrophobicity.....	246
Figure 10.2 The relationship between net charge and viscosity	249
Figure 10.3 The relationship between net charge and water binding capacity (A), hydrophobicity and water binding capacity (B).....	250
Figure 10.4 The relationship between surface tension air-water interface and oil-water interface	251
Figure 10.5 The relationship between net charge and interfacial tension (air-water) of 0.001% (w/w) dephosphorylated α_{s1} -casein solutions (◆) and 0.02% (w/w) succinylated α_{s1} -casein solutions (■).	252
Figure 10.6 The relationship between surface hydrophobicity and interfacial tension (air-water) of 0.001% (w/w) dephosphorylated α_{s1} -casein solutions (◆) and 0.02% (w/w) succinylated α_{s1} -casein solutions (■).....	252
Figure 10.7 The relationship between net charge and particle size $d_{(3,2)}$ of canola oil droplet in emulsions made with α_{s1} -casein (A), and between hydrophobicity and particle size $d_{(3,2)}$ of canola oil droplet in emulsions made with α_{s1} -casein (B).....	254

List of Tables

Table 1.1 Characteristics of major whey proteins components.	5
Table 1.2 Properties of the casein proteins in milk	9
Table 1.3. The concentration of principal elements in milk	14
Table 2.1: The list of chemicals and their supplier	46
Table 2.2 Preparation of stock solutions for SDS-PAGE	52
Table 2.3 Preparation of stock solutions for urea-PAGE	55
Table 2.4 The preparation of OPA reagent.....	56
Table 3.1 The mass to charge ratio of native and dephosphorylated α_{s1} -casein at incubation times of 20 min and 180 min.....	77
Table 3.2 The level of secondary structure of native and dephosphorylated α_{s1} -casein estimated by CD	103
Table 4.1 Parameters for the calcium ions binding on to α_{s1} -casein calculated using the Langmuir model.....	120
Table 4.2 The volumes of native and dephosphorylated α_{s1} -casein foam.	141
Table 5.1 The level of secondary structure of native and succinylated α_{s1} -casein estimated by CD.	169
Table 6.1 The volumes of native and succinylated α_{s1} -casein foam.....	183
Table 7.1 The mass to charge ratio of peptide Lys ₇ -Arg ₂₂ from native α_{s1} -casein and TGA-modified α_{s1} -casein at incubation time 120 min.	196
Table 7.2 The level of secondary structure of native and TGA-treated α_{s1} -casein estimated by CD	208
Table 8.1 The volumes of foam from native and TGA-treated α_{s1} -casein.	224
Table 9.1 The surface zeta potential of native α_{s1} -casein and fully succinylated α_{s1} -casein-coated 60 nm and 100 nm latex particles.	239
Table 9.2 The surface zeta potential of native α_{s1} -casein-coated 60 nm and 100 nm latex particles, and the effect of succinylation on the surface zeta potential.	242
Table 10.1 The changes in the physicochemical and functional properties of modified α_{s1} -caseins.	245

List of Symbols

pI	Isoelectric point
pK_a	The negative base-10 logarithm of the acid dissociation constant (K _a) of a solution.
S	Sedimentation coefficient
S₀	Initial slope
θ	Mean residue molar ellipticity

List of Abbreviations

ANS	1-Anilinonaphthalene-8-sulphonic acid
APS	Ammonium persulphate
AU	Alkaline urea
AUC	Analytical ultracentrifuge
BSA	Bovine serum albumin
CCP	Colloidal calcium phosphate
CD	Circular dichroism
Citr	Citrate
DDT	Dithiothreitol
ESI-MS	Electrospray ionization mass spectrometry
FTIR	Fourier transform infra-red
HLB	Hydrophilic-lipophilic balance
IEF	Isoelectric focusing
IEF	Isoelectrofocusing
Ig	Immunoglobulins
ISE	Ion selective electrode
MFGM	Milk fat globule membrane
NEM	N-ethylmaleimide
NMR	Nuclear magnetic resonance
OPA	o-Phthaldialdehyde
PAGE	Polyacrylamide gel electrophoresis
PRODAN	6-Propionyl-2-(N,N-dimethylamino)-naphthalene

RFI	Relative fluorescence intensity
RP-HPLC	Reversed phase high performance liquid chromatography
SDS	Sodium dodecyl sulphate
TCA	Trichloroacetic acid
TEM	Transmission electron micrograph
TEMED	Tetramethylethylenediamine
TGA	Transglutaminase
Tris-base	Tris (hydroxymethyl) methylamine
UV	Ultraviolet
WPI	Whey protein isolate

Chapter 1 Introduction and literature review

The primary purpose of bovine milk is to meet the nutritional requirements of the neonate, to supply essential amino acids, essential fatty acids, minerals (especially calcium), vitamins, and lactose (Fox, 2003; Meisel, 2005). Because of its high nutritional value, bovine milk has been widely commercialized as a general daily food source, and has been processed into a large number of consumer products such as yoghurt and cheese that maintain the nutritional value but prolong the shelf life. Moreover, novel technical methods have been developed to produce bovine milk protein products with specific or enhanced functionalities. Thus, bovine milk as a raw material or ingredient plays an important role in modern food systems (Szwajkowska et al., 2011).

The physicochemical properties of milk protein play an important role in dairy products, impacting on viscosity, emulsifying properties, solubility, texture and heat stability. Protein modifications can alter the physicochemical properties of the proteins by changing their net charge and hydrophobicity. These will affect the overall functional properties of these proteins in dairy food systems. Thus, it is necessary to understand how these molecular interactions with and between dairy proteins control the functional properties of dairy products.

In this study, α_{s1} -casein, a key protein in dairy products, was modified with three modification approaches: phosphatase-induced dephosphorylation, succinylation with succinic anhydride, and transglutaminase-catalysed protein crosslinking and deamidation. This project aims to investigate the impact of protein modification on the functionalities of these proteins and to explore the correlation between the physicochemical and functional properties of these dairy proteins.

The objectives of the study were:

1. To create a range of modified protein ingredients with a range of controlled levels of modifications.
2. To investigate the effect of these modifications on the physicochemical properties of protein, such as charge, hydrophobicity, secondary structure and self-association behaviour.
3. To investigate the functionality of modified proteins, such as emulsifying properties, viscosity, water binding capacity, and foaming properties.
4. To understand how the interactions of these proteins with each other and with other food components, control the overall properties and functionalities of dairy foods.

This literature review describes bovine milk composition and focuses on the fundamental knowledge of milk proteins. The review then introduces three modification approaches: dephosphorylation, transglutaminase modification and succinylation, and their effects on the physicochemical and functional properties of milk proteins and milk products.

1.1 Milk composition

Bovine milk consists of approximately 86% water and 14% dry matter that is dissolved or suspended in the water. The major components of milk are summarized in Figure 1.1. The actual composition of milk can be affected by many factors such as variations between individual cows, different breeds, seasons, feed regimes and stage of lactation (Bylund, 1995; Elsasser et al., 2007; Fox, 2009; Jensen et al., 2012b; Litwinczuk et al., 2011; Ostersen et al., 1997). Milk proteins provide high nutritional value, including essential amino acids such as sulphur amino acids essential for the

metabolic system of the body (Smithers, 2008; Szwajkowska et al., 2011). Apart from the proteins, milk also contains fat, lactose, minerals and vitamins, that supply the energy and micro-nutrients needed for the growth of the neonate (Walstra et al., 2005).

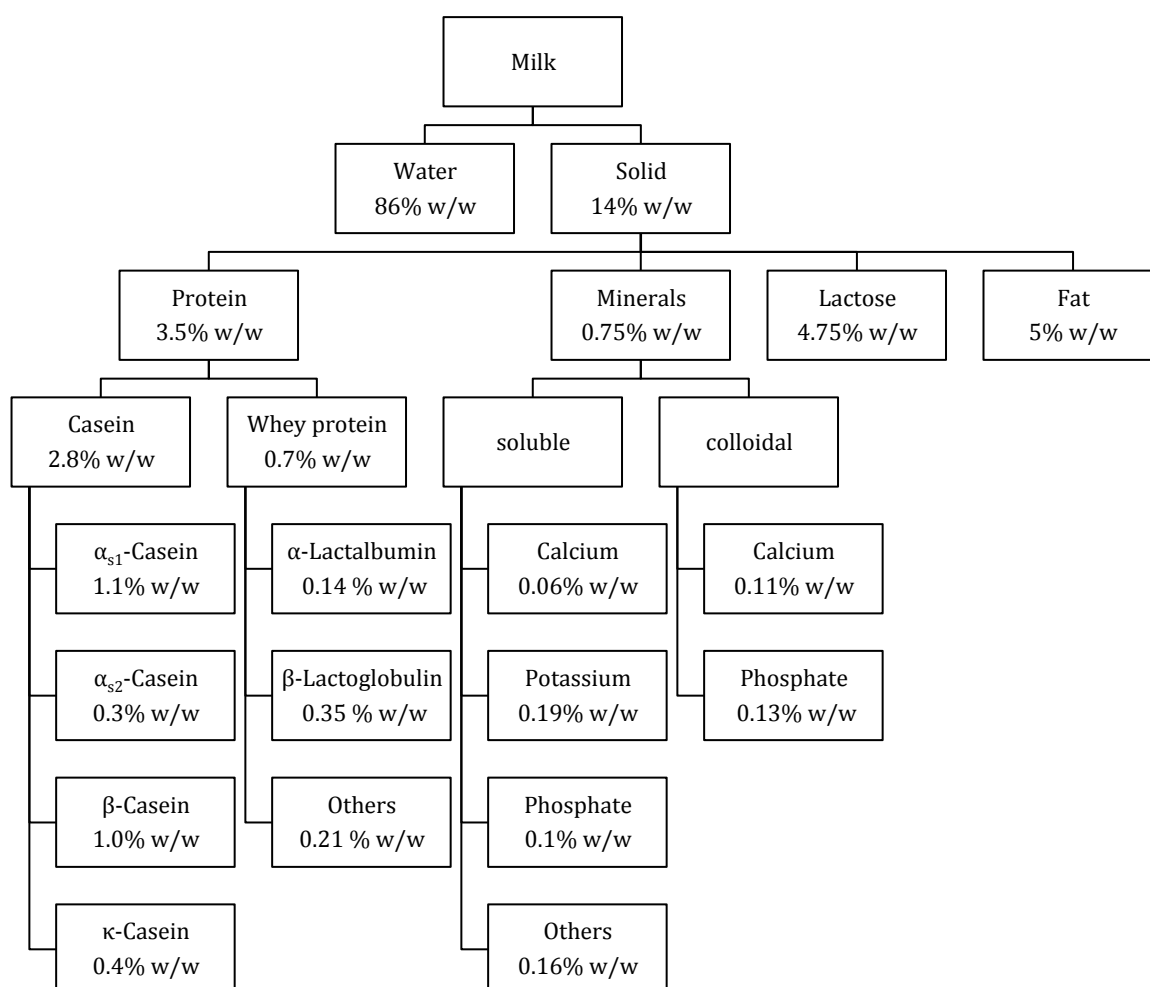


Figure 1.1 Milk composition. (Bylund, 1995; Swaisgood, 1982; Wang et al., 2009).

1.1.1 Proteins in milk

Milk contains approximately 3.5% total protein, with casein and whey proteins the two main classes of protein in milk. Casein and whey proteins account for 20% and 5% of the total dry matter in whole milk, respectively. The general definition for the caseins is based on the solubility at their isoelectric point that is about pH 4.6.

Caseins are precipitated at pH 4.6 and 20°C while native whey proteins are soluble under these conditions. Thus, isoelectric precipitation is the most widely used method for separating casein proteins from native whey proteins. Caseins can also be separated from whey proteins by other methods such as ultracentrifugation, microfiltration, salting-out and rennet coagulation. Rennet coagulation, as used in cheese and rennet casein manufacture, is a different process and it results in different composition of whey proteins due to proteolysis of caseins (Fox, 2009; Fox, 1982; Walstra & Jenness, 1984; Wang et al., 2009).

1.1.2 Whey proteins

Whey protein makes up approximately 20% of the total protein composition in milk. The major whey proteins are β -lactoglobulin (β -lg, approximately 50% of whey protein) and α -lactalbumin (α -lac, approximately 20% of the whey proteins). There are numerous minor whey proteins that make up the remaining 30%, in particular the immunoglobulins (Ig, approximately 10% of the whey proteins), bovine serum albumin (BSA, approximately 6% of the whey proteins), and lactoferrin (Lf, approximately 1% of the whey proteins). The proteose peptones (approximately 10% of the whey proteins) is a complex mixture of proteins and peptides, with some of the peptides derived from the proteolysis of casein by indigenous milk enzymes (Fox, 2009). Some characteristics of the major whey proteins components are summarized in Table 1.1 (Fox, 2003; Paulsson, 1990).

Table 1.1 Characteristics of major whey proteins components.

	β -lg	α -lac	Ig	BSA	Lf
Molecular weight (kDa)	18	14	150-900	66	80
pI	5.0-5.3	4.2-4.5	5.5-8.3	5.3	8.7
Amino acid residues (per molecule)	162	123		607	689
Cystine (per molecule)	2	4	21	17	17
Cysteine residues S-H (per molecule)	1	0	0	1	0

β -Lactoglobulin

β -Lg has 162 amino acids and a monomer molecular weight of ~18,000 Da. Although there are ten known genetic variants for β -lg, most bulk milks are composed of the two common variants, A and B, in roughly equal concentrations (Fox, 2009; Ganai et al., 2009; Mercadante et al., 2012; Merin et al., 2001). β -Lg can be a monomer, a dimer or an octamer, dependent on the pH, concentration, temperature and ionic strength (Figure 1.2; Elofsson, 1996). The β -lg monomer has two intramolecular disulfide bonds (-S-S-) and one free sulfhydryl group (-SH) (Figure 1.3; Edwards & Jameson, 2009). Two monomers can join together by hydrophobic interaction to form a dimer, and this is the predominant oligomeric state between pH 5.5 and 7.5 (Figure 1.4). The dimers can associate with each other to form octamers with a molecular weight of 144,000 Da in the pH range of 3.5-5.5. When the pH is below 3.5, the electrostatic repulsion disrupts the dimers to re-form monomers (Fox, 2003; Mercadante et al., 2012; Swaisgood, 1982; Walstra et al., 2005).

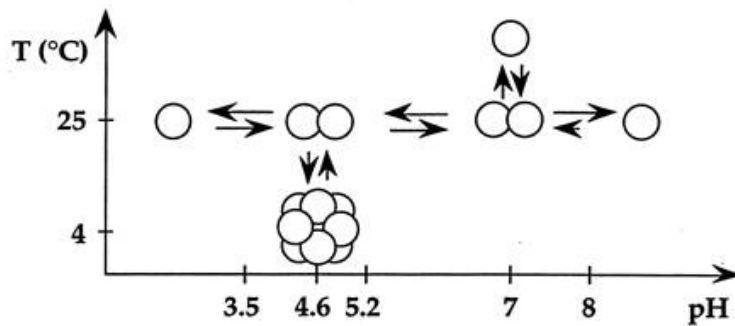


Figure 1.2 The self-association behaviour of β -lg as a function of pH and temperature (Elofsson, 1996).

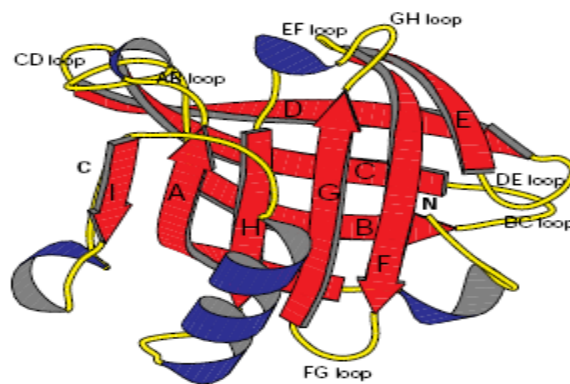


Figure 1.3 The structure of a monomer of bovine β -lg (Brownlow et al., 1997).

The secondary structure of β -lg has about 15% α -helix, 50% β -sheet and 15-20% reverse turn. β -Strands A to D and strands E to H combine to form the calyx, which is flanked by a three-turn α -helix. The final ninth strand I forms part of a dimer interface (Figure 1.3 and 1.4; Brownlow et al., 1997). One of the cysteine residues (Cys121) is in the free thiol state and is buried between β -strand H and the three-turn α -helix; thus, it has a low activity in the native state of β -lg. The other four cysteine residues form two pairs of disulphide bonds. Cys66 is the cysteine residue on loop CD and is disulphide bonded with Cys160, which is near the C-terminus (Figure 1.4). Cys106 on strand G is disulphide bonded with Cys119 on strand H (Brownlow et al., 1997; Mercadante et al., 2012; Muhammad et al., 2013).

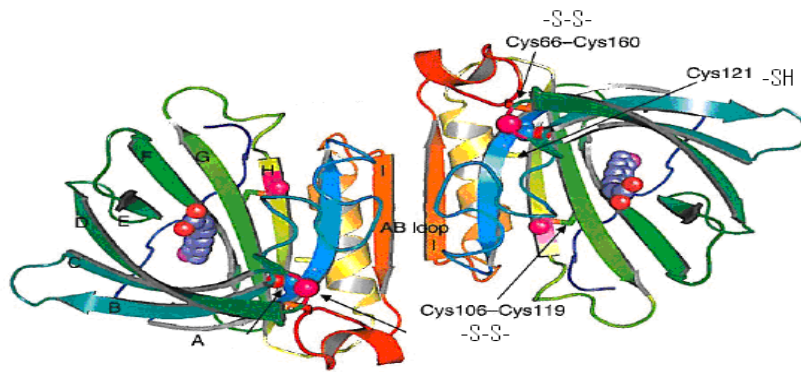


Figure 1.4 The structure of a dimeric form of β -lg. A-I, β -strands; Cys, cysteine residues; -SS-, disulfide bond; -SH, Trp, tryptophan residues (purple dot); thiol group (Edwards et al., 2009).

α -Lactalbumin

α -Lac has 123 amino acids and a monomer molecular weight of 14,000 Da (Merin et al., 2001). The genetic variant A of α -Lac is common in bovine milk, whereas other variants are rare (Visker et al., 2012). α -Lac has four intra-molecular disulphide bonds, but no free thiol group. α -Lac is a metallo protein, and is associated with a calcium ion in its native state. The calcium ion plays an important role in stabilizing the protein conformation. α -Lac denaturation occurs at low pH (pH<4) as the calcium ion is dissociated, and this results in partial unfolding of the protein to form a molten globular state (Edwards & Jameson, 2009; Fox, 1982; Walstra & Jenness, 1984).

The secondary structure of α -lac has 26% α -helix, 14% β -structure and a 60% unordered structure (Robbins & Holmes, 1970). The tertiary structure of α -lac consists of an α -lobe and a β -lobe. The α -lobe has three α -helices and two short 3_{10} -helices, and the β -lobe has three-stranded β -sheets and a short 3_{10} -helix (Figure 1.5). The α -lobe contains two disulphide bonds (Cys6-Cys120 and Cys28-Cys111) and the β -lobe contains one (Cys60-Cys77), with the two lobes bound together by a disulphide bond (Cys73- Cys90) (Brew, 2003; Muhammad et al., 2013).

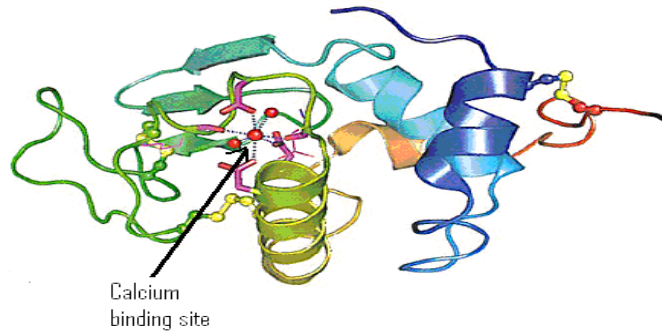


Figure 1.5 The structure of α -lac showing the Ca^{2+} binding site (Edwards & Jameson, 2009).

Minor whey proteins

BSA has a molecular weight of 66,000 Da and it accounts for approximately 6% of whey proteins. BSA has one sulfhydryl group and seventeen disulphide bonds. BSA is not strictly a milk protein, it is transferred to the mammary gland from the blood (Fox, 2003; Walstra & Jenness, 1984).

The Igs are a family of large globular proteins with a common antibody activity and similar structural elements. Igs are found at very high levels in colostrum and they provide multiple specific functions in the immunity system. Some are also derived from blood in a similar way to BSA (Fox, 2009). The basic sub-units in Igs consists of two heavy polypeptide chains (MW about 50-70,000 Da) and two light polypeptide chains (MW 22,400 Da), linked by three inter-polypeptide disulphide bonds (Figure 1.6). Each heavy chain and light chain contains two and four cystines, respectively (Fox, 1989).

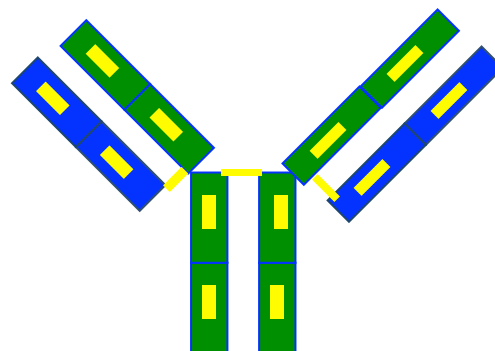


Figure 1.6 Immunoglobulin monomer showing intermolecular and intramolecular disulphide bonds (S-S, yellow), heavy chain (green) and light chain (blue).

Lactoferrin, lactolin, glycoprotein and blood transferrin are minor proteins in whey and collectively account for only 5% of the total whey protein content. Lactoferrin is also known as a component of the immune system of the human body and provides antimicrobial activity, particularly to human infants (Fox, 2009).

1.1.3 Casein proteins

Casein makes up approximately 80% of the total protein composition of cow's milk. Casein has four gene products: α_{s1} -, α_{s2} -, β - and κ -casein, and they account for approximately 38%, 10%, 35% and 12% of whole casein, respectively. Casein proteins have high levels of the amino acid proline that has a ring structure at the N-terminus. The proline is relatively uniformly distributed along the protein chains, and due to the fixed ring structure, the flexibility of the protein chain is reduced and large regions of α -helix and β -sheet structures cannot be formed. As a consequence, the high proline content contributes to low levels of a secondary and tertiary structure in the caseins. Casein has a high heat stability and high surface hydrophobicity, due to the lack of secondary and tertiary structure. Each of the caseins also has an amphipathic structure due to the non-uniform distribution of its hydrophobic and hydrophilic residues. The hydrophobic binding domains between caseins cause casein molecules to associate (Fox, 2009; Huppertz et al., 2006; Walstra et al., 2005).

The properties of the casein fractions in milk are listed in Table 1.2. All the caseins are phosphorylated at some of the serine amino acid residues.

Table 1.2 Properties of the casein proteins in milk (Fox, 2009).

	α_{s1} -casein	α_{s2} -casein	β -casein	κ -casein
Molecular weight (kDa)	23.6	25.2	24.0	19.6
pI	5.0	5.3	5.2	5.5
Amino acid residues (per molecule)	199	207	209	169
Phosphate residues (per molecule)	8-9	10-14	4-5	1-2
Cysteine residues (per molecule)	0	2	0	2

α_{s1} -Casein

α_{s1} -Casein has 199 amino acids and a monomer molecular weight of 23,600 Da. α_{s1} -Casein contains 8 to 9 phosphoserine residues that are highly charged, but no cysteine residues. The most common genetic variant of α_{s1} -casein is variant B. The phosphoserine residues are not distributed uniformly and form two clusters (Figure 1.7 a, blue). The phosphate clusters can bind metal ions, mainly calcium (Ca^{2+}) in milk. Thus, α_{s1} -casein is very sensitive to calcium ion concentration, it precipitates at a calcium ion concentration of 3-8 mM at 20°C and above (Holt, 1985). α_{s1} -Caseins can self-associate by interactions through the hydrophobic regions of the molecules to form worm-like chain polymers (Figure 1.7 b; Horne, 1998). The self-association of α_{s1} -casein can be affected by pH and ionic strength. Oligomerization of α_{s1} -casein occurs with increased ionic strength from 0.003 to 0.01 at pH 6.6; however, with decreased ionic strength, only small polymers are formed. The polymerization of α_{s1} -casein is favoured at higher pHs (Swaisgood, 2003).

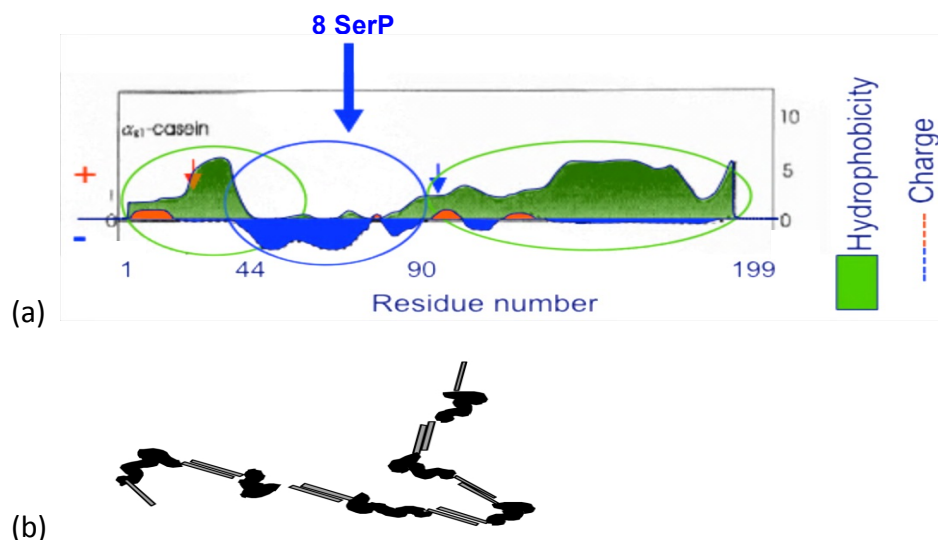


Figure 1.7 (a) The distribution of hydrophobic residues and charge along the α_{s1} -casein protein chain, hydrophobic residues at the N-terminus and C-terminus (green), 8 phosphoserine residues in the negatively charged region between residues 44 and 90 (blue). (b) Diagrammatic representations of the polymeric structures of α_{s1} -casein, showing linkages through interaction of hydrophobic regions of the molecules (rectangular bars), with α_{s1} -casein forming a linear polymer (Horne, 1998).

α_{s2} -Casein

α_{s2} -Casein has 207 amino acids and a monomer molecular weight of 25,200 Da. α_{s2} -Casein has a higher calcium sensitivity and hydrophilicity compared to α_{s1} -casein, due to a higher content of phosphoserine residues. At 20°C and above, α_{s2} -casein is precipitated at calcium ion concentrations of 2 mM (Holt, 1985). α_{s2} -Casein contains 10-13 phosphoserine groups that form three clusters, in which the clusters are separated by hydrophobic regions (Figure 1.8; Fox, 1982; Swaisgood, 2003). α_{s2} -Casein contains two cysteine residues that occur as intermolecular disulphide bonds that link some of the α_{s2} -casein to form dimers. The genetic variant A in α_{s2} -casein is more common than variant B, C and D in bovine milk. α_{s2} -Caseins can be self-associated by hydrophobic and/or electrostatic interactions, which is analogous to the self-association of α_{s1} -caseins. α_{s2} -Casein associations are affected by ionic strength and strong associations occur at an optimal ionic strength 0.2 M (Schmidt, 1982; Swaisgood, 2003).



Figure 1.8 The distribution of hydrophobic residues and charge along the α_{s2} -casein protein chain, hydrophobic residues at N-terminus and at C-terminus (green), 8 phosphoserine residues in the negatively charge region between residues 1 and 58; 3 phosphoserine residues in the negatively charge region between residues 58 and 143 (blue).

β -Casein

β -Casein has 209 amino acids and a molecular weight of 24,000 Da. β -Casein contains five phosphoserine groups in one cluster at the hydrophilic N-terminus (Figure 1.9 a). β -Casein is less calcium ion sensitive than α_{s2} -casein as it precipitates at calcium ion concentrations of 8-15 mM when the temperature is above 20°C

(Holt, 1985). There are 12 known genetic variants of β -casein, but the common variants are A1, A2 and B. β -Casein has a high hydrophobicity due to the large hydrophobic C-terminal region. The hydrophilic N-terminus and hydrophobic C-terminal regions contribute to an amphiphilic structure of β -casein (Fox, 1982). At neutral pH, the first 21 amino acid residues of most β -casein sequence are charged, while the remainder of the molecule is uncharged (Darewicz et al., 2000). β -Casein can be self-associated by interactions in the hydrophobic regions to form a surfactant-like micellar polymer (Figure 1.9 b). The association of β -casein is strongly affected by temperature and micellar polymers are formed at temperatures above 8.5°C, whereas only monomers are present at 4°C (De Kruif & Grinberg, 2002; Swaisgood, 2003).

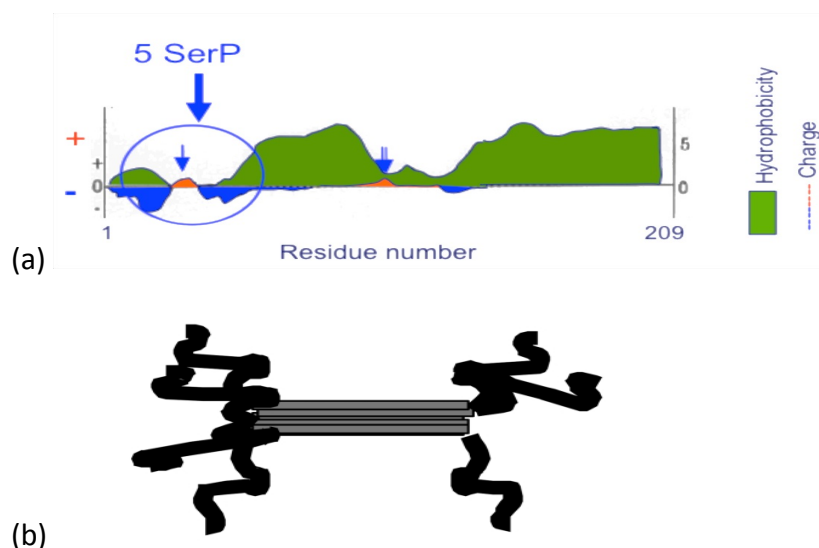


Figure 1.9 (a) The distribution of hydrophobic residues and charge along the β -casein protein chain, hydrophobic residues at N-terminus and at C-terminus (green), 5 phosphoserine residues in the negatively charge region (blue). **(b)** Diagrammatic representations of polymeric structures of β -casein, showing linkages through interaction of hydrophobic regions of the molecules (rectangular bars), with β -casein forming a surfactant-like micellar structure (Horne, 1998).

κ -Casein

κ -Casein has 169 amino acids and a monomer molecular weight of 19,550 Da. κ -Casein contains only one phosphoserine group and therefore this protein weakly

binds calcium ions (Figure 1.10; Jeyarajah & Allen, 1994). The major feature of κ -casein is a variable degree of glycosylation. The most common κ -casein variants in bovine milk are the A and B variants. κ -Casein has a much lower calcium ion sensitivity compared to other casein fractions; it can stabilize other caseins against aggregation in the presence of calcium. κ -Casein has a hydrophilic C-terminal region and a hydrophobic N-terminal region that has two cysteine residues (Swaigood, 1982). κ -Casein can form monomers with an internal disulphide bond and oligomers of up to 12 or more monomers by disulphide bonds between the monomers. The oligomers can further associate via hydrophobic interactions to form larger polymers with soap-like micelle structures that containing around 30 monomers. κ -Casein can also interact with other caseins (Holland et al., 2008; Swaigood, 2003; Walstra & Jenness, 1984).

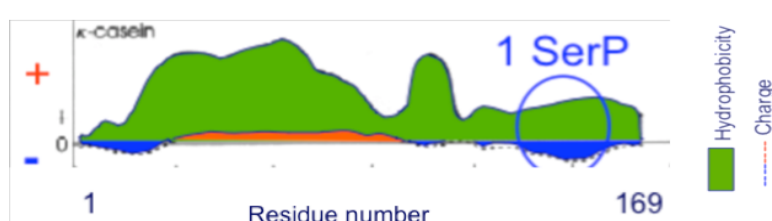


Figure 1.10 The distribution of hydrophobic residues and charge along the κ -casein protein chain, hydrophobic residues at N-terminus and C-terminus (green), 1 phosphoserine residue in the negatively charge region (blue).

1.2 Minerals and other components in milk

Milk contains organic and inorganic salts. The concentration of various principal mineral components in milk is shown in Table 1.3. Milk also contains trace amounts of minor elements (e.g. Zn, Fe, Mo, Cu, and Se) that are also important in a nutritional food. In milk, some of the minerals, in particular calcium and phosphate are partially distributed in the serum phase and partially associated with the casein micelles. The calcium and phosphate is referred to as colloidal calcium phosphate (CCP), when they are associated with the casein. The distribution of calcium and phosphate between the soluble and colloidal phases is strongly dependent on pH and temperature and it is also affected by milk concentration. Only ~34% of the

calcium and ~43% of the phosphate are soluble at the natural pH of milk (~pH 6.7) and at ~20°C. Calcium phosphate becomes more soluble at decreased milk pH or decreased temperature. All calcium and phosphate is soluble at pH 4.6 (Fox, 2009; Silva et al., 2001).

Table 1.3. The concentration of principal elements in milk (Fox, 2009).

	Concentration (mg/l)	Colloidal form (%)	Soluble form (%)	
Na	500	8	92	Completely ionized
K	1450	8	92	Completely ionized
Cl	1200	0	100	Completely ionized
S	100	0	100	Completely ionized
P (Inorganic)	750	57	43	10% bound to Ca^{2+} and Mg^{2+} 54% H_2PO_4^- 36% HPO_4^{2-}
Citr	1750	6	94	85% bound to Ca^{2+} and Mg^{2+} 15% Citr^{3-}
Ca	1200	66	34	35% Ca^{2+} 55% bound to citrate 10% bound to phosphate
Mg	130	33	67	Similar to calcium

In addition to water (86%), milk also contains lactose (about 4.75%) and lipids (milk fat, 5%) at high levels. Water in milk acts as a solvent for minerals, lactose and proteins; it affects the stability of milk and milk products (Fox, 2009). Lactose is the key carbohydrate in milk; it is a disaccharide of glucose and galactose (Figure 1.11). Lactose is a reducing sugar and involved in Maillard reactions during the heating/storage of milk products (Fox, 2009; Holsinger, 1997).

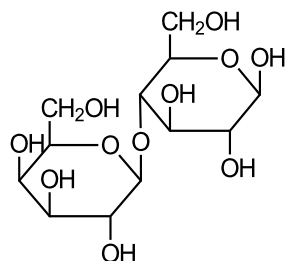


Figure 1.11 Structural formula of α -lactose.

Moreover, various different lipids exist in milk; the major lipid is triglyceride that accounts for about 98% of milk fat. Triglycerides contain three fatty acids that covalently bound to a glycerol molecule (Dewettinck et al., 2008). The triglycerides are present in fat globules and these globules are stabilized by a complex layer of protein and phospholipids. This complex layer is referred as the milk fat globule membrane (MFGM, Figure 1.12). The triglyceride core is surrounded by an inner monolayer of hydrophilic lipids; and a double layer of hydrophilic lipids surrounds the inner monolayer. The membrane proteins are distributed along the membrane and most of phospholipids and glycolipids are located on the outer layer of the membrane (Dewettinck et al., 2008). These polar lipids on the membrane maintain the milk fat globules stability as natural emulsifiers (Fox, 2009).

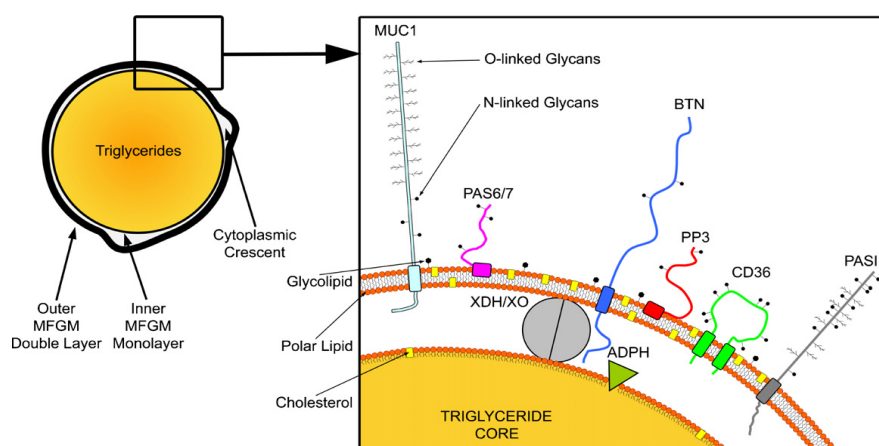


Figure 1.12 Structure of fat globules in milk (Dewettinck et al., 2008).

Milk also contains low but nutritionally significant levels of vitamins. Sufficient amounts of all the vitamins exist in milk, such as biotin (B_7), riboflavin (B_2),

cobalamine (B₁₂) and retinol (A); these are important for the normal maintenance for neonate.

1.2.1 Casein micelles

In milk, caseins are in the form of colloidal particles called 'casein micelles' with molecular weights ranging from 10⁶ to 10⁹ Da and diameters ranging from 50 to 500 nm. On a dry basis, casein micelles consist of 94% protein and 6% of mineral components, predominantly calcium phosphate. These mineral components associated with the casein micelles are CCP in the form of nanoclusters of about 2.5 nm in diameter, and these are uniformly distributed through the micelle. Casein micelles are highly hydrated, and contain 2-4 g H₂O/g protein (Fox, 2009; Huppertz et al., 2006). Casein micelles can be disrupted by addition of a strong calcium ion sequestrant (e.g. EDTA), addition of chemicals that disrupt hydrophobic interactions (e.g. urea), by dialysis against a phosphate-free buffer, or increasing the pH (Horne, 2009).

Several models of casein micelle structure have been proposed and have been extensively refined or developed as more information on the structure and interactions has become available. However, the exact structure of the casein micelle has not been unequivocally established. Two principal categories of casein micelle models have been proposed, which are sub-micelle models and non-sub-micelle models.

Sub-micelle models

Sub-micelle models of the casein micelle structure were initially proposed after electron microscopy showed an irregular distribution of caseins in the casein micelles (Slattery & Evard, 1973). The most widely accepted sub-micelle model was developed by Schmidt (1982), and refined by Walstra (1990). In this model, the casein micelle contains 2 types of sub-micelle and each sub-micelle is around 8-20 nm in diameter. One type of sub-micelle consists of α_{s1} -, α_{s2} -, and β -caseins and with

high levels of κ -caseins and one type of sub-micelle consists of α_{s1} -, α_{s2} -, and β -caseins but with low levels of κ -caseins. The sub-micelles are held together via hydrophobic interactions forming a hydrophobic core (Figure 1.13 A). Sub-micelles with low levels of κ -caseins are located in the centre of the casein micelle, whereas sub-micelles with high levels of κ -caseins are located at the surface of the casein micelle. The sub-micelles are linked via interactions between CCP and phosphoserine clusters of caseins to form a casein micelle (Figure 1.13 B and 1.14). As κ -casein does not contain a high level of serine phosphates, it cannot link sub-micelles. Therefore the size of casein micelle does not grow when its surface is fully covered by κ -casein rich sub-micelles (De Kruif et al., 2012; Schmidt, 1982).

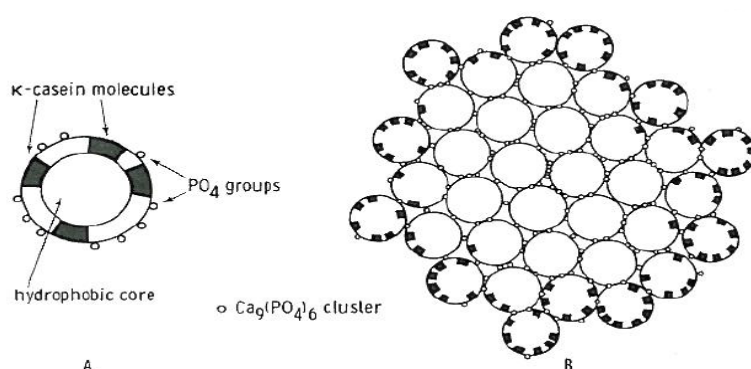


Figure 1.13 Casein sub-micelle structure. A. A sub-micelle with the hydrophobic core; B. Casein micelle consisting of numerous sub-micelles (Schmidt, 1982).

In the casein sub-micelle model, CCP play an important role in linking the sub-micelles together. It was proposed that CCP is formed as an amorphous calcium phosphate structure, with the serine phosphates of the caseins being incorporated as part of the calcium phosphate structure. CCP and the phosphoserine residues of caseins are negatively charged, and they link to each other via binding with positively charged calcium ions (Schmidt, 1982).

A hairy casein micelle model was proposed by Walstra (1990). This model was similar to the original sub-micelle model (Schmidt, 1982) apart from the hairy layer structure. In this model, the surface of micelles was covered by κ -casein. The hydrophobic region of κ -casein is associated with the casein micelle core, and the

highly charged hydrophilic region sticks out from the micelle surface into the serum and forms the 'hairy layer' (Figure 1.14; Walstra, 1990). κ -Caseins on the surface of casein micelles stabilize the casein micelles against coagulation by predominantly steric repulsion, although electrostatic effects may also play a role. The negative charge on the hydrophilic regions of κ -caseins contributes to an electrostatic repulsion, which causes the hydrophilic regions of κ -caseins to stretch out from the surface of the micelle. When two casein micelles approach one another, the hydrophilic regions of κ -caseins are restricted in movement due to the volume restriction which leads to repulsion. The resulting repulsion will occur if the interaction between the hydrophilic regions of κ -caseins and solvent is favoured; if this interaction is not favoured, attraction will occur between the casein micelles (Holt & Horne, 1996; Walstra, 1990).

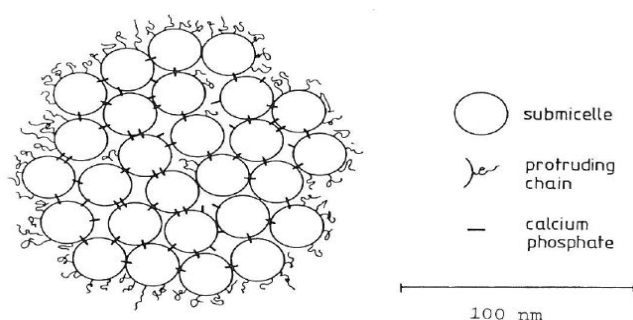


Figure 1.14 Hairy casein sub-micelle structure (Walstra, 1990).

In the original Schmidt/Walstra casein sub-micelle models (Figure 1.13 and 1.14), it was proposed that CCP linked sub micelles together and therefore would be found at the periphery of the submicelles and not uniformly distributed throughout the micelle (Knoop et al., 1973; Holt et al., 1986). However, recent studies suggested that the CCP was uniformly distributed throughout the casein micelles. To accommodate this finding, the hairy casein micelle structure was modified by Walstra (1999). In this model, the CCP is distributed throughout the sub-micelles, and the sub-micelles are linked together via hydrophobic interactions rather than through CCP (Figure 1.15). The electrostatic repulsion within sub-micelles is reduced by the CCP neutralizing the charges of the serine phosphates of the caseins within the sub-micelles. Therefore, the sub-micelles shrink and these submicelles are

hydrophobically linked together to form casein micelles (Walstra, 1999).

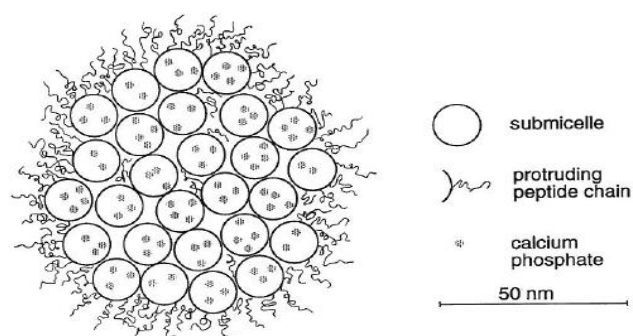
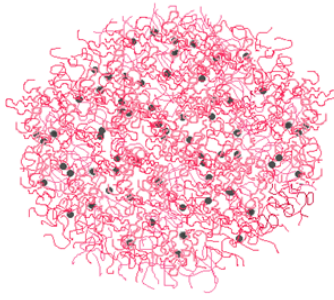


Figure 1.15 Modified hairy casein sub-micelle structure (Walstra, 1999).

However, the sub-micelles were not observed from transmission electron micrograph (TEM) analysis with newly developed cryopreparation methods (McMahon & McManus, 1998). The casein micelles were proposed to be intact after the cryopreparation. It is also questionable why there are 2 types of sub-micelles: κ -casein rich sub-micelle and κ -casein poor sub-micelle rather than only one type of sub-micelle containing a mixture of all the casein proteins (Horne, 2006). Therefore, sub-micelle models become less acceptable and these evolved to non-sub-micelle models.

Non sub-micelle models

The first non-submicellar model of casein micelle was proposed by Holt (1992) and has been referred to as the nano-cluster model. In the model, the CCP is in the form of nanoclusters and these nanoclusters have a dominant role in determining the structure and size of the casein micelles. The nanoclusters of CCP are randomly distributed throughout the casein micelle, binding to the phosphoserine of α_{s1} , α_{s2} , and β -caseins and cross-linking them to form a three-dimensional network of casein molecules (Figure 1.16). The κ -caseins are located on the surface of the casein micelles (De Kruif, 2003; Holt, 1992; Horne, 2006).



Holt

Figure 1.16 Casein nanocluster structure (Holt, 1992).

However, the nano-cluster model did not have a specific role for κ -caseins or a rationale for how κ -caseins locate on the surface of the casein micelles to control the micelle size; it relied only on the CCP to hold the micelle together and control the growth of casein micelles.

The dual-binding model has been developed by Horne (1998), which has a role for κ -casein and hydrophobic interactions. In the dual-binding model of the casein micelle, caseins are described in loop/train models where the loop represents the hydrophilic region and the train represents the hydrophobic region. α_{s1} -, α_{s2} -, β - and κ -Caseins are amphiphilic and they contain hydrophobic regions that are separated from hydrophilic and highly charged regions. Only α_{s1} -, α_{s2} - and β -caseins contain clusters of phosphoserines in the charged regions; these clusters of phosphoserines can bind high levels of calcium ions/calcium phosphate. In the dual-binding model of the casein micelle structure, casein molecules are cross-linked via two types of bonding: hydrophobic interactions where hydrophobic regions of caseins interact with each other, and calcium phosphate bridging where the CCP bridges the caseins through their serine phosphate groups. κ -Casein can only interact with other caseins through its hydrophobic regions. The hydrophilic region of κ -casein does not contain phosphoserine clusters and it cannot extend the association via calcium phosphate bridging. Therefore, κ -casein terminates the growth of casein micelles, as it cannot continue growth through CCP, and this builds up a casein micelle with κ -casein at the surface (Figure 1.17; Horne, 1998, 2009).

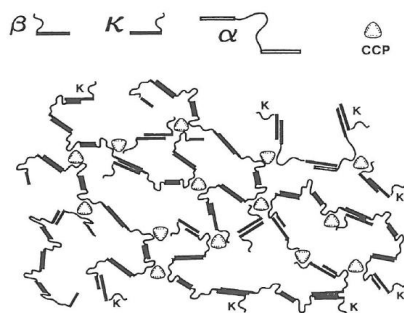


Figure 1.17 Casein dual-binding structure (Horne, 1998).

The dual-binding model only described how the caseins bind together. However, the ability of β -casein to diffuse in and out, and the high hydration of the casein micelles are not understood. In addition, it does not explain the ability of small molecules such as denatured whey protein to interact with the micelle surface and the ability of large molecules such as other casein micelles to be repelled. Hence the Dalglish model was developed to overcome the limitations of dual-binding model.

In 2011, Dalglish proposed a new casein micelle, which has unevenly distributed κ -caseins on the micelle surface and specific role of free β -casein (Figure 1.18). Overall, in this model, the interactions involved in casein associations are the same as in the dual-binding model, in which α_{s1} , α_{s2} caseins and part of the β -caseins are cross-linked together via the interaction between the nanoclusters of CCP and phosphoserine clusters of the caseins. Strands formed from CCP/casein nanoclusters and water channels form the internal structure of the micelle as a bicontinuous system. In this model, β -casein is mainly in the micellar interior. Some β -caseins hydrophobically bind to other caseins and the hydrophilic regions of β -caseins remain in the water channel; these caseins are named free β -casein. The distribution of water channels results in extensive hydration of the micelles. However, non-polar regions of β -casein possess significant hydrophobic character, which is incompatible with β -casein being highly hydrated. Therefore, this leads to water channels unevenly distributed throughout the micellar interior.

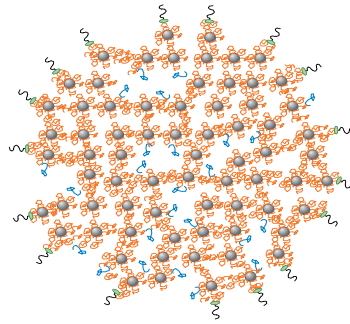


Figure 1.18 Schematic structure of the casein micelle, incorporating calcium phosphate nanoclusters (grey) with their attached caseins (orange) and the surface-located κ -casein (para- κ -casein: the hydrophobic region of κ -casein, green; caseinomacropeptide chains: the hydrophilic region of κ -casein, black). The “hydrophobically bound” mobile β -casein is shown in blue, within the water channels inside the micelle (Dalgleish & Corredig, 2012).

β -Casein and other small protein molecules can diffuse through the micellar interiors, which is dependent on the temperature. When milk is cooled down to 4°C at its natural pH, β -casein can be present as monomers and diffuse out from the casein micelles and therefore result in extensive dissociation of the micelles; removing the dissociated β -casein or recooling does not lead to further dissociation of β -casein. However, increasing the temperature of milk to 37°C, or even to room temperature, the free β -casein diffuses in to the casein micelles and reassembles via hydrophobic binding.

κ -Casein also plays an important role in stabilizing the casein micelle structure, it is unevenly attached on the surface of the casein micelles via hydrophobic binding (Dalgleish, 2011). The uneven distribution of κ -casein leads to clefts or pores on the surface of the micelles, which allows small molecules such as denatured whey proteins to reach the surface/interior of micelles. Denatured whey proteins can be attached to the cysteine residues of κ -casein that is buried close to the surface of micelle. However, when large molecules such as other casein micelles approach the micelles, the hairy layer of κ -casein will deny access of the large molecules to the interior of the micelle via steric repulsion mainly, and therefore stabilize the casein micelle structure (Dalgleish, 2011).

1.3 Protein modifications

Milk protein modifications can be accomplished by chemical, enzymatic or physical approaches. Chemical modifications such as acetylation, succinylation, glycosylation and phosphorylation can modify the structure and functionalities of milk proteins. Enzyme-catalysed modifications result in proteolytic hydrolysis, protein cross-linking or specific changes to functional groups attached to the proteins. Physical modifications mainly include heat treatment and polymer complexing (Kester & Richardson, 1984). These modifications can manipulate the surface charge, apparent pI, surface hydrophobicity, size and shape of the proteins, and enhance or alter the functional properties of proteins (Morand et al., 2011a).

In order to understand the impact of the casein interactions on the functionalities of proteins, the casein interactions will be altered by using different modification approaches. In this review, dephosphorylation, succinylation and TGA modification approaches were highlighted as these three modifications have been reported to have a significant impact on the physicochemical properties and functionalities of dairy proteins (Meyer et al., 1981; Morand et al., 2011a; Tang et al., 2005b).

1.4 Protein modifications catalysed by phosphatases

Enzymatic dephosphorylation can modify the physicochemical properties of caseins by removing the phosphate groups from serine residues (Molina et al., 2007). Dephosphorylation can decrease the net negative charge and the calcium ion binding ability of the caseins, as well as increasing the hydrophobicity of proteins (Meyer et al., 1981; Yeung et al., 2001). Consequently, dephosphorylation also changes the solubility, foaming ability, emulsion stability and calcium ion sensitivity of whole casein proteins (Darewicz et al., 1999).

The dephosphorylation of protein can be achieved by both chemical and enzymatic modifications. A fast and simplified chemical dephosphorylation method employs

hydrofluoric acid or hydrogen fluoride-pyridine (Kuyama et al., 2003). Alkali-induced dephosphorylation of β -casein, by dilute aqueous solutions of sodium hydroxide has been studied (Manson & Carolan, 1972). However, chemical modifications of protein are not generally acceptable in food systems. Enzymatic dephosphorylations of protein by alkaline and acid phosphatases which are commercially available have been studied and provided better solubility and emulsion stability of milk protein (Darewicz, et al., 1999). The figure of enzymatic dephosphorylation reaction is in Section 3.1.

1.4.1 Phosphatases

Both alkaline and acid phosphatases exist in bovine milk. Milk acid phosphatase is active on the phosphoserine residues of casein and is stable under heat conditions (Shahani, 1966). Milk alkaline phosphatase can be destroyed by pasteurization and has very low activity in milk (Lorient & Linden, 1976). Acid phosphatase has a high enzymatic activity that can affect rennet coagulation and syneresis during cheese making (Pearse et al., 1986). It has also shown proteolytic activity that can result in the formation of hydrophobic peptides. However, there was no noticeable proteolysis observed in dephosphorylation by alkaline phosphatase (Darewicz et al., 1999; Lorenzen & Reimerdes, 1992; Molina et al., 2007; Pepper & Thompson, 1963). In comparison, alkaline phosphatase has contributed to better creaming stability of dephosphorylated α_s - and β -casein than acid phosphatase, at the same degree of dephosphorylation (Lorenzen & Reimerdes, 1992). Therefore, alkaline phosphatase has been commonly used for milk protein dephosphorylation in order to avoid the proteolysis of milk protein (Darewicz et al., 1999; Darewicz et al., 2000; Koudelka et al., 2009; Lichan & Nakai, 1989; Lorenzen & Reimerdes, 1992; Molina et al., 2007; Pearse et al., 1986; Pepper & Thompson, 1963).

The pH for optimum activity of general bovine alkaline phosphatase is dependent on the substrate, such as pH 8.6 for phosphoserine, pH 6.8 for micellar casein and whole casein at 40°C. In addition, alkaline phosphatase from calf intestine has its optimum activity at pH 8.0 for whole casein (Lorient & Linden, 1976). Lichan and

Nakai (1989) also reported that calf intestinal alkaline phosphatase can hydrolyse clustered phosphoserine residues, but its activity towards whole casein is low.

Different phosphatases can also attack their substrates in different ways (West & Towers, 1976). Alkaline phosphatase in the calf intestine has different properties of heat stability and chemical inhibition compared with the phosphatase in liver and spleen (Ashok et al., 2008). In a study by West & Towers (1976), a 1.4% solution of β -casein and the derived phosphopeptide from β -casein (consist of the first 25 residues of the protein chain, including the 4 phosphoseryl residues in the cluster) were incubated with different levels of bovine spleen phosphatase at pH 5.8 and/or *Escherichia coli* alkaline phosphatase at pH 8.0 (West & Towers, 1976). The cellulose acetate electrophoresis results showed that the dephosphorylation of both β -caseins and its derived peptides by bovine spleen phosphatase proceeded in a sequential manner and all the organic phosphate groups were substrates for the enzymatic reaction. The dephosphorylation of both samples was completed well within the incubation time of 24 hours, which was established by measuring the amount of released inorganic phosphate.

Escherichia coli alkaline phosphatase dephosphorylated both β -casein and its derived peptides in an organized manner, with 2 of the 5 phosphate groups being removed at pH 8.0, which is similar to the samples treated with bovine spleen phosphatase. However, the remaining 3 phosphate groups were resistant to attack by the enzyme. When the incubation time was increased to 24 hours, the dephosphorylation of both samples treated with *Escherichia coli* alkaline phosphatase was not completed. When the pH was decreased to pH 5.8, the derived peptide was completely dephosphorylated. Therefore, hydrolysis of three phosphate groups from the derived peptide that were resistant to enzymatic attack could be removed by lowering the pH (West & Towers, 1976). However, which phosphate group from the substrates was resistant to attack by *Escherichia coli* alkaline phosphatase and the mechanisms of the resistance is not yet clear.

In order to achieve a desired degree of dephosphorylation, several inhibitors of phosphatase can also be used to control the enzymatic activity. Studies have shown that a Na_2WO_4 solution can be used to inhibit intestinal alkaline phosphatase (Yeung et al., 2001). Trichloroacetic acid (TCA) has been used to stop casein dephosphorylation by bovine alkaline phosphatase (Lorient & Linden, 1976) and/or by potato acid phosphatase (Molina et al., 2007). Addition of NaOH to alkaline pH 9-10 (Yoshikawa et al., 1974) or H_2SO_4 (West & Towers, 1976) has also been added to stop the dephosphorylation of β -casein treated by bovine spleen phosphatase. Heat treatment at 80°C for 5 minutes has also been commonly used to inhibit alkaline or acid phosphatase activity (Darewicz et al., 2000; Lorenzen & Reimerdes, 1992).

1.4.2 Dephosphorylation of protein fractions

The phosphate groups, which are removed during the enzyme-catalysed reaction, are dependent on the protein substrate, therefore, dephosphorylated groups have been studied in different casein fractions. Molina and co-workers observed random dephosphorylation occurring in both α - and β - casein when incubated with potato acid phosphatase at pH 5.8 (Molina et al., 2007). In the study, a 0.25% solution of whole casein, containing α -casein and β -casein, was incubated with potato acid phosphatase (96 U/g protein) at 37°C for 6 hours. The dephosphorylated samples were then analysed by Electrospray Ionization Mass Spectrometry (ESI-MS) and urea-PAGE. The results revealed that six phosphate groups of α -casein were successfully dephosphorylated, including phosphate groups 1, 2, 4, 6, 7 and 8 numbered from the amino terminus of the protein. It was also observed that phosphate groups 1 and 2 were lost in the incubated α - and β - casein control samples without phosphatase addition. The partial dephosphorylated α - and β -casein in control samples might be the result of the presence of natural phosphatase in the milk (Molina et al., 2007).

Phosphatase has lower activity on whole casein substrates than in individual casein fractions (Lichan & Nakai, 1989). It was observed that when casein protein solutions (2%) were incubated individually with the same amount of calf intestinal alkaline

phosphatase at 37°C, only 10% of phosphoserine residues were hydrolysed in whole casein after 60 minutes, while 50% of phosphoserine residues were dephosphorylated in both α_{s1} - and β -casein fractions after 30 minutes. The different hydrolysis rate may be due to the low accessibility of phosphoserines in whole casein protein (Lichan & Nakai, 1989). Moreover, it has been reported that dephosphorylation of whole casein was inhibited by the presence of whey protein, lactose and phosphate ions at pH 6.8 in the milk system; β -lg as an activator when the pH was above pH 8.0 (Lorient & Linden, 1976). In the study, casein proteins in a 25 mM borate buffer (containing 1 mM MgCl_2) and/or in an artificial milk system (mineral solution with a composition similar to ultrafiltrated milk, with the addition of varying amounts of whey protein and/or lactose and/or phosphate ions) was incubated with calf intestinal alkaline phosphatase (500 U/g protein) at 40°C for 2 hours. The degree of dephosphorylation was established by the amount of phosphate released in the supernatant after centrifugation. Results revealed that the artificial milk system (containing β -lactoglobulin and/or lactose and/or phosphate ions) was less favourable to dephosphorylation than the borate buffer solution at pH 6.8. Lorient and Linden (1976) proposed that the genetic variants of β -lactoglobulin might have different inhibitory effects on the alkaline phosphatase. It was also found that individual casein fractions were dephosphorylated more quickly than its mixtures (Lorient & Linden, 1976). The dephosphorylation rate decreased in the following order: individual casein > mixture of α_s -, β - and κ -caseins / micellar casein > mixture of α_s - and β -caseins.

Dephosphorylation of α_{s1} -casein reduced complex formation between α_{s1} -casein and κ -casein in the presence of calcium ions (Schmidt & Poll, 1989). In the study, artificial casein micelles were prepared from mixtures of native and/or dephosphorylated α_s -, β -, and κ - in a mass ratio of 3:3:1. Different levels of dephosphorylated α_s - and/or β - and/or κ -casein were achieved by incubation with potato acid phosphatase (for 15 minutes to 12 hours) with dialysis during the incubation. Lower turbidity and smaller particle sizes were observed in the samples with dephosphorylated α_{s1} -casein compared to the control samples without phosphatase treatment. The degree of dephosphorylation was estimated by measuring the phosphorus in the serum phase

after centrifugation of samples. The stability and size distribution of the casein micelles was estimated by turbidity measurement and by means of electron microscopy (Schmidt & Poll, 1989). Moreover, results revealed that phosphorylation of κ -casein reduced its ability to stabilize α_{s1} - and β -casein against precipitation by calcium ions. The capacity was regained when the phosphorylated κ -casein was subsequently dephosphorylated in the mixed system, which was analysed by turbidity and size distribution measurements (Schmidt & Poll, 1989).

Dephosphorylation of β -casein can protect α_{s1} -casein from precipitation in the presence of Ca^{2+} ions (Darewicz et al., 1999). 0.5% β -casein (intact and/or dephosphorylated) and 0.5% native α_{s1} -casein were dissolved in imidazole buffer (pH 7) with the addition of Ca^{2+} ions. There was a higher α_{s1} -casein content in the supernatant of the sample containing dephosphorylated β -casein than that containing intact β -casein, which was determined by PAGE and reversed phase high performance liquid chromatography (RP-HPLC) after centrifugation of the samples. It was concluded that dephosphorylated β -casein possessed the amphiphilic structure that can associate with native α_{s1} -casein, and thus protect α_{s1} -casein against calcium ion precipitation (Darewicz et al., 1999; Darewicz et al., 2000).

Both native α_s - and β -caseins can prevent α -lactalbumin (α -lac) from aggregation. However, the propensity to inhibit α -lac aggregation is significantly reduced by dephosphorylation of α_s - and/or β -caseins (Koudelka et al., 2009). In the study, 1% casein solutions (pH 7.8) were incubated with alkaline calf intestine phosphatase (125 U/g protein) at 37°C for 8 hours. During the incubation, the samples were dialyzed against ammonium bicarbonate buffer. The degree of dephosphorylation was established by measuring inorganic phosphate using a fluorescence spectrophotometer as well as analysis by MS combined with SDS-PAGE. The dephosphorylated caseins were separated on SDS first and then the separated fractions were extracted and analysed by MS. The native and/or dephosphorylated casein solutions with the addition of α -lac (in molar ratio 3:1) were incubated with a reducing agent 1,4-dithiothreitol (DTT) at 37°C for 6 hours to achieve aggregation of the α -lac. More precipitation in dephosphorylated α_s - and/or β -casein solutions

was observed in comparison to in native α_s - and/or β -casein solutions, which was analysed by a turbidity measurement. Therefore, dephosphorylation reduces the hydrophilicity of α_s - and β -caseins and decreases their ability to solubilize unfolded α -lac (Koudelka et al., 2009).

Dephosphorylation of β -casein also increased its solubility in the presence of Ca^{2+} ions in comparison to native β -casein (Yoshikaw et al., 1974). In this study β -casein (pH 5.8) was incubated with bovine spleen phosphatase at 35°C in the presence of CaCl_2 . Results showed that the amount of sediment in a dephosphorylated β -casein sample was higher than in a native β -casein sample, as measured by the PAGE method after centrifugation (Yoshikaw et al., 1974). This result is in agreement with Darewicz et al. (1999), who suggested that dephosphorylation of β -casein decreased the overall net negative charge of the N-terminus. As a result, the pI of dephosphorylated β -casein was increased to the neutral pH range and the solubility was also increased in acidic conditions. In the study, β -casein solution was incubated with potato acid phosphatase (50 U/g protein) at 20°C for 1 hour, followed by a heat treatment at 100°C for 5 minutes to terminate the interaction. The degree of phosphorylation was estimated by measuring inorganic phosphorous using a microscale colorimetric method and the pI was measured using isoelectrofocusing (IEF) analysis (Darewicz et al., 1999). During dephosphorylation, the hydrophilic phosphate groups from β -casein are removed, the hydrophilicity, electrostatic and steric repulsion between the dephosphorylated molecules is reduced, and consequently the interactions between protein and solvent decrease. In addition, the association of β -casein molecules in solution is decreased as the phosphate groups that can bind the Ca^{2+} are removed. Therefore, the micelle of β -casein is less likely to be formed and it is more soluble in the solution with the presence of Ca^{2+} ions (Darewicz et al., 1999).

1.4.3 Emulsion properties of dephosphorylated caseins

The degree of dephosphorylation is related to the stability of emulsions, prepared from the modified proteins (Lorenzen & Reimerdes, 1992). In this study, 1% α_s -

and/or β -casein solutions (pH 8.0) were incubated with acid or alkaline phosphatase (50 U/g protein). Both of the enzymes achieved rapid dephosphorylation in the first 8 hours of incubation time, which was measured by urea-PAGE. When the incubation time was increased to 24 hours, both samples were completely dephosphorylated by acid phosphatase. The samples were only partially dephosphorylated by alkaline phosphatase in 24 hours with a further incubation time needed (42 hours total) for complete dephosphorylation. The emulsifying properties of dephosphorylated samples were measured by a radio analytical method, which measures the time required for 50% creaming of o/w emulsions that were prepared using the treated samples. It was observed that samples dephosphorylated by acid phosphatase showed slightly better emulsifying properties than alkaline phosphatase at 24 hours. However, after complete dephosphorylation, the emulsifying properties of both α_s - and β -casein treated by alkaline phosphatase had increased 2-fold in comparison to both α_s - and β -casein treated by acid phosphatase. Therefore, the emulsifying properties of modified casein fractions can be related to the specificity of phosphatase used for incubation. Moreover, the dephosphorylation by alkaline phosphatase contributed to a 6-fold increase in α_s -casein creaming stability and a 10-fold increase in β -casein in comparison to samples without dephosphorylation treatment. Therefore, a higher degree of dephosphorylation contributed to a better stability of dephosphorylated β -casein, but this was also dependent on the type of enzyme used (Lorenzen & Reimerdes, 1992).

Darewicz et al. (2000) reported that dephosphorylation of β -casein and its peptide did not significantly affect the emulsifying properties. In the study, a 0.25% solution (pH 8.0) of intact β -casein and/or β -casein fragment (1-105/107) was incubated with alkaline phosphatase (2000 U/g protein) at 37°C for 24 hours. All the samples were completely dephosphorylated as measured by RP-HPLC combined with MS. The o/w emulsions containing 0.44% dephosphorylated β -casein and/or β -casein fragment were prepared in order to determine the effect of dephosphorylation on the emulsifying properties of β -casein. The foaming ability and stabilizing properties against coalescence of all samples was analysed by particle size distribution and by

measurement of the turbidity after homogenizing. The particle size results and turbidity measurements showed that there was no noticeable difference between dephosphorylated and native samples. This conclusion is in conflict with previous results reported by Lorenzen and Reimerdes (1992).

This conflicting result could be due to different experimental conditions and measuring methods. The creaming of dephosphorylated protein emulsions was measured in the previous study by Lorenzen & Reimerdes, (1992), while the particle sizes and turbidity of dephosphorylated protein emulsions were determined in the study by Darewicz et al. (2000). Moreover, it has also been observed that dephosphorylated β -casein showed an increased α -helix and decreased random coil structure when compared to native β -casein, which was measured by Far-UV Circular Dichroism (CD) (Darewicz et al., 2000). It has also been reported that partial dephosphorylation of β -casein significantly increased the formation of α -helix in both β -casein fragments (1-28) and (1-52) in the presence of trifluoroethanol (TFE) (Clark et al., 1992). The above two findings are in agreement with Koudelka et al. (2009), who reported that dephosphorylation increased the α -helix and β -sheet structure in both dephosphorylated α_s - and β -casein. β -Casein is the best emulsifier of the caseins and it can stabilize emulsion droplets before coalescence occurs due to its fast adsorption at the o/w interface (Dalgleish, 1996). Its secondary structure can be changed when the protein is adsorbed onto the o/w interface in a emulsion (Maste et al., 1997). Thus, in this experiment, the native and/or dephosphorylated protein solutions were loaded and absorbed on Teflon lattices to mimic the protein-adsorbed state of o/w emulsions. The Teflon lattices were centrifuged off and the secondary structure of proteins was analysed by CD. In the absorbed state, the secondary structure of dephosphorylated β -casein and its peptide had increased in comparison to native β -casein and its peptide. However, the change in secondary structure did not correlate with its emulsifying properties (Darewicz et al., 2000).

1.4.4 Phosphorylation

Phosphorylation of proteins can be achieved by covalent binding with chemical reagents such as phosphorus oxychloride, sodium trimetaphosphate, phosphorus pentoxide dissolved in phosphoric acid, phosphoramidate, and phosphoric acid combined with trichloroacetonitrile (Kester & Richardson, 1984). Chemical phosphorylation of soy protein isolate with sodium trimetaphosphate generated the derivatization of the hydroxyl oxygen of serine residues and the amino groups of lysine residues, which showed improved solubility, water-holding capacity and emulsifying capacity of soy proteins (Sung et al., 2006). Emulsions prepared with the phosphorylated β -lactoglobulin were more stable at pH 5 and pH 7 when compared with emulsions prepared with native β -lactoglobulin (Woo & Richardson, 1983). Campbell et al. (1992) also proposed that phosphorylated soy protein showed enhanced solubility and emulsifying property over a pH range of 3-6, but with lower foam stability.

Chemical phosphorylation of caseins with phosphorus oxychloride results in crosslink formation within the protein structure, which might be attributed to phosphate bridges or isopeptide linkages. The phosphorylated caseins showed an increase in water absorption properties; however, their solubility was decreased (Matheis et al., 1983). Chemical superphosphorylated whole bovine caseins at pH 5 had improved foam stability but decreased solubility and emulsion stability than the controls (Van Hekken et al., 1996; Van Hekken & Strange, 1997). Therefore, the degree of phosphorylation needs to be controlled to achieve the improved functionalities.

The change in physicochemical properties of phosphorylated bovine caseins is dependent on the pH of phosphorylation of caseins, covalent bonds between phosphate groups and formation of different specific amino acids (Medina et al., 1992). The solubility of phosphorylated caseins was increased near the isoelectric point (pH 4.6) and decreased at alkaline and acidic pH in the presence of Ca^{2+} when compared with unmodified caseins (Medina et al., 1992). This is in agreement with Nayak et al. (2006) who reported that in the presence of Ca^{2+} , the phosphorylated

caseins from buffalo milk had lower solubility than native caseins (used as the control) at pH 3, while they had higher solubility than the control around pH 4.6. However, the solubility of phosphorylated caseins was decreased when calcium ion concentration was increased at pH 4.6. Therefore, phosphorylation could shift the isoionic point of caseins towards acidic pH (Nayak et al., 2006).

1.5 Protein modifications catalysed by transglutaminase

1.5.1 Transglutaminase

Transglutaminase (TGA) has been extensively studied as a processing aid for food protein modification. It naturally exists in animal tissues and bodily fluids, plays a key role in blood-clot formation, and it has also been discovered in plants and microorganisms (Motoki & Seguro, 1998). Both microbial TGA and GTGA (from guinea pig liver) have been commercialized. The enzymatic activity of GTGA is dependent on the presence of Ca^{2+} , while microbial TGA is Ca^{2+} -independent (Jaros et al., 2006). Microbial TGA is most commonly used in food systems, such as meat, fish products (Hwang, 2004), bakery (Gerrard & Sutton, 2005; Schuster et al., 2002) and dairy products (e.g. cheese and yogurt) (Han & Spradlin, 2000; Jaros et al., 2006). It has been proposed that transglutaminase may act with gliadin proteins in dough to produce an epitope that is associated with coeliac disease (Gerrard & Sutton, 2005). However, this risk is specific to bakery products.

Microbial TGA is a monomeric enzyme containing 331 amino acids in a single polypeptide chain, and its secondary structure consists of 8 β -sheets and 11 α -helices (Kanaji et al., 1993). Microbial TGA has an isoelectric point of approximately 8.9 and a molecular weight of 38,000 to 40,000 Da. The optimum pH and temperature for TGA activity is pH 5 to 8, and 50°C, respectively. TGA is active at the freezing point of water and at temperatures up to 70°C. However, heat treatment (~85°C) and N-ethylmaleimide (NEM) can inhibit enzyme activity by blocking the sulfhydryl group of cysteine 64 in the enzyme's active site (Motoki & Seguro, 1998).

1.5.2 Transglutaminase-catalysed reactions

TGA can induce protein modification by deamidation, acyl-transfer and enzymatic cross-linking of the protein side chains. The enhancement of protein functionality in food systems has generally been attributed to the cross-linking reaction (Hiller & Lorenzen, 2009), but other activities may also alter functionality (Hamada & Swanson, 1994b; Yasir et al., 2007) and need systematic investigation. TGA catalyses an acyl-transfer reaction between the γ -carboxamide group of a protein-bound glutamine (acyl donor) and various primary amines (acyl acceptors) to form both inter- and intra-molecular isopeptide bonds (Boenisch et al., 2008). The intermolecular crosslinks are formed between proteins, while the intramolecular crosslinks are formed within a protein (Gerrard, 2002). ϵ -N-(γ -Glutamyl)lysine crosslinks are formed by the TGA-catalysed reaction between a γ -carboxamide group and the ϵ -amino group of a lysine residue (Jaros et al., 2010; Singh, 1991). However, when amine groups are absent, water molecules can act as the acyl acceptors, yielding the deamidation of glutamine residues (Ikura et al., 1992; Motoki & Seguro, 1998). TGA-induced reactions are described in more detail in Section 7.1.

1.5.3 Transglutaminase in whey proteins

TGA-induced crosslinking is dependent on the macromolecular structure of the protein substrate. For example, casein crosslinking catalysed by TGA is a more favourable reaction than that of native whey protein in a milk system. However, when whey protein is denatured by heat treatment or a reducing agent, its globular structure is denatured, which allows casein-whey protein and/or whey-whey protein crosslinking (Ikura et al., 1984; Nonaka et al., 1989; Traore & Meunier, 1992). The reduced whey proteins have glutamine and lysine residues, which have better accessibility to the TGA active site. SDS-PAGE results showed that there were more crosslinks formed when whey proteins were treated with dithiothreitol (DDT) or heated at 90°C compared to untreated whey proteins (De Jong & Koppelman, 2002).

The amount of TGA enzyme added and the time for which it is incubated with the substrate can also have significant effects on the functionality of the resulting modified proteins. Some studies have shown that moderate TGA treatment will diminish the thermal stability of β -lg, while extensive TGA treatment led to a significant increase (Tang & Ma, 2007). In the study by Tang and Ma (2007), β -lg solutions were incubated with TGA at 37°C. After incubation, the TGA was inactivated by heating at 75°C for 15 minutes, and then soluble aggregates in the heat-treated solutions were measured by size-exclusion chromatography combined with on-line multi-angle laser light scattering and UV detection. Sharma et al. (2001) proposed that the primary TGA reaction occurring in the first 30 minutes was dominated by crosslinking, while amine incorporation and/or deamidation were more dominant after 30 minutes. After incubation of skim milk with TGA at 40°C at different times, the total TGA-catalysed reactions were analysed by monitoring the levels of ammonia released using the Boehringer Mannheim Ammonia Kit colorimetric assay, while TGA-induced ϵ -N-(γ -glutamyl)lysine crosslinking was established by detection of amino acids after proteolysis using ion-exchange-chromatography. The results showed that the amount of ammonia released during the first 30 minutes of incubation was similar to the amount of ϵ -N-(γ -glutamyl)lysine. However, the amount of ϵ -N-(γ -glutamyl)lysine had little or no change after 30 minutes, while the amount of ammonia had significantly increased. Therefore, an increased amount of ammonia was released from TGA-catalysed non-crosslinking reactions (Sharma et al., 2001).

Other studies showed that treatment with TGA increased the surface hydrophobicity of both whey protein concentrate and sodium caseinate (Tang & Jiang, 2007). Proteins were dissolved in Tris-HCl buffer (pH 8.0) containing glycerol and incubated with TGA at 37°C for different times, then heated at 80°C for 30 minutes to inactivate TGA; all the treated samples were cast onto levelled glass plates covered with polyethylene films and air-dried at room temperature for 24 h to form protein films. The films were peeled off the plates and then analysed by surface angle measurement. The contact angle between the protein film surface and the water droplet was measured. TGA treated samples had a higher contact angle and a higher

contact angle values indicated higher surface hydrophobicity (Tang & Jiang, 2007).

1.5.4 Transglutaminase in casein proteins

The formation of α -casein and/or β -casein crosslinks catalysed by TGA can prevent κ -casein dissociation from the micelle, even under conditions that would usually destroy their integrity (Anema & de Kruif, 2012; Huppertz & de Kruif, 2007a; Huppertz & G de Kruif, 2007; Huppertz et al., 2007; Huppertz & de Kruif, 2008; Moon et al., 2009; O'Sullivan et al., 2002a; O'Sullivan et al., 2002b; Smiddy et al., 2006). Thus, TGA treatment increases the stability of casein micelles. It has been suggested that β -casein has better accessibility to TGA than α -casein in UHT-treated milk. β -Casein is primarily located in the outer space of the casein micelle structure when compared with α -casein, which is mainly located in the centre, thus an isopeptide network is formed in the outer β -casein rich "layer" of the micelle structure (Partschfeld et al., 2009). However, Tang et al. (2005a) have reported that the accessibility of sodium caseinate protein fractions to TGA decreased in the following order: κ -casein > α -casein > β -casein. In this study, sodium caseinate solutions were incubated with TGA at 37°C. After incubation, the degree of protein polymerization was analysed by SDS-PAGE (Figure 1.19) and size-exclusion HPLC (Tang et al., 2005a). The conflicting results from these studies indicate that the accessibility of protein fractions to TGA can be affected by the structure of the proteins, the availability of the reactive groups and their surrounding residues (Jaros et al., 2006). Bonisch et al. (2004) found that TGA had a higher activity towards sodium caseinate than native casein micelles in a milk serum system; native casein micelles showed higher capacity for cross-linking when dissolved in distilled water than in milk serum. All the solutions were incubated with TGA at 40°C for different times and analysed by the degree of polymerization using size exclusion chromatography. These results were in agreement with Jaros' hypothesis that the structure of proteins and their surrounding residues can affect the accessibility of protein fractions to TGA. However, when casein micelles in milk serum solutions were heated at 140°C for 20 seconds before treatment with TGA, the casein cross-linking significantly increased

in comparison to the unheated sample. Therefore, it has been suggested that the presence of a TGA inhibitor in milk serum decreased the formation of casein micelle cross-link and the inhibitor can be inactivated by heat treatment (Bonisch et al., 2004).

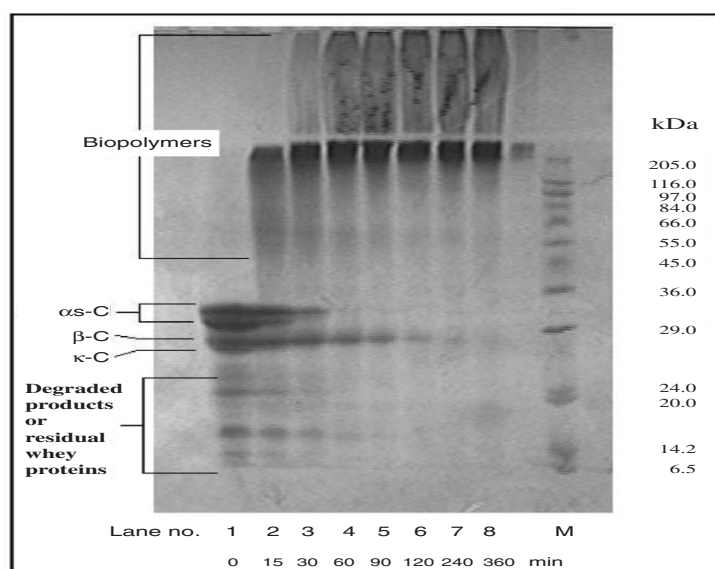


Figure 1.19 Reduced SDS-PAGE profiles of sodium caseinate and its different biopolymers induced by TGA. Lanes 1–8 are sodium caseinate samples incubated with TGA for 0, 15, 30, 60, 90, 120, 240 and 360 min at 37°C, respectively. Lane M indicates standard protein markers. Biopolymers indicate dimer, trimer and polymers (Tang et al., 2005a).

TGA-catalysed intermolecular cross-linking can lead to formation of protein oligomers and/or polymers, which can also affect protein functionality (Hiller & Lorenzen, 2009). Protein oligomerization has been examined in a 5% sodium caseinate solution incubated with TGA at 40°C for different times, and analysed by spontaneous SDS-PAGE. It was observed that casein oligomerization increased significantly during the first 60 minutes, which also corresponded with an increase in gel firmness measured by a penetration test; additional incubation time (~150 minutes) did not further increase oligomerization, therefore, the formed oligomers might bind with water to form a stable network (Hiller & Lorenzen, 2009; Jaros et al., 2010). It has also been found that excessive cross-linking leads to the formation of large oligomers, which inhibit uniform development of protein gels (Jaros et al., 2010). This is in agreement with other research, which suggests that, in comparison

to untreated reference protein gels, prolonged incubation of β -casein or whey protein with TGA resulted in weaker protein gels (DeJong & Koppelman, 2006; Eissa & Khan, 2005).

Faergemand et al. (1998) reported that limited TGA-induced cross-linking increased the overall stability of milk protein emulsions by preventing their coalescence, whereas extensive cross-linking reduced coalescence stability. In this study, sodium caseinate or β -lg was added to an oil-in-water emulsion followed by incubation with TGA. After incubation, all the samples and control samples without TGA were analysed by SDS-PAGE and a Malvern Mastersizer to detect protein cross-linking and droplet size. It was observed that the average droplet size was more stable in crosslinked emulsions than control emulsions. Therefore, TGA could be a means of improving emulsifying properties in milk or milk products.

1.6 Succinylation

Succinylation with succinic anhydride is a common chemical modification used in food protein applications. Succinylation of proteins decreases the pI by converting the amino groups of the lysine residues into carboxyl groups, thereby increasing the negative charge (Morand et al., 2011b). Thus, the electrostatic repulsive forces can lead to more extensive unfolding of the polypeptide chain, which enables water molecules to penetrate the partially unfolded protein structure (Kester & Richardson, 1984). Succinylation is described in more detail in Section 5.1.

1.6.1 Succinylation of whey proteins and other food proteins

Varying degrees of succinylation (32%-64% succinylated lysine residues) of whey protein complexes were generated by controlling the concentration of succinic anhydride in the protein solutions, the zeta potential results showed a shift in pI of the whey protein complexes from pH 4.9 to pH 3.8 (Morand et al., 2011b). In their study, the succinylated lysine residues of whey proteins were identified by mass

spectrometry and the level of succinylated lysine residues was determined using the *o*-phthaldialdehyde colorimetric assay. A small change was observed in secondary structure and surface hydrophobicity of the succinylated whey protein complexes, that were determined using a fourier transform infra-red (FTIR) spectrometer and the 6-propionyl-2-(*N,N*-dimethylamino)-naphthalene (PRODAN) probe, respectively (Morand et al., 2011b).

In a protein succinylation study by Yang et al. (2015), about a 10% increase in the β -sheet content was observed in 82% succinylated yak casein micelles compared to native yak casein micelles, which was measured using a FTIR spectrometer. The same effect of a high level of succinylation on the level of secondary structure was also found in other proteins measured using CD spectrometer. Batra et al. (1990) reported that 97% succinylation of ovalbumin led to an increase in the level of β -sheet (~8%) and a reduction in the level of α -helix (~14%), the random coil structure was relatively unchanged.

Moreover, a high level of succinylation has been reported to decrease the surface hydrophobicity of proteins (Shilpashree et al., 2015; Yang et al., 2015). In their study, 82% succinylated yak casein micelles and 96% succinylated sodium caseinate at pH 7.0 showed a large reduction in the surface hydrophobicity in comparison to unmodified proteins, which was measured using 1-anilinonaphthalene-8-sulphonic acid (ANS) fluorescence probe technique. It also has been reported that the surface hydrophobicity of canola protein isolate at pH 7.0 decreased as the level of succinylation increased (Paulson & Tung, 1987).

Succinylation had a significant impact on whey protein conformation and the resulting functional properties of the protein (Kester & Richardson, 1984). In their study, it was found that succinylation of 77% of the available amino groups resulted in increased solubility, emulsion properties and water-holding capacities of heat denatured acid whey proteins. It has also been observed that succinylated oat protein isolate had a higher water-binding capacity than native oat proteins (Mirmoghtadaie et al., 2009). However, in their studies, the water-binding capacity

of succinylated proteins was measured using a centrifugation method that compares the weight difference of protein sediment (Kester & Richardson, 1984; Mirmoghtadaie et al., 2009). This measurement is lacking in accuracy due to proper separation of the sediment from the supernatant; therefore, a more advanced technique is required to establish the water binding capacity.

Succinylation had a significant effect on the functionalities of food proteins (Franzen & Kinsella, 1976; Kim & Kinsella, 1986; Mirmoghtadaie et al., 2009; Paulson & Tung, 1987). The viscosity of succinylated soy protein was found to increase with increasing level of succinylation (Franzen & Kinsella, 1976; Kim & Kinsella, 1986). On the other hand, succinylation enhanced solubility and emulsifying properties of oat protein isolate, but decreased foaming capacity (Mirmoghtadaie et al., 2009). In the study, succinylated oat protein (0.4% w/v, pH 7) stabilized emulsions were made with 25% (v/v) soybean oil. The absorbance of the emulsion was determined at 500 nm at room temperature. After the emulsion had formed, the emulsion stability was examined by measuring the half-life of the turbidity. The foam capacity of oat protein solution (3% w/v, pH 7) was determined by measuring the overall volumes of foam at 0, 10, 30, 60 and 120 min after mixing. However, the level of succinylation of oat protein was not determined in the study. The reduction in the foam stability was also observed in succinylated soy protein and flax protein (Franzen & Kinsella, 1976; Wanasundara & Shahidi, 1997).

1.6.2 Succinylation of casein proteins

Although the effect of succinylation on the physicochemical and functional properties of whey and other food proteins has been intensely studied, there are limited reports on effect of succinylation on the physicochemical and functional properties of casein proteins. Shilpashree et al. (2015) reported that succinylation decreased the surface hydrophobicity and enhanced the solubility, viscosity and emulsifying properties of sodium caseinate. In their study, 64% to 99% of succinylated sodium caseinate were generated, and emulsions were prepared with 0.8% (w/v) of succinylated proteins and 20% (v/v) soybean oil. After mixing the

emulsions, the emulsions were centrifuged and the height of emulsified layer in the tube was measured at room temperature as the emulsifying property index. The foam capacity and foam stability of these succinylated sodium caseinate were also determined. The protein foam was generated by whipping 100 mL of 3% (w/v) succinylated protein solutions in 0.05 M phosphate buffer (pH 7) (Shilpashree et al., 2015). The volume of foam obtained immediately after whipping was measured as the foam capacity index. Foam stability was examined as the volume of foam that remained after 30 min expressed as a percentage of the initial foam volume. The results showed that the foam stability of sodium caseinate decreased with increasing the level of succinylation, but the foam capacity of succinylated sodium caseinate did not have a noticeable change in comparison to native sodium caseinate.

1.7 Other protein modifications

1.7.1 Acetylation

Acetylation of proteins with acid anhydrides acetylates the amino groups of lysine residues (Figure 1.20). Acetylation with acetic anhydride attaches the neutral acetyl groups to the amino group of the protein. Therefore, the electrostatic attraction between oppositely charged amino acid residues is decreased, which leads to a partial unfolding of the protein backbone. Acetylation improved the aqueous solubility and reduced the isoelectric point of proteins (Kester & Richardson, 1984). However, acetylation has a much lower impact on protein conformation and the resulting functional properties of the protein, compared to succinylation (Kester & Richardson, 1984).

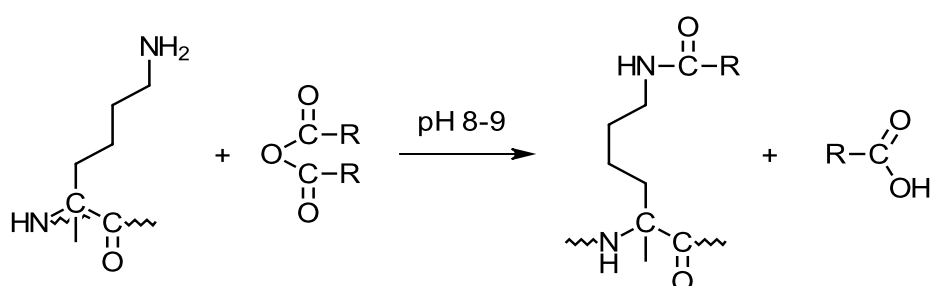


Figure 1.20 Schematic diagram of the acetylation reaction (Morand et al., 2012).

Acylation of heat-induced whey protein complexes has been achieved by anhydride derivatives with various chain lengths, such as acetic, butanoic, hexanoic or succinic anhydride. Acylation of the heat-induced whey protein complexes increased the surface hydrophobicity of complexes; with the exception of succinylation, which did not affect the surface hydrophobicity of the protein complexes. The longer the attached carbon chain is to the protein, the higher the increase in surface hydrophobicity of the complexes. Furthermore, the degree of acylation and the type of anhydride derivative used also had an effect on the pI of the complexes; however, the size and thiol/disulphide distribution of the complexes was unaffected (Morand et al., 2012). In a study, glucono- δ -lactone was added to selected suspensions of modified heat-induced whey protein complexes, which have similar pI values (3.7 ± 0.2), but with different surface hydrophobicities, to form acid-gels. Results showed that increasing the surface hydrophobicity of the whey protein heat-induced complexes increased the pH of acid gelation (Morand et al., 2012).

1.7.2 Reductive alkylation

Reductive methylation can be accomplished via interaction of protein amino groups with formaldehyde and sodium borohydride (Figure 1.21), by attachment of methyl groups to the protein (Kester & Richardson, 1984). Reductive methylation of casein and whey proteins have a small effect on the physicochemical properties of these proteins, such as solubility and electrophoretic mobility. Methylation of 80% β -lg only increased the isoelectric point one pH unit (Olson et al., 1978; Rowley et al., 1979). However, when caseins were highly alkylated by isopropyl, cyclopentyl, hexyl and benzyl groups, respectively, the alkylated caseins showed enhanced water absorption and emulsifying properties (Sen et al., 1981). Therefore, the altered functionalities of alkylated proteins are dependent on the size and hydrophobicity of incorporated alkyl groups (Kester & Richardson, 1984).

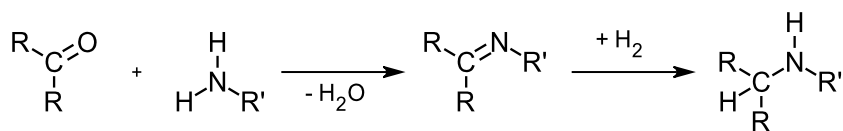


Figure 1.21. Schematic diagram of the reductive methylation (Kester & Richardson, 1984).

Reductive methylation can couple sugars to milk proteins in the presence of sodium cyanoborohydride. Glycosylation of proteins contributed to a decreased pI and increased hydrophilicity of β -lg through incorporation of negatively charged glycosyl groups, which might modify the solubility, viscosity, and gelation characteristics of β -lg (Kester & Richardson, 1984). Moreover, glycosylation of heat-induced whey protein using dextran molecules has been shown to enhance the water-binding capacity. The improved water-binding capacity might be a result of the addition of charges to the heat-induced whey protein (Morand et al., 2011a).

1.7.3 Genetic variation

The net charge of proteins can be altered through the protein's genetic variants (Bonfatti et al., 2009; Ganai et al., 2009; Jensen et al., 2012a; Jensen et al., 2012b; Ostersen et al., 1997; Visker et al., 2011). For example, the negative net charge of β -lg variant A (ASP₆₄, VAL₁₁₈) is higher than that β -lg variant B (GLY₆₄, ALA₁₁₈) (Farrell Jr et al., 2004); the negative charge of κ -casein variant B (ILE₁₃₆, ALA₁₄₈) is slightly more than A (THR₁₃₆, ASP₁₄₈) though κ -casein is weakly negatively charged (Cayot & Lorient, 1998). The net charge of κ -casein can be increased by glycosylation, and the κ -casein variant B is more glycosylated than A (Heck et al., 2009; Robitaille et al., 1991; Vreeman et al., 1986). Therefore, the physicochemical properties of milk proteins can also be affected by the genetic variation of proteins.

1.7.4 Conclusions

The physicochemical properties and functionalities of modified food proteins have been extensively studied (as described above). Some specific functionalities of these food proteins were enhanced with the selected modification approaches, although

some modification approaches showed adverse effect on the functionalities of food proteins. Thus, modifying the surface of casein proteins with selected modification approaches may improve their functionalities in dairy products.

α_{s1} -Casein has been reported to have good functional properties such as surface properties (de Jongh & Broersen, 2012). α_{s1} -Casein is a key component of ingredients in dairy products and could be incorporated into different food products to enhance nutritional and functional properties (Crowley et al., 2002; Modler, 1985). Therefore, α_{s1} -casein was selected as the protein modification material to investigate the effect of modifications on the functionalities of proteins. Acid α_{s1} -casein is separated from whey proteins by acidifying skim milk to the isoelectric point of α_{s1} -casein (Walstra & Jenness, 1984; Fox, 2009). When the pH of the acid α_{s1} -casein solutions is adjusted with sodium hydroxide to a neutral pH, a α_{s1} -caseinate is obtained (Bylund, 1995).

In this study, dephosphorylation, succinylation and TGA modification were selected to modify the α_{s1} -casein, as these three modification approaches have different effects on the physicochemical properties of proteins. Dephosphorylation and succinylation alter the net charge and hydrophobicity of proteins in different ways (Meyer et al., 1981; Morand et al., 2011a). Unlike dephosphorylation and succinylation, TGA modification could alter the molecular weight of proteins (Tang et al., 2005a). The changes in the physicochemical properties of caseins due to these modifications will be studied to correlate to the functional properties of proteins.

1.8 Thesis aims

The aim of this thesis was to investigate the correlations between the physicochemical properties and functionalities of α_{s1} -casein through the modifications of proteins. To achieve the aim the following objectives were set up:

1. To synthesise a range of modified proteins including dephosphorylated, succinylated and TGA-modified α_{s1} -casein.

2. To determine the physicochemical and functional properties of the modified proteins.
3. To correlate the physicochemical properties with the functionalities of the modified proteins.

Outline

Chapter two provides the materials and methods used in this study.

Chapter three presents the physicochemical properties of dephosphorylated α_{s1} -casein.

Chapter four discusses the effect of dephosphorylation on the functionalities of α_{s1} -casein.

Chapter five presents the physicochemical properties of succinylated α_{s1} -casein.

Chapter six discusses the effect of succinylation on the functionalities of α_{s1} -casein, and the correlation between the physicochemical and functional properties.

Chapter seven presents the physicochemical properties of TGA-treated α_{s1} -casein.

Chapter eight discusses the effect of TGA treatment on the functionalities of α_{s1} -casein, and the correlation between the physicochemical and functional properties.

Chapter nine presents the change in the structure of modified α_{s1} -casein on latex surface.

Chapter ten includes the final conclusions and key findings of the thesis.

Chapter 2 Experimental

The experiments in this thesis studied the effects of physicochemical properties on the functionalities of α_{s1} -casein by generating 4 protein modifications to α_{s1} -casein: dephosphorylation, succinylation, crosslinking and deamidation. The materials and techniques adopted for analysis are described below.

2.1 Materials

2.1.1 Proteins and protein solutions

The α_{s1} -casein enriched protein powder, containing around 64.6 % α_{s1} -casein, was an acid casein product and was obtained from Fonterra Co-operative Group, New Zealand. The contaminants were β -casein (~10% w/w), other milk protein fractions (~16 % w/w), moisture (~7.4% w/w), lactose (0.01% w/w), fat (~0.3% w/w) and Ca^{2+} (0.23% w/w) as well as trace amounts of other minerals.

An α_{s1} -casein solution (6% w/w on milk protein basis) was prepared fresh by dispersing the appropriate quantity of α_{s1} -casein powder in Milli-Q water (UltraPure water system, Australia; resistivity $\geq 18 \text{ M}\Omega \text{ cm}^{-1}$), and was then adjusted to pH 7 ± 0.1 with stirring until the casein was fully dissolved.

2.1.2 Chemicals

Table 2.1 provides a detailed list of key chemicals used in this research and their suppliers.

Table 2.1: The list of chemicals and their supplier

Bio-Rad Laboratories, Hercules, CA, U.S.A.	Acrylamide, ammonium persulphate (APS), Tetramethylethylenediamine (TEMED)
Fisher Scientific UK, Leics, U.K.	Propan-2-ol, sodium dodecyl sulphate (SDS)
Merck KGaA, Darmstadt, Germany	Glacial acetic acid, glycine, Tris (hydroxymethyl) methylamine (Tris-base)

Sigma – Aldrich Co., St Louis, MO, U.S.A.	2-Mercaptoethanol, phosphate buffered saline, NH_4HCO_3 , 1-anilinonaphthalene-8-sulphonic acid, trypsin (analytical grade), o-phthaldialdehyde, succinic anhydride, commassie Brilliant blue R-250, alkaline phosphatase from bovine intestinal mucosa (Lot # SLBL7932V, one unit of phosphatase will hydrolyze 1 μmole of 4-nitrophenyl phosphate per minute at pH 9.8 at 37 °C)
Davis Trading Co., Palmerston North, New Zealand	Canola oil
Ajinomoto Foods Deutschland GmbH, Hamburg, Germany	Transglutaminase (Activa MP) from <i>Streptomyces mobaraensis</i> (one unit of transglutaminase will catalyze the formation of 1 μmole of hydroxamate per min from Z-Gln-Gly-OH and hydroxylamine at pH 6.0 at 37°C)

2.2 Methods

2.2.1 Dephosphorylation of α_{s1} -casein

The α_{s1} -casein was dephosphorylated with alkaline phosphatase using a method modified from those of Koudelka et al. (2009), Lorenzen and Reimerdes (1992) and Pearse et al. (1986). The stock α_{s1} -casein solution (6% protein, Section 2.1.1) was stirred for at least 1 h at room temperature. The solution was adjusted to pH 7.8 ± 0.1 with 6 M NaOH while stirring. The pH adjusted α_{s1} -casein solution (50 mL) was then mixed with 50 mM ammonium bicarbonate buffer (pH 7.8) containing 1 mM MgCl_2 at a ratio of 1:1. The final solution (pH 7.8) contained 3% protein, 25 mM ammonium bicarbonate and 0.5 mM MgCl_2 . The solution was placed in a 4°C cold room until use. The temperature of the α_{s1} -casein solution was adjusted to $18 \pm 0.5^\circ\text{C}$ in a thermostatically controlled water bath. When the temperature of the solution reached 18°C, alkaline phosphatase was added to 100 mL of the α_{s1} -casein solution

at a level of 0.25 U/mg casein. The mixture was transferred to another water bath at 37°C and samples were collected after 5, 10, 20, 30, 60, 90, 120 and 180 min incubation. All samples taken at the different time points were heat-treated at 85°C for 5 min using a heat block to inactivate the phosphatase. After heating, the samples were cooled in ice.

The resulting solutions (5 mL from each incubation time) were transferred into dialysis bags, and each sample was dialyzed overnight at 4°C against 5 L of stirred distilled water. After dialysis, all the dephosphorylated protein solutions were adjusted to equal concentrations with Milli-Q water, with the protein concentration determined using an ultraviolet spectrophotometry method. In all experiments, a standard sample of untreated native α_{s1} -casein solution and a control sample were also included. The control sample was a standard sample that had no enzyme added but had undergone heat treatment at 85°C for 5 min. All the samples were stored in a -20 °C freezer until use.

2.2.2 Succinylation of α_{s1} -casein

α_{s1} -Casein was succinylated with succinic anhydride using a method modified from that of Fayle (1998). The stock protein solution (6% protein, measured by ultraviolet spectrophotometry method, Section 2.2.4) was stirred for at least 1 h at room temperature and then diluted to 3% protein with Milli-Q water. Based on a preliminary experiment, seven portions of succinic anhydride (6.2, 7.4, 12.2, 16.2, 46, 94 and 110 mg) were prepared, and each portion of succinic anhydride was gradually added into 10 mL aliquots of the diluted protein solutions with constant stirring. For those solutions containing 46, 94 and 110 mg of succinic anhydride, the succinic anhydride was dissolved in 3 steps over a period of 3 hours. In each step, 1/3 of the amount of the succinic anhydride was gradually added and this was followed by an hour of stirring. The pH was maintained at 7 between the additions of succinic anhydride by the dropwise addition of 1 M sodium hydroxide.

The resulting solutions (10 mL from each succinylated solution) were transferred into dialysis bags, and each sample was dialysed overnight at 4°C against 2 L of stirred distilled water. After dialysis, all the succinylated protein solutions were adjusted to equal protein concentrations with Milli-Q water, with the protein concentration determined using an ultraviolet spectrophotometry method (as described in section 2.2.4). In all experiments, a standard sample of native α_{s1} -casein solution without the addition of succinic anhydride was also prepared and all the samples were stored in a -20 °C freezer until use.

2.2.3 Crosslinking of α_{s1} -casein

α_{s1} -Casein was cross-linked with transglutaminase using a method modified from that of Jaros et al. (2006) and Jaros et al. (2010). The stock protein solution (6% protein, Section 2.1.1) was stirred for at least 1 h at room temperature before dilution with Milli-Q water to give a 3% protein solution. The solution was placed in a 4°C cold room until use.

The temperature of the α_{s1} -casein solution was adjusted to 20 ± 1 °C in a thermostatically controlled water bath. When the temperature of the solution reached 20°C, transglutaminase (TGA Activa® MP, around 100 U/g powder) was added to 100 mL of the α_{s1} -casein solution at a level of 0.007 U/mg casein. The mixture was then incubated in another water bath at 45°C and samples were collected after 1, 3, 5, 10, 20, 30, 60, 90 and 120 min. All samples taken at the different time points were heat-treated at 85°C for 5 min using a heat block to inactivate the transglutaminase. After heating the samples were cooled in ice.

The resulting solutions (5 mL from each incubation time) were transferred into dialysis bags, and each sample was dialyzed overnight at 4°C against 5 L of stirred distilled water. After dialysis, all the cross-linked protein solutions were adjusted to an equal concentration with Milli-Q water, with the protein concentration measured by an ultraviolet spectrophotometry method (as described in Section 2.2.4). In all experiments, a standard sample of untreated native α_{s1} -casein solution and a control

sample were included. The control sample was a standard sample that had no enzyme added but had undergone the heat treatment at 85°C for 5 min. All the samples were stored in a -20 °C freezer until use.

2.2.4 Ultraviolet – spectrophotometry

The concentration of the protein solutions was measured using a Jasco V-560 UV/Vis Spectrometer (Jasco Corporation, Tokyo, Japan). The protein solutions were diluted with Milli-Q water and then the diluted samples were transferred into a quartz cuvette for the absorbance reading at both 280 nm and 320 nm wavelengths. Proteins have a maximum absorbance at 280 nm wavelength, which is mainly due to the amino acids tryptophan, tyrosine and cysteine. The absorbance at 320 nm was measured to determine the background scattering. The absorption coefficient is specific for each protein depending on the relative concentrations of these three amino acids.

The protein used in this study is a mixture of α_{s1} -casein, β -casein and other milk protein fractions, with a total of 90.5% w/w protein based on a nitrogen test and a conversion factor of 6.38 (Tremblay et al., 2003). Standard protein solutions (0-0.1% w/w protein based on the composition of the α_{s1} -casein powder) were prepared and the absorbances ($A_{280}-A_{320}\times 1.7$) were plotted against the protein concentration to give a calibration curve (Figure 2.1).

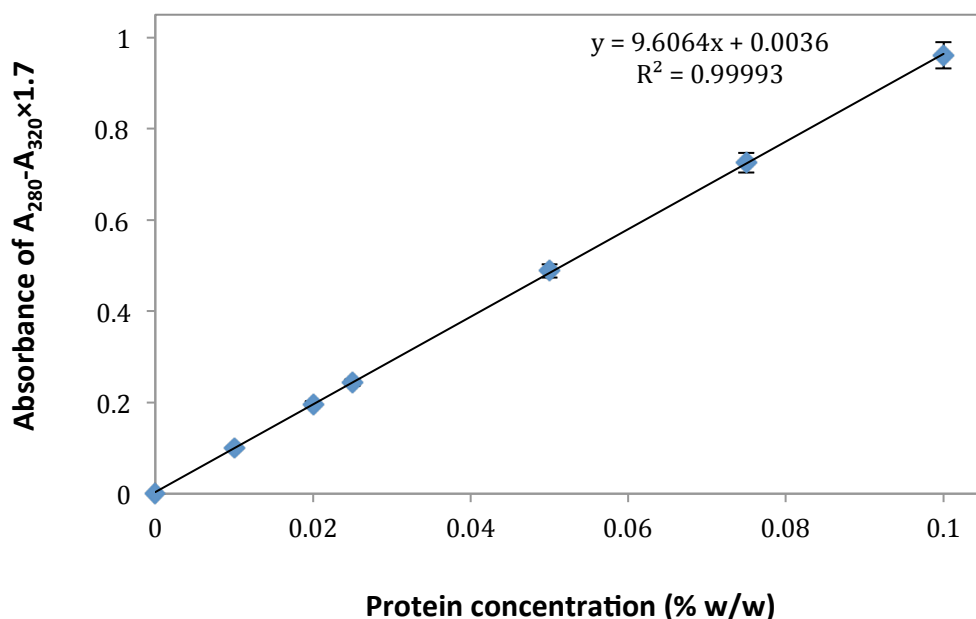


Figure 2.1 Standard curve of absorbance ($A_{280}-A_{320} \times 1.7$) against protein concentration. Error bars represent the standard deviation of the mean of three replicates.

The concentration of the protein in the solutions can be calculated using Equation 2.1.

$$\text{Concentration} = \frac{A_{280} - (A_{320} \times 1.7) - b}{m} \times \text{Dilution factor} \quad \text{Equation 2.1}$$

Constant m = the gradient of the trend line for standard curve

Constant b = the point at which the line crosses the y-axis of the standard curve

$A_{280/320}$ = absorbance of protein solutions read against Milli-Q blank at 280 or 320 nm

When a narrow beam passes through a volume, the beam will lose intensity due to the adsorption and scattering processes. The scattering intensity has a strong dependence on the diameter of the particles (d), it is proportional to d^6 . In addition to this, the intensity of light scattered by particles is proportional to $1/(\lambda^4)$. Thus, a particle at 280 nm scatters 1.7 times more light than the sample particle at 320 nm. In order to correct for the wavelength dependence of the scattering of particles at 280 and 320 nm, the correction factor 1.7 was used in Equation 2.1 (Holland et al., 2011).

2.2.5 Sodium dodecyl sulphate and alkaline urea polyacrylamide gel electrophoresis

In this study, both SDS-PAGE and urea-PAGE were performed using a Bio-Rad mini-gel slab electrophoresis unit (Bio-Rad Laboratories, Richmond, CA, U.S.A) and the method of Laemmli (1970), as described in detail by Manderson et al. (1998) and Havea et al. (1998). The composition and preparation details of stock solutions for SDS-PAGE are listed in Table 2.2.

Table 2.2 Preparation of stock solutions for SDS-PAGE

Stock solutions	Reagent	volume
30% Acrylamide solution	30 g of mixture of 37.5:1 of acrylamide and N,N'-methylene-bis-acrylamide	Made up to 100 mL with Milli-Q water
10% (w/v) Ammonium persulphate (APS) prepared fresh each day	100 mg of APS	In 1 mL of Milli-Q water
10% (w/v) SDS	10 g of SDS	Made up to 100 mL with Milli-Q water
Bromophenol blue 0.4% (w/v)	1.6 g of Bromophenol blue	In 400 mL of 1.75 mM NaOH
Resolving buffer (1.5 M Tris-HCl buffer)	18.15 g of Tris-base	Made up to 100 mL with Milli-Q water, pH was adjusted to 8.8 using 6 M HCl
Stacking buffer (0.5 M Tris-HCl buffer)	6.0 g of Tris-base	In 60 mL of Milli-Q water, pH was adjusted to 6.8 using 6 M HCl.
SDS Sample buffer	500 mL of Milli-Q water, 125 mL of 0.5 M Tris-HCl buffer (pH 6.8), 100 mL glycerol, 200 mL of 10% SDS and 25 mL of 0.4% bromophenol blue solution	

SDS Electrode stock buffer (5× concentration)	15 g of Tris-base, 72 g of glycine, 5 g of SDS	In 1 L of Milli-Q water. pH 8.2 (± 0.2)
Staining solution	0.5 g of Coomassie Brilliant blue R-250	Made up to 1 L with 250 mL isopropanol, 100 mL glacial acetic acid and Milli-Q water
Destaining solution	100 mL of isopropanol, 100 mL of glacial acetic acid	In 800 mL of Milli-Q water

Preparation of SDS-PAGE resolving and stacking gels

The resolving and stacking gel solutions were prepared according to the following description. For the resolving gel solution, Milli-Q water (3.00 mL), 1.5 M Tris-HCl buffer (3.75 mL) and 30% acrylamide solution (7.95 mL) were mixed and degassed under vacuum with constant stirring for 15 min in a Buchner flask. After degassing, 150 μ L of 10% (w/v) SDS solution, 7.5 μ L of TEMED and 75 μ L of 10% (w/v) APS were added and the solution was mixed well. For the stacking gel solution, Milli-Q water (6.10 mL), 0.5 M Tris-HCl buffer (2.5 mL) and 30% acrylamide solution (1.3 mL) were mixed and degassed for 15 min in a Buchner flask with constant stirring. After degassing, 100 μ L of 10% (w/v) SDS solution, 10 μ L of TEMED and 50 μ L of 10% (w/v) APS were added and the solution was mixed well.

Gel making procedure

For each gel, 3 mL of the resolving gel mixture was poured between the casting plates (Bio-Rad Laboratories, Richmond, CA, U.S.A) with the addition of 1 mL of water on the top of the gel solution. The resolving solution was allowed to stay at room temperature for 1 h to complete the polymerization. After 1 h, the water on the top layer of resolving gel was poured off and the residual water on the gel surface was removed with filter paper. The stacking gel solution was prepared fresh and transferred on to the top of the set resolving gel to fully fill the space between the glass plates. A 10 well plastic comb was then inserted between the glass plates

immediately. The gel was set at room temperature overnight to allow complete polymerization.

Sample treatment measurement

All the modified protein samples were diluted with sample buffer to give a final protein concentration of 4 mg/mL, as measured by the ultraviolet spectrophotometry method. The samples were analyzed under reduced conditions, with 2 μ L of β -ME added to each 20 μ L of diluted sample. The solutions were then heated at ~ 100 °C for 4 min. The treated samples (4 μ L) were loaded into each well of the gel using a syringe. After loading all the samples, the gel was run using a Bio-Rad power supply unit (Model 1000/500, Bio-Rad, Richmond, CA USA) for approximately 1.1 h, with setting parameters: voltage 210 V, current 70 mA and power 6.5 W.

When the electrophoresis process was completed, as indicated by the bromophenol dye front reaching the end of the gel, the gels were removed from the glass plates and placed into a plastic container containing 50 mL of staining solution and allowed to stain for 1 h with rocking. After staining, the stain was poured away and replaced with 100 mL of destaining solution and the gel rocked for one hour. This destaining procedure was repeated twice, and then the gels with replaced fresh destaining solution were rocked overnight to achieve a clear background. After the destaining procedure was completed, the gels were scanned using an Image Scanner III (GE Healthcare, Bio-Sciences AB, Sweden).

Urea-PAGE preparation

The preparation procedure for urea-PAGE is the same as the preparation procedure for SDS-PAGE (as described above) apart from the different stock solutions required for the urea gel. The preparation of stock solutions for urea-PAGE are listed in Table 2.3.

Table 2.3 Preparation of stock solutions for urea-PAGE

Stock solutions	Reagent	volume
Resolving buffer	9.2 g of Tris methylamine, 0.8 mL of HCl (concentrated), 54 g of urea	Made up to 200 mL with Milli-Q water, pH was adjusted to 8.8 with 1 M HCl
Stacking buffer	1.08 g of Tris methylamine, 36 g of urea, 0.55 g of boric acid, 92 mg of EDTA	Made up to 100 mL with Milli-Q water, pH was adjusted to 8.4 with 1 M HCl
Sample buffer	Same as stacking buffer + 2.5 mL of 0.4% (w/v) Bromophenol Blue solution	Made up to 100 mL with Milli-Q water, pH was adjusted to 8.4 with 1 M HCl
Electrode stock buffer (5× concentration)	10.7 g of Tris base, 5.5 g of boric acid, 0.9 g EDTA	Made up to 1 L with Milli-Q water, pH was adjusted to 8.4 with 1 M HCl

In urea-PAGE, the resolving gel solution was made by mixing resolving gel buffer (8.9 mL) and 30% acrylamide solution (6.0 mL). The mixture was then degassed under vacuum for 15 min in a Buchner flask with constant stirring. After degassing, 7.5 µL of TEMED and 75 µL of 10% (w/v) APS was added to the solution and mixed well. For the stacking gel solution, stacking gel buffer (8.65 mL) and 30% acrylamide solution (1.3 mL) were mixed and degassed for 15 min in a Buchner flask with constant stirring. After degassing, 10 µL of TEMED and 50 µL of 10% (w/v) APS were added and mixed well. The staining and destaining procedures were same as for SDS-PAGE gels.

2.2.6 Isoelectric focusing electrophoresis

The isoelectric point of the proteins was measured using Novex® pH 3-7 Isoelectric focusing electrophoresis (IEF) protein gels of 1.0 mm thickness and containing 10 wells (Invitrogen, CA USA). This measurement method was modified from that described by Kim and Jimenez-Flores (1994). All the modified protein samples were diluted with Milli-Q water to give a final protein concentration of 1.5% (w/w). The

diluted samples were mixed with the Novex® IEF Sample Buffer (pH 3-7, Invitrogen) in a ratio of 1:1. The samples were analyzed under reducing conditions, with 2 µL of β-ME added to each 20 µL of diluted sample. The samples were then heated at ~ 100 °C for 4 min. The treated samples (4 µL) were then loaded into each well of the gel using a syringe. After loading the samples, the gel was run using a Bio-Rad power supply unit (Bio-Rad model 1000/500) with Novex® IEF Anode Buffer and Novex® IEF Cathode Buffer pH 3-7 (Invitrogen). This IEF gel was run at a voltage of 100 V for 1 h, 200 V for 1 h and 500 V for 30 min. The staining and destaining procedures were same as for SDS-PAGE gels.

2.2.7 *o*-Phthaldialdehyde colorimetric assay

The *o*-phthaldialdehyde (OPA) method was used for lysine estimation and the method developed by Fayle et al. (2000) was used, which builds on an existing method from Bertrand-Harb et al. (1993). The OPA solution was prepared fresh as outlined in Table 2.4 immediately prior to the assay.

Table 2.4 The preparation of OPA reagent.

Reagent	Vol (mL)
0.1 M Sodium borate	25
20% SDS solution	2.5
40 mg of OPA	in 1 mL methanol
2-Mercaptoethanol	0.1
Milli-Q water	21.4

For construction of a calibration curve, lysine standards ranging from 0.125 to 1 mM (prior to addition to 1 mL of OPA) were prepared in Milli-Q water in triplicate from a 1 mM lysine stock prepared in Milli-Q water.

All of the protein samples were diluted to 2 mg/mL with Milli-Q water in triplicate. The lysine availability was assayed by adding 50 µL of sample into a cuvette containing 1 mL of OPA reagent, mixing thoroughly, and incubating for 2 min at

room temperature. The A_{340} was recorded in a spectrophotometer against Milli-Q water. The absorbances were plotted against concentration and a calibration curve was generated. The R^2 value of a linear regression of the standard curve was also determined.

2.2.8 Mass spectrometry

The mass spectrometry method was adapted from a Fonterra in-house method. α_{s1} -Casein solution was diluted with Milli-Q water to give 1% protein in the final solution. Trypsin (0.05% w/v) was dissolved in a 0.2 M ammonium bicarbonate buffer (pH 7.8). The diluted α_{s1} -casein solution was mixed with the trypsin solution in a 1:1 ratio and incubated at 37°C for 17 h in an incubator. After incubation, 10 μ L of 50% formic acid was added to 1 mL of the mixture and mixed well. The final mixture was centrifuged at 13,000 rpm for 1 min (Multifuge 15-R, Thermo Scientific, Germany) and the supernatant was analyzed using an Ion LTQ-Orbitrap mass spectrometer (Thermo Finnigan, USA) interfaced to a capillary high-performance liquid chromatograph (Dionex Ultimate 3000, Thermo Scientific, USA).

The hydrolyzed α_{s1} -casein samples were separated by RP-HPLC performed using an HPLC equipped with an Acclaim PepMap 100 (Dionex, USA) C18 column (300 μ m i.d. x 15 cm, 3 μ m, 100 Å). The auto-sampler was set to 6 °C. The column was held at 40°C. Solvent A was 0.2% formic acid in water (v/v) and solvent B was 0.2% formic acid in 90% acetonitrile (v/v). The LC gradient was carried out as follows: solvent B was held at 5% during the first 8 min then increased to 90% by 55 min, this was kept constant for another 10 min before dropping back to 10% over 70 min; finally the column was re-equilibrated for 15 min at 10% solvent B before the next injection. The flow rate was 3 μ L/min.

Liquid eluant from the column was directly injected into the source of an ion trap mass spectrometer equipped with an electrospray ionization source, via a 75 μ m i.d. fused silica capillary. Data dependent acquisition experiments were performed according to the following parameters: full scan (m/z 200-2000) carried out on the

OrbiTrap with 30000 resolution, followed by MS/MS of the top 4 most intense peaks in the LTQ. Former target ions were excluded for 15 s. The source temperature was 220 °C. Spectra were acquired in positive ion mode; the capillary voltage was 4 kV. Helium was used as collision gas. Spectra were processed using the software furnished with the instrument, and the characterization of modified residues of α_{s1} -casein were processed using the Mascot Distiller Database (Liu et al., 2007; Stephan et al., 2010). Mascot assigns a raw score for a peptide match, which takes into account the number of peaks in the spectrum that match predicted fragments based on peptide sequences in the database. A score greater than 50 was considered to be a peptide match.

2.2.9 Zeta potential measurements

The zeta potential of both the modified and unmodified α_{s1} -casein were measured using a Malvern Zetasizer Nano-ZS (Malvern Instruments Ltd, Worcestershire, UK) connected with an autotitrator (Malvern Instruments Ltd, Worcestershire, UK). This method was modified from the method of Anema and Klostermeyer (1996) and Morand et al. (2011c). The electrophoretic mobility of the particle in solution was measured under an applied electric field of 40 V. The refractive index and viscosity of dispersant (Milli-Q water) are 1.330 and 1.0031cP, respectively. The dispersant dielectric constant (Milli-Q water) and temperature were set as 80.4 and 20°C, respectively (Anema & Klostermeyer, 1996). The Henry equation is used to calculate the zeta potential. In the Henry equation, a value of 1.5 is used for the Henry's function $f(Ka)$ when the zeta potential was measured in aqueous solutions at low ionic strength, which is referred to as the Smoluchowski approximation. All the α_{s1} -casein samples were diluted with Milli-Q water to give a final protein concentration of 0.2% (w/w). The pH of the measured samples was adjusted with 0.1 M, 1 M HCl and 1 M NaOH using the autotitrator.

2.2.10 1-Anilinonaphthalene-8-sulfonic acid fluorescence probe

The 1-anilinonaphthalene-8-sulfonic acid (ANS) probe method is a well established

technique for protein hydrophobicity measurements. In this study, the protein surface hydrophobicity using an ANS probe was determined using a method modified from that of (Kato & Nakai, 1980). Stock solutions of 8 mM ANS were prepared in 0.01 M phosphate buffer (pH 7.0). The ANS stock solution was stored in a screw-capped tube wrapped in aluminium foil at room temperature.

The α_{s1} -casein solution was diluted with 0.01 M phosphate buffer (pH 7.0) to five concentrations in the range of 0.0025% - 0.02% w/w. The 0.01 M phosphate buffer was used as the blank for these measurements. ANS stock solution (10 μ L) was added to 2 mL of diluted protein solution and/or a blank buffer and mixed well. A 200 μ L mixture was loaded into each well of a black 96-well plate with a clear bottom (Greiner, Germany) and the relative fluorescence index (RFI) of treated samples was measured using the SpectraMax® M5 Multi-Mode Microplate Reader (Molecular Devices LLC, USA) at excitation and emission wavelengths of 390 and 470 nm, respectively. For standardization of the ANS assay, the measured RFI for 10 mL of methanol with 10 μ L of ANS was corrected to a value of 15. The initial slope (S_0) of the net RFI versus percentage protein concentration plot was calculated by linear regression analysis with Microsoft Excel and used as an index of the protein surface hydrophobicity. All the surface hydrophobicity values were determined at least twice.

2.2.11 Sodium dodecyl sulphate (SDS) binding

The surface hydrophobicity of modified proteins was determined using the SDS binding colorimetric assay using the SpectraMax® M5 Multi-Mode Microplate Reader (Molecular Devices LLC, USA). This method was modified from that of Hettiarachchy et al. (1995).

All protein samples were diluted with Milli-Q water to a final protein concentration of 0.2% (w/w). The diluted protein solutions were mixed with a 0.14 mM SDS solution in a ratio of 1:1. The protein solutions were left to stand at room temperature for 30 min. The mixed protein solutions were then dialyzed against 0.02

M phosphate buffer pH 7.0 at 4°C overnight. After dialysis, 1 mL of the dialyzed protein solution was transferred into a 25 mL screw-capped test tube containing 10 mL chloroform and mixed well. Methylene blue solution (2.5 mL of a 0.0024% solution) was added to the test tube and mixed well. The mixed samples were centrifuged at $800 \times g$ to separate the water and insoluble protein from the chloroform. Finally, the SDS-methylene blue mixture in the chloroform layer was transferred into a quartz cuvette for the absorbance measurement at a wavelength of 655 nm. A calibration curve, obtained using the above methods with known amounts of SDS, is used to determine the amount of SDS bound to the proteins. The SDS binding capacity (μg of SDS bound to 1 mg protein) is a measure of the hydrophobicity of the proteins.

2.2.12 Calcium ion activity

The calcium ion activity of all the modified protein samples titrated with CaCl_2 was measured at room temperature using a PHM 85 precision pH/mV-meter (Radiometer, Copenhagen) coupled with a calcium ion selective electrode. This method was modified from a method by Lin et al. (2006). The electrode was calibrated using 5 mL of CaCl_2 solutions (concentrations ranging from 0 to 4 mM) with the addition of 100 μL of KCl solution (4 M). Dephosphorylated α_{s1} -casein solutions were diluted to 0.4% (w/w) with Milli-Q water. The diluted α_{s1} -casein solutions (5 mL) were transferred to flat-bottom screw-top tubes, and 100 μL of KCl solution (4 M) was added. Then a total of 290 μL of a CaCl_2 solution (80 mM) was added into each of the protein solutions in 13 increments, with constant stirring. The potential difference was measured after each increment of CaCl_2 was added.

2.2.13 Circular dichroism

The secondary structure of native and modified α_{s1} -casein was analyzed using circular dichroism (CD) spectrometry with a method modified from Farrell Jr et al. (2001) and Hoagland et al. (2001). All CD spectra were recorded using a JASCO J-815 spectro-polarimeter (Easton, MD, USA) with a temperature controller (JASCO PET-

423S Easton, MD, USA) and using a quartz cuvette of 1 mm path length. Spectra were recorded over the wavelength range of 190-250 nm with a bandwidth of 1.0 nm at 20°C. All spectra were baseline corrected for the contribution of the solvent.

The succinylated, dephosphorylated and cross-linked α_{s1} -casein samples were all dialyzed overnight against Milli-Q water at 4°C. After dialysis, all the protein samples and dialyzed water, except cross-linked α_{s1} -casein, were filtered through 0.45 μ m pore filters. The filtered succinylated, dephosphorylated α_{s1} -casein and unfiltered cross-linked α_{s1} -casein were diluted with the filtered solvent to a final protein concentration of 0.2 mg/mL. The filtered solvent was used as the baseline samples for the CD measurement.

2.2.14 Analytical ultracentrifugation

The sedimentation velocity experiments were performed using a Beckman Coulter Model XL-I analytical ultracentrifuge equipped with UV/Vis scanning optics. The measurement method was modified from that of Nazmi et al. (2014). Reference buffer solutions and sample solutions were loaded into 12-mm double-sector cells with quartz windows, and the cells were then mounted in an An-50 Ti 8-hole rotor. Samples at protein concentrations of 1, 2 and 3 mg/mL (380 μ L) and reference (400 μ L) were centrifuged at 50,000 rpm at 20°C, and absorbance data were collected in continuous mode at 295 nm without averaging. Data were fitted to a continuous size-distribution model using the SEDFIT program (Lebowitz et al., 2002). The partial specific volume of the sample (0.728 mL/g), buffer density (1.00545 g/mL) and buffer viscosity (0.01020 cp) were calculated using the SEDNTERP program (Malin et al., 2005).

All the dephosphorylated, succinylated and cross-linked α_{s1} -casein solutions were dialyzed against 0.01 M phosphate buffer (containing 0.0027 M potassium chloride and 0.137 M sodium chloride, pH 7.4) at 4°C overnight. For AUC measurements, each of the modified α_{s1} -casein protein solutions was diluted with their dialyzed buffer to a protein concentration of 1, 2 and 3 mg/mL, respectively.

2.2.15 Nuclear magnetic resonance spectroscopy

The water binding capacity of modified proteins was measured using NMR using a method modified from that of Fabri et al. (2005). All the modified protein solutions were diluted to a concentration of 1% (w/w) with Milli-Q water. The T2 relaxation constant for protons of the diluted protein samples was measured using a Bruker MSL200 NMR spectrometer (Bruker, Germany) at 200MHz. The T2 measurements were performed using a standard Carr± Purcell/Meiboom±Gill (CPMG) pulse sequence. The excitation pulse (90°) was 5.5 micro sec and refocusing pulse (180°) was 11 micro sec with a recycle time of 10 sec. All the samples were measured at 22°C. The T2 constants fitted with Bruker Topspin version 1.4 NMR software.

2.2.16 Viscosity measurements of modified α_{s1} -casein

The viscosity of native and modified α_{s1} -casein solutions was measured with a method modified from Buzzell and Tanford (1956). The viscosity measurement was performed using a glass capillary viscometer (C384, 75, Cannon, USA) that was immersed in a $20 \pm 0.1^\circ\text{C}$ water bath. The time required for the level of the liquid to drop from one mark to the other was measured with a timer. The average of three readings gives the flow time of the liquid to be examined. The kinematic viscosity ($\text{mm}^2\cdot\text{s}^{-1}$) was calculated using the equation:

$$\eta = \kappa t \quad \text{Equation 2.2}$$

κ : is the constant of the viscometer, expressed in mm/sec^2 , which was determined using Milli-Q water as a viscometer calibration liquid in this study. t : is the flow time, in sec, of the liquid to be examined.

In order to examine the difference in the viscosity between native and modified protein solutions, a preliminary experiment was required to determine the upper and/or lower limits of protein concentrations for the viscosity measurement. All the protein solutions with a protein concentration range of 1% to 3% were prepared by

diluting the stock protein solutions with Milli-Q water for the viscosity measurement. Based on the results of the preliminary experiment, 3% dephosphorylated α_{s1} -casein solutions, 1% succinylated α_{s1} -casein solutions and 1% cross-linked α_{s1} -casein solutions were prepared by diluting the stock solutions with Milli-Q water.

2.2.17 Surface tension (air-water) measurement - Wilhelmy plate method

The surface tension measurements between air and water were conducted at $20 \pm 0.5^\circ\text{C}$ by a Wilhelmy plate method using a roughened platinum plate. A Krüss Processor tensiometer K12 (Hamburg, Germany) with an external circulating water bath was used. The Wilhelmy plate method was modified from that described by Rodríguez Niño and Rodríguez Patino (1998). The measurement was set up with a vessel diameter of 6.65 cm, vessel height of 3.75 cm, measurement intervals of 10 sec and the number of values as 10.

Due to the fact that adsorption measurements are sensitive to the presence of impurities, extreme care was taken to ensure that all materials and instruments used were clean. The platinum plate was washed with ethanol, rinsed with deionized water, heated in a Bunsen burner flame, and left to cool to room temperature.

For the preliminary experiments, the stock native protein solutions were diluted with Milli-Q water to a protein concentration range of 0.001% to 1%. The surface tension of these diluted protein samples were measured.

Based on the results from the preliminary experiments, all the stock protein solutions were diluted with Milli-Q water to give a final concentration of 0.001% dephosphorylated α_{s1} -casein, 0.02% succinylated α_{s1} -casein and 0.02% TGA-treated α_{s1} -casein. Each diluted protein solution (25 mL) was transferred into a flat-bottom screw-top tube. All the samples were kept in a 20°C water bath before measurements. Prior to each measurement of protein samples, a surface tension measurement of Milli-Q water was undertaken to ensure no contamination was present in the system. Milli-Q water has a surface tension of approximately 72

mN/m at 20°C (Rodríguez Niño & Rodríguez Patino, 1998).

2.2.18 Interfacial tension (oil-water) measurement – the pendant drop method

The method of surface tension measurement used was modified from Tripp (1993) and as described by Tripp et al. (1995). The parameters were set with 5 s frame intervals and 80 frames. Canola oil, which has a density around 0.92 g/mL, was used as the light phase for the interfacial tension measurements.

A preliminary experiment was performed to examine the optimum protein concentration for the surface tension measurements. The stock native protein solutions were diluted with Milli-Q water to a protein concentration range of 0.001% to 0.08%. The surface tension of these diluted protein samples was measured.

Based on the results from the preliminary experiment, all stock protein solutions were diluted with Milli-Q water to give a final protein concentration of 0.002% (w/w) for dephosphorylated α_{s1} -casein and 0.02% (w/w) for succinylated and TGA-treated α_{s1} -casein. Prior to each measurement of protein samples, a surface tension measurement of Milli-Q water was undertaken to ensure no contamination was present in the system. The interfacial tension between water and oil is approximately 35 mN/m (Peters & Arabali, 2013).

2.2.19 Foaming property measurements

The foaming property measurement of proteins was based on that described by Martínez-Padilla et al. (2014), with modifications as follows. All protein samples were adjusted to a 3% protein concentration with Milli-Q water. The adjusted protein solutions (9 mL) were transferred into a 50 mL graduated centrifuge tube and whipped using a milk frother (Steven Deluxe Frother with two AA batteries) for 5 min at room temperature. The volume of protein foam and the time for 7.5 mL of serum to separate from the foam was recorded as the foaming index for the protein solutions.

2.2.20 Particle size measurement using laser light scattering

The emulsion particle size distributions and mean diameters ($d_{3,2}$) of emulsion droplets were determined by laser light scattering using a Malvern Mastersizer 2000. The method was carried out according to the method of Ye (2011). This measurement was performed with a pump speed of 2975 rpm and optical parameters: 1.330 and 1.456 for the refractive index of water and canola oil, respectively, and 0.001 for the particle absorption.

2.2.21 Emulsion preparation

Emulsions containing 0.2% protein with different levels of oil (2.5 to 17.5%) were prepared by diluting the stock modified protein solutions with Milli-Q water and canola oil. The mixture of the emulsion samples was then pre-homogenized at 24,000 rev min⁻¹ for 3 min using an Ultra-Turrax T25 (IKA® -Werke GmbH & Co. KG, Staufen, Germany) to form a coarse emulsion. The coarse emulsion was homogenized using a sonicator (Qsonica Q125, USA) at a 100% amplitude for a total of 10 min of sonication (in cycles of 15 sec ON and 15 sec OFF). During the sonication, the sample temperature was controlled at 20 ± 1°C using a water bath.

2.2.22 Protein-coated latex samples preparation and measurement

Polystyrene latex particles of nominal diameters of 60 and 100 nm were obtained from the Duke Scientific Corp. (3060A and 3100A, Nanospheres™, Palo Alto, CA, USA). All the polystyrene latex particles were supplied as aqueous solutions. For the light scattering experiments, the latex solutions were prepared by adding 50 µL of the 60 and 100 nm latex particles to 5 mL of imidazole buffer (20 mM imidazole, pH 7.0), respectively. Bovine α_{s1} -casein purchased from Sigma was dissolved in the Milli-Q water to 9.79 mg/mL (pH 6.55). Working solutions were prepared by mixing the α_{s1} -casein solution with 20 mM imidazole buffer (pH 7) at a ration of 1:1.

The size and zeta potential of protein-coated latex particles were measured using a Malvern Zetasizer Nano-ZS (Malvern Instruments Ltd, Worcestershire, UK) with a method adapted from Anema (1997). The measurements of the dynamics of the scattered light were collected at a scattering angle of 173°. The temperature of the samples was maintained at 20°C and/or 37°C for the duration of the experiments. The dispersant (imidazole buffer) was considered to have the properties of water with a reflective index of 1.330 and viscosity of 1.0031 cP (Anema & Klostermeyer, 1997). The average diffusion coefficients were analysed by the method of cumulates and translated to average particle diameters using the Stokes-Einstein relationship for spheres (Anema & Li, 2003). The electrophoretic mobility of the α_{s1} -casein coated particles was also measured using the above method. The sample preparation of the α_{s1} -casein coated particles is described in the following section.

Dephosphorylated sample preparation

The latex particles were coated with dephosphorylated α_{s1} -casein in two ways: dephosphorylated α_{s1} -casein coating latex particles and dephosphorylation on α_{s1} -casein coated latex particles. For the dephosphorylated α_{s1} -casein coated latex particles, the latex particle solutions were titrated with fully dephosphorylated α_{s1} -casein at 20°C. The completely dephosphorylated α_{s1} -casein was prepared by adding alkaline phosphatase to the α_{s1} -casein solution at a level of 0.25 U/mg α_{s1} -casein, and then incubated at 37°C for 24 hours. For dephosphorylation on α_{s1} -casein coated latex particles, the latex particle solutions were coated with native α_{s1} -casein and followed by the centrifugation and re-suspension procedure. In order to remove the excess native α_{s1} -casein from the latex particles, the coated particles were centrifuged at 14,000 rpm and at 25°C for 20 min. After centrifugation, the supernatant was removed and the sediment was re-dispersed with imidazole buffer. This centrifugation and re-suspension step was repeated three times. After the centrifugation and re-suspension procedure, the coated latex particle solutions were incubated with different amounts of alkaline phosphatase at 37°C up to 12 hours.

Succinylated sample preparation

The latex particles were coated with succinylated α_{s1} -casein in two ways: succinylated α_{s1} -casein coating latex particles and succinylation on α_{s1} -casein coated latex particles. For the succinylated α_{s1} -casein coating latex particles, the latex particle solutions were titrated with fully succinylated α_{s1} -casein at 20°C. The fully succinylated α_{s1} -casein was prepared by adding succinic anhydride to the α_{s1} -casein solution at a level of 0.5 mg/mg α_{s1} -casein, and then mixed at 20°C for 3 hours. For succinylation on α_{s1} -casein coated latex particles, the latex particle solutions were coated with native α_{s1} -casein and followed by the centrifugation and re-suspension procedure. In order to remove the excess native α_{s1} -casein from the latex particles, the coated particles were centrifuged at 14,000 rpm and at 25°C for 20 min. After centrifugation, the supernatant was removed and the sediment was re-dispersed with imidazole buffer. This centrifugation and re-suspension step was repeated three times. After the centrifugation and re-suspension procedure, the succinic anhydride (0.4 mg/ mg casein) was added into the coated latex particle solutions.

2.3 Statistical analysis

All experiments were carried out at least twice for both sample treatments and sample analyses. Standard deviations were used where appropriate to indicate the variability between repeated experiments or measurements. The R-squared value was calculated to analyse the relation between the dependent variable and the other independent variables. The initial slope of a regression line was used to test the significance of a linear relationship between the dependent variable and independent variable.

Chapter 3 Characterization of dephosphorylated α_{s1} -casein

3.1 Introduction

α_{s1} -Casein is a phosphoprotein and commonly contains 8 phosphoserine residues that form phosphate clusters that can bind metal ions, mainly calcium (Ca^{2+}) in milk (as described in Section 1.1.3; Holt, 1985). α_{s1} -Casein that contains 9 phosphoserine residues has also been reported, but it is less common (Fox, 1982). The phosphoserine residues have a significant effect on the characteristics of the casein including its amphiphilic character, association behaviour and the bioavailability of divalent cations (Lorenzen & Reimerdes, 1992; Molina et al., 2007). Phosphorylation can occur on several amino acids; however, the phosphorylation of serine residues is the most common, followed by threonine (Cohen, 2002; Thomason & Kay, 2000).

Enzymatic dephosphorylation can modify the physicochemical properties of caseins by removing the phosphate groups from the serine residues (as described in Section 1.3). Figure 3.1 shows the dephosphorylation reaction for serine phosphate residues (Molina et al., 2007). The level of dephosphorylation of caseins can be manipulated by controlling the incubation time of the dephosphorylation reaction (Koudelka et al., 2009; Lorenzen & Reimerdes, 1992; Pearse et al., 1986). The dephosphorylation of caseins has been studied (Anderson & Kelley, 1959; Bingham et al., 1971; Clark et al., 1992; Darewicz et al., 2000); however, these previous studies did not focus on the correlation between physicochemical properties and functionalities of dephosphorylated α_{s1} -casein.

The aim of this work was to carry out controlled dephosphorylation of α_{s1} -casein and investigate the physicochemical properties of the dephosphorylated protein. The dephosphorylated α_{s1} -casein solution was prepared by incubating α_{s1} -casein with

alkaline phosphatase (as described in Section 1.2.1) and its resulting properties were examined using a variety of methods, such as alkaline urea-PAGE (AU-PAGE), mass spectrometry, light scattering, IEF-PAGE, etc. The results will help improve the understanding of how the isoelectric point, charge and hydrophobicity of α_{s1} -casein can be manipulated using different degrees of dephosphorylation.

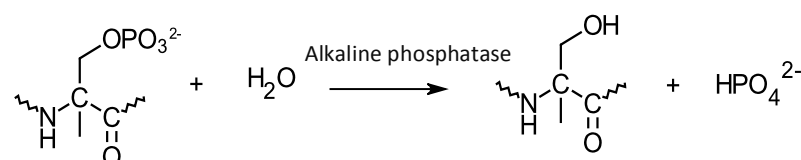


Figure 3.1 Dephosphorylation of the serine phosphate residues with alkaline phosphatase (Anderson & Kelley, 1959).

3.2 Results and discussion

α_{s1} -Casein genetic variant B was used in this study. Variant B is the most abundant in Western dairy cow populations (~94%); variant A is extremely rare (< 0.3%) and variant C is uncommon (~6%) (Berry et al., 2014). As expected, a mass spectrometry analysis showed that the major fraction of native α_{s1} -casein had eight phosphate moieties attached to serine residues (as described in Section 2.2.8 and Appendix C). Figure 3.2 shows the abbreviated amino acid sequence of α_{s1} -casein genetic variant B with the eight common phosphoserine residues highlighted in red, and the ninth rare phosphoserine residue highlighted in blue (as described in Section 1.2.1). (Anderson & Kelley, 1959; Molina et al., 2007)



Figure 3.2 Abbreviated sequence of α_{s1} -casein: Asn₃₈-Glu₅₀, Glu₆₁-Glu₇₇, Pro₁₁₃-Arg₁₁₉, highlighting the eight common phosphoserine residues (red) and the ninth rare phosphoserine residue (blue) in the sequence (Fox, 1989).

3.2.1 Determination of dephosphorylation of α_{s1} -casein

Gel electrophoresis is used to separate proteins according to their electrophoretic mobility, which is a function of the length of a polypeptide chain and its charge. In sodium dodecyl sulphate polyacrylamide gel electrophoresis (SDS-PAGE), the proteins are separated based on their molecular mass as proteins retain only the primary structure and have a constant charge to mass ratio in the SDS-environment. In the presence of SDS, the hydrophobic and hydrogen bonds of proteins are disrupted and negative charge is introduced to the protein (Andrews, 1990).

In alkaline urea polyacrylamide gel electrophoresis (AU-PAGE), the proteins are separated on the basis of size and charge as urea allows the casein proteins to migrate as monomers (Andrews, 1990). AU-PAGE has been extensively used for the determination of casein fractions, and it was effective for examining whole caseins or β -caseins that were dephosphorylated by potato acid phosphatase (Lorenzen & Reimerdes, 1992; Ohmiya et al., 1983). Both, AU-PAGE and mass spectrometry were used in this study, to monitor the level of dephosphorylation and identify the dephosphorylated serine residues of α_{s1} -casein (as described in section 2.2.5 and 2.2.8).

AU - PAGE

The degree of dephosphorylation of α_{s1} -casein was manipulated by controlling the incubation time with the enzyme at a constant temperature of 37°C and at pH 7.8. Figure 3.3 shows the AU-PAGE pattern for α_{s1} -casein incubated with alkaline phosphatase. The band intensities and protein band positions in the standard sample (Lane 1) represent the total amount and the type of proteins in the native α_{s1} -casein without heat treatment. The band intensities and positions in the control sample (Lane 2) show the total amount of protein and the type of proteins in the native α_{s1} -casein with heat treatment, where the heat treatment was applied to deactivate the enzyme in the dephosphorylated samples. The shift in band intensities and band positions of the other samples (Lanes 3 to 10) was due to the change in the net charge of proteins, which correspond to an increasing degree of dephosphorylation at increasing incubation times.

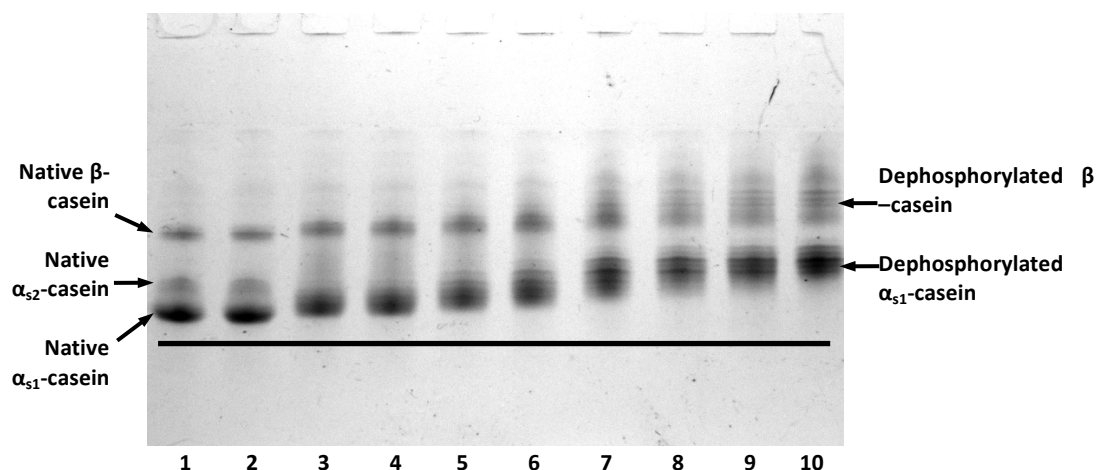


Figure 3.3: AU-PAGE for dephosphorylation of α_{s1} -casein at different incubation times with alkaline phosphatase. From left to right: standard sample (native α_{s1} -casein without heat treatment, Lane 1); control sample (native α_{s1} -casein with heat treatment at 85°C for 5 min, Lane 2); α_{s1} -casein incubated with alkaline phosphatase at incubation times: 5 min (Lane 3), 10 min (Lane 4), 20 min (Lane 5), 30 min (Lane 6), 60 min (Lane 7), 90 min (Lane 8), 120 min (Lane 9), and 180 min (Lane 10).

There was no difference in the band intensities and band positions between the standard (Lane 1) and control samples (Lane 2) confirming that the difference in the incubated samples is due to the enzyme and not the heat treatments. The bands representing the dephosphorylated α_{s1} -casein and β -casein (Lanes 3 to 10) gradually shifted to higher positions (slower migration) compared to the native proteins (Lanes 1 and 2), and the longer the incubation time, the slower the protein band migration. This indicates that the dephosphorylated caseins are low negatively charged and therefore have a slower electrophoretic mobility than the native caseins.

The protein band patterns (Figure 3.3) also show that the dephosphorylated α_{s1} -casein bands consisted of several thin bands as seen more clearly in Lanes 5 to 10. This is consistent with different levels of serine dephosphorylation resulting in different levels of negative charge and different electrophoretic mobility. In addition, there was a small amount of β -casein in the sample, which shows less band-shifting with increased incubation time when compared with α_{s1} -casein (Figure 3.3). This indicates that the total negative charge of β -casein was reduced to a lesser extent

compared with α_{s1} -casein. This is because β -casein has fewer serine phosphate residues (4 to 5 per protein) than α_{s1} -casein (8 to 9 per protein) (Holt, 1985). There is a blurry protein band between the native β -casein and α_{s1} -casein (Figure 3.3, Lane 1 and 2), which could be due to α_{s2} -casein, but it is not seen in the dephosphorylated samples (Lane 3 to 10). As α_{s2} -casein contains 11 phosphoserine residues, dephosphorylation of α_{s2} -casein will result in more phosphate groups being removed and a higher level of reduction in the net charge compared to α_{s1} -casein and β -casein. Thus the dephosphorylated α_{s2} -casein would have a higher level of reduction in the electrophoretic mobility than dephosphorylated β -casein, which may lead to the dephosphorylated α_{s2} -casein shifting under the β -casein bands on the gel.

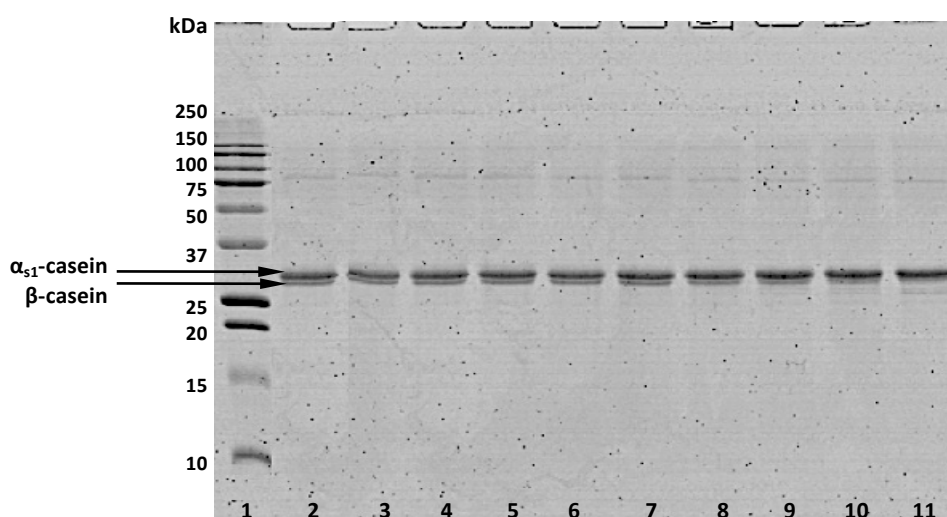


Figure 3.4 SDS-PAGE for dephosphorylation of α_{s1} -casein at different incubation times with alkaline phosphatase. From left to right: molecular weight (Lane 1); standard sample (native α_{s1} -casein without heat treatment, Lane 2); control sample (native α_{s1} -casein with heat treatment at 85°C for 5 min, Lane 3); α_{s1} -casein incubated with alkaline phosphatase at incubation times: 5 min (Lane 4), 10 min (Lane 5), 20 min (Lane 6), 30 min (Lane 7), 60 min (Lane 8), 90 min (Lane 9), 120 min (Lane 10), and 180 min (Lane 11).

The SDS-PAGE pattern in Figure 3.4 confirms that the α_{s1} -casein sample contains a small amount of β -casein. There was no noticeable difference in the band intensities and band positions between the standard (Lane 2), control samples (Lane 3) and

dephosphorylated samples (Lane 4 to 11). These SDS-PAGE patterns also show that there were no additional bands with molecular weight smaller than α_{s1} -casein on the gel, and the intensity of dephosphorylated α_{s1} -casein did not decrease in comparison to native α_{s1} -casein. This indicates that the bovine intestinal alkaline phosphatase did not have any proteolytic effect on the caseins.

Mass spectrometry of dephosphorylated α_{s1} -casein

An LTQ-Orbitrap mass spectrometer is defined as an electrostatic high resolution mass spectrometer. In the analysis, the sample was injected onto an LC column and separated according to differences in hydrophobicity. The components eluted from the LC column were ionized then transmitted to the MS detector where they were analyzed. For electrospray ionization, a combination of high voltage and heat is used to provide the ionization that is needed to produce the ions. The high voltage field nebulizes the column effluent resulting in charged droplets directed toward the mass analyzer. These droplets become smaller as they approach the entrance to the mass analyzer, and individual ions are formed in a process that is referred to as ion-evaporation (Makarov & Scigelova, 2010).

The process of capturing ions in the C-trap which is a curved linear trap and injection into the analyzer takes several milliseconds, but the process of detection requires a much longer period of time than injection. Thus, a linear ion trap mass was interfaced and synchronized to the C-trap (Figure 3.5). These ions are stored in the C-trap and then injected into the Orbitrap analyzer in a short pulse. These ion packets are focused on the entrance of an outer curved electrode of the Orbitrap analyzer. The Orbitrap analyzer surrounds the curved central electrode which is sustained at a high voltage. When ion packets are injected tangentially into the electric field, ramping the voltage on the inner electrode leads to an increase in the electric field. The ions are squeezed towards the inner electrode. When the ions reach the desired orbit inside the trap, the ramping is stopped. Each ion packet contains a large number of ions of different velocities spread over a certain volume. Thus, ions will move with the same axial frequency and different rotational frequencies. This leads to ions of specific mass to charge ratios spread into rings

which oscillate along the central electrode with a period proportional to $(m/z)^{1/2}$. A broadband detection of this signal is followed by a fast Fourier transform to convert the recorded time-domain signal into a frequency, and then into the m/z spectrum (Makarov & Scigelova, 2010).

For MS/MS analysis, in the first stage, the ions of one mass-to-charge ratio (the parent ions) are selected and all other ions are ejected from the mass analyzer. The parent ions are collided with background gas and fragmented to produce one or more product ions. In the second stage of mass analysis, the product ions from the first stage are stored in the mass analyzer and consecutively scanned to produce a full product ion mass spectrum. Finally, the ion profile is compared to those in a database to determine the protein's sequence (Korfmacher, 2005).

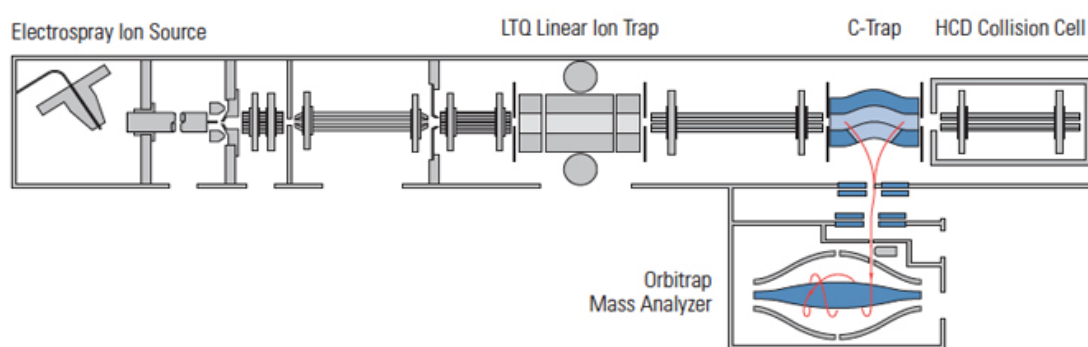
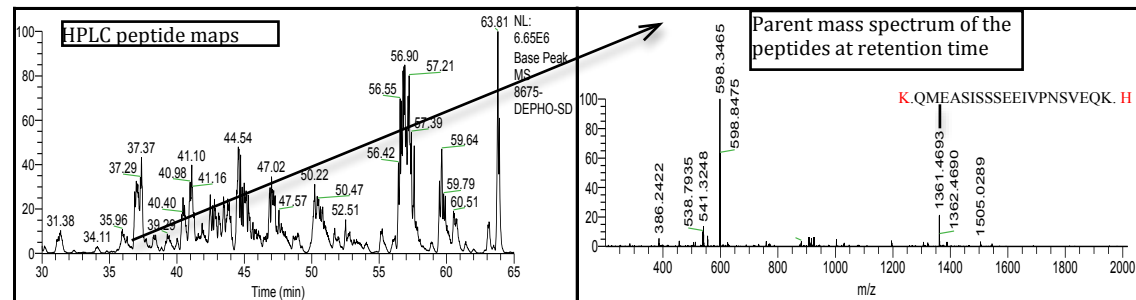


Figure 3.5 Schematic layout of the LTQ Orbitrap mass spectrometer. (Figure taken from Aligent Technologies basic LC/MS manual 2001).

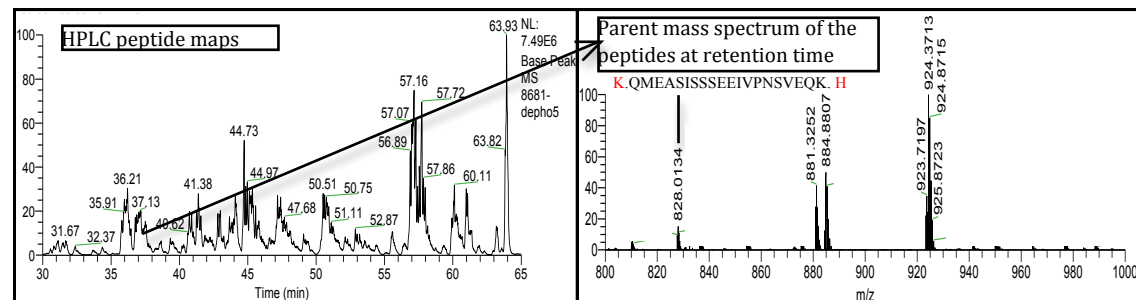
Mass spectrometry is well established as a method to identify modified amino acid residues of proteins. Therefore, the dephosphorylation of α_s - and β -caseins was able to be confirmed by mass spectrometry (Koudelka et al., 2009). In this study, the serine residues of dephosphorylated α_{s1} -casein were identified by linear Orbitrap mass spectrometry (as described in Section 2.2.8). The mass spectrometry chromatograph of peptides of interest from trypsin-digested native and dephosphorylated α_{s1} -casein is shown in Figure 3.6. The peaks were labelled with

mass to charge ratio and sequenced. All the peaks were used in a database search to map the dephosphorylated serine residues.

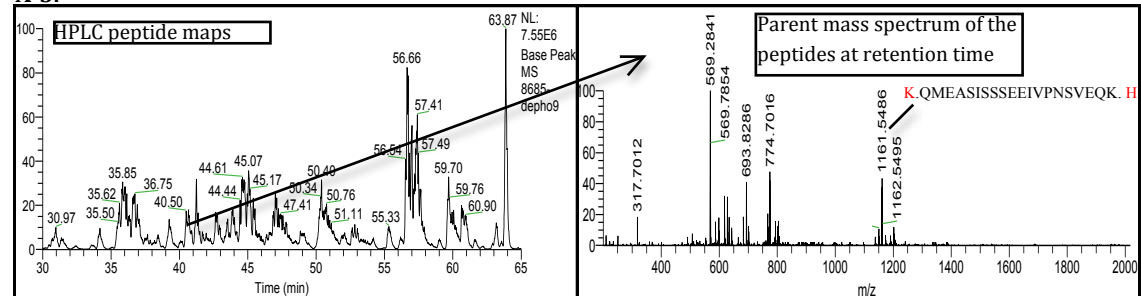
A-1.



A-2.



A-3.



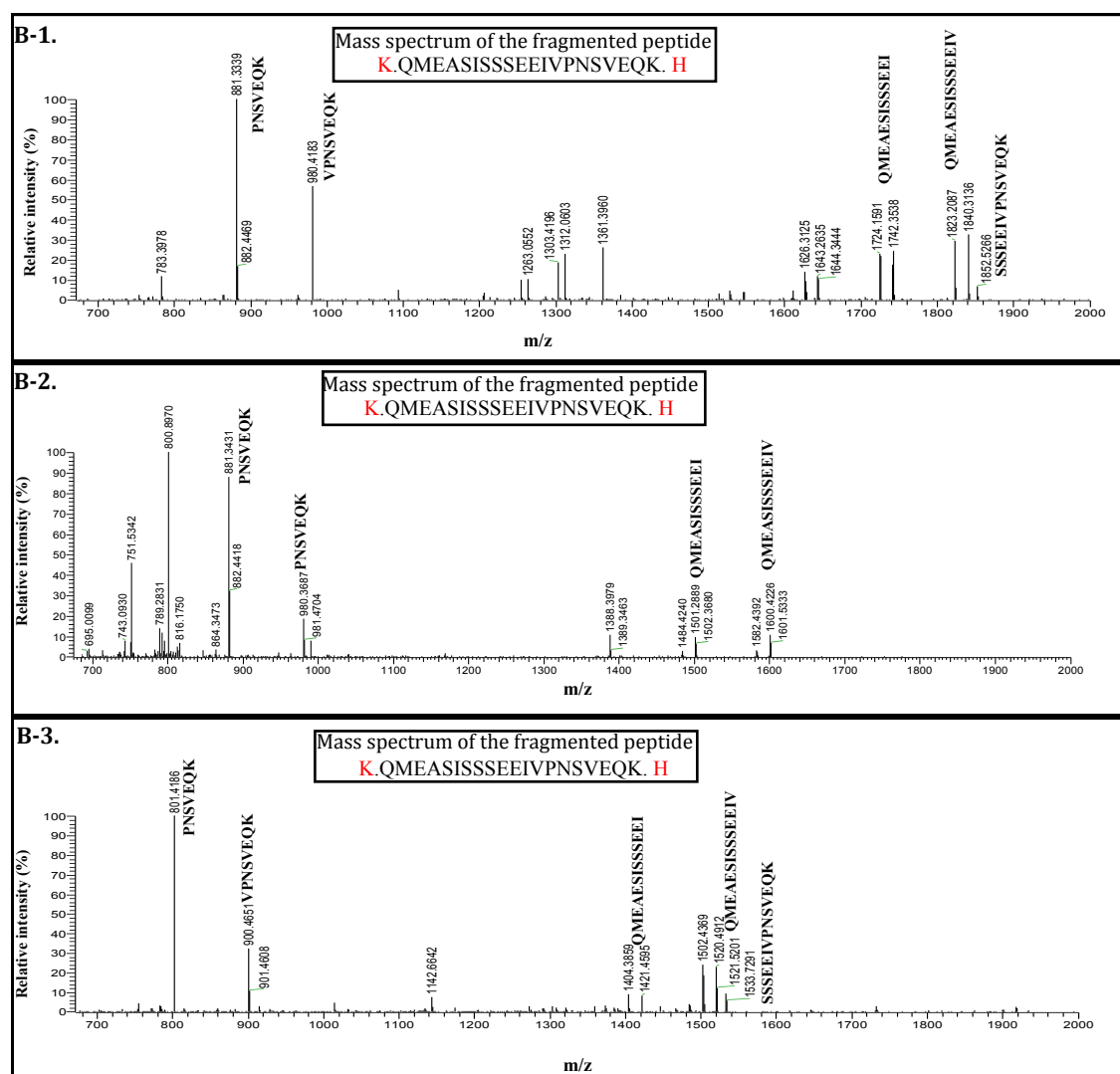


Figure 3.6 HPLC peptide maps, parent mass spectrum (A) and mass spectrum of fragmented peptide Gln₅₉-Lys₇₉ (B) from trypsin-digested native α_{s1} -casein (1), dephosphorylated α_{s1} -casein at incubation time of 20 min (2) and 180 min (3). Peak assignments corresponding to the phosphopeptides of α_{s1} -casein are indicated.

The HPLC peptide maps show different patterns between native and dephosphorylated α_{s1} -casein at the retention times between 35 to 43 min (Figure 3.6 A). The parent mass spectrum is given in Figure 3.6 A, and the peptide Gln₅₉-Lys₇₉ was selected to represent a typical mass spectrum. The trypsin cleavage sites for peptide Gln₅₉-Lys₇₉ are highlighted in red. Figure 3.6 A shows that the retention time for peptide Gln₅₉-Lys₇₉ increased as the phosphatase incubation time increased. This indicates that dephosphorylation contributed to an increase in the

hydrophobicity of the peptide Gln59-Lys79, which is due to the reduction in the net charge of dephosphorylated α_{s1} -casein.

The fragmentation patterns of peptide Lys₇-Arg₂₂, which are shown in Figure 3.6 B, were used to identify the dephosphorylated serine residues. The fragmented peptide map showed the change in the mass to charge ratio between the native and dephosphorylated peptide. The peptide fractions labelled in Figure 3.6 B were identified as carrying one positive charge, thus the difference in the mass to charge ratio between native and dephosphorylated α_{s1} -casein (Figure 3.6 B) indicated the loss of phosphate groups; the results are summarized in Table 3.1.

Table 3.1 The mass to charge ratio of native and dephosphorylated α_{s1} -casein at incubation times of 20 min and 180 min. All the peptide fractions carried one positive charge.

Peptide fractions	Native α_{s1} -casein	Dephosphorylated α_{s1} -casein 20 min			Dephosphorylated α_{s1} -casein 180 min		
		Mass (m/z)	Δ mass	No. PO ₄	Mass (m/z)	Δ mass	No. PO ₄
PNSVEQK	881.3339	881.3431	0 (0)	0	801.4186	80 (1)	1
VPNSVEQK	980.4183	980.3637	0 (0)	0	901.4651	79 (1)	1
QMEAESSISSEEI	1724.1591	1484.4240	240 (3)	3	1404.3589	320 (4)	4
QMEAESSISSEIIV	1840.3136	1600.4226	240 (3)	3	1521.5201	319 (4)	4

In order to monitor the specific phosphoserine residues that were dephosphorylated at different incubation times, the identified dephosphorylated serine residues of α_{s1} -casein were compared with the results obtained from the AU-PAGE. The peptides were sequenced using Mascot Distiller Database as described in Section 2.2.8. The ninth serine residue is labelled as fully dephosphorylated as only a minor fraction of α_{s1} -casein had nine phosphoserines (Figure 3.7). When the α_{s1} -casein was incubated with alkaline phosphatase for 20 min, serine residues 1 to 8 were partially dephosphorylated (Figure 3.7). By the time the incubation reached 180 min, serine residues 1, 2, 4, 6 and 8 were fully dephosphorylated.

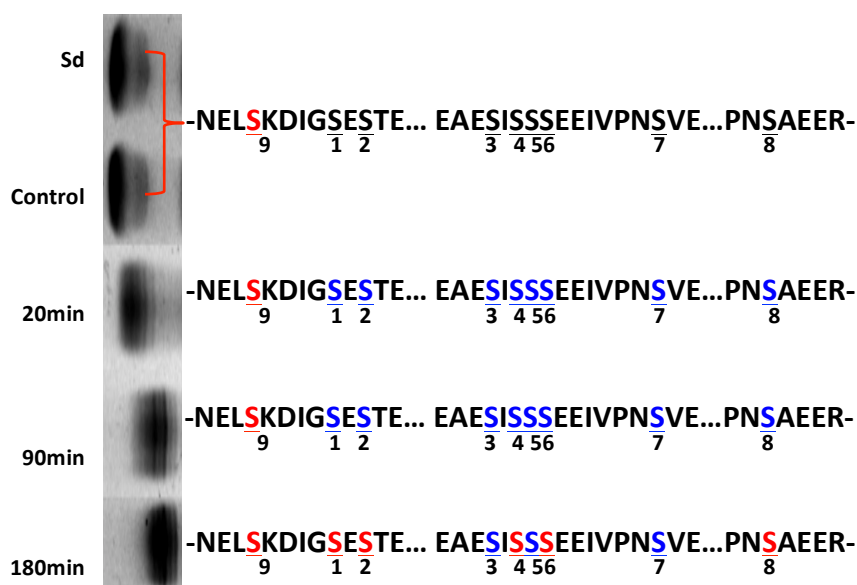


Figure 3.7 Dephosphorylated serine residues at incubation times of: 20 min, 90 min and 180 min, monitored by AU-PAGE (left PAGE pattern) and mass spectrometry (right). S (black): phosphorylated serine residues of α_{s1} -casein; S (blue): partially dephosphorylated serine phosphate residues of α_{s1} -casein; S (red): fully dephosphorylated serine phosphate residues of α_{s1} -casein.

3.2.2 Discussion of the dephosphorylation of α_{s1} -casein

The AU-PAGE results indicate that the heat treatment of 85°C for 5 minutes did not affect the charge of the caseins. The degree of dephosphorylation gradually increased as the incubation time with the enzyme increased. Proteins with a higher degree of dephosphorylation had more negatively charged phosphate groups removed and less total negative charge remained on the protein. Therefore, when the incubation time was increased and more serine residues were dephosphorylated, the migration distance of the proteins consistently decreased on the AU-PAGE (Figure 3.3). These findings are in agreement with a study by Molina et al. (2007) who reported that the migration distance of the dephosphorylated casein fractions was reduced on the AU-PAGE due to the modification of net charge.

The degree of dephosphorylation was manipulated by controlling the incubation time whilst keeping the temperature constant, and the results obtained are in agreement with a study by Lorenzen and Reimerdes (1992). The partial dephosphorylation of caseins can also be achieved by controlling the amount of bovine intestinal alkaline phosphatase added (Pearse et al., 1986). However, in the study carried out by Pearse et al. (1986), the AU-PAGE pattern did not show a considerable change in the degree of dephosphorylation by simply controlling the amount of phosphatase added when compared with controlling the incubation time of dephosphorylation, as shown in Figure 3.3. This might be due to the fact that the phosphatase is very active at its optimal pH and temperature conditions, and in these experiments the level of phosphorylation is not able to be controlled within the experimental time frame when excess phosphatase is added at the optimal reaction conditions. Therefore, controlling the incubation time of dephosphorylation at defined temperatures and pH conditions is a more controlled approach for manipulating the level of dephosphorylation.

The dephosphorylation of α_{s1} -casein was observed when incubated with bovine intestinal alkaline phosphatase at pH 7.8. The dephosphorylated serine residues were monitored at different incubation times. Mass spectrometry showed that the serine residues gradually lost the phosphate groups during the incubation, and there were more phosphate groups lost as the incubation time increased (Figure 3.7). When the incubation time of dephosphorylation of α_{s1} -casein reached 180 minutes, the phosphoserine residues 1, 2, 4, 6 and 8 were completely dephosphorylated. However, the phosphoserine residues 3, 5 and 7 were only partially dephosphorylated at an incubation time of 180 minutes.

The partial dephosphorylation might result from the fact that the alkaline phosphatase became unstable and less active when the incubation time increased to 180 min. The alkaline phosphatase is most stable in the pH range 7.5-9.5, the pH optimum for enzymatic activity is pH 8-10 at 25°C. The pH optimum will change depending upon the substrate, the substrate concentration, temperature and ionic strength (Latner et al., 1971). At constant temperature and substrate concentration,

the pH optimum decreases with increased ionic strength (Shukla, 2009). However, Shukla (2009) did not report the level of the change in the ionic strength that affects the pH optimum of the enzyme. The concentration of the α_{s1} -casein solution was around 1.2 mM, and each α_{s1} -casein molecule has eight phosphate groups. Each phosphate group was assumed to have two negative charges at pH 7.8. When the dephosphorylation incubation time increased close to 180 min, the released phosphate groups in the solution were predicted to increase the ionic strength of the solution environment by 20 mM when fully dephosphorylated. The physiological ionic strength is generally in the range 100 to 200 mM (Scopes, 1993). At lower than the physiological value, the enzyme activity is normally not affected. Thus, a change in the ionic strength of 20 mM due to the released inorganic phosphate from the α_{s1} -casein to the solution is not considered sufficient to cause an extensive inhibition of phosphatase.

Although the small change in ionic strength does not have an impact on the phosphatase activity, the released inorganic phosphate is reported to be a strong inhibitor of alkaline phosphatase (Coburn et al., 1998; Shukla, 2009). Iqbal (2011) has reported that increasing the concentration of serum phosphate from ~0 to 0.1 mM led to a significant reduction in the activity of alkaline phosphatase at pH 9.8 (Figure 3.8). This is due to the inorganic phosphate binding to the active sites of the alkaline phosphatase, which inhibit a substrate from entering the active sites and consequently inhibiting the enzyme catalysed reaction (Fernley & Walker, 1967). When the α_{s1} -casein was fully dephosphorylated at pH 7.8, the concentration of inorganic phosphate in the serum phase increased from ~0 to 9.6 mM. This increase in the level of serum phosphate could cause a substantial inhibition of alkaline phosphatase. On the other hand, the alkaline phosphatase has a lower activity at pH 7.8 than pH 9.8. Therefore, the experimental conditions and inorganic phosphate levels may have contributed to the partial dephosphorylation of serine residues 3, 5 and 7 of α_{s1} -casein at incubation time of 180 min.

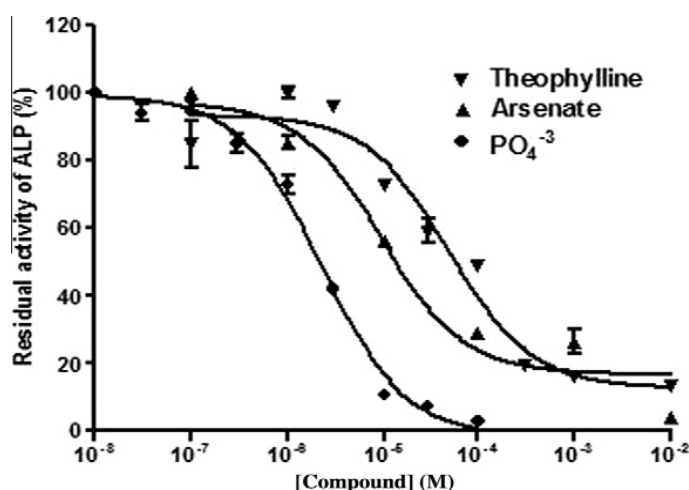


Figure 3.8 The effect of concentration of theophylline, arsenate and PO_4^{3-} on the inhibition of calf intestinal alkaline phosphatase at pH 9.8 (Iqbal, 2011).

The dephosphorylation of casein fractions has been examined in previous studies using mass spectrometry (Koudelka et al., 2009; Molina et al., 2007). Molina and co-workers have reported that random dephosphorylation occurs in both α - and β -casein when incubated with potato acid phosphatase at pH 5.8, although proteolysis of α -casein was also observed. Their results revealed that six phosphate groups were successfully removed in 89.2% dephosphorylated α -casein, including phosphate groups 1, 2, 4, 6, 7 and 8 (Molina et al., 2007). Therefore, the dephosphorylation of α_s -casein was induced by either the potato acid phosphatase with a proteolytic effect or alkaline phosphatase without a proteolytic effect.

In summary, mass spectrometry along with the AU-PAGE method confirmed that the level of dephosphorylation of α_{s1} -casein can be manipulated by controlling the incubation time with alkaline phosphatase. Furthermore, incubation with alkaline phosphatase for 180 minutes led to almost complete dephosphorylation of α_{s1} -casein.

3.2.3 Isoelectric point of dephosphorylated α_{s1} -casein

The results obtained from AU-PAGE analysis indicated that the total negative charge of dephosphorylated α_{s1} -casein decreased as the dephosphorylation time increased. This was predicted to result in an isoelectric point (pI) difference between the native and dephosphorylated α_{s1} -casein. The pI is the pH value at which the zeta potential is approximately zero. In this section, the pI of the native and dephosphorylated α_{s1} -casein was examined by measuring the zeta potential using both laser Doppler electrophoresis and IEF-PAGE (as described in Section 2.2.9 and 2.2.6, respectively). The laser Doppler electrophoresis technique offers a simple, fast and accurate way to measure the zeta potential of colloidal particles. IEF-PAGE is a type of zone electrophoresis performed by running the proteins in a gel matrix. It has an advantage that the overall charge on the protein of interest is a function of the pH of its surrounding environment.

Calculation of theoretical pI

The theoretical charges of native and dephosphorylated α_{s1} -casein with pH were calculated. The α_{s1} -casein sequence without phosphate groups was extracted from the Uniprot database (access code: P02662) and inserted into the SCRIPPS protein calculator V 3.4 (<http://protcalc.sourceforge.net>) to calculate the relationship between pH and protein charge. The charge of phosphate groups at different pHs was then calculated with the CurTiPot software package (Gutz, 2012). The pK_a values of phosphate groups used for the charge calculation were $pK_{a1} = 2$ and $pK_{a2} = 6.2$ (Connors, 1986). One to nine phosphate groups were added to the non-phosphorylated α_{s1} -casein. The total charge of α_{s1} -casein containing one to nine phosphate groups was calculated at different pHs. Finally, the plot of pH versus charge of α_{s1} -casein containing zero to nine phosphate groups was generated to demonstrate the shift in the isoionic point of α_{s1} -casein with phosphorylation level (Figure 3.9). The isoionic point is different from the pI in that pI is the pH value at which the net charge of proteins, including bound ions is zero, whereas the isoionic point is the pH where the protein has a net zero charge in a deionized solution.

Therefore, the isoionic point and pI are equal when the concentration of charged species in the solution is zero.

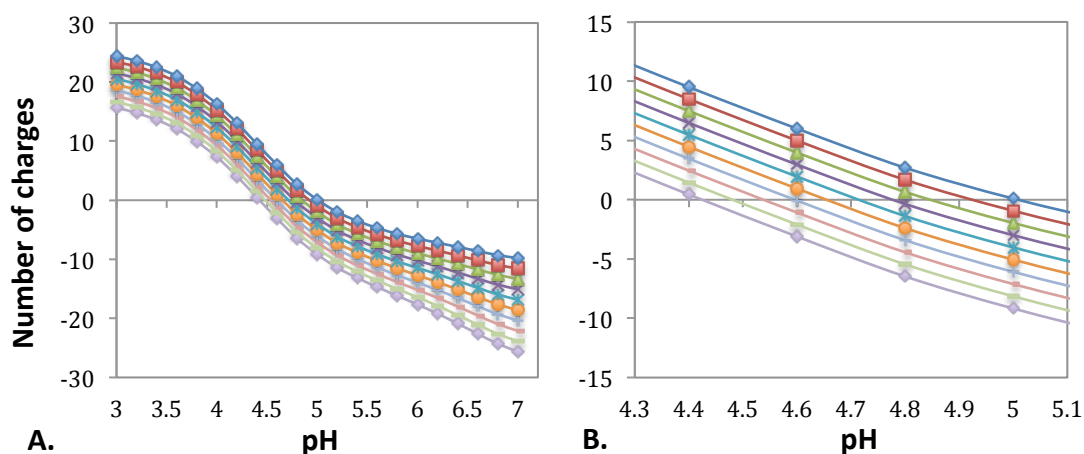


Figure 3.9 A. The calculated charge of α_{s1} -casein with different numbers of phosphate groups (zero to nine) at pH range of 3.0 to 7.0. **B.** The calculated charge of α_{s1} -casein with different numbers of phosphate groups (zero to nine) at pH over the range of 4.2 to 5.2. α_{s1} -Casein with 9 (\blacklozenge), 8 ($-$), 7 ($-$), 6 ($+$), 5 (\bullet), 4 ($*$), 3 ($*$), 2 (\blacktriangle), 1 (\blacksquare) and 0(\blacklozenge) phosphate groups.

The curves of calculated charge versus pH for α_{s1} -casein gradually shifted from lower to higher pH values as the phosphate group content decreased (Figure 3.9). This indicates that the isoionic point of α_{s1} -casein increased as the phosphate group content decreased. The change in the isoionic point with the number of phosphate groups is plotted in Figure 3.10.

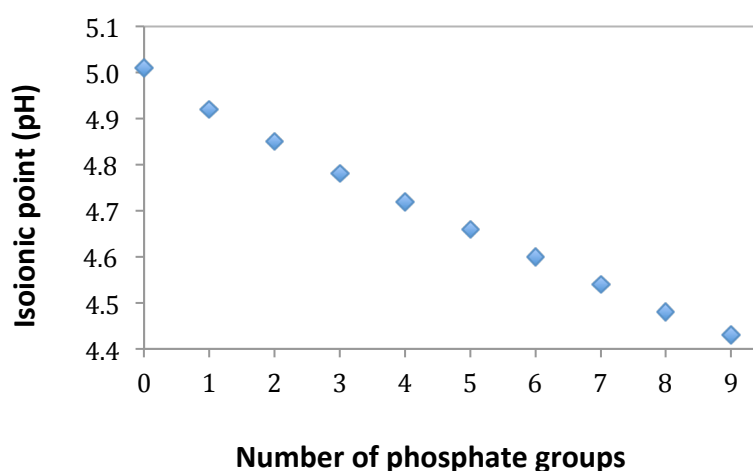


Figure 3.10 The isoionic pH of α_{s1} -casein with different numbers of phosphate groups attached.

The isoionic pH of α_{s1} -casein was predicted to increase when the level of dephosphorylation increased from 0% to 100% (Figure 3.10). The isoionic point of α_{s1} -casein with 100% dephosphorylation (i.e. when the 8 phosphate groups were completely removed) increased by about 0.51 pH units when compared with native α_{s1} -casein. This is due to the fact that the negative charge was reduced as the level of dephosphorylation increased.

Zeta potential

When a particle with a charged surface is suspended in solution, the ions of opposite charge to that of the particle will re-distribute and concentrate at the surface of the particle. The liquid layer surrounding the particle forms an inner layer (Stern layer) and an outer layer (diffuse layer) on the surface of the particle. The ions are strongly bound at the inner layer and less firmly associated at the outer region. A slipping plane is inside of the outer layer and the ions and particles form a stable entity within the outer layer. When a particle moves, ions within the boundary move with it. Those ions beyond the boundary stay with the bulk dispersant. The potential at this boundary is the zeta potential (Figure 3.11).

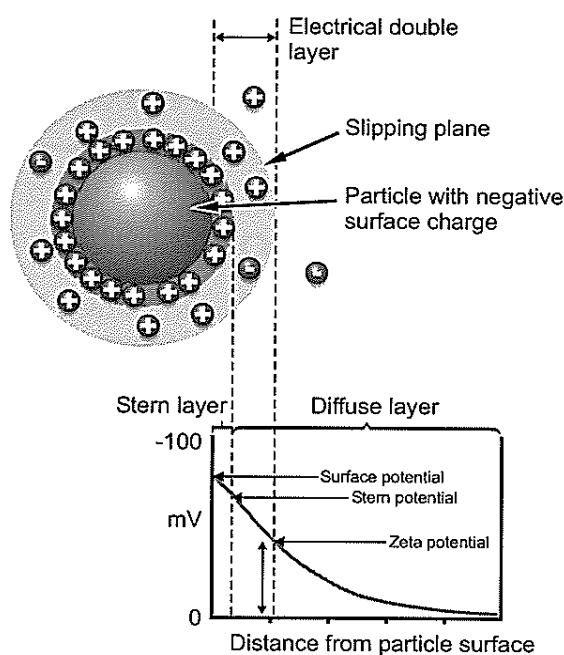


Figure 3.11 Schematic representation of the zeta potential of a particle. Source: Instruction Manual of Malvern-Instrument (Malvern-Instruments, 2007).

The multi-purpose titrator (MPT2) used in conjunction with a Zetasizer allows for the automatic determination of isoelectric points of proteins (Morand et al., 2011b). Proteins are negatively charged when the pH of the protein solution is higher than its pI and, in that situation, the zeta potential of proteins have negative values. Proteins are positively charged when the pH is lower than the pI of protein, and then the zeta potential of proteins has a positive value. When the pH of proteins reaches their pI, proteins have no charge on their surface, and the zeta potential has a zero value. Therefore, the apparent pI of proteins corresponds to the pH value where proteins have a zeta potential of zero.

After dephosphorylation, the net negative charge of α_{s1} -casein decreased and the proteins need fewer positive charges to reach their pI in comparison to native α_{s1} -casein. Therefore, the higher the level of dephosphorylation and the more negative charge was removed from serine residues, the higher the pI of dephosphorylated α_{s1} -casein.

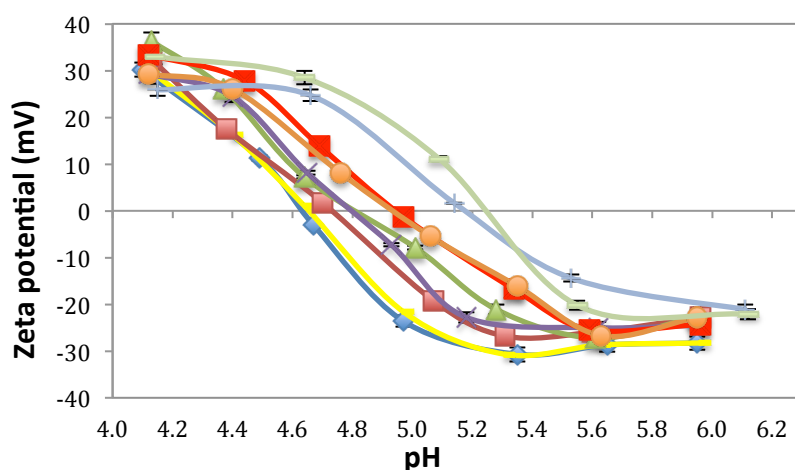


Figure 3.12 Zeta potentials of the native and dephosphorylated α_{s1} -casein at different incubation times: standard sample (native α_{s1} -casein without heat treatment, \blacklozenge); control sample (native α_{s1} -casein with heat treatment at 85°C for 5 min, —); α_{s1} -casein incubated with alkaline phosphatase at incubation time: 5 min (\blacksquare), 20 min (\blacktriangle), 30 min (\ast), 60 min (\blacksquare), 90 min (\bullet), 120 min (\blackplus), 180 min (— green). Each data point is an average of two replicates. Error bars represent the standard deviation of the mean of the replicates.

The α_{s1} -casein showed a negative zeta potential at low pH and a positive zeta potential at high pH (Figure 3.12). Figure 3.12 also shows the different shape of the curve in comparison to Figure 3.9, which is due to the fact that zeta potential is measured from the surface charge of proteins and the calculated pI is based on the overall net charge of proteins.

The pH where the α_{s1} -casein sample had a zero zeta potential was shifted from pH 4.66 to pH 5.25 as the incubation time increased (Figure 3.12 and Figure 3.13). This indicates that the apparent pI of dephosphorylated α_{s1} -casein increased as the incubation time increased. The zeta potential results also indicate that the heat treatment of α_{s1} -casein at 85°C for 5 min did not affect the pI of α_{s1} -casein. The pI of dephosphorylated α_{s1} -casein at an incubation time of 180 min increased about 0.59 to 0.61 units in comparison to standard or control samples.

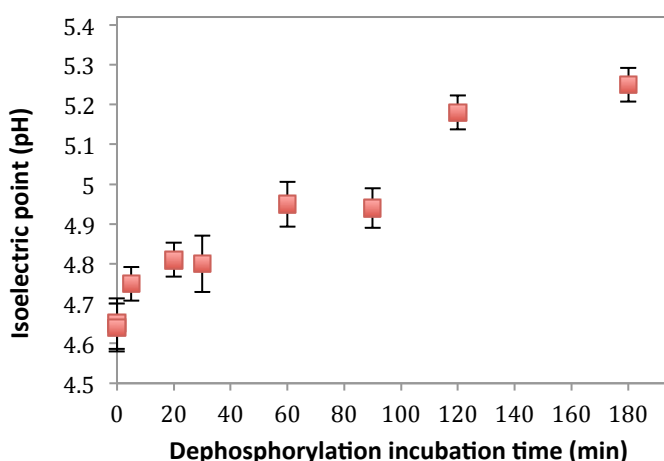


Figure 3.13 The isoelectric point of dephosphorylated α_{s1} -casein at different incubation times. Each data point is an average of two replicates. Error bars represent the standard deviation of the mean of the replicates.

IEF-PAGE

Isoelectric focusing electrophoresis (IEF) separates proteins according to their isoelectric point. The separation is performed on a polyacrylamide gel that contains a mixture of ampholytes that establish a stable pH gradient. For a protein in a pH

region below its isoelectric point, the protein is positively charged and therefore migrates towards the cathode. If the protein is in a pH region above its isoelectric point, it is negatively charged and therefore migrates towards the anode. The charge of the protein will decrease as the protein migrates through the pH gradient towards the electrode of opposite charge. When the protein reaches the pH that corresponds to its isoelectric point, the protein has a zero net charge and stops migrating (Figure 3.14; Alberts et al., 2007; Allen et al., 1984).

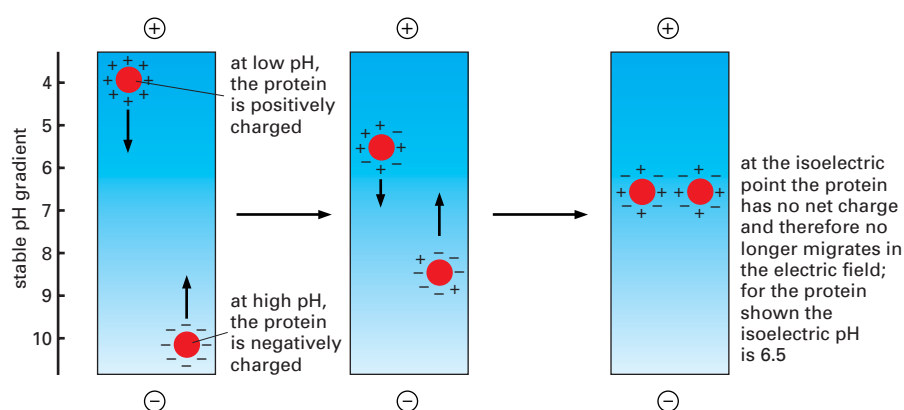


Figure 3.14 Separation of protein molecules by isoelectric focusing (Alberts et al., 2007).

IEF-PAGE does not determine the exact pI values of the proteins, but it can corroborate the pI change and any pI shift of proteins (Kim & Jimenez-Flores, 1994). After dephosphorylation of α_{s1} -casein, its net charge was reduced and therefore the apparent pI was increased. The IEF-PAGE showed the shift in apparent pI between the native and dephosphorylated α_{s1} -casein (Figure 3.15).

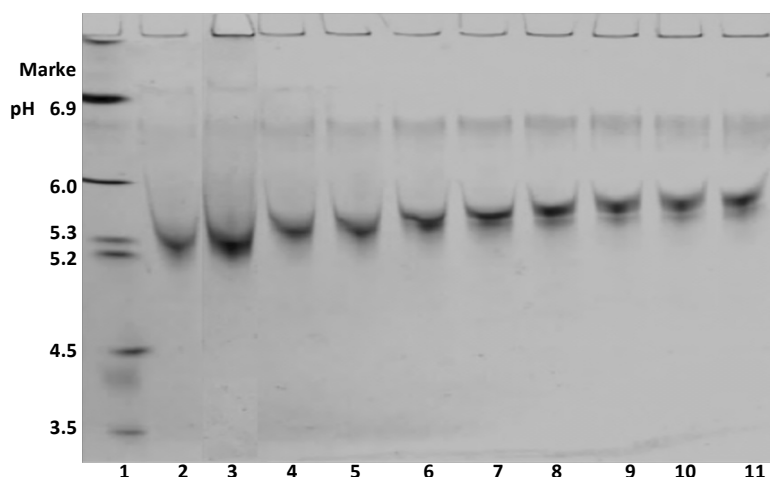


Figure 3.15 IEF-PAGE for the dephosphorylation of α_{s1} -casein at different incubation times. From left to right: pH marker (Lane 1); standard sample (native α_{s1} -casein without heat treatment, Lane 2); control sample (native α_{s1} -casein with heat treatment at 85°C for 5 min, Lane 3); α_{s1} -casein incubated with alkaline phosphatase at incubation time: 5 min (Lane 4), 10 min (Lane 5), 20 min (Lane 6), 30 min (Lane 7), 60 min (Lane 8), 90 min (Lane 9), 120 min (Lane 10), 180 min (Lane 11).

The IEF protein marker used for the IEF-PAGE experiments represented a pH range of 3.0 to 7.0 (Figure 3.15; Lane 1). There was no difference in the band positions between the standard and control α_{s1} -casein samples (Lane 2 and Lane 3). The bands representing the dephosphorylated α_{s1} -casein (Lanes 4 to 11) gradually shifted to higher positions compared to the native proteins (Lanes 2 and 3). This indicates that the dephosphorylated caseins have a shorter migration distance which represents a higher pH. The migration distance decreased as incubation time increased, which is due to the fact that the dephosphorylated α_{s1} -casein with reduced net charge will migrate a shorter distance to neutralise the net charge in comparison to native α_{s1} -casein.

The IEF-PAGE shows that the pI of α_{s1} -casein increased with increasing incubation time of dephosphorylation. The standard and control samples gave similar pI values around pH 5.25 (Lanes 2 and 3) and the pI of dephosphorylated α_{s1} -casein increased within the range of pH 5.25 to 5.85 as the incubation time of dephosphorylation increased from 5 minutes to 180 minutes (Lanes 4 to 11). Across the range of

incubation times, the observed apparent pI of dephosphorylated α_{s1} -casein increased from pH 5.25 to 5.85 (Figure 3.15 and Figure 3.16).

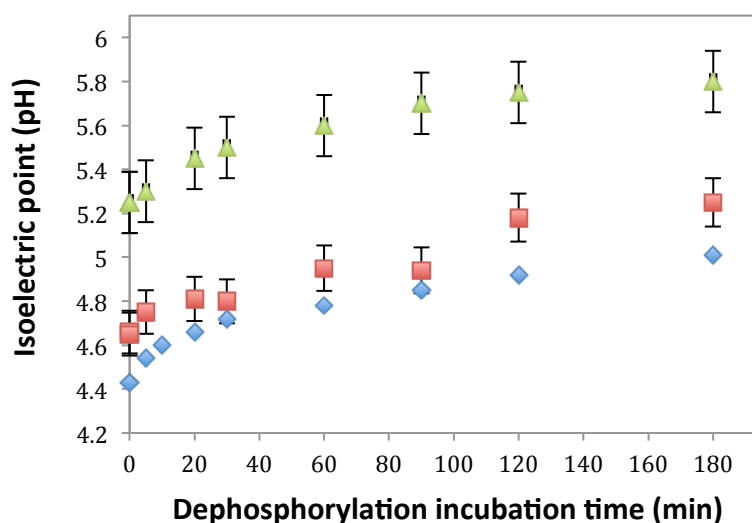


Figure 3.16 The isoelectric point of dephosphorylated α_{s1} -casein at different incubation times that were determined using IEF gel (\blacktriangle), zeta potential measurement (\blacksquare) and charge calculation (\blacklozenge). Each pI value from IEF gel is an average of two replicates. Error bars represent the standard deviation of the mean of the replicates.

In order to compare zeta potential, IEF and charge calculation methods for the pI measurement, the pI values from the various methods are plotted in Figure 3.16. The relative change in pI of dephosphorylated α_{s1} -casein calculated by the plot of charge versus pH is in agreement with the results from the zeta potential and IEF measurements, which showed that the pI increased by approximately 0.6 units when α_{s1} -casein is dephosphorylated for 180 minutes (Figure 3.16). The IEF-PAGE data corroborate these results. Figure 3.16 shows that the IEF measurement gave a much higher pI value than charge calculation and zeta potential methods; whereas the pI results from zeta potential methods were slightly higher than by charge calculation. However, a linear relationship was found when the calculated pI was plotted against the pI from IEF gel ($R=0.99$, $p<0.0001$) and the pI from zeta potential measurement ($R=0.95$, $p<0.0001$) (Figure 3.17). Figure 3.17 confirmed that the charge calculation,

IEF gel and zeta potential methods provided consistent results and that dephosphorylation contributed to an increase in the pI of α_{s1} -casein.

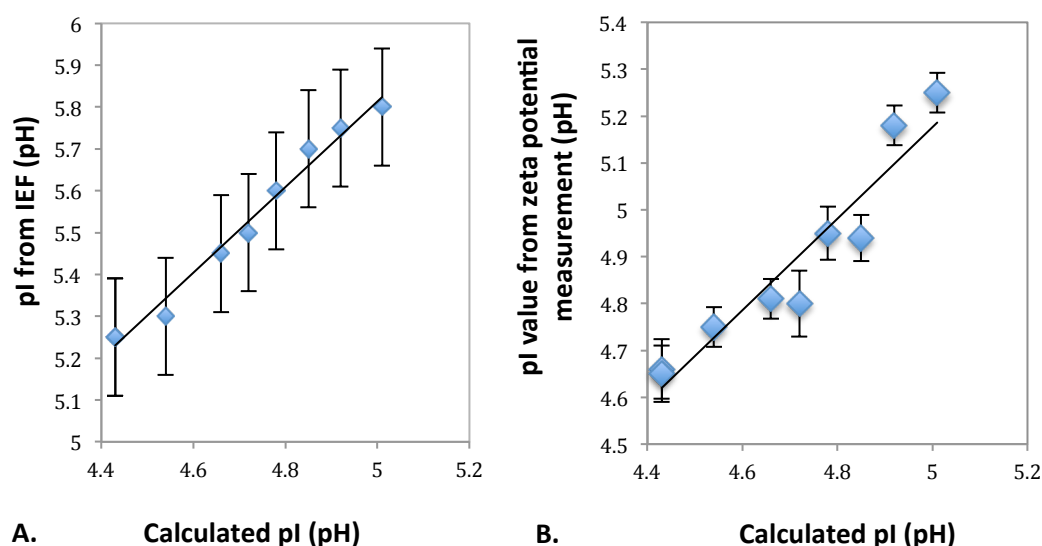


Figure 3.17 The relationship between charge calculation and IEF gel method (A), or charge calculation and zeta potential method (B) for measuring the pI of native and dephosphorylated α_{s1} -casein. Error bars represent the standard deviation of the mean of the replicates.

The pI of native and dephosphorylated α_{s1} -casein, as measured by zeta potential, was close to the isoionic point determined by charge calculation (Figure 3.16). This is due to the fact that the isoionic point was calculated assuming deionized water as a medium. By contrast, the zeta potential measurement was conducted in an ammonium bicarbonate buffer (1.67 mM) containing a very low level of salt (0.03 mM MgCl_2). The salt content in the buffer could affect the pI values by zeta potential measurement, as salt can shield the surface charge of proteins. Dukhin and Parlia (2014) have shown that the absolute value of the zeta potential of BSA decreased when the concentration of KCl increased from 0 to 0.4 M. On the other hand, zeta potential measurements only determine the surface charge of proteins; it does not measure the total charge of proteins. Therefore, the pI results from zeta potential measurement was slightly higher compared to charge calculation method, but the pI changes from both methods were comparable.

Unlike the zeta potential measurement, the pI measurement using IEF is based on the total net charge of proteins, which should provide pI values close to the theoretical pI from the charge calculation. However, the IEF gel measurement resulted in a higher pI value compared to that calculated, or that determined by the zeta potential measurement. In this study, commercial precast native IEF gels were used for pI measurement. Native IEF is often limited by the fact that proteins have low solubility close to their pI (Righetti, 1998). Therefore, when α_{s1} -casein migrates to a position close to its pI, the migration could be inhibited by the low solubility of α_{s1} -casein, which may result in a higher pI value in comparison to zeta potential and charge calculation methods. In this case, denaturing IEF is employed, in which reducing agents are often used in conjunction with urea for solubilisation of proteins (Righetti, 1998). However, urea is not stable in aqueous solution, so precast IEF gels are not manufactured with urea.

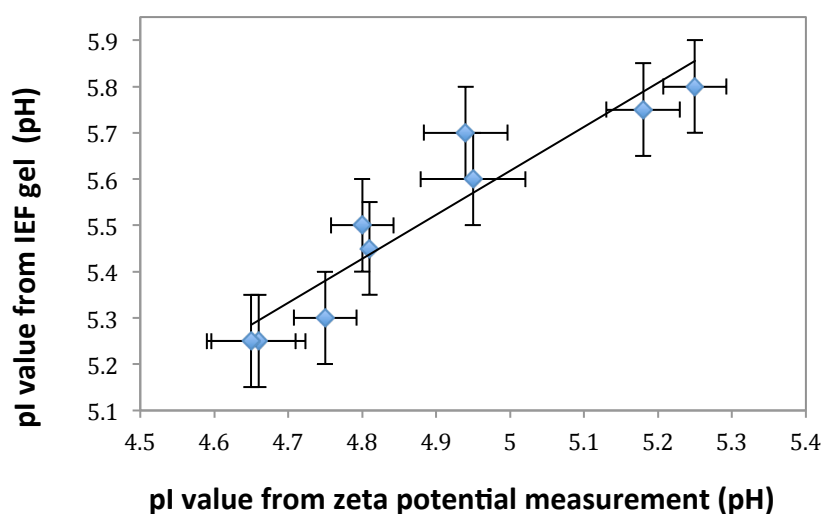


Figure 3.18 The relationship between zeta potential and IEF gel methods for measuring the pI of native and dephosphorylated α_{s1} -casein. Error bars represent the standard deviation of the mean of the replicates.

The pI values from IEF gel showed a reasonably linear relationship with the pI values from zeta potential measurement ($r=0.94$, $p<0.0001$) (Figure 3.18). Figure 3.18 shows that when the dephosphorylation incubation time of α_{s1} -casein increased

from 0 min to 180 min, the pI increased from pH 4.65 to pH 5.25 and pH 5.25 to 5.85 measured by zeta potential and IEF gel, respectively.

The observation that dephosphorylation increases pI is consistent with previous findings. For example the pI of β -casein was measured by IEF gels and the results showed that the dephosphorylation of β -casein decreased the overall net negative charge of the N-terminal sequence. As a result, the pI of dephosphorylated β -casein was increased to a higher pH compared to native β -casein (Darewicz et al., 1999). The pI determined using IEF-PAGE of dephosphorylated β -casein increased to pH 6.48 compared to native β -casein, which had a pI of 5.72. The β -casein sequence without phosphate groups was extracted from the Uniprot database (access code: P02666). Figure 3.19 shows that the isoionic point of β -casein shifted from pH 5.20 to pH 4.75, when 4 phosphate groups were removed from native β -casein. Although different phosphatase and casein fractions were used in the study of Darewicz et al. (1999) in comparison to this study, which used alkaline phosphatase and α_{s1} -casein, the same general effect of dephosphorylation was observed. Darewicz et al. (1999) showed that the pI values of β -casein obtained from the IEF gel is higher than the pI values determined from charge calculations, which was also observed in this study.

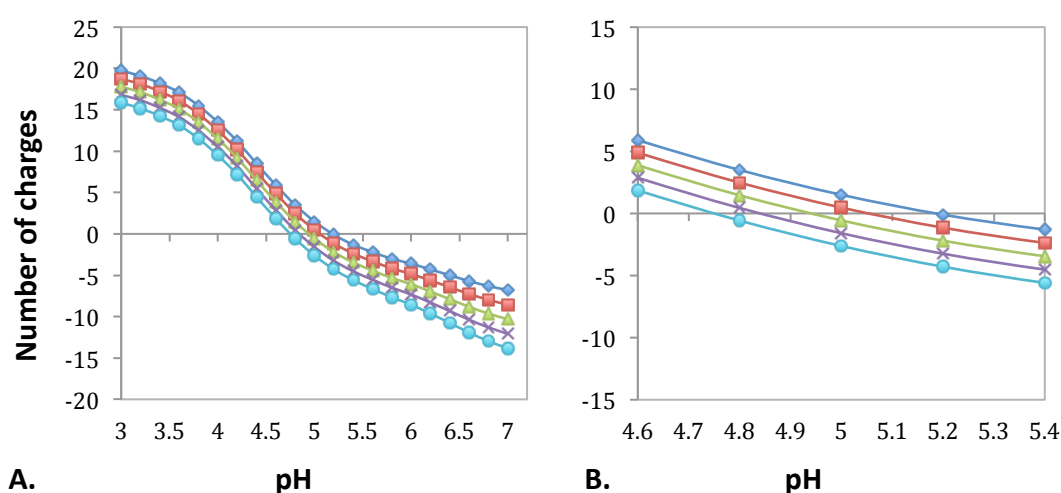


Figure 3.19 A. The charge of β -casein with different numbers of phosphate groups (0-4) over the pH range of 3.0 to 7.0. **B.** The charge of β -casein with different numbers of phosphate groups (0-4) over the pH range of 4.6 to 5.4. β -Casein with 4 (●), 3 (×), 2 (▲), 1 (■) and 0 (◆) phosphate groups.

3.2.4 Hydrophobicity of dephosphorylated α_{s1} -casein

Surface hydrophobicity of milk proteins is related to their surface functional properties, such as those responsible for emulsifying and foaming (Moro et al., 2001). In early studies, reversed phase-high pressure liquid chromatography results showed slight changes in the retention times of α_{s1} -casein and β -casein as a result of dephosphorylation (Strange et al., 1991). This indicated that the hydrophobicity of casein fractions was modified by dephosphorylation. After dephosphorylation, the decreased net charge of α_{s1} -casein was predicted to change the apparent hydrophobicity of α_{s1} -casein. Thus, measurements of the surface hydrophobicity may provide an indication of changes in the functionality of α_{s1} -casein. In this study, the apparent hydrophobicity of both native and dephosphorylated α_{s1} -casein was examined using an ANS fluorescence probe and an SDS colorimetric assay (as described in Section 2.2.11 and 2.2.10, respectively).

SDS binding assay

The SDS colorimetric assay used was adapted from Kato et al. (1984). This method has been used previously to determine the hydrophobicity of modified soy proteins (Hettiarachchy et al., 1995). In their study, the hydrophobicity of modified soy proteins increased in comparison to unmodified soy proteins. In addition, an ANS method was used as a cross-reference method for the hydrophobicity measurement in that study, which also showed an increase in the hydrophobicity of modified soy proteins compared to unmodified proteins. However, the ANS results suggested greater increases in hydrophobicity than the SDS results.

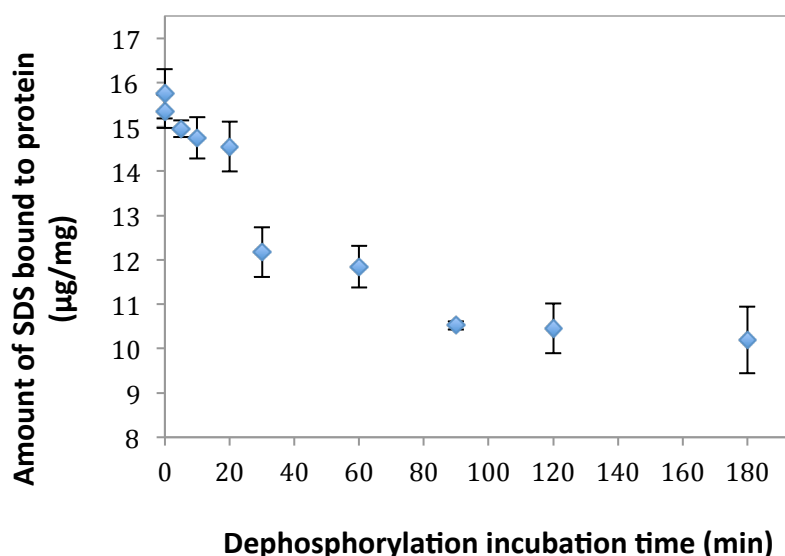


Figure 3.20 Amount of SDS (μg) bound per mg of α_{s1} -casein for native α_{s1} -casein and α_{s1} -casein dephosphorylated for different times. Each data point is an average of two to four replicates. Error bars represent the standard deviation of the mean of the replicates.

In this study, the amount of SDS bound to α_{s1} -casein was found to decrease as the dephosphorylation time increased (Figure 3.20). When the dephosphorylation incubation time increased from 0 to 180 min, the amount of SDS bound to α_{s1} -casein decreased from 16 to 9.5 $\mu\text{g}/\text{mg}$. In addition, Figure 3.20 shows that there was no significant difference in the amount of SDS bound to standard and control samples.

The results presented in Figure 3.20 indicated that the hydrophobicity of α_{s1} -casein decreased progressively as it was dephosphorylated, if the amount of SDS bound to protein is an indication of hydrophobicity. However, the hydrophobicity of α_{s1} -casein was expected to increase after dephosphorylation, which is contrary to the results from SDS binding. Phosphoserine residues of α_{s1} -casein are responsible for the existence of hydrophilic areas of strong negative charge (Varnam, 2012). A hydrophobic portion of a protein can be turned into a very hydrophilic portion by adding a phosphate ion (PO_4^{3-}) to a polar R group of an amino acid residue (López et al., 2012). Thus, removing the phosphate groups and negative charge from the phosphoserine residues is expected to make α_{s1} -casein less hydrophilic rather than

decrease the hydrophobic portion of α_{s1} -casein (Darewicz et al., 2000; Meyer et al., 1981; Molina et al., 2007; Strange et al., 1991; Yeung et al., 2001).

The reduction in the amount of bound SDS might be due to the self-association behaviour of α_{s1} -casein. The self-association of α_{s1} -casein is affected by the hydrophobicity and net charge of proteins (Horne, 1998; Horne, 2002). Thus, dephosphorylation could lead to an increase in the self-associated species of α_{s1} -casein due to the reduced net charge, with more hydrophobic regions of α_{s1} -casein buried in the interior of the associated structure. The results from analytical ultracentrifuge measurement showed an increase in the self-association behaviour of dephosphorylated α_{s1} -casein (as described in Section 3.2.5).

SDS has a hydrophobic tail that interacts strongly with the hydrophobic regions of a protein. The amount of SDS binding depends on the structure of the protein, for example, it was reported that BSA bound only 0.9 g of SDS per gram of protein without reduction, but 1.4 g upon reduction of disulphide bonds (Pitt-Rivers & Impiombato, 1968; Reynolds & Tanford, 1970). The amount of SDS used in this study was around 0.02 g of SDS per gram of α_{s1} -casein, which is not sufficient to disrupt the self-associated behaviour of α_{s1} -casein. Thus, it is possible that the SDS only coated the surface of the self-associated species of α_{s1} -casein and could not access the internal hydrophobic regions, resulting in less SDS binding to the dephosphorylated α_{s1} -casein.

ANS fluorescence probe

ANS is a fluorescent “hydrophobic probe” that can bind to the exposed hydrophobic regions of proteins. The quantum yield of fluorescence and the wavelength of maximum fluorescence emission of ANS are dependent on the polarity of the environment. The unbound ANS probe has a low fluorescence intensity in aqueous solution. When ANS binds to the hydrophobic regions of proteins, the fluorescence intensity increases (Koudelka et al., 2009; Wu et al., 1998). The ANS fluorescence method is well established for determining the hydrophobicity of proteins (Koudelka et al., 2009). In this study, the hydrophobicity of dephosphorylated α_{s1} -casein was

measured using the ANS probe according to the method of Alizadeh-Pasdar and Li-Chan (2000). A plot of the initial slope (S_0) of the relative fluorescence intensity (RFI) versus protein concentration was used as an index of the protein hydrophobicity. A correlation between the charge and S_0 of α_{s1} -casein was determined.

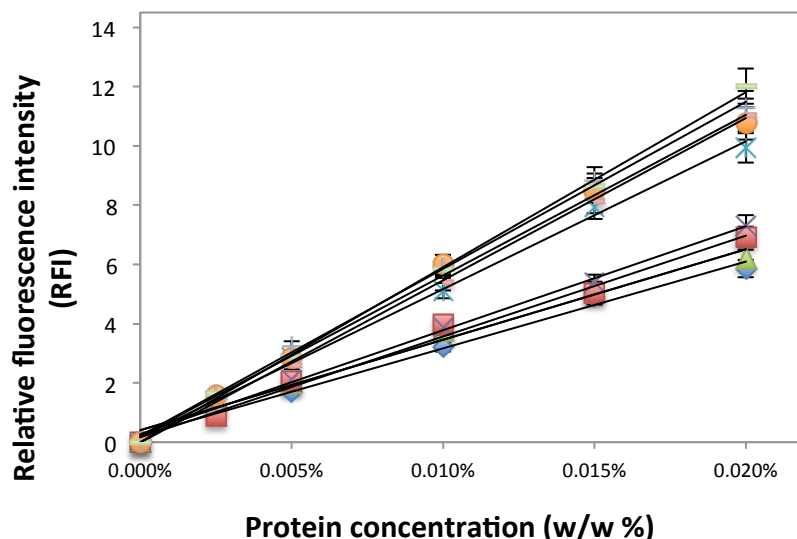


Figure 3.21 Relative fluorescence intensity of α_{s1} -casein: standard (◆), native α_{s1} -casein without heat treatment); control (▲), native α_{s1} -casein with heat treatment at 85°C for 5 min); α_{s1} -casein incubated with alkaline phosphatase at incubation time: 5 min (■), 20 min (×), 30 min (*), 60 min (●), 90 min (+), 120 min (-) and 180 min (-). Each data point is an average of three replicates. Error bars represent the standard deviation of the mean of the replicates.

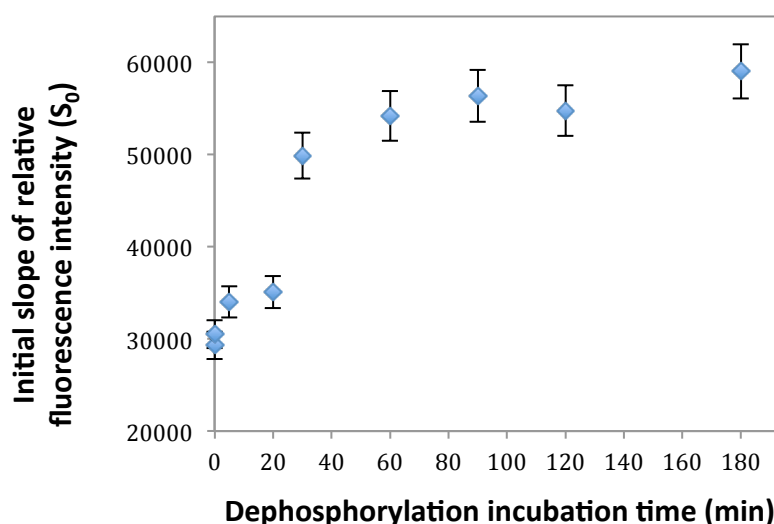


Figure 3.22 Initial slope (S_0) of the relative fluorescence intensity versus dephosphorylation incubation time of α_{s1} -casein. Error bars represent the standard deviation of the mean of the replicates.

The RFI of α_{s1} -casein was found to increase as the protein concentration increased (Figure 3.21). The RFI of dephosphorylated α_{s1} -casein over a protein concentration range of 0.0025% to 0.02% increased as the incubation time of dephosphorylation increased (Figure 3.21). There was no noticeable difference in the S_0 change between the standard and control samples (Figure 3.22). This indicates that the heat treatment (85°C, 5 min) did not affect the hydrophobicity of α_{s1} -casein. The S_0 significantly increased when the incubation time of dephosphorylation increased from 0 to 60 min, and then plateaued between incubation times of 60 and 180 min (Figure 3.22). The RFI results indicated that dephosphorylation led to an apparent increase in hydrophobicity of α_{s1} -casein. The hydrophobicity of dephosphorylated α_{s1} -casein incubated for 180 minutes almost doubled in comparison to the standard sample.

There are reports that using ANS as a probe for determining protein hydrophobicity has limitations (Moro et al., 2001). Moro and co-workers suggested that the ANS probe can bind to proteins by both electrostatic and hydrophobic interactions, which may contribute to overestimating the hydrophobicity. However, other researchers

suggested that the hydrophobic interactions play a dominant role in the association between ANS and proteins rather than the electrostatic interactions (Kato & Nakai, 1980; Nakai et al., 1996). The ANS anion can bind to cationic groups of water-soluble proteins through ion pair formation (Matulis & Lovrien, 1998). However, dephosphorylation only removed the negatively charged phosphate groups from the phosphoserine residues of α_{s1} -casein, and did not modify the cationic groups of the proteins. Therefore, it is reasonable to attribute the increase in the RFI of dephosphorylated α_{s1} -casein to the increased hydrophobic binding of ANS rather than electrostatic interactions.

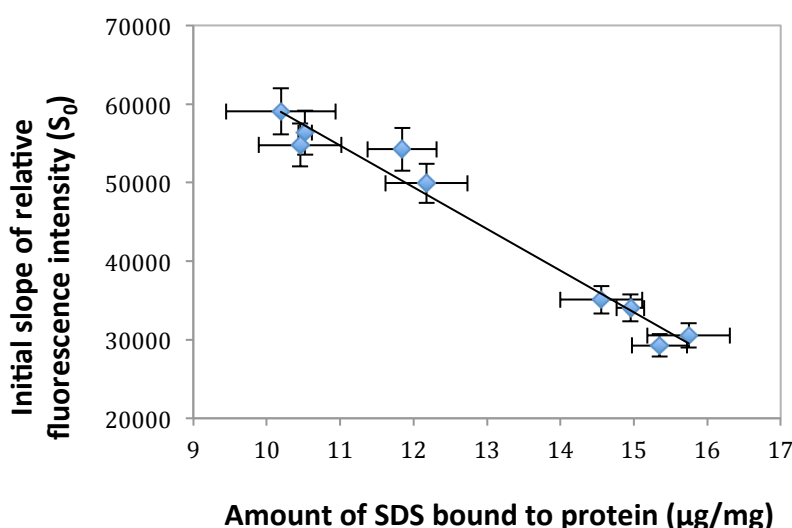


Figure 3.23 The relationship between SDS binding and ANS probe methods for measuring the apparent hydrophobicity of native and dephosphorylated α_{s1} -casein. Error bars represent the standard deviation of the mean of the replicates.

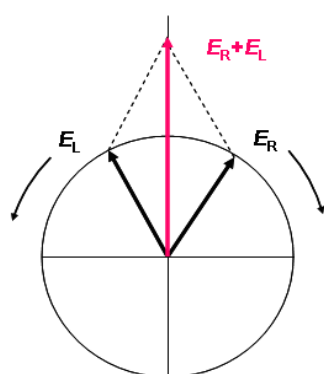
The ANS probe method showed that the apparent hydrophobicity of dephosphorylated α_{s1} -casein increased when compared with native α_{s1} -casein. However, the SDS binding method showed the opposite result from the ANS probe, where the hydrophobicity decreased as the level of dephosphorylation increased. The hydrophobicity results from the SDS binding method against ANS probe method were plotted (Figure 3.23). A linear inverse relationship between the SDS and ANS methods was observed ($r=0.99$, $p<0.0001$). Unlike SDS, ANS has a compact structure,

thus, ANS could access the buried hydrophobic regions of the self-associated α_{s1} -casein. The ANS fluorescence probe was chosen for hydrophobicity measurements in further studies, as it was considered to provide a more reliable measure of changes in hydrophobicity.

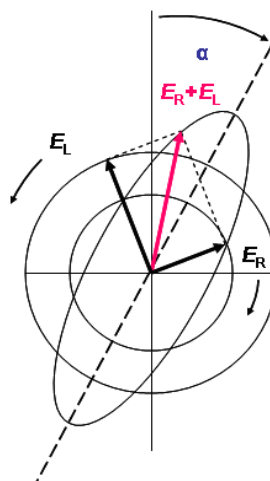
3.2.5 Secondary structure of dephosphorylated α_{s1} -casein

Circular dichroism (CD) refers to the differential absorption of two circularly polarized components of plane-polarized radiation of equal magnitude: one rotating counter-clockwise (left handed circular, L) and the other clockwise (right handed, R) (Solomon & Lever, 2006). After passage of plane-polarized radiation through the sample being examined, if the L and R components are not absorbed or are absorbed to equal extents, the recombination of L and R will regenerate radiation polarised in the original plane (Figure 3.24). However, if L and R are absorbed to different extents, the resulting radiation will produce elliptical polarisation (Figure 3.24; Berova et al., 2000). The CD spectrometer reports the difference in the absorbance between the L and R circularly polarized components in terms of the ellipticity (θ) in degrees (Kelly et al., 2005).

A1.



A2.



B.

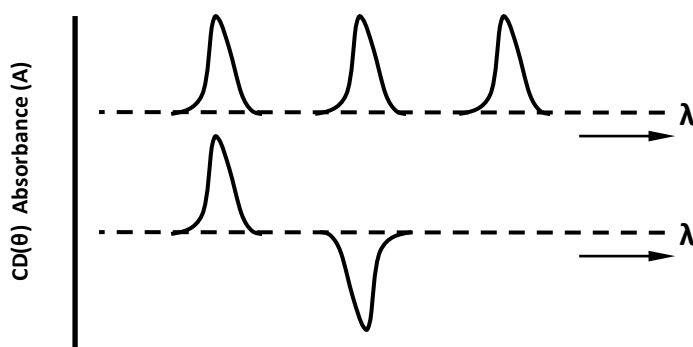


Figure 3.24 Origin of the CD effect. (A) The left (L) and right (R) circularly polarised radiation: (1) the two components have the same amplitude and when combined generate plane polarised radiation; (2) the components are of different magnitude and the resultant (dashed line) is elliptically polarised. (B) The relationship between absorbance and CD spectra. Band 1 has a positive CD spectrum with L adsorbed more than R; band 2 has a negative CD spectrum with R absorbed more than L; band 3 is due to an achiral chromophore (Kelly et al., 2005).

CD signals arise where the absorption of radiation occurs, and thus spectral bands are assigned to distinct structural features of proteins. The far UV CD spectra (≤ 240 nm) have been commonly used to estimate the secondary structure composition of proteins, which is due mainly to the peptide bonds (Berova et al., 2000; Kelly et al., 2005). The different types of regular secondary structure found in proteins give rise to a characteristic CD spectra in the far UV (Figure 3.25; Kelly et al., 2005).

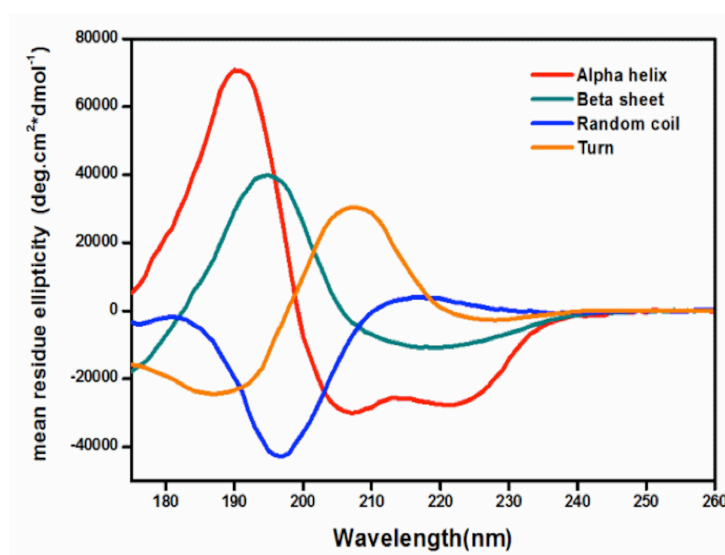


Figure 3.25 Far UV CD spectra associated with various types of secondary structure: α -helix, β -sheet, random coil and turn structure (Kelly et al., 2005).

When comparing the CD spectra of different proteins, or the same protein at different concentrations, or when using the data to estimate the secondary structure content, it is usual to normalise the machine units of millidegrees ellipticity by conversion to mean residue molar ellipticity using the following equation (Equation 3.1; Kelly et al., 2005).

$$\theta(deg.cm^2.dmol^{-1}) = \frac{Ellipticity(mdeg).10^6}{Pathlength(mm).[Protein](\mu M),n}$$

Equation 3.1

Where n is the number of peptide bonds in the protein and 'ellipticity' is the raw data from the instrument.

The dephosphorylation of α_{s1} -casein resulted in a decrease in the overall charge of α_{s1} -casein (as described in Section 3.2.2). This change in the charge of α_{s1} -casein might have an effect on the conformational arrangement of the protein. Therefore, the secondary structure of dephosphorylated α_{s1} -casein was compared with that of the native casein using CD spectrometry (see Section 2.2.13).

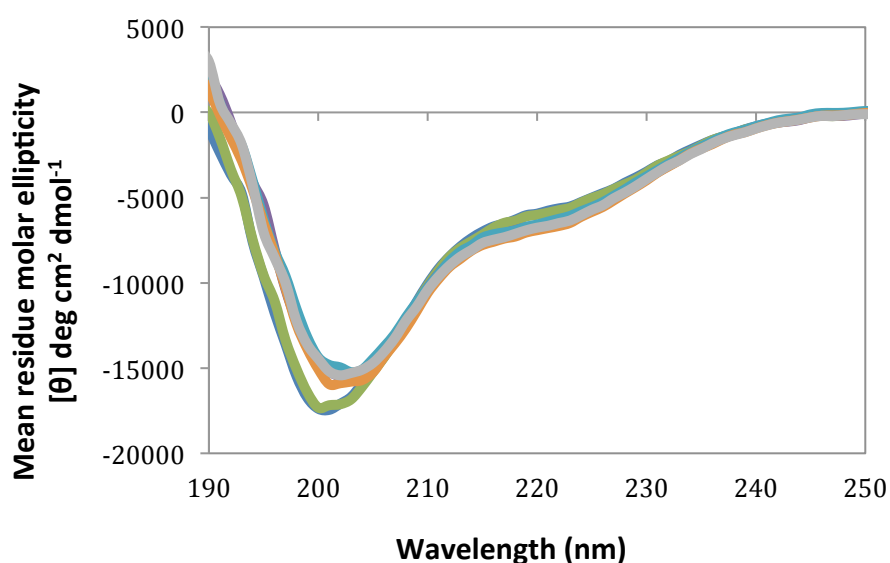


Figure 3.26 Effect of dephosphorylation levels on the far-UV CD mean residue ellipticity $[\theta]$ of α_{s1} -casein expressed in degree cm^2/dmol . Standard - native α_{s1} -casein (blue); control – native α_{s1} -casein with heat treatment at 85°C for 5 min (green); α_{s1} -casein incubated with alkaline phosphatase at incubation time: 20 min (purple), 60 min (light blue), 90 min (orange) and 180 min (grey). All α_{s1} -casein samples were measured at same protein concentration.

The far-UV CD spectrum showed that after dephosphorylation of α_{s1} -casein, the absolute value of mean residue ellipticity slightly increased between wavelength 190 and 205 nm and decreased between wavelength 215 and 230 nm (Figure 3.26). Kelly et al. (2005) have reported that the far-UV CD spectra of an α -helix exhibited troughs at 207 and 220 nm, respectively. The β -sheet exhibited a trough at 215 nm and a trough between 208 and 235 nm, whereas the random coil structure exhibited a trough at 197 nm and a trough between 180 and 210 nm.

The raw data from CD spectrum was inserted into a CD on-line analysis software package (<http://perry.freeshell.org/raussens.html>) to calculate the secondary structure (Raussens et al., 2003). The calculated secondary structural features for each composition spectrum in Figure 3.26 are given in Table 3.2. The standard and control samples contained 12% helix, 30% β -sheet and 40% random coil structure. The level of helix and β -sheet of native α_{s1} -casein is in agreement with the

studies of Kumosinski et al. (1993) and Malin et al. (2005) who reported that 8-15% α -helix, 18-40% β -sheet and 24-35% random coil was observed in native α_{s1} -casein using CD spectroscopy. However, the random coil structure (40%) observed in this study is higher when compared to previous studies (24-35%). The α_{s1} -casein sample used in this study contained ~10% (w/w) β -casein, and β -casein is reported to contain 42-72% random coil structure (Caessens et al., 1999; Graham et al., 1984). Thus, the impurity of β -casein in the α_{s1} -casein might account for the slightly higher levels of random coil structure. The level of secondary structure of native α_{s1} -casein has also been reported in previous studies, with a 13% α -helix and 20% β -sheet being determined using Raman spectroscopy (Horne, 2002; Michael Byler et al., 1988).

The levels of secondary structure of dephosphorylated α_{s1} -casein at different incubation times are also shown in Table 3.2. The amount of α -helix, β -sheet and random coil structure remains relatively invariant at about 12% ($p=0.10$), 30% ($p=0.09$) and 40% ($p=0.69$), respectively (Table 3.2). Although the effect of dephosphorylation on the secondary structure of α_{s1} -casein has not been reported before, Farrell Jr et al. (2002) have reported that dephosphorylation of β -casein showed little or no secondary structural changes of the protein, which is consistent with the results for α_{s1} -casein.

Table 3.2 The level of secondary structure of native and dephosphorylated α_{s1} -casein estimated by CD (fifteen accumulations for one determination; standard error given for three determinations, standard errors less than 1 are not stated).

Dephosphorylation incubation time (min)	α -Helix (%)	β -Sheet (%)	Random coil (%)
0 min standard	12 \pm 1	30 \pm 1	40 \pm 1
0 min control	12 \pm 1	30	40 \pm 1
20 min	13 \pm 1	29 \pm 1	40
60 min	14	29	40 \pm 1
90 min	13	29 \pm 1	40
180 min	14	30	40

The far-UV CD spectra results confirm that the levels of secondary structure in native α_{s1} -casein are consistent with literature reports. The results indicate that neither the dephosphorylation nor heat treatment significantly affected the secondary structure of α_{s1} -casein.

3.2.6 Self-association behaviour of dephosphorylated α_{s1} -casein

In an analytical ultracentrifuge (AUC), a sample being spun can be monitored in real time through an optical detection system using ultraviolet light absorption (Figure 3.27). This technique can monitor the sample concentration versus the axis of rotation profile as a result of the applied centrifugal field. Two kinds of experiments are commonly performed on this instrument: sedimentation velocity experiments and sedimentation equilibrium experiments (Van Holde, 1975).

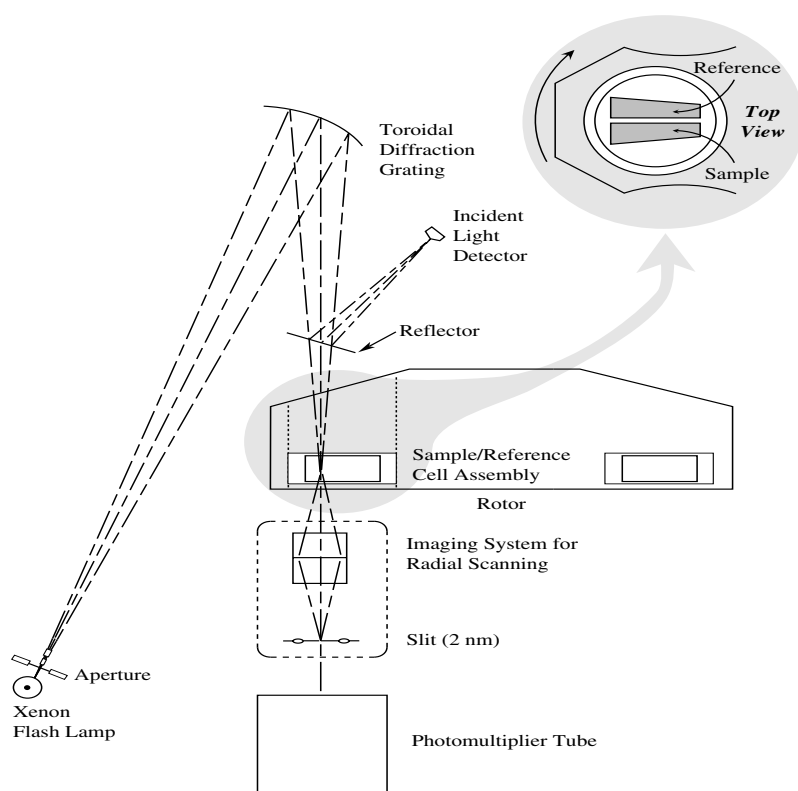


Figure 3.27 Schematic diagram of the optical system of the analytical ultracentrifuge (Beckman Optima XL-A Analytical Ultracentrifuge manual).

Sedimentation velocity experiments aim to interpret the entire time-course of

sedimentation, and report on the shape and molar mass of the dissolved macromolecules, as well as their size-distribution (Van Holde, 1975). The Lamm equation is applied to show the evolution of the concentration distribution variations of the molecules in a centrifugal field as a function of time with the two competing processes: diffusion and sedimentation terms (Equation 3.2).

Lamm equation:

$$\frac{\partial x(r,t)}{\partial t} = \frac{1}{r} \frac{d}{dr} \left[r D(r) \frac{dx(r,t)}{dr} - s(r) \omega^2 r^2 x(r,t) \right] \quad \text{Equation 3.2}$$

c : solute concentration (g/L)

t : time (sec)

ω : rotor angular velocity (radians/sec)

r : radial position (mm)

D : diffusion constant coefficient

S : sedimentation constant coefficient (10^{-13} sec)

Initially a uniform solution is placed in the cell and a sufficiently high angular velocity is used to cause relatively rapid sedimentation of solute towards the bottom of the cell. This produces a depletion of solute near the meniscus and the formation of a sharp boundary between the depleted region and the uniform concentration of the sedimenting solute (Figures 3.28). The rate of movement of this boundary is measured (Figure 3.29) which leads to the determination of the sedimentation coefficient, S (Equation 3.3). The sedimentation coefficient depends on the mass of the particles and inversely on the frictional coefficient, which is, in turn, a measure of effective size (Van Holde, 1975).

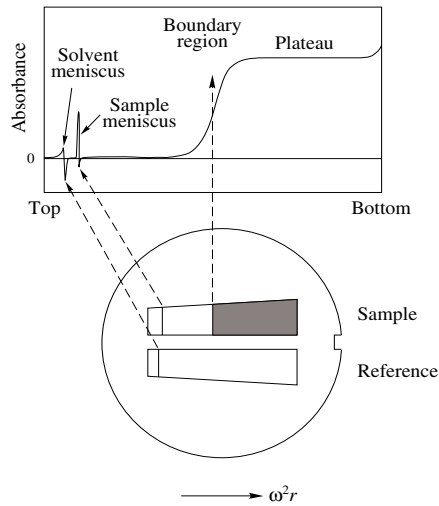


Figure 3.28 Double-sector centrepiece. The sample solution is placed in one sector, and sample of the solvent is placed in the reference sector. The reference sector is usually filled slightly more than the sample sector, so that the reference meniscus does not obscure the sample profile (Ralston, 1993).

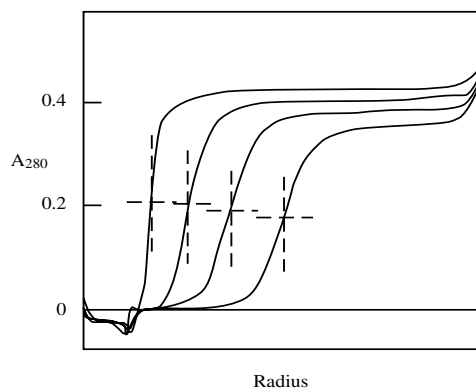


Figure 3.29 An example of an AUC experiment: movement of the boundary in a sedimentation velocity experiment with a recombinant malaria antigen protein. As the boundary progress down the cell, the concentration in the plateau region decreases from radial dilution, and the boundary broadens from diffusion (Ralston, 1993).

$$S = \frac{u}{\omega^2 r} = \frac{u}{\alpha} \quad \text{Equation 3.3}$$

α : centrifugal acceleration

ω : rotor angular velocity (radians/sec)

r : radial position (mm)

u : constant velocity

Measurement of the rate of spreading of a boundary can lead to the determination of the diffusion coefficient, D , which depends on the effective size of the particles:

$$D = \frac{RT}{Nf} \quad \text{Equation 3.4}$$

where R is the gas constant ($8.314 \text{ J mol}^{-1} \text{ K}^{-1}$) and T the absolute temperature in Kelvin.

The ratio of the sedimentation to diffusion coefficient gives the molecular weight:

$$M = \frac{s^0 RT}{D^0 (1 - v\rho)} \quad \text{Equation 3.5}$$

where M is the molar weight of the solute (g/mol), v its partial specific volume (mL), and ρ is the solvent density (g/mL) (Van Holde, 1975).

α_{s1} -Casein has been reported to exhibit self-association behaviour to form dimers, tetramers and hexamers, etc. The level of self-association is dependent on the protein concentration, pH, ionic strength and temperature of the solution (Ho & Waugh, 1965; Schmidt, 1970; Swaisgood, 2003). In order to understand the effect of charge and hydrophobicity on the self-association behaviour of α_{s1} -casein, the sedimentation velocity of native and dephosphorylated α_{s1} -casein was measured using an analytical ultracentrifugation method (see Section 2.2.14).

The native α_{s1} -casein showed a major peak at a sedimentation coefficient of 2 to 7 S, (Figure 3.30 A, B and C). The sedimentation distribution of the standard sample at a concentration of 1, 2 and 3 mg/mL was similar to the control samples (Figure 3.30 A). The higher sedimentation coefficient value corresponds to the larger size of associated species of proteins. The heat treatment at 85°C for 5 min for native α_{s1} -casein did not have a significant effect on the self-association behaviour of α_{s1} -casein.

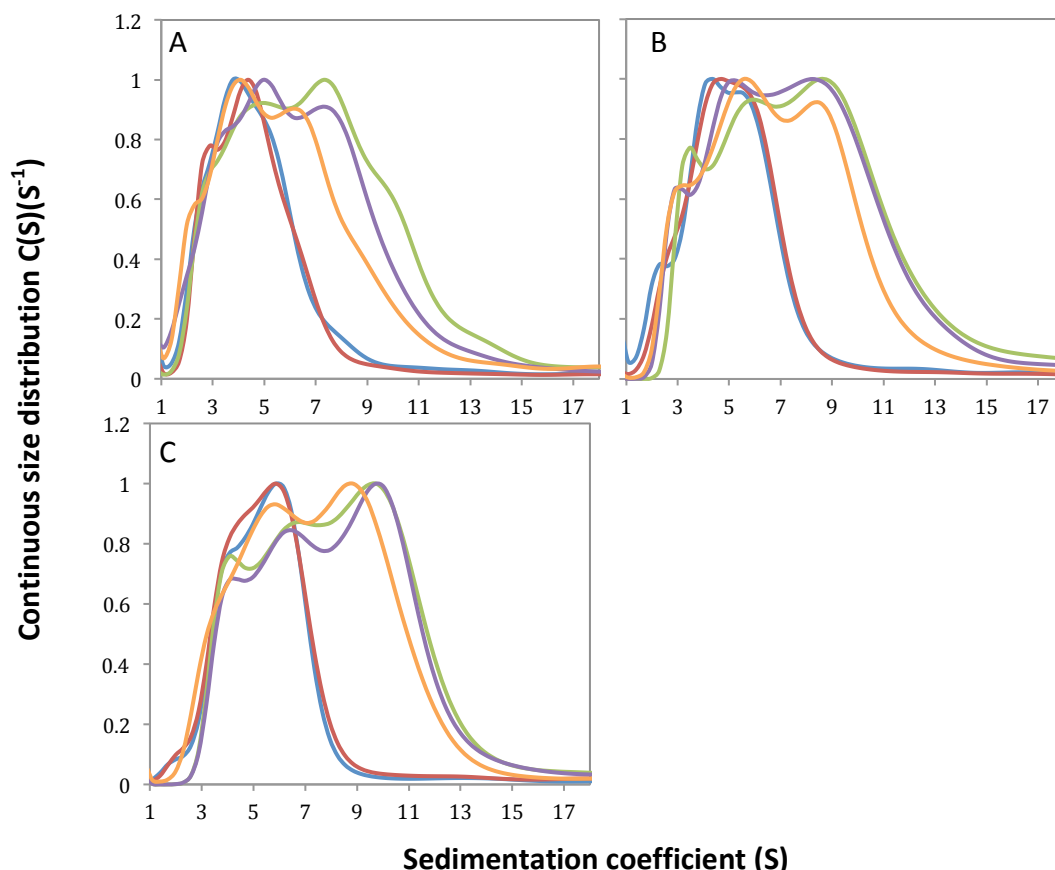


Figure 3.30 Sedimentation coefficient distribution of native and dephosphorylated α_{s1} -casein in 10 mM phosphate buffer (containing 2.7 mM KCl and 137 mM NaCl, pH 7.4) at protein concentrations of: A: 1 mg/mL, B: 2 mg/mL and C: 3 mg/mL. Standard native α_{s1} -casein (blue); control native α_{s1} -casein with heat treatment at 85°C for 5 min (red); α_{s1} -casein incubated with alkaline phosphatase at incubation time: 20 min (green), 60 min (purple) and 180 min (orange). Confidence level in all the measurements was set to 99% for the final fits. The sedimentation coefficient distribution of α_{s1} -casein was determined with rmsds of 0.0048 ± 0.0003 , 0.0050 ± 0.0005 , and 0.0053 ± 0.0003 for measurement A, B and C, respectively.

Dephosphorylation resulted in an increase in the sedimentation coefficient of α_{s1} -casein. The dephosphorylated α_{s1} -casein showed major peaks at a broad range of sedimentation coefficients from 3 to 11S (Figure 3.30 A, B and C). When the protein concentration increased to 3 mg/mL, the major sedimentation coefficient peak of

dephosphorylated α_{s1} -casein shifted to 11S with a low level of sedimentation coefficients distributed at 4 to 9S (Figure 3.30 C).

The sedimentation coefficient distribution results indicate that the dephosphorylated α_{s1} -casein exhibited a higher level of associated species compared to native α_{s1} -casein. The dephosphorylated α_{s1} -casein was found to contain a major species with large polymers. The formation of polymers is probably due to the fact that dephosphorylation resulted in an increase in the apparent hydrophobicity of α_{s1} -casein as the hydrophilic phosphate groups were removed from serine residues. Therefore, the higher level of self-association of dephosphorylated α_{s1} -casein may have occurred via increased hydrophobic interactions. In addition, the overall net charge of dephosphorylated α_{s1} -casein decreased, which led to a reduction in the electrostatic repulsion between α_{s1} -casein molecules.

The self-association of the α_{s1} -casein may be driven by hydrophobic interactions but the size of the polymers and degree of association is limited by electrostatic repulsions (Horne, 1998; Horne, 2002). The hydrophobic interactions of protein self-association lead the hydrophobic regions of proteins to be shielded at the inner layer of the associated species and expose the charged hydrophilic regions of proteins at the outer layer of the associated species. Therefore, further growth of the associated proteins is limited by the electrostatic repulsive interactions on the outer layer of the associated species. Consequently, decreasing the electrostatic repulsion allows the formation of larger associated species of caseins (Payens et al., 1969; Schmidt, 1970).

The self-association behaviour of α_{s1} -casein is dominated by the pH and ionic strength of the solutions. At 20 °C, pH 6.6 and an ionic strength of 0.003 M, only monomers are present. When the ionic strength increases, the monomers exist in a rapid equilibrium with oligomers, and a further increase in the ionic strength results in the appearance of larger oligomers in equilibrium with smaller oligomers and monomers (Ho & Waugh, 1965; Schmidt & Van Markwijk, 1968; Schmidt, 1970). However, when the ionic strength reaches 0.2 M, dimers and tetramers are favoured

while the formation of large oligomers becomes progressively less favourable (Ho & Waugh, 1965; Schmidt, 1970). Thus, at constant pH and temperature conditions, the buffer environment has a significant effect on the self-association behaviour of α_{s1} -casein.

At protein concentrations of 1, 2, and 3 mg/mL, α_{s1} -casein at dephosphorylation times of 180 min was found to contain a lower level of large associated species (sedimentation coefficient > 7S) compared to those dephosphorylated for 60 min and 20 min (Figure 3.30 A and B). This indicated that the longer dephosphorylation incubation times resulted in a lower level of large associated species in comparison to moderate incubation times.

The difference in the size of associated species between dephosphorylated α_{s1} -casein at different incubation times may be due to the change in the electrostatic repulsions. Under suitable conditions of pH, ionic strength, or in the presence of low levels of ionic calcium, the α_{s1} -casein could aggregate in a closed flower-like petal arrangement, which might appear in scattering studies as a spherical or plate-like particle (Horne, 2002). Dephosphorylation increased the size of self-associated α_{s1} -casein due to the increased hydrophobic interactions. However, the reduction in electrostatic repulsions within the self-associated polymer chain or the flower-like ring structure could be more intensive than between the self-associated structures, which lead the self-associated polymer chain or the flower-like ring structure to fold or shrink rather than the associated structure to further grow. The longer dephosphorylation incubation time resulted in a higher level of reduction in the electrostatic repulsions, which contributed to the higher level of folding or shrinking of the self-associated structures. Thus, the dephosphorylated α_{s1} -casein at longer incubation time formed a higher level of smaller oligomers.

3.3 Conclusions

α_{s1} -Casein was dephosphorylated using bovine intestinal alkaline phosphatase

without the interference from proteolysis that has confounded previous studies (Darewicz et al., 1999; Darewicz et al., 2000; Koudelka et al., 2009; Lichan & Nakai, 1989; Lorenzen & Reimerdes, 1992; Molina et al., 2007; Pearse et al., 1986; Pepper & Thompson, 1963). Dephosphorylation led to an increase in the apparent pI and surface hydrophobicity of α_{s1} -casein, but did not affect the secondary structure. However, the changes in the electrostatic repulsions and hydrophobicity enhanced the self-association behaviour of α_{s1} -casein as the level of self-associated α_{s1} -casein increased after dephosphorylation.

The findings of this chapter provide a starting point for understanding the correlations between the physicochemical and functional properties of proteins. The functionality of dephosphorylated α_{s1} -casein is investigated in next chapter.

Chapter 4 Functional properties of

dephosphorylated α_{s1} -casein

4.1 Introduction

In Chapter 3, it was demonstrated that the dephosphorylation has a significant effect on the physicochemical properties of α_{s1} -casein, impacting on the overall negative net charge, pI and hydrophobicity. All of these physicochemical parameters were able to be manipulated by controlling the incubation time of dephosphorylation.

Previous studies have shown that dephosphorylation can change the solubility, foaming ability, emulsion stability and calcium ion sensitivity of whole casein proteins (Darewicz et al., 1999; Meyer et al., 1981; Yeung et al., 2001). However, previous work on the dephosphorylation of casein proteins has not investigated how the physicochemical parameters impact on the functionalities of caseins. The correlation between physicochemical properties, interfacial properties and functional properties of α_{s1} -casein has not been well studied.

This chapter will discuss how the pI/charge, hydrophobicity and calcium binding affect the interfacial properties of α_{s1} -casein. In addition, this chapter will look at the impact of the physicochemical properties on the functionalities of α_{s1} -casein, such as the emulsifying activity and the foaming properties.

4.2 Results and discussion

4.2.1 Calcium ion binding of dephosphorylated α_{s1} -casein

An ion selective electrode (ISE) measures the activity of an ion in a solution by measuring the electric potential formed across a membrane when the electrode is submerged in the solution (Ross, 1967). A calcium ISE has a PVC membrane, which is

soaked with an organic molecule that selectively binds and transports Ca^{2+} ions. In the internal system of the calcium ISE, a fixed concentration of CaCl_2 is added to the KCl/AgCl solution of the reference system (Figure 4.1).

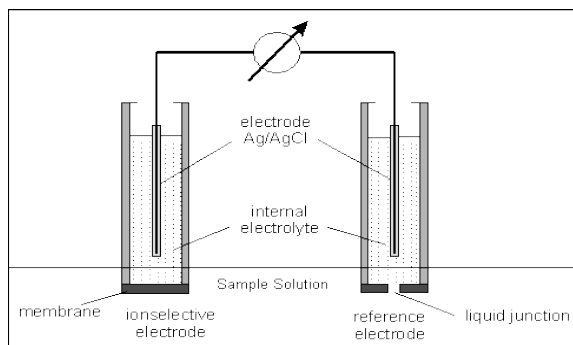


Figure 4.1 Schematic representation of the ion-selective electrode (Wojciech Wroblewski, CSRG, University of Warsaw, Poland).

When the electrode is dipped in a sample solution that contains calcium ions, the ions diffuse from the membrane side with higher concentration to the lower concentration, which is due to the diffusion pressure. The inside of the membrane is coated with positively charged ions, which corresponds to an increasing negative charge outside of the membrane. Therefore, an electrical potential difference occurs across the membrane, which causes the calcium ion migration to slow down. The calcium ions stop migration, when the diffusion pressure is balanced due to the difference in calcium ions concentration by the electrostatic repulsion (Arnold & Meyerhoff, 1984; Craggs et al., 1974; Koryta, 1986; Meyerhoff & Opdycke, 1986).

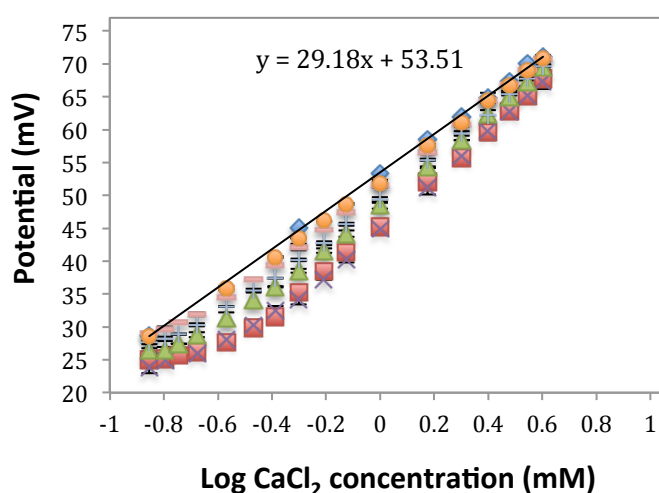
Inside the ISE, the positive charge at the membrane surface obtains electrons from the silver wire. Consequently, the silver ions in the internal reference system lose their charge and attach on the wire. Thus electrons are drawn through the external wiring from the meter and thence from the external reference electrode. Chloride ions migrate to the silver chloride-coated wire and combine with the silver ions. In order to balance the lost positive charge of calcium ions, potassium ions transfer into the sample solution across the liquid junction. The sum of all potential differences

formed in this system is measured in millivolts (mV) and expressed as the calcium ion activity (Craggs et al., 1974; Meyerhoff & Opdycke, 1986).

A unique attribute of casein is its phosphate group content, and these phosphate groups can bind calcium ions (Holt, 1985). The calcium ion binding capacity of α_{s1} -casein can be determined by a calcium ion activity measurement using an ion-selective electrode. The measured electrical potential of calcium ions represents the calcium ion activity, thus a high electrical potential correlates to lower calcium ion binding with α_{s1} -casein and a low electrical potential correlates to higher calcium ion binding with α_{s1} -casein.

The electrical potential for both the calcium ion standard and α_{s1} -casein samples increased when the calcium chloride concentration increased (Figure 4.2 A). However, the electrical potential of α_{s1} -casein within the calcium ion concentration ranges of 0.14 – 1.16 mM ($\log[\text{CaCl}_2]$ of -0.85 to 0.06) did not increase linearly like the calcium ion standard, except for the dephosphorylated α_{s1} -casein incubated for 180 min (Figure 4.2 A and B). This indicated that calcium ion binding with α_{s1} -casein occurred when the calcium ion was added into the α_{s1} -casein solution, and this resulted in a lower calcium ion activity compared to the calcium chloride standard sample. The dephosphorylated α_{s1} -casein sample incubated for 180 min and the standard calcium chloride both had a similar level of change in electrical potential (Figure 4.2 A), indicating that no significant calcium ion binding with α_{s1} -casein occurred in the dephosphorylated α_{s1} -casein incubated for 180 min. Figure 4.2 A demonstrates that at the calcium chloride concentration range above 1.16 mM ($\log[\text{CaCl}_2] > 0$), the electrical potential of all α_{s1} -casein samples linearly increased. Thus, there was no additional calcium ion binding with α_{s1} -casein formed at the higher calcium chloride concentration range.

A.



B.

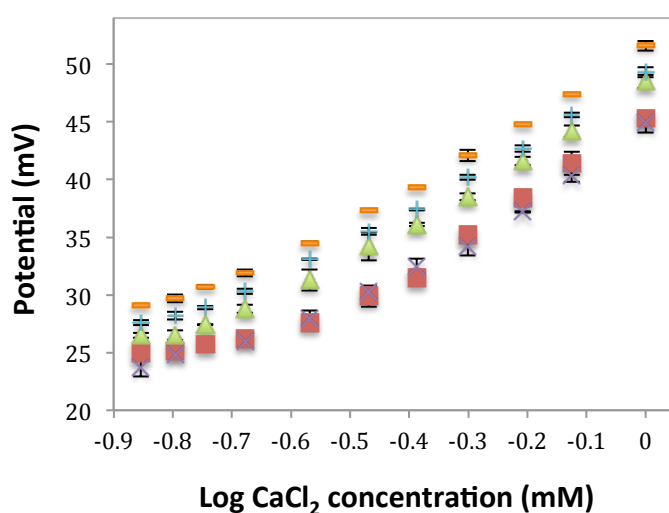


Figure 4.2 Electrical potential of dephosphorylated α_{s1} -casein containing different levels of calcium chloride measured using the ion-selective electrode. A. Potential of free calcium ions of α_{s1} -casein with the calcium ion concentration range of 0.14 mM – 4 mM. B. Potential of free calcium ions of α_{s1} -casein with the calcium ion concentration from 0.14 to 0.16 mM. CaCl_2 standard curve (\blacklozenge), standard-native α_{s1} -casein (\blacksquare), control-native α_{s1} -casein with heat treatment at 85°C for 5 min (\times), α_{s1} -casein incubated with phosphatase for 5 min (\blacktriangle), 30 min ($+$), 90 min ($-$) and 180 min (\bullet), respectively, followed by heat treatment. Each data point is an average of two replicates. Error bars represent the standard deviation of the mean of the replicates.

There is no noticeable difference in the electrical potential between the standard and control samples (Figure 4.2 A and B), indicating that there is no difference in the

calcium ion binding capacity between the samples. Figure 4.2 A shows that the standard and control samples had the lowest electrical potential compared to dephosphorylated α_{s1} -casein and the electrical potential increased as the incubation time of dephosphorylation increased. This was especially apparent in the calcium ion concentration ranges of 0.14 – 1.16 mM (Figure 4.2 B), where a significant difference was observed between the standard sample and dephosphorylated α_{s1} -casein with different incubation times. The Ca^{2+} binding capacity of dephosphorylated α_{s1} -casein decreased compared to the standard and control samples and the longer incubation time of dephosphorylation resulted in a lower Ca^{2+} binding capacity. The findings from this study are in agreement with the suggestion from previous work that dephosphorylation can decrease the calcium ion binding ability of casein fractions (Meyer et al., 1981; Yeung et al., 2001).

The levels of free calcium ions in the serum were calculated based on the electrical potential of α_{s1} -casein samples with the equation derived from the calcium ion standard curve in Figure 4.2. The calculated serum calcium ion concentration is given in Figure 4.3.

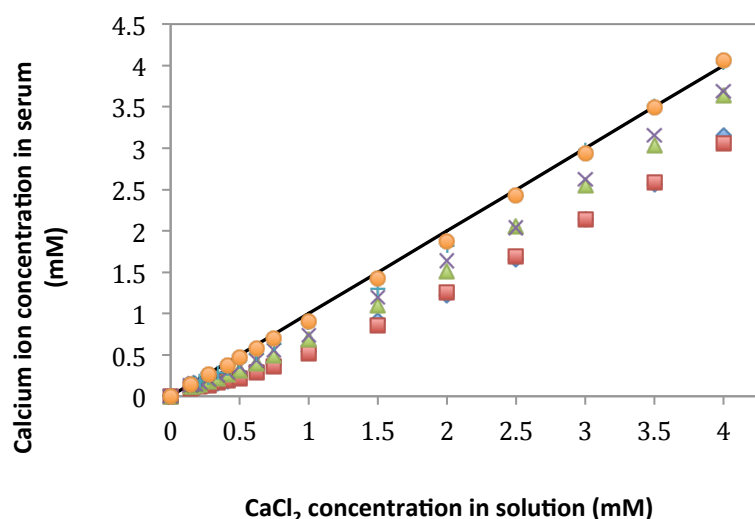


Figure 4.3 Calcium ion levels in the serum phase of standard CaCl_2 solution (solid line), standard-native α_{s1} -casein (\blacklozenge), control-native α_{s1} -casein with heat treatment at 85°C for 5 min (\blacksquare), α_{s1} -casein incubated with phosphatase for 5 min (\blacktriangle), 30 min (\times), 90 min ($+$) and 180 min (\bullet).

Figure 4.3 shows that the serum calcium ion level in the α_{s1} -casein samples increased with increased dephosphorylation time. The differences in the levels of serum calcium ion concentration between the standard curve and the α_{s1} -casein samples represent the levels of bound calcium ions in the α_{s1} -casein samples, which is given in Figure 4.4.

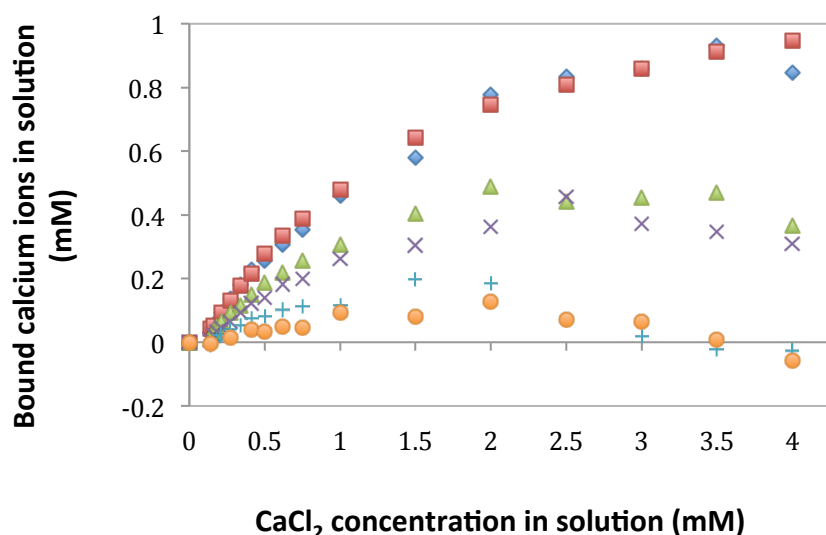


Figure 4.4 Bound calcium ion levels in standard-native α_{s1} -casein (◆), control-native α_{s1} -casein with heat treatment at 85°C for 5 min (■), α_{s1} -casein incubated with phosphatase for 5 min (▲), 30 min (×), 90 min (+) and 180 min (●).

Figure 4.4 shows that the curves of bound calcium ions in α_{s1} -casein samples shifted to lower values as the dephosphorylation incubation time increased. When the concentration of calcium chloride in the samples increased, the levels of bound calcium ions increased and then plateaued as they reached the maximum level of calcium ion binding. The curve of bound calcium ions of dephosphorylated α_{s1} -casein at an incubation time of 180 min showed very small changes (Figure 4.4). There are two negative values of the levels of bound calcium in dephosphorylated α_{s1} -casein at incubation times of 90 and 180 min, which suggested that the calcium ion content in the samples was slightly higher than the standard curve. This could be a result of slight variations in titration concentrations of calcium ions. The results from Figure 4.4 indicate that during the calcium chloride titration, a higher level of dephosphorylation resulted in a faster saturation of calcium binding in α_{s1} -casein consistent with the loss of serine phosphate groups.

In order to obtain the maximum level of bound calcium ions in α_{s1} -casein samples from Figure 4.4, the units of the levels of bound calcium ions (mM) and serum calcium ions (mM) were converted to mg/g (amount of bound calcium ions per gram of α_{s1} -casein) and g/L, respectively. These experimental calcium ion binding data (Figure 4.3 and 4.4) were fitted using a Langmuir model in the computer program R (Version 3.3.2 GUI) to obtain the best fit non-linear curve (Tercinier et al., 2013).

The Langmuir model is commonly used for protein adsorption on surfaces. It calculates the level of adsorbed proteins on a surface (Luo & Andrade, 1998; Mura-Galelli et al., 1991; Wahlgren & Arnebrant, 1991). This model is ideally used for a monolayer adsorption system that assumes the sorbate species binds to a series of distinct sites on a solid surface of sorbent. A sorbate complex is formed between the binding sites and empty sites on the surface of sorbent. The adsorption process will stop when an equilibrium is established between the bound sorbate species and the serum sorbate (Mura-Galelli et al., 1991; Wahlgren & Arnebrant, 1991). In this study, the calcium binding of α_{s1} -casein was assumed as a single layer adsorption process, as α_{s1} -casein has a polymer chain structure that can be assumed as a monolayer surface.

In the Langmuir model, the maximum amount of bound calcium ions on α_{s1} -casein (q_m , mg/g) and the Langmuir affinity constant (K , L/g) were calculated using the Langmuir Equation 4.1.

$$q = q_m \times \frac{Kp}{1+Kp} \quad \text{Equation 4.1}$$

Where q is the bound calcium ions on α_{s1} -casein (mg/g), p is the calcium ion concentration at equilibrium, which is the same as the serum calcium ion concentration (g/L).

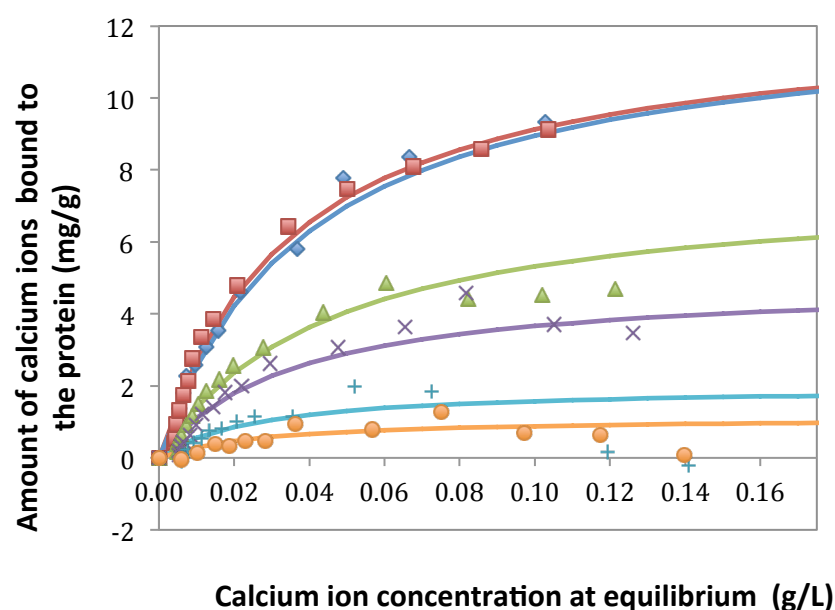


Figure 4.5 Isotherms of calcium ions bound to α_{s1} -casein and the fitted Langmuir model curves (solid line). Standard-native α_{s1} -casein (\blacklozenge), control-native α_{s1} -casein with heat treatment at 85°C for 5 min (\blacksquare), dephosphorylated α_{s1} -casein at incubation times of 5 min (\blacktriangle), 30 min (\times), 90 min ($+$) and 180 min (\bullet).

Using the Langmuir model, the non-linear curves of calcium ions binding to α_{s1} -casein were plotted against the concentration of free calcium ions in the serum (Figure 4.5). In order to obtain the best-fit curve, the negative values of bound calcium ions were excluded from the Langmuir model. Figure 4.5 shows that there is no difference in the curve between native α_{s1} -casein and heat-treated α_{s1} -casein. When the dephosphorylation incubation time increased, the curves plateaued at a lower level of bound calcium ions. This indicates that the maximum amount of bound calcium ions on α_{s1} -casein decreased when the level of dephosphorylation increased (Table 4.1 and Figure 4.6). The q_m and K values were obtained from the average of the repeated measurements. Based on the analysed data in the Langmuir model, the difference in the q_m values of replicated measurements were only observed in the second decimal place, thus, the accuracy of the q_m measurement is at least 1 decimal place. In this experiment, the Langmuir model provided the best fit for the maximum calcium ion binding analysis, but not for the affinity constant. Therefore, the K values were unchanged by the treatment.

Table 4.1 Parameters for the calcium ions binding on to α_{s1} -casein calculated using the Langmuir model.

Dephosphorylation Incubation time (min)	Affinity constant, K (L/g)	Maximum binding, q_m (mg/g)	Maximum binding q_m (M/M)
0 -standard	25.6 ± 3.8	12.5 ± 0.8	7.4 ± 0.5
0 -control	28.2 ± 2.9	12.4 ± 0.5	7.3 ± 0.3
5	22.3 ± 4.7	7.7 ± 0.9	4.6 ± 0.5
30	28.8 ± 7.8	4.9 ± 0.5	2.9 ± 0.3
90	28.5 ± 3.8	2.0 ± 0.5	1.2 ± 0.3
180	25.4 ± 5.5	1.1 ± 0.3	0.7 ± 0.2

The maximum levels of bound calcium ions to α_{s1} -casein were calculated in moles from the parameter q_m (mg/g) and these are given in Table 4.1. Table 4.1 shows that the heat treatment did not affect the calcium binding to α_{s1} -casein. In theory, native α_{s1} -casein can bind 8 M calcium ions, as it contains eight phosphoserine residues. Native α_{s1} -casein bound 7.35 M calcium ions, which is close to the maximum if each phosphate group binds one calcium ion. The α_{s1} -casein sample used in this study contained ~10% (w/w) β -casein that has 4-5 phosphoserine residues. This contamination could lead to the experimental calcium binding being slightly lower than the theoretical binding. The results from Table 4.1 were plotted against the zeta potential results in Figure 4.6, which shows that when the apparent pI of dephosphorylated α_{s1} -casein increased, the level of bound calcium decreased.

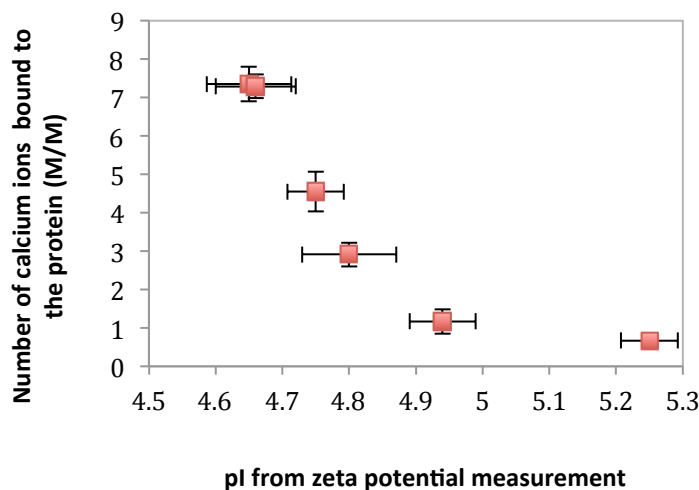


Figure 4.6 Bound calcium ions on α_{s1} -casein at different pI values of dephosphorylated α_{s1} -casein.

The apparent pI of α_{s1} -casein increased with increased dephosphorylation incubation time, which is due to the increased loss of net charge of α_{s1} -casein (as described in Section 3.2.2 and 3.2.3). This is consistent with the results from experimental calcium ion binding, as the calcium ion binding gradually decreased with increased dephosphorylation incubation time (Figure 4.6). The isoionic point of α_{s1} -casein at different dephosphorylation incubation times was calculated based on the predicted numbers of dephosphorylated serine residues (as described in Section 3.2.2). When the calcium ion binding based on the predicted numbers of dephosphorylated serine residues was calculated and plotted against the experimental calcium ion binding, a non-linear relationship was found (Figure 4.7). The number of calcium ions bound to the α_{s1} -casein decreased when the net charge of proteins decreased. Therefore, the prediction of dephosphorylated serine residues at different incubation times reasonably indicated the change in the calcium ion binding of dephosphorylated α_{s1} -casein.

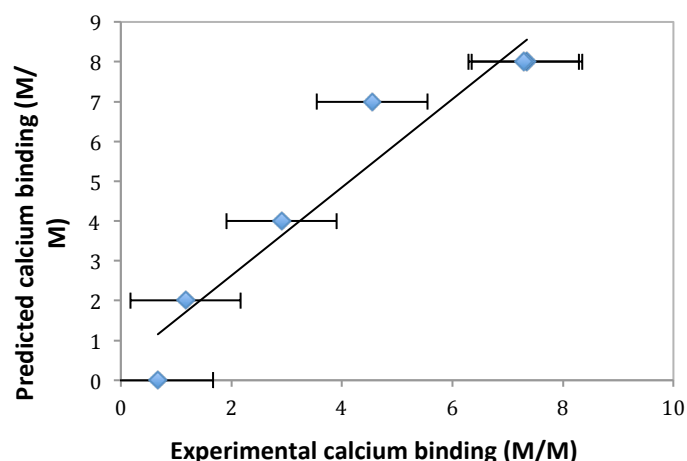
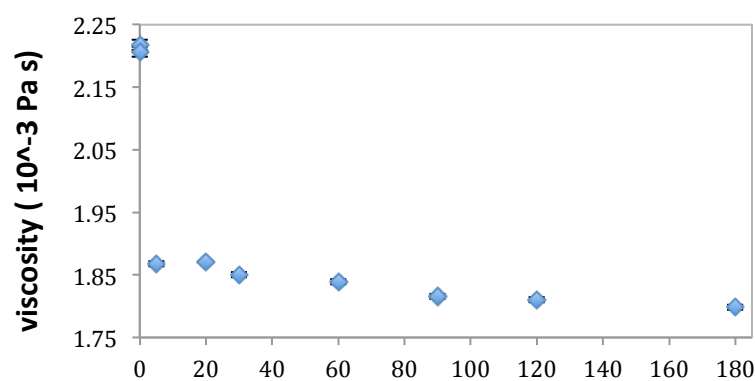


Figure 4.7 The relationship between predicted calcium ion binding and experimental calcium ion binding.

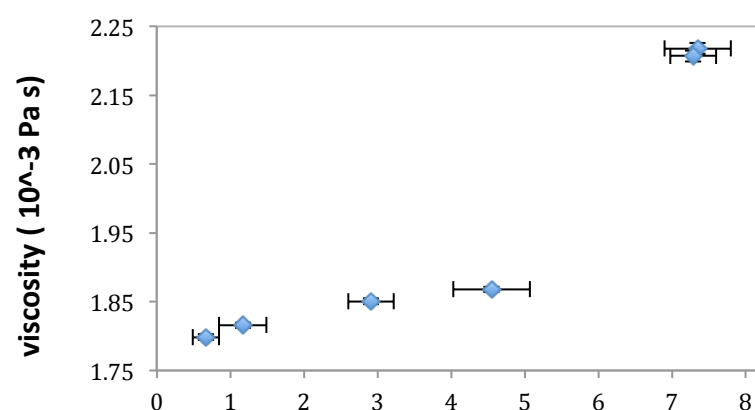
Dephosphorylation led to a significant increase in the surface hydrophobicity of α_{s1} -casein when the incubation time of dephosphorylation increased from 0 to 60 min, and a plateau between an incubation time of 60 and 180 min (as described in Section 3.2.3). In the experimental calcium ion binding study, a major reduction in the levels of bound calcium ions was observed between native α_{s1} -casein and dephosphorylated α_{s1} -casein at 90 min incubation time, and a minor reduction between the incubation times of 90 and 180 min (Figure 4.6). The change in the surface hydrophobicity of dephosphorylated α_{s1} -casein is mostly consistent with the results of experimental calcium ion binding.

4.2.2 Viscosity of dephosphorylated α_{s1} -casein

The results from Section 3.2.2 showed that the overall net negative charge of α_{s1} -casein decreased and the apparent hydrophobicity increased as the incubation time of dephosphorylation increased. These modified physicochemical parameters might also affect the functional properties of α_{s1} -casein. Therefore, the viscosity of dephosphorylated α_{s1} -casein was determined using a capillary viscometer (as described in Section 2.2.16).



A. Dephosphorylation incubation time (min)



B. Experimental calcium ions binding (M/M)

Figure 4.8 Viscosity of dephosphorylated α_{s1} -casein solutions incubated with phosphatase for different times (A). Viscosity of dephosphorylated α_{s1} -casein that bound to different numbers of calcium ions (B). Each data point is an average of three replicates. Error bars represent the standard deviation of the mean of the replicates.

The viscosity of the dephosphorylated α_{s1} -casein solutions decreased in comparison to the standard and control samples (Figure 4.8 A). Figure 4.8 A also shows that there was only a moderate reduction in the viscosity between dephosphorylated α_{s1} -casein incubated for 5 min and 180 min in comparison to the viscosity reduction between the standard and dephosphorylated α_{s1} -casein incubated for 5 min. This is consistent with the results of experimental calcium binding that a big reduction in the calcium binding for the dephosphorylated α_{s1} -casein incubated for 5 min (Figure 4.8 B). In addition, there was no noticeable difference in viscosity between standard and control samples.

These observations can be explained by the negative charge on the hydrophilic phosphate groups of α_{s1} -casein contributing to an electrostatic repulsion. Buzzell and Tanford (1956) reported that when the charge of protein was altered by changing the pH of the protein solution with the addition of appropriate amounts of HCl, KOH and KCl, the viscosity of the protein increased with net charge at a constant ionic strength. After dephosphorylation, the overall negative charge of α_{s1} -casein was reduced, which caused the electrostatic repulsion between α_{s1} -casein molecules to also decrease. The decreased intermolecular repulsive force led to a lower resistance to flow (Michael & Rosalind, 2000). Thus, dephosphorylation reduced the viscosity of α_{s1} -casein solution.

In addition, the shape and size of the molecule will affect the viscosity (Viswanath et al., 2007). Dephosphorylation enhanced the self-association behaviour of α_{s1} -casein (described in Section 3.2.5), which may lower the viscosity of α_{s1} -casein. When the self-associated species of dephosphorylated α_{s1} -casein were formed, the associated species occupied less space in the solution compared to the dissociated molecules, which resulted in a reduction in the overall volume of α_{s1} -casein particles. Therefore, a higher level of self-association may have contributed to a lower viscosity of α_{s1} -casein,

The most significant reduction in viscosity was observed between the standard sample and the dephosphorylated α_{s1} -casein incubated for 5 min. This might be due to the fact that the highest level of self-association was formed in the dephosphorylated α_{s1} -casein at an incubation time of 5 min, which could significantly reduce the viscosity of α_{s1} -casein. The AUC results showed that a higher level of dephosphorylation led to a lower self-associated α_{s1} -casein, as the α_{s1} -casein dephosphorylated for 20 min had a higher level of self-association than those dephosphorylated α_{s1} -caseins with longer incubation times (as described in Section 3.2.5). Thus, most of the change in self-association occurred within the first 20 min of dephosphorylation, and it is apparent that this was also observed for viscosity of dephosphorylated α_{s1} -caseins. The self-association of dephosphorylated α_{s1} -casein at

the incubation time of 5 min was not monitored, but it seems likely that this might be similar to the sample incubated for 20 min based these viscosity results.

4.2.3 Water binding properties of dephosphorylated α_{s1} -casein

Nuclear Magnetic Resonance (NMR) spectroscopy is an analytical technique used to determine content, purity and molecular structure. The principle of NMR is that the nuclei of all elements are electrically charged and the nuclei with an odd atomic number have a “nuclear spin”, such as ^1H and ^{13}C . The nuclei of elements will develop a magnetic field and these elements are randomly oriented. However, when an external magnetic field is applied, these spins line up parallel or opposed to the applied field. The more highly populated state is the lower energy spin state, the spin aligned situation (Figure 4.9). The gap between the higher and lower energy corresponds to radio frequency; when the spin returns to its base level, the energy is released at the same frequency. The matched signal of energy transfer is measured and processed to generate an NMR spectrum (Freeman, 1997).

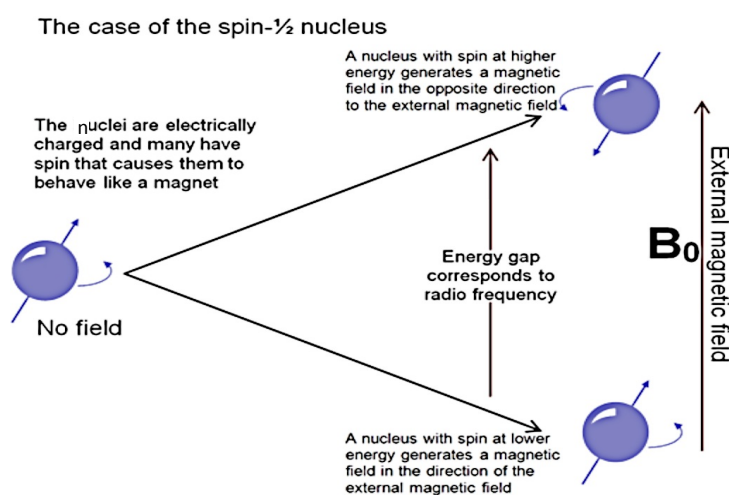


Figure 4.9 The basis of NMR (Hoffman & Ozery, 2013)

T2 relaxation (spin-spin) relaxation is the progressive dephasing of spinning dipoles following the 90°C pulse, which is expressed as a time constant characterizing the signal decay. The 90°C pulse is the angle to which the net magnetization is rotated to the main magnetic field direction by the application of an excitation pulse. When the

energy between dipoles facing parallel and antiparallel is transferred to the external magnetic field, the dipoles flip in opposite directions. The rate of flipping or transfer of energy between dipoles is related to the rate of rotation and translation of neighbouring water molecules (Freeman, 1997; Mitchell et al., 1987).

The magnetic moment of the proton precesses around the external magnetic field and the rate of precession is known as the Larmor frequency. If the frequency of variation of the local magnetic field approaches the Larmor frequency, the rate of flipping or transfer of energy between dipoles increases. In pure water, the water molecules move faster than the Larmor frequency, as a consequence the rate of flipping between dipoles increases, resulting in a longer T2 time. In protein solutions, the slower motion of protons in the protein is closer to the Larmor frequency and the water molecules are attracted to the surface of the proteins, which contribute to a much faster relaxation time (Fabri et al., 2005; Freeman, 1997; Mitchell et al., 1987).

Water molecules that bind to the polar groups or ionic sites of proteins are known as 'bound water' (Berlin et al., 1973; Fennema, 1996). The bound water forms water layers around the protein molecules and is therefore unable to act as a solvent. By contrast, the less structured and ordered water molecules that form the outer water layers are available to act as a solvent, thus they are known as 'free water' (Berlin et al., 1973; Fennema, 1996). Dephosphorylation was shown to have an impact on the charge and hydrophobicity of α_{s1} -casein, as previously described in Section 3.2. In addition to this it has been hypothesized that the amount of bound water might be affected by dephosphorylation (Zhang et al., 2012). Therefore, the water binding capacity of dephosphorylated α_{s1} -casein was determined by measuring the T2 relaxation constant using NMR (as described in Section 2.2.15).

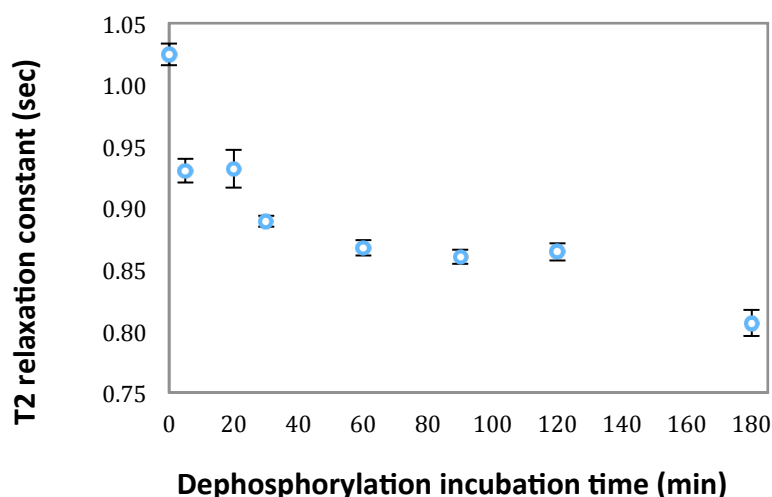


Figure 4.10 T2 relaxation constant time for α_{s1} -casein incubated with phosphatase for different times. Each data point is an average of two replicates. Error bars represent the standard deviation of the mean of the replicates.

Overall, the T2 relaxation constant of dephosphorylated α_{s1} -casein was found to decrease as the incubation time of dephosphorylation increased (Figure 4.10). The standard sample also had a very similar T2 relaxation constant ($1.024 \pm 0.009s$) compared to the control sample ($1.025 \pm 0.007s$). All in all, these results indicate that the water binding capacity of dephosphorylated α_{s1} -casein was higher than the standard and control samples, and a longer incubation time of dephosphorylation prompted a higher water binding capacity for α_{s1} -casein.

Figure 4.10 shows two major reductions in the T2 relaxation constant. There was about a 0.09 s reduction in the T2 relaxation constant between the standard sample and dephosphorylated α_{s1} -casein which was incubated for 5 to 10 min and when the incubation time of dephosphorylation was increased from 10 min to 180 min, the T2 relaxation constant of α_{s1} -casein decreased by about 0.06 s. Therefore, compared to native α_{s1} -casein, the water binding capacity of α_{s1} -casein was significantly improved during the first 5 min of incubation. Furthermore the longest incubation time (180 min) led to the maximum water binding capacity for dephosphorylated α_{s1} -casein.

The interaction between molecules of water and the hydrophilic groups of the protein side chains occurs *via* hydrogen bonding (Zayas, 1997). After dephosphorylation, the apparent hydrophobicity of α_{s1} -casein had increased compared to the native α_{s1} -casein, due to less hydrophilic serine residues were formed in comparison to the phosphate serine residues (Chapter 3, Section 3.3). Thus, the amount of bound water with dephosphorylated α_{s1} -casein was predicted to be reduced in comparison to native α_{s1} -casein. However, this study showed that the water binding capacity of α_{s1} -casein increased as the incubation time of dephosphorylation increased (Figure 4.10).

There might be other factors that contribute to the increased water binding capacity of dephosphorylated α_{s1} -casein. The exposed hydroxyl group might play a role, as it has been reported that the water binding of proteins can be related to the attached hydrophilic groups, such as the amino, carboxyl, hydroxyl, carbonyl, and sulfhydryl groups. Hydrophilic amino acid side chains have a specific water binding affinity and capacity that is directly affected by the type and number of these hydrophilic groups in the polypeptide chain (Kuntz, 1971). The hydroxyl groups can form hydrogen bonds with water molecules, helping to dissolve proteins in a deionized environment (Zumdahl & Zumdahl, 2012). Therefore, the introduced hydroxyl group may increase the water binding capacity of dephosphorylated α_{s1} -casein. By contrast, the hydrophobicity of dephosphorylated α_{s1} -casein was measured in a phosphate buffer, which is an ionized environment (as described in Section 2.2.10). The hydroxyl groups may have a lower affinity to bind with water molecules at higher ionic strength.

In addition, the heat treatment of native α_{s1} -casein (85°C, 5 min) did not affect the water binding capacity of α_{s1} -casein. Although there have been several studies looking at enzymatic dephosphorylation of caseins (Yamauchi & Yoneda, 1978; Yeung et al., 2001; Yoshikaw et al., 1974), the water binding capacity of dephosphorylated α_{s1} -casein has not been previously reported.

4.2.4 Surface tension of air-water interfaces of dephosphorylated α_{s1} -casein

The Wilhelmy plate method is a force measurement in which the normal force acting on the liquid surface, allows the liquid to conform to its smallest surface area (Rodríguez Niño & Rodríguez Patino, 1998). In this method, a platinum plate is thoroughly cleaned and attached to a scale or balance via a thick metal wire. The plate is lowered parallel to the liquid surface. The liquid is then raised until it just touches the bottom edge of the plate. The force on the plate increases due to wetting of the liquid against the plate, which is measured via the balance (Figure 4.11; Rodríguez Niño & Rodríguez Patino, 1998).

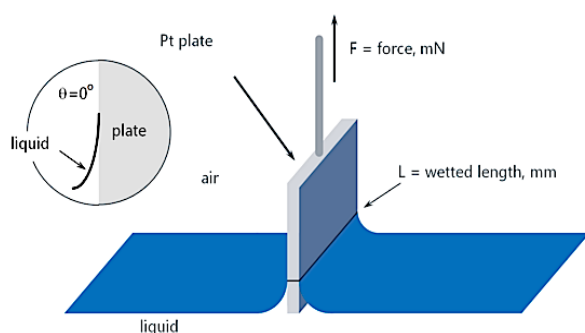


Figure 4.11 Schematic diagram of the Wilhelmy plate method (Krüss Processor tensiometer K12 manual).

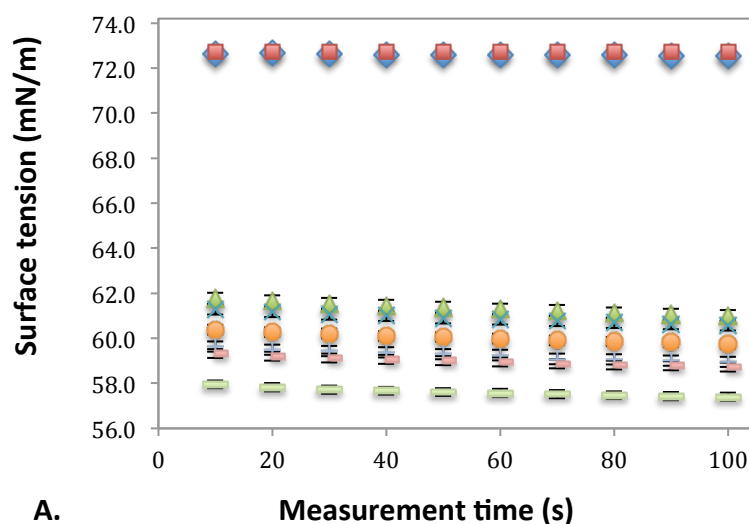
A platinum plate is applied in the measurement of surface tension as it is chemically inert and easy to clean, and because it can be optimally wetted on account of its very high surface free energy and therefore generally forms a contact angle, θ , of 0° ($\cos \theta = 1$) with liquids. If the contact angle between the liquid and the plate is zero due to perfect wetting, then the surface tension (σ mN/m) is calculated using the Wilhelmy equation (Equation 4.2; Abercrombie-Thomas et al., 2010):

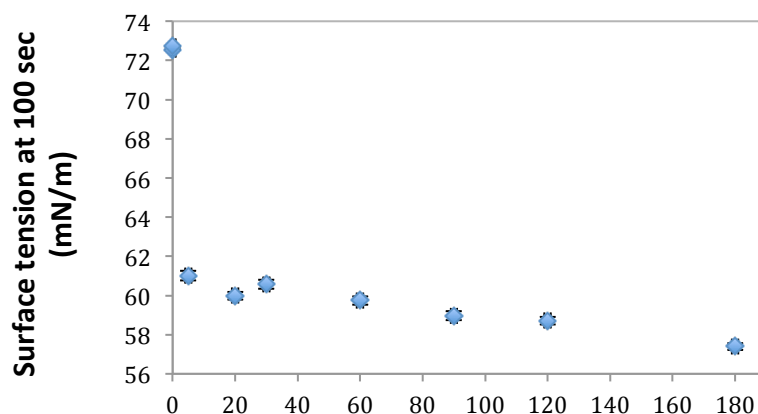
$$\sigma = \frac{F}{L \cdot \cos \theta} \quad \text{Equation 4.2}$$

where F is the force on the plate (mN), L is the wetted perimeter (m) ($2w + 2d$, where w is plate width and d is plate thickness) of the Wilhelmy plate and θ is the

contact angle between the liquid phase and plate.

Surface tension is a contractive tendency of the surface of a liquid that allows it to resist an external force. At air-water interfaces, the high attraction of water molecules to each other is greater than to the molecules in the air, which contributes to the surface tension of water. Water has a relatively high surface tension compared to other liquids (72.8 milliNewtons per meter (mN/m) at 20°C (Defay, 1996)). α_{s1} -Casein contains both hydrophilic and hydrophobic regions, and it can reduce the surface tension by adsorbing the hydrophilic head groups in the water leaving the hydrophobic tails facing towards the air (Gonzalez-Tello et al., 2009). Surface tension as a functional parameter can play an important role in the functionality of proteins and therefore the surface tension of dephosphorylated α_{s1} -casein was measured using the Wilhelmy plate method (as described in Section 2.2.17).





B. Dephosphorylation incubation time (min)

Figure 4.12 Surface tension (air-water) of dephosphorylated α_{s1} -casein solutions measured using the Wilhelmy plate method. Standard-native α_{s1} -casein (incubation time – 0, \blacklozenge); control-native α_{s1} -casein with heat treatment at 85°C for 5 min (incubation time – 0, \blacksquare); α_{s1} -casein incubated with phosphatase for 5 min (\blacktriangle), 30 min (\times), 60 min (\bullet), 90 min ($+$), 120 ($-$) and 180 min ($-$), respectively (A). Surface tension of dephosphorylated α_{s1} -casein at different incubation times (B). Each data point is an average of four replicates. Error bars represent the standard deviation of the mean of the replicates.

The surface tension of native and dephosphorylated α_{s1} -casein between the air and water interface was measured (Figure 4.12). In order to remove free phosphate from the protein solutions, all the protein samples were dialyzed against Milli-Q water before the surface tension measurement. The surface tension of dephosphorylated α_{s1} -casein decreased as the incubation time of dephosphorylation increased (Figure 4.12 B). There was a significant reduction (around 10 mN/m) in the surface tension between the standard sample and the dephosphorylated α_{s1} -casein incubated for 5 min. After 5 min of incubation time, the surface tension of dephosphorylated α_{s1} -casein decreased gradually until 180 min of incubation time. Both the standard and control samples having surface tension values of about 72.5 mN/m, which is similar to the surface tension of water (72.9 mN/m, also measured in this study). Based on the results from the preliminary experiments, a low concentration of α_{s1} -casein (0.001% protein concentration) was used for the surface tension measurement, as the use of such a low protein concentration can avoid the saturation of protein

adsorption on the Wilhelmy plate but still provide enough of a change range for the surface tension for dephosphorylated α_{s1} -casein. The surface tension of milk proteins has been well studied, and it has been reported that the surface tension of milk proteins was dependent on the experimental conditions such as protein concentration, ionic composition, pH and temperature (Kitabatake, 1982; Miller et al., 2004; Rodríguez Niño & Rodríguez Patino, 1998).

The decreased surface tension of dephosphorylated α_{s1} -casein could result from the increased apparent hydrophobicity of the dephosphorylated α_{s1} -casein (Section 3.2.4). Proteins adsorbed onto the surface due to the hydrophobic properties of the interface would decrease the surface tension of the proteins (Benjamins et al., 1975; Pezennec et al., 2000; Walstra & De Roos, 1993). The key driving force is the entropy increase that is generated from dehydration of the hydrophobic regions and the hydrophobic interface of the protein surface (Dickinson & McClements, 1996). Kato and Nakai (1980) reported that effective hydrophobicity shows significant correlations with interfacial tension of the proteins; the higher hydrophobicity of proteins leads to a lower surface tension.

A longer incubation time for dephosphorylation contributed to more charged phosphate groups being lost, which consequently resulted in the serine residues being less hydrophilic than the charged phosphate serine residues. Thus, the non-phosphate serine residues tend to move closer to the interface due to their lower hydrophilicity compared to phosphate serine residues. However, the NMR results indicated that the serine residues of α_{s1} -casein bound more water than phosphate serine residues in a deionized solution (as described in Section 4.2.3). Unlike the solution environment of the NMR measurement, the water molecule loses the hydrogen bond at a hydrophobic surface (Chalikian, 2001), thus the hydroxyl groups of the serine residues could lose the bound water at the interface. This indicated that the water binding capacity of α_{s1} -casein in a solution might not be suitable for the prediction of the interfacial tension of α_{s1} -casein.

In addition, the reduced amount of overall negative charge could result in the surface tension of α_{s1} -casein being diminished. Boström et al. (2001) have suggested that proteins experience different forces near the air-water interface that might be attractive or repulsive, but acting together they lead to an increase or decrease in concentration near the interface. The change in concentration leads to the change in surface tension (Boström et al., 2001). In this study, the repulsive force between α_{s1} -casein molecules was reduced due to the decreased negative charge, which may have contributed to dephosphorylated α_{s1} -casein molecules moving closer to the air-water interface. The increased concentration of dephosphorylated α_{s1} -casein at the air-water interface would result in a reduced surface tension.

4.2.5 Surface tension of oil-water interfaces of dephosphorylated α_{s1} -casein

In the pendant drop method the interfacial tension is determined by analysing the shape of a drop of liquid hanging from the needle of a syringe. The interfacial tension can be calculated by Equation 4.3 (Jůza, 1997; Morita et al., 2002):

$$\gamma = \frac{\Delta\rho g(R_0^2)}{\beta} \quad \text{Equation 4.3}$$

where γ is surface tension, $\Delta\rho$ is the density difference between fluids, g is the gravitational constant, R_0 is the radius of the drop curvature at the apex and β is the shape factor. β is defined through the Young-Laplace equation that is shown in Figure 4.13.

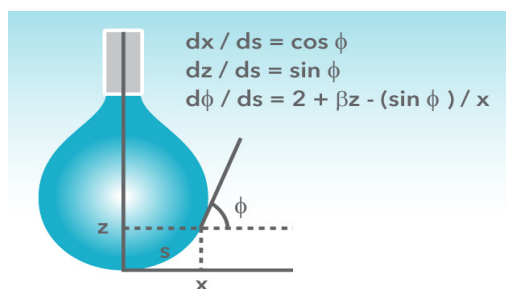


Figure 4.13 A pendant drop showing the characteristic dimension, the parameter, s is the arc length to the point from the drop apex, z is the axial coordinate of the described point to the drop apex, x is the distance of the point from the axis of the drop, X , Z and S are dimensionless parameters made by dividing x , z , and s , respectively, by R_0 (KSV CAM 200 manual).

The interfacial tension measurement can be done with a pendant drop method that provides a convenient way to determine the interfacial tension between oil and water. The KSV CAM 200 pendant drop instrument is designed for measuring the interfacial tensions of liquids. This measurement is based on the video capture of images and automatic image analysis.

Proteins are very surface-active substances, which means that they readily adsorb onto air-water and oil-water interfaces, even at low concentrations. The interfacial properties of protein between oil and water play an important role in food emulsions. In order to understand the relationship between the physicochemical and functional properties, the surface tension of dephosphorylated α_{s1} -casein at an oil-water interface was examined using a pendant drop tensiometer (as described in Section 2.2.18).

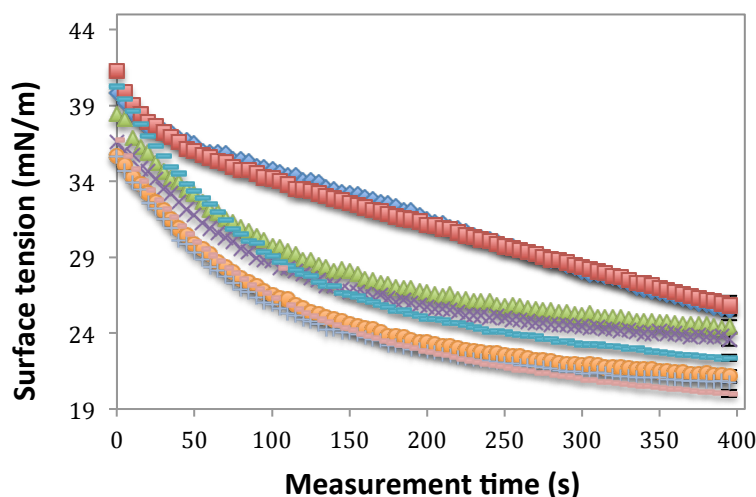


Figure 4.14 Interfacial tension (oil-water) of dephosphorylated α_{s1} -casein measured using a pendant drop tensiometer. Standard-native α_{s1} -casein (incubation time – 0, \blacklozenge); control-native α_{s1} -casein with heat treatment at 85°C for 5 min (incubation time – 0, \blacksquare); α_{s1} -casein incubated with phosphatase for 5 min (\blacktriangle), 30 min (\times), 60 min ($-$), 90 min (\bullet), 120 ($+$) and 180 min ($-$), respectively. Each data point is an average of two replicates. Error bars represent the standard deviation of the mean of the replicates.

The results showed that the surface tension of dephosphorylated α_{s1} -casein between the water and oil interface decreased in comparison to the standard sample and overall the longer incubation time contributed to a lower surface tension (Figure 4.14). Moreover, there is no noticeable difference in the surface tension between the standard and control samples.

The principle of the surface tension change on the oil-water interface is similar to the change on the air-water interface that was discussed previously. The decreased surface tension of dephosphorylated α_{s1} -casein on the oil-water interface is due to the increased hydrophobicity and decreased negative charge of dephosphorylated α_{s1} -casein. For the oil-water interface, the hydrophobic part of the α_{s1} -casein is adsorbed into the oil phase and the hydrophilic part of the α_{s1} -casein remains in the water phase (Beverung et al., 1999; Binks et al., 2000; Chandler, 2005; Paunov, 2003). Therefore, more dephosphorylated α_{s1} -casein was adsorbed onto the oil-water interface resulting in a lower interfacial tension compared to native casein.

4.2.6 Emulsifying properties of α_{s1} -casein

Many different techniques are available for measuring particle size distribution, but a laser diffraction technique is commonly used, as it can be applied for both solid and liquid samples (Sochan et al., 2012). The Mastersizer 2000 (Malvern instrument Ltd, UK) uses the technique of laser diffraction to measure the size of particles. It can detect the particles size in the range of 0.02 to 2000 micron (Malvern laser light guide, 1998). During a laser diffraction measurement, particles are passed through a focused laser beam and scatter light at an angle (Figure 4.15). The angular intensity of the scattered light is inversely proportional to their size, which is measured by photosensitive detectors. The angular scattering intensity data are then analyzed using the Mie scattering model, which calculates the size of the particles. Large particles scatter light at small angles with high intensities, whereas, small particles scatter light at wide angles with low intensities. The particle size is reported as the volume equivalent sphere diameter: $d_{(3,2)}$ is the volume/surface mean diameter and $d_{(4,3)}$ is the volume mean diameter (Wedd, 2003).

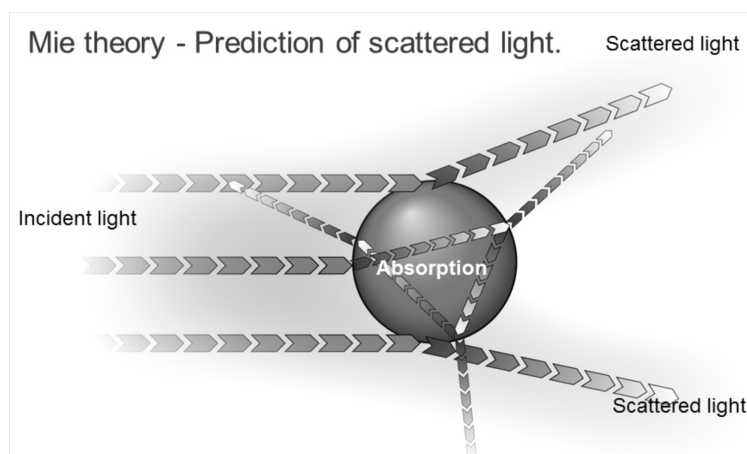


Figure 4.15 A schematic diagram of the light scattering of a particle (Mastersizer manual, Malvern instrument Ltd, UK).

In order to explore the emulsifying properties of dephosphorylated α_{s1} -casein, especially the relationship between the interfacial properties and the formation of

the emulsion, the particle sizes of a canola oil droplet in an emulsion were measured by static light scattering using a Malvern Mastersizer 2000. In oil in water emulsion systems, oil droplets are covered with emulsifier and dispersed in the water phase. The emulsifier covers the oil droplets to inhibit the droplets from coalescence, and consequently stabilized the dispersions. The coalescence leads to large oil droplets being formed, and uncontrolled coalescence will result in a phase separation of emulsions. Thus, the size of the oil droplets is an important factor in the emulsion stabilization. Canola oil is commonly used in food systems that require vegetable oil as an ingredient. Thus, the emulsions were prepared with all protein samples and canola oil (as described in Section 2.2.21).

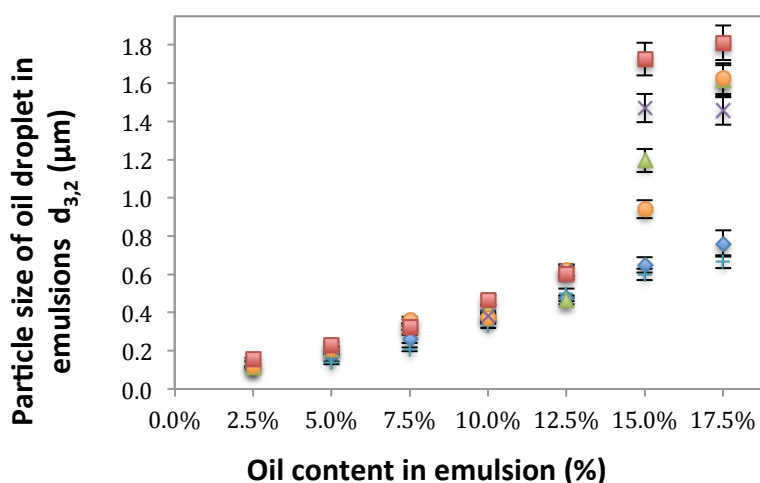


Figure 4.16 Particle size $d_{(3,2)}$ of canola oil droplet in emulsions made with α_{s1} -casein. Standard-native α_{s1} -casein (incubation time – 0, ♦); control-native α_{s1} -casein with heat treatment at 85°C for 5 min (incubation time – 0, 0); α_{s1} -casein incubated with phosphatase for 5 min (▲), 30 min (●), 90 min (×) and 180 min (■), respectively. Each data point is an average of two replicates. Error bars represent the standard deviation of the mean of the replicates.

Figure 4.16 shows that the particle sizes in the emulsions made from all α_{s1} -casein samples increased with increasing oil concentration from 2.5% to 17.5%. This suggested that at a low oil concentration, the initially formed small oil droplets were completely covered with sufficient α_{s1} -casein and were stabilized in the emulsion. When the oil concentrations increased to a high level, there was not enough α_{s1} -

casein to fully cover the small oil droplets and large oil droplets formed due to coalescence. The formation of the large oil droplets reduces total surface area in the emulsions, thus, the coalescence will stop until the oil droplets are fully covered with α_{s1} -casein and the emulsions are stabilized.

In all the emulsions containing 2.5 – 10% oil, there was no noticeable difference in particle sizes between emulsions made from native α_{s1} -casein and the dephosphorylated α_{s1} -casein (Figure 4.16). However, when the oil content was increased above 12.5%, the particle sizes in the emulsions with dephosphorylated α_{s1} -casein dramatically increased compared to the standard samples, especially in the emulsions containing both 15% and 17.5% oil (Figure 4.16). In general, the longer the incubation times for dephosphorylation the larger the particle sizes were in the emulsions containing more than 12.5% oil. Also, the particle size for the standard sample was similar to that of the control sample (around 0.7 μm at 12.5% oil content). The result that coalescence occurred at lower oil concentration for emulsions made from dephosphorylated α_{s1} -casein than for native α_{s1} -casein suggested that more dephosphorylated α_{s1} -casein was required to completely cover the surface of the oil droplets than the native α_{s1} -casein.

The particle size measurements for the emulsions in this study indicated that native α_{s1} -casein had better emulsifying properties than dephosphorylated α_{s1} -casein. Dephosphorylation resulted in a change in the surface hydrophobicity of α_{s1} -casein. Thus, the hydrophilic-lipophilic balance (HLB) of dephosphorylated α_{s1} -casein is changed compared to native α_{s1} -casein. When the oil-water emulsion is prepared with the protein, the hydrophobic heads of the protein are adsorbed to the surface of the oil droplets and the hydrophilic tails of the protein are oriented to the water phase. The hydrophilic tails stabilize the emulsion by covering the oil droplets to inhibit their coalescence (Chandler, 2005; Kato et al., 1993; Nakamura et al., 1993; Sánchez & Patino, 2005). Therefore, the changed hydrophilic-lipophilic balance contributes to the decreased emulsifying properties of dephosphorylated α_{s1} -casein. It has been suggested that surface hydrophobicity is one of the characteristics of the protein most likely to define its surface behaviours and consequently its emulsifying

properties (Graham & Phillips, 1979; Nakai et al., 1980; Nakai, 1983; Nakai et al., 1986).

In addition, the reduced overall negative net charge of dephosphorylated α_{s1} -casein could diminish the emulsifying capacity of α_{s1} -casein. It has been reported that the addition of an electrical charge can prevent flocculation and increase the resistance to coalescence, which contributes to improving the emulsifying properties of the protein (Dagorn-Scaviner et al., 1987; Graham & Phillips, 1976; Nagasawa et al., 1996). The electrostatic repulsions between protein chains on the surface of oil droplets allow the native α_{s1} -casein to spread and cover the surface of the oil droplets. Dephosphorylation decreased electrostatic repulsions between protein chains due the reduction in the net charge, which limited the α_{s1} -casein chains to spread on the surface of the oil droplets. Thus, dephosphorylated α_{s1} -casein occupied less surface area than native α_{s1} -casein. As the result of insufficient dephosphorylated α_{s1} -casein covering on the surface, coalescence occurred between these oil droplets to form large droplets until the surface was fully covered with enough dephosphorylated α_{s1} -casein (Figure 4.17).

On the other hand, the reduction in the electrostatic repulsions between protein covered oil droplets could promote a faster coalescence. When the net charge is increased the repulsive forces are strong enough and the oil droplets covered by proteins are repelled before they can make contact and coalesce, and the emulsion is stable (Moro et al., 2001; Nagasawa et al., 1996; Urrutia, 2006). By contrast, when the overall charge was reduced after dephosphorylation of α_{s1} -casein, the repulsive forces between the oil droplets covered by dephosphorylated α_{s1} -casein decreased. In this case, a faster coalescence of oil droplets occurred and the larger droplets formed, associated with poor emulsifying property of dephosphorylated α_{s1} -casein.

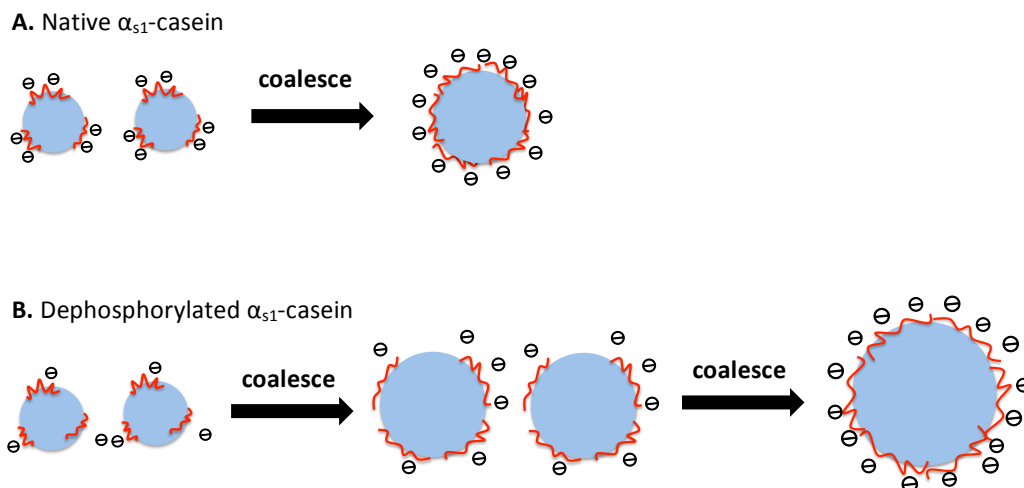


Figure 4.17 The proposed mechanisms of emulsion coalescence: native α_{s1} -casein (A) occupies more surface of oil droplets than dephosphorylated α_{s1} -casein (B).

In an oil-water emulsion system, the viscosity of the continuous phase (protein solutions in this study) affects the diffusion rate of proteins from bulk solution to the oil-water interface, which is dependent on the emulsification (Piacentini et al.; Sikorski, 2002). An increase in the viscosity of the continuous phase by adding polysaccharides can slow the movement and coalescence of oil droplets in a protein-stabilized emulsion (Kiosseoglou & Paraskevopoulou, 2011). This coalescence will be stopped when the oil droplets were stabilized by being fully covered with proteins, which is mainly dependent on the stabilization capacity of the proteins. Behrend et al. (2000) reported that there is no clear relationship between the viscosity of the continuous phase and the size of stabilized oil droplets in an oil-water emulsion generated by ultrasound emulsification. Therefore, the change in the viscosity of α_{s1} -casein due to dephosphorylation probably did not have an impact on the size of oil droplets of emulsions.

4.2.7 Foaming properties of dephosphorylated α_{s1} -casein

A commonly used method to measure foam stability is the half-life of the foam, which reflects the required time to reduce the foam volume to half of its original

value (Dickinson & Izgi, 1996). The decrease in foam volume occurs as a result of liquid drainage from the foam, gas diffusion, coalescence, and disproportionation of gas bubbles (Huppertz, 2010). The rate of drained liquid can be accurately determined as an index of the foam stability. Caseins are well-known for their good foaming and emulsifying properties, and for these reasons they are widely used in various food formulations (Dalglish et al., 1997; Damodaran, 1997). In order to understand the correlation between the physicochemical properties and the foaming properties of α_{s1} -casein, the proteins foaming properties were investigated by measuring the volume of foam formation and the serum separation time (as described in Section 2.2.19).

Table 4.2 The volumes of native and dephosphorylated α_{s1} -casein foam.

Incubation time (min)	0 Standard	0 Control	5	20	30	60	90	120	180
Volume of foam (mL)	25±1	25±1	25±1	25±1	25±1	25±1	25±1	25±1	25±1

The volumes of protein foam formation generated were very similar between the native α_{s1} -casein and dephosphorylated α_{s1} -casein. About 25 mL of foam was formed during whipping of the protein solutions (Table 4.2).

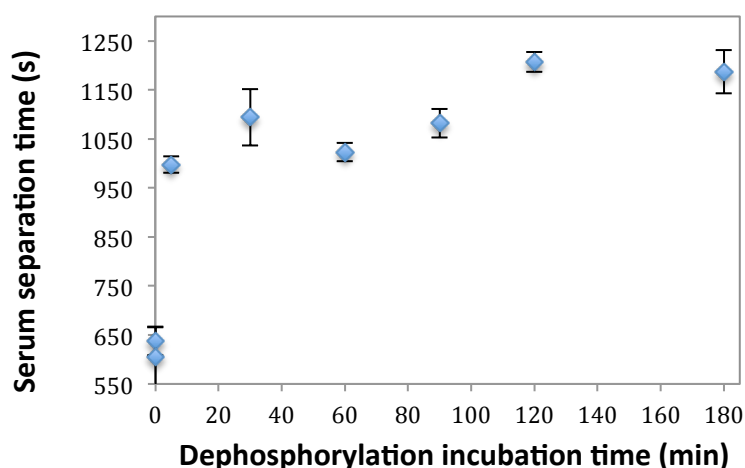


Figure 4.18 Protein serum separation time for samples incubated with phosphatase for different times. The duplicate points at time 0 are the standard-native α_{s1} -casein and control-native α_{s1} -casein with heat treatment at 85°C for 5 min. Each data point is an average of two to four replicates. Error bars represent the standard deviation.

The time of serum separation from the protein foam increased as the incubation time of dephosphorylation increased (Figure 4.18). Figure 4.18 shows that dephosphorylated α_{s1} -casein incubated for 5 min had a significant increase in the serum separation time compared to the standard sample (about 1.7 times). After 5 min of incubation, the serum separation time increased gradually until 180 min of incubation. In addition, the standard sample had a similar serum separation time to the control sample (Figure 4.18). Thus, the foam containing dephosphorylated α_{s1} -casein collapsed slower than the foam containing native α_{s1} -casein and the longer incubation times of dephosphorylation contributed to a slightly more stable foam. The surface tension (air-water interface) of dephosphorylated α_{s1} -casein decreased as the incubation time of dephosphorylation increased, due to the increased hydrophobicity of dephosphorylated α_{s1} -casein (Section 4.2.4).

It has been reported that the foaming characteristics of sodium caseinate are dependent on the rate of diffusion to the air-water interface (Sánchez et al., 2005). Proteins with high surface hydrophobicity will increase surface pressure rapidly, due to the affinity for the air-water interface, and have a low rate of desorption. High foaming ability has been correlated with a low surface tension that resulted in a high

rate of increase in surface pressure (Hill, 1996; Klitzing & Müller, 2002; Sánchez & Patino, 2005; Wilde, 2000a). After dephosphorylation, a decreased surface tension of dephosphorylated α_{s1} -casein contributed to the increased surface pressure; as a result the foaming stability of dephosphorylated α_{s1} -casein was enhanced. This is in agreement with previous studies showing that foaming capacity has been linked to surface hydrophobicity; and increased surface hydrophobicity enhanced the foaming stability of whey protein concentrate (Moro et al., 2001; Townsend & Nakai, 1983).

The foam stability of dephosphorylated α_{s1} -casein incubated for 5 min was significantly improved compared to native α_{s1} -casein (Figure 4.18). This enhanced foam stability is consistent with the change in air-water surface tension. The dephosphorylation incubation time for 5 min resulted in a significant reduction in the surface tension of α_{s1} -casein in comparison to native α_{s1} -casein (Figure 4.12). In addition, the heat treatment (85°C, 5 min) of α_{s1} -casein did not affect foam stability. It has been reported that electrostatic forces can also significantly influence the foaming properties of whey proteins, such as their stability, interfacial properties and adsorption rates (Foegeding et al., 2006; Roth et al., 2000). Electrostatic repulsion is expected to be more prominent during adsorption; the reduction in electrostatic repulsion facilitates adsorption to the air-water interface (Davis et al., 2004; Dickinson, 1999b). The stability of a foam depends on the electrostatic double-layer force that relates to the strength of the protein film between air bubbles and the ability of the adsorbed molecules to associate (Belitz et al., 2008; Bergeron et al., 1996). The results are consistent with the net charge of α_{s1} -casein being reduced by dephosphorylation, and the electrostatic repulsion between protein molecules being reduced and more protein adsorbing to the interface (Figure 4.19). This is proposed to contribute to the overall net charge increasing on the interface of bubbles, even though the net charge of each single molecule was reduced. The total repulsive force would therefore increase between bubble layers due to increased protein adsorption, which resulted in a stronger film forming between bubbles. Consequently, the increased repulsive force between air bubbles and the stronger film stabilizing the air bubbles prevents them from collapsing.

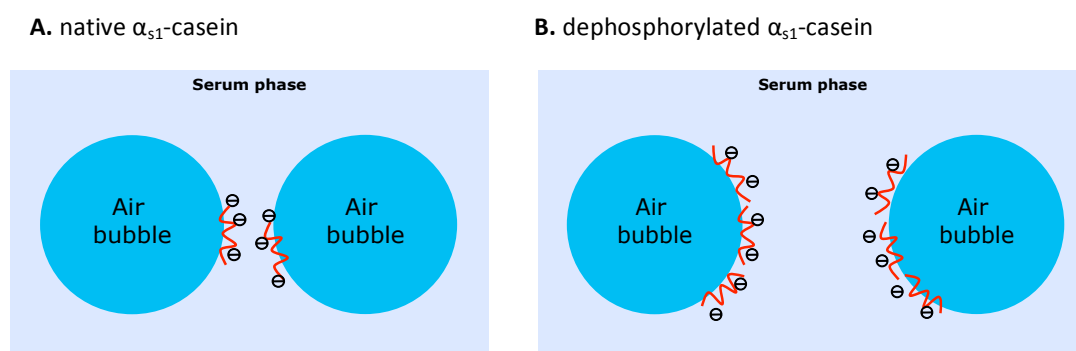


Figure 4.19 The diagram illustrates proposed electrostatic repulsion between air bubbles coated with **A. native α_{s1} -casein** and **B. dephosphorylated α_{s1} -casein** in a foam system.

Unlike the emulsion system, the foam stability is maintained by the thickness of the liquid films between the bubbles. A high viscosity of the continuous phase may retard the film thinning and rupture, consequently slowing the drainage rate (Kiosseoglou & Paraskevopoulou, 2011; Wang & Narsimhan, 2006; Wilde, 2000a). However, the drainage rate of α_{s1} -casein containing foam decreased with increasing dephosphorylation incubation time, though dephosphorylation led to a reduction in the viscosity of continuous phase (α_{s1} -casein solution). Therefore, the hydrophobicity and electrostatic repulsion may play a dominant role in the foam stability rather than the continuous phase viscosity.

4.3 Conclusions

This chapter investigated the impact of dephosphorylation on the functional properties of α_{s1} -casein. The functional properties of dephosphorylated α_{s1} -casein were discussed in relation with the changes in the physicochemical properties of α_{s1} -casein. The surface tension was found to have an impact on the foaming stability of α_{s1} -casein, but it did not have any impact on the volume of the foam. Hydrophobicity and net charge plays a dominant role in the interfacial properties, emulsifying capacity and foaming stability. Therefore, the functional properties of food proteins

can be manipulated by simply modifying the surface hydrophobicity and net charge of proteins.

The calcium ion binding capacity diminished after dephosphorylation of α_{s1} -casein and this might have an effect on other functionalities of proteins in a food system. Thus, the dephosphorylated α_{s1} -casein needs to be tested in a real food model system to help understand the relationship between calcium ion binding and the rheological properties of food proteins.

The dephosphorylated α_{s1} -casein exhibited enhanced water binding capacity and foaming stability, even though it resulted in a poor emulsifying capacity. After dephosphorylation, the phosphate group on the serine residues was replaced with the hydroxyl group. The introduced hydroxyl group might be a functional group on serine residues. Alternately the change in the self-association of α_{s1} -casein caused by dephosphorylation may contribute to the improved water binding capacity of α_{s1} -casein.

Chapter 5 Characterizations of succinylated α_{s1} -casein

5.1 Introduction

The succinylation of proteins with succinic anhydride is a chemical modification that converts the amino groups of the lysine residues into carboxyl groups (Figure 5.1; Morand et al., 2011b). Succinylation can modify the physicochemical properties of caseins by capping their lysine residues. The aim of the work described in this chapter is to understand how the physicochemical properties of α_{s1} -casein are affected by succinylation. To do this, α_{s1} -casein was succinylated to different levels by adding different amounts of succinic anhydride to native α_{s1} -casein solutions (as described in Section 2.2.2). The physicochemical properties of the native and succinylated α_{s1} -casein were examined using a variety of techniques.

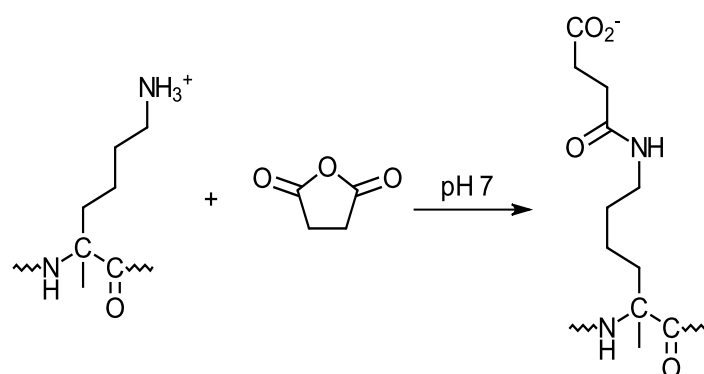


Figure 5.1 The capping of lysine residues with succinic anhydride (Morand et al., 2012).

The degree of succinylation of α_{s1} -casein was examined using the *o*-phthaldialdehyde (OPA) colorimetric assay, reduced SDS-PAGE and mass-spectrometry (as described in Sections 3.2.7, 3.2.5 and 3.2.8). The pI of all samples was measured using laser Doppler electrophoresis and IEF-PAGE (as described in Section 2.2.9 and 3.2.6). The hydrophobicity of α_{s1} -casein was investigated using 1-

anilinonaphthalene-8-sulfonic acid (ANS) fluorescence (as described in Section 2.2.10).

5.2 Results and discussion

5.2.1 Determination of succinylation of α_{s1} -casein

The exact level of succinylation was determined using the OPA colorimetric assay and the specific succinylated lysine residues of α_{s1} -casein were confirmed by mass spectrometry. In addition, reduced SDS-PAGE was used to monitor the change in the mobility of succinylated α_{s1} -casein.

OPA colorimetric assay

The spectrophotometric assay using *o*-phthaldialdehyde (OPA) provides a simple and fast method of lysine quantification. This assay is based on the reaction of primary amino groups of proteins with OPA in the presence of 2-mercaptoethanol, which yields 1-alkylthio-2-substituted isoindoles that absorb light at a wavelength of 340 nm (Figure 5.2; Church et al., 1983; Morand et al., 2011b; Simons Jr & Johnson, 1976; Švedas et al., 1980). Fluorescence is highly dependent on the presence of 2-mercaptoethanol, which is required for formation of the chromophore (Fig 5.2; Švedas et al., 1980).

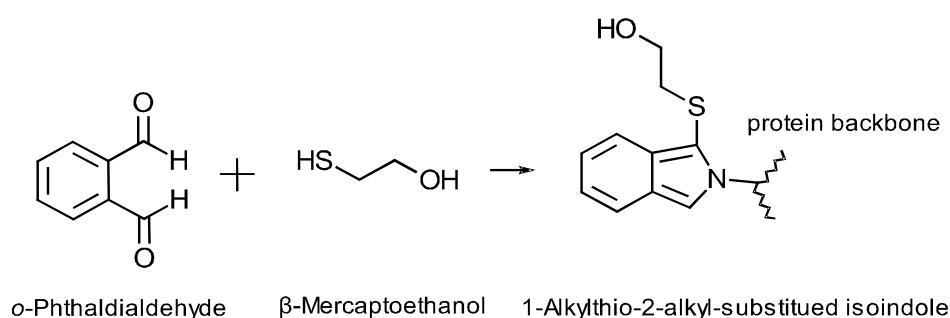


Figure 5.2 Reaction of OPA with amine and 2-mercaptoethanol (Simons Jr & Johnson, 1976; Švedas et al., 1980)

After succinylation, the lysine residues of α_{s1} -casein have been capped, as depicted in Figure 5.1. The level of succinylated lysine residues was expressed as the degree of succinylation of α_{s1} -casein, which was quantified using the OPA colorimetric assay. The degree of succinylated α_{s1} -casein was manipulated by controlling the amount of succinic anhydride used in the experiment.

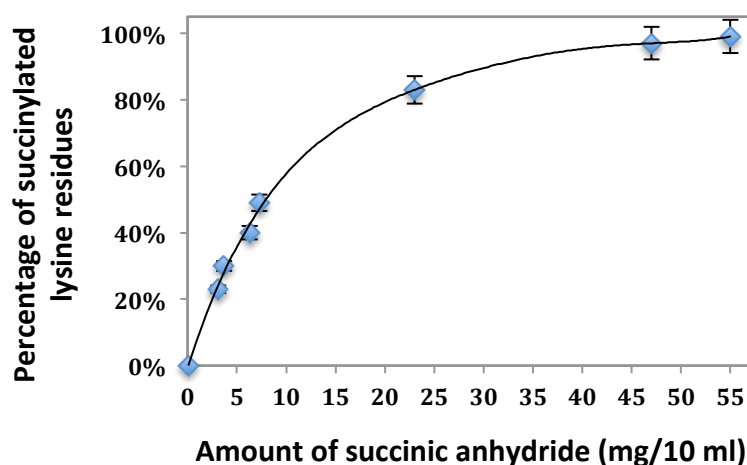


Figure 5.3 α_{s1} -Casein solutions with the addition of different amounts of succinic anhydride (as described in Section 2.2.2). The percentage of succinylated lysine residues was calculated based on a molar basis. Each data point is an average of three replicates. Error bars represent the standard deviation of the mean of the replicates.

The degree of succinylation of α_{s1} -casein was found to increase as the level of succinic anhydride in the solution was increased (Figure 5.3). The standard sample (native α_{s1} -casein) was prepared with no succinic anhydride. Figure 5.3 shows that the level of succinylated α_{s1} -casein increased linearly to approximately 50% as the amount of added succinic anhydride increased to 7.3 mg/10 mL. However, a gradual increase in the level of succinylated α_{s1} -casein was observed when the amount of added succinic anhydride was further increased to 55 mg/10 mL.

Reduced SDS – PAGE

The succinylated α_{s1} -casein was further analysed using reduced SDS-PAGE to assess the change in the mobility of succinylated α_{s1} -casein. Equal amounts of protein were loaded on the gel, and the gel was stained with Coomassie blue, which binds to

positively charged amino acid residues (Schägger & von Jagow, 1991; Tal et al., 1985). The SDS-PAGE results for the succinylated α_{s1} -casein are shown in Figure 5.4. The band intensities and positions in the standard sample (Lane 1) represent the total amount of native α_{s1} -casein. The change in band intensities in the other samples (Lanes 2 to 8) shows the α_{s1} -casein with increasing levels of succinylation.

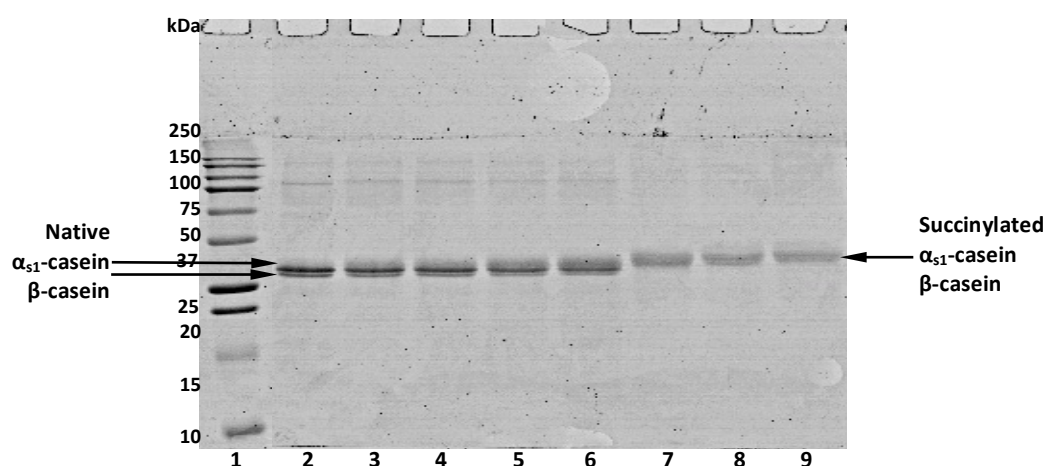


Figure 5.4 Reduced SDS-PAGE of α_{s1} -casein with different levels of succinylation. From left to right: molecular weight standards (Lane 1); α_{s1} -casein with 0 mg (standard sample – native α_{s1} -casein, Lane 2), 3.1 mg (Lane 3), 3.7 mg (Lane 4), 6.3 mg (Lane 5), 7.3 mg (Lane 6), 23 mg (Lane 7), 47 mg (Lane 8) and 55 mg (Lane 9) succinic anhydride added.

The native α_{s1} -casein had the highest band intensity (Lane 2), and the intensities of protein bands diminished as the amount of succinic anhydride added into α_{s1} -casein solutions increased from 3.1 to 55 mg/10 mL (Lanes 3 to 9). This result is consistent with the binding affinity of Coomassie blue being reduced as the positively charged lysine residues were succinylated. Figure 5.4 shows that the band of succinylated α_{s1} -casein gradually shifted to a higher position with increased amounts of succinic anhydride (Lane 2 to 6). When the amount of added succinic anhydride was increased from 23 to 55 mg/10 mL, the band position of succinylated α_{s1} -casein slightly moved to a higher position on the SDS gel (Lane 7, 8 and 9).

In the SDS-environment, proteins are separated based on their molecular mass (as described in Section 3.2.1). After succinylation, one to 14 succinic anhydride

molecules with a molar mass of 0.1 kDa could be introduced onto the α_{s1} -casein molecule as α_{s1} -casein contains 14 lysine residues. Therefore, when the level of succinylation increased from 0 to 49% (Figure 5.4 Lane 3 to 6), the molecular weight of succinylated α_{s1} -casein increased 0.64 kDa, which was not easily resolved in the gel. At higher succinylation levels (Figure 5.4 Lane 7 to 9), more succinic anhydride groups were added onto α_{s1} -casein with greater increase in the molecular weight (1.1 – 1.4 kDa), which could be more easily resolved in the gel.

The intensity of native and succinylated α_{s1} -casein on the SDS gel was quantified using ImageQuant software. Figure 5.5 shows that the band intensity of α_{s1} -casein linearly decreased to approximately 65% as the amount of added succinic anhydride increased to 23 mg/10 mL. When the amount of added succinic anhydride further increased to 55 mg/10 mL, the intensity of α_{s1} -casein gradually decreased to approximately 53% of the initial intensity (Figure 5.5).

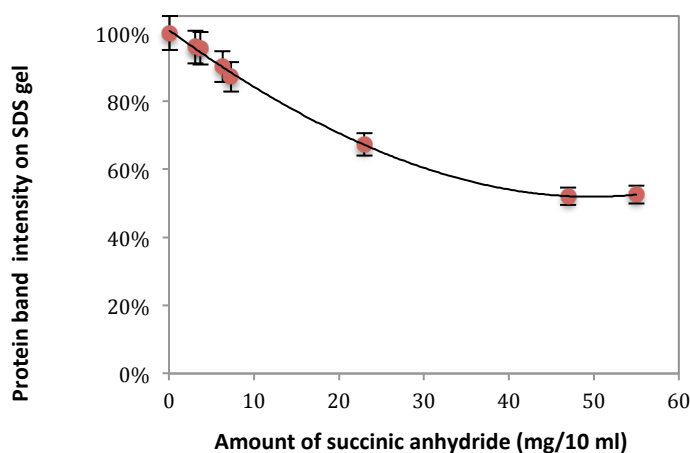


Figure 5.5 The band intensity of α_{s1} -casein with the addition of different amounts of succinic anhydride on SDS gel.

When the intensity of succinylated α_{s1} -casein, quantified from the SDS gel, was plotted against the level of succinylation determined using OPA method, a non-linear relationship was found between these two methods (Figure 5.6). One Coomassie blue molecule binds to the positively charged amino acid residues of a protein by electrostatic interactions, and up to two more dye molecules may interact with

adjacent amino acid residues through hydrophobic interactions (Tal et al., 1985). Succinylation resulted in a reduction in the lysine binding with the dye, which may affect the ability of adjacent amino acid residues to bind with the dye by the hydrophobic interactions. The introduced negative charge on the succinylated lysine residues may inhibit the dye binding to the adjacent amino acid residues by the increased electrostatic repulsions between succinylated lysine and the dye. Therefore, the change in the intensity is dependent on the number of succinylated lysine residues and the adjacent amino acid binding with the dye. By contrast to the SDS gel, the level of succinylation of α_{s1} -casein determined using OPA method is based on the number of available lysine residues.

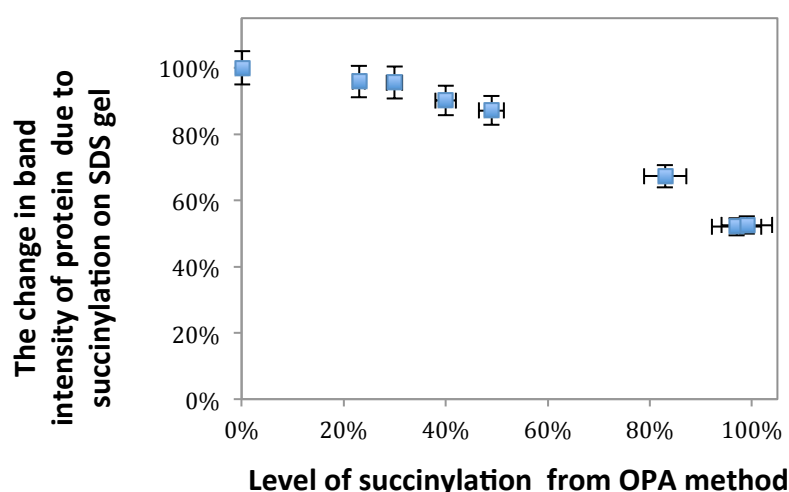


Figure 5.6 The relationship between SDS gel and OPA methods. Error bars represent the standard deviation of the mean of the three replicates.

Mass spectrometry of succinylated α_{s1} -casein

The succinylated lysine residues of α_{s1} -casein were identified using mass spectrometry (as described in Section 2.2.8). Trypsin cleaves peptide chains mainly at the carboxyl side of the lysine or arginine amino acids except when either is followed by a proline residue (Rodriguez et al., 2007). Trypsin is not able to cleave the peptide bond adjacent to lysine residues that were capped by succinic anhydride (Simpson, 2006). This will lead to different peptide fractions being formed between trypsin-digested native and succinylated α_{s1} -casein. The mass spectrometry

chromatographs of trypsin-digested native and succinylated α_{s1} -casein are shown in Figure 5.7. All the peaks were used in a database search to map the succinylated lysine residues (as described in Section 2.2.8 and Appendix C).

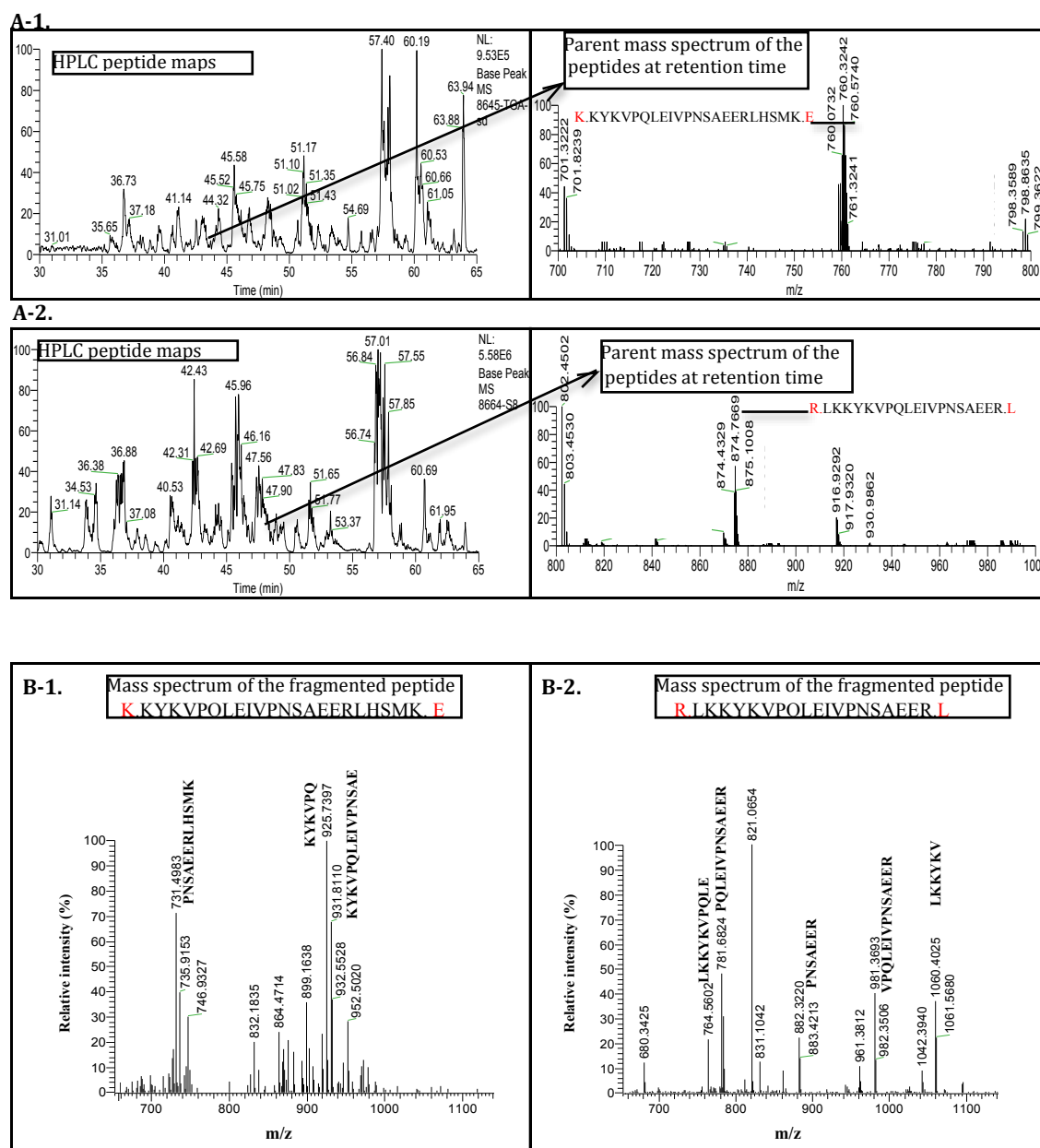


Figure 5.7 HPLC peptide maps, parent mass spectrum (A) and mass spectrum of fragmented peptide Lys₁₂₃-Lys₁₄₄ (B) from the trypsin-digested native α_{s1} -casein (1) and Arg₁₂₀-Arg₁₃₉ from the trypsin digested 99% succinylated α_{s1} -casein (2). Peak assignments corresponding to the native and succinylated lysine residues are indicated.

The HPLC peptide maps for native and succinylated α_{s1} -casein show very different patterns in the retention times between of 30 to 65 min (Figure 5.7 A). This is due to the fact the different peptides were generated between trypsin-digested native and succinylated α_{s1} -casein, as trypsin does not cleave succinylated lysine residues. The difference in the parent mass spectrum between the trypsin-digested native α_{s1} -casein and succinylated α_{s1} -casein confirmed the differences in the cleavage patterns (Figure 5.7 A). The peptide Lys₁₂₃-Lys₁₄₄ from native α_{s1} -casein and peptide Arg₁₂₀-Arg₁₃₉ from succinylated α_{s1} -casein were found in the parent mass spectrum and selected as representative mass spectra, with the trypsin cleavage sites highlighted in red. This confirmed that, as the result of succinylation, the arginine residues were the preferred cleavage sites.

The fragmentation patterns of peptide Lys₁₂₃-Lys₁₄₄ from native α_{s1} -casein and Arg₁₂₀-Arg₁₃₉ from succinylated α_{s1} -casein were used to identify the succinylated lysine residues within this peptide. Figure 5.7 B shows the mass to charge ratio of sequenced fractions from these peptides. The differences in the fragmentation patterns between trypsin-digested native and succinylated α_{s1} -casein are the result of succinylation. These fragmented peptides were processed with database mapping to calculate the change in the mass due to succinylation. This procedure was also performed for other digested peptides to identify all native and succinylated lysine residues in the whole α_{s1} -casein sequence.

In order to identify the specific lysine residues succinylated at different levels of added succinic anhydride, the identified lysine residues of α_{s1} -casein by mass spectrometry were compared with the results obtained from the SDS-PAGE. The peptides sequence was processed using Mascot Distiller Database. Figure 5.8 shows the abbreviated α_{s1} -casein genetic variant B sequence with the “K” highlighted to represent the succinylated lysine residues.

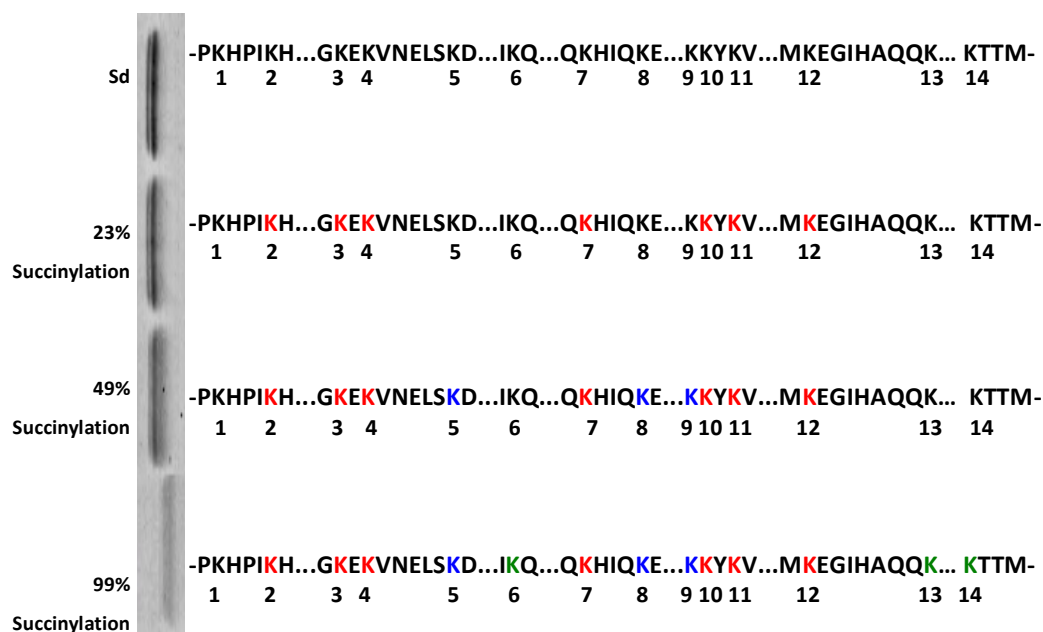


Figure 5.8 α_{s1} -Casein with different levels of succinylation monitored by reduced SDS-PAGE and mass spectrometry. K (black): un-succinylated lysine residues of native α_{s1} -casein (Sd), K (red): lysine residues succinylated at 23% succinylation of α_{s1} -casein, K (blue): lysine residues succinylated at 49% succinylation of α_{s1} -casein, K (green): lysine residues succinylated at 99% succinylation of α_{s1} -casein, which was determined using OPA method.

In the 23% succinylated α_{s1} -casein sample, lysine residues 2, 3, 4, 7, 10, 11, and 12 were succinylated (Figure 5.8). The succinylated lysine residues 5, 8 and 9 were succinylated next in the 49% succinylated α_{s1} -casein solution. When the level of succinylation increased to 99%, the lysine residues 6, 13 and 14 were succinylated (Figure 5.8).

Figure 5.8 shows that lysine residue 1 remained un-succinylated, even in the 99% succinylated α_{s1} -casein sample, presumably because accessibility was inhibited by the adjacent proline residue. It has been reported that lysine residues adjacent to the proline have low accessibility for trypsin digestion (Simpson, 2006). Thus, the proline residue could block the enzyme or chemicals to access the adjacent amino residues, such as trypsin, succinic anhydride and OPA.

For the α_{s1} -casein sample with 55 mg added succinic anhydride, 99% succinylation was obtained as judged by the OPA colorimetric assay. However, if the level of succinylation is calculated from the mass spectrometry results, the level of succinylation was 93% as only 13 out of 14 lysine residues were succinylated. This difference could be due to the blocked accessibility of the first lysine residue by the adjacent proline, which may also inhibit OPA binding to this lysine residue in both native and succinylated α_{s1} -casein. Therefore, the level of succinylation calculated from the absorbance reading of OPA colorimetric assay may be based on a total 13 available lysine residues in α_{s1} -casein rather than 14 available lysine residues.

In previous studies, around 32-94% of succinylation of whey proteins was achieved by controlling the concentration of succinic anhydride in the protein solutions (Morand et al., 2012). Morand and co-workers identified the succinylated lysine residues of whey proteins by mass spectrometry and the level of succinylated lysine residues was in agreement with the OPA results. In general, the results obtained for the succinylated α_{s1} -casein using the three different analytical approaches showed some changes due to succinylation, although the level of succinylated lysine residues determined using the OPA method was different from the mass spectrometry method. The mass spectrometry method provided detailed information on the succinylated lysine residues, whereas, the OPA assay offered a simple and fast method to determine the level of succinylation. The OPA and electrophoresis methods showed a non-linear relationship for the measurement of the level of succinylation. The electrophoresis method can be used as an indication of change in mobility and intensity of proteins, but not for the quantitative assessment.

5.2.2 Isoelectric point of succinylated α_{s1} -casein

Calculation of the theoretical pI

The theoretical pI of succinylated α_{s1} -casein (with 8 phosphoserine residues) was expressed as the isoionic point (as described in Section 3.2.2). The charge of succinylated α_{s1} -casein (containing one to 13 succinylated lysine residues) was

calculated using an online database (as described in Section 3.2.2). Based on the mass-spectrometry results (Section 5.3.1), when the level of succinylation increased, one to 13 lysine residues were capped by succinic anhydride. Each lysine residue carries one positive charge over the pH range of two to seven (Davies, 2000; Morand et al., 2011b). Therefore, the α_{s1} -casein lost one to 13 positive charges due to succinylated lysines and obtained one to 13 negative charges from the introduced carboxylate groups after succinylation. The pK_a value of the introduced succinyl group on the lysine residues is unknown. Thus, the pK_a value of 2.0 for α -carboxyl groups of amino acids was used to estimate the charges of proteins (Reginald & Charles, 2012). The charges of the α -carboxylate groups were calculated at different pHs with the CurTiPot software (Gutz, 2012). The plot of pH versus charge of α_{s1} -casein with one to 13 succinylated lysine residues was generated to demonstrate the shift in isoionic point on succinylation (Figure 5.9).

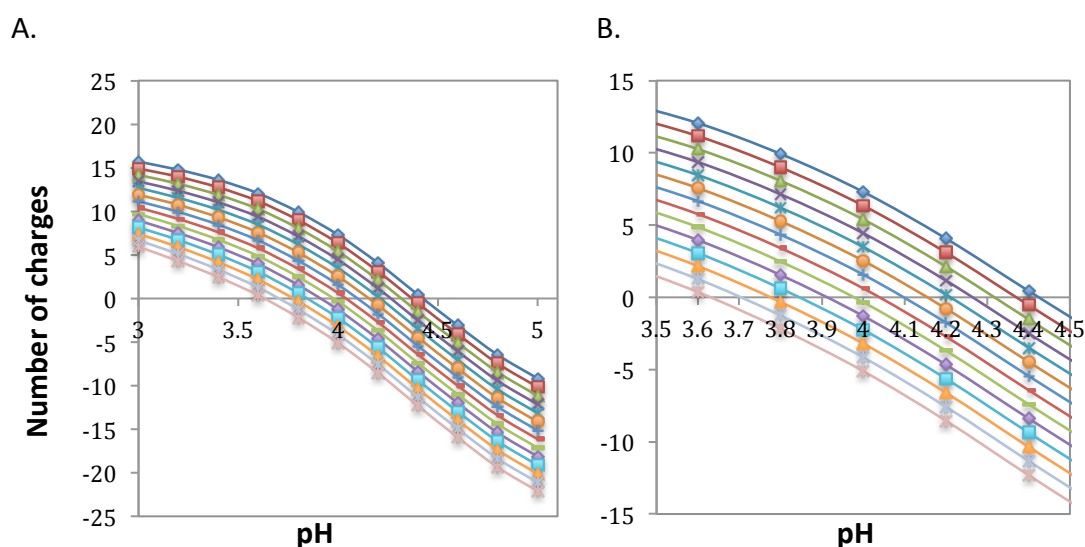


Figure 5.9. The calculated charge of α_{s1} -casein with eight phosphoserine residues and different numbers of succinylated lysine residues (0-13) at pH over the range of 3.0 to 5.0 (A) and at pH over the range of 3.5 to 4.5 (B). Casein with 0 (\blacklozenge), 1 (\blacksquare), 2 (\blacktriangle), 3 (\times), 4 ($*$), 5 (\bullet), 6 ($+$), 7 ($-$), 8 ($-$), 9 (\blacklozenge), 10 (\blacksquare), 11 (\blacktriangle), 12 (\times) and 13 ($*$) succinylated lysine residues. The net charge at each pH for the succinylated α_{s1} -casein is equal to the net charge of native α_{s1} -casein minus the positive charge of succinylated lysine, plus the negative charge of the carboxyl groups from the succinic group.

The graphs in Figure 5.9 A and B show that the variation of charge versus pH for α_{s1} -casein gradually shifted from higher to lower pH values as the number of succinylated lysine residues increased, indicating a decrease in the isoionic point. Figure 5.9 shows that succinylated α_{s1} -casein had more negative charge at higher pH ($> \text{pH } 4.4$) and less positive charge at lower pH ($< \text{pH } 3.6$) compared with native α_{s1} -casein.

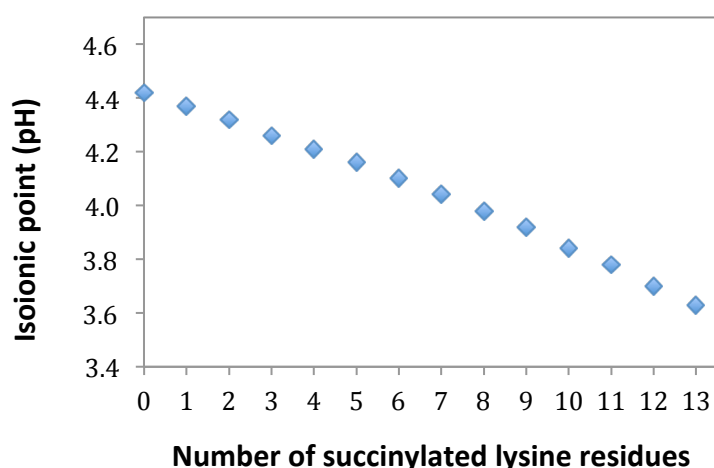


Figure 5.10 The calculated isoionic point of α_{s1} -casein with different numbers of succinylated lysine residues.

The relationship between the isoionic point of succinylated α_{s1} -casein and the level of succinylation is shown in Figure 5.10. This plot is based on the numbers of succinylated lysine residues out of the total of 13 lysine residues, corresponding to the level of succinylation. This calculated isoionic point of α_{s1} -casein was obtained from the plot of charge versus pH, which showed a decrease of 0.79 units in the pH as zero to 13 of the lysine residues of α_{s1} -casein were systematically succinylated (Figure 5.10). The isoionic point of α_{s1} -casein decreased approximately linearly from pH 4.42 to pH 3.63 as the level of succinylation increased (Figure 5.10).

Zeta potential

The change in the net charge of succinylated α_{s1} -casein was predicted to have a significant impact on the measured pI of the protein. Thus, the zeta potential of both native and succinylated α_{s1} -casein samples were measured at different pHs (as

described in Section 3.2.2). The pH of the samples was adjusted to a pH in the range of 5.6 – 2.6 prior to the experiment (as described in Section 2.2.9).

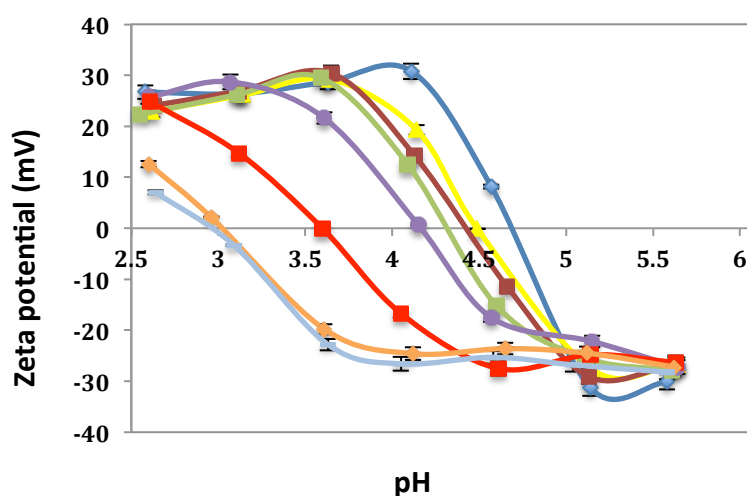


Figure 5.11 The zeta potentials of native and succinylated α_{s1} -casein at different pH values: standard sample (native α_{s1} -casein, ♦); α_{s1} -casein with different level of succinylation: 23% succinylation (▲), 30% succinylation (■), 40% succinylation (■), 49% succinylation (●), 83% succinylation (■), 97% succinylation (◆), 99% succinylation (—). Each data point is an average of two replicates. Error bars represent the standard deviation of the mean of the replicates.

The pH at which α_{s1} -casein had zero zeta potential was shifted to a lower pH as the level of succinylation increased (Figure 5.11). The pH where the native α_{s1} -casein had zero zeta potential was about pH 4.69, whereas the pH where the 99% succinylated α_{s1} -casein had zero zeta potential was about pH 2.95. These zeta potential results indicate that native α_{s1} -casein had a much higher apparent pI in comparison with succinylated α_{s1} -casein, and the lowest apparent pI was observed at highest level of succinylation (Figure 5.11).

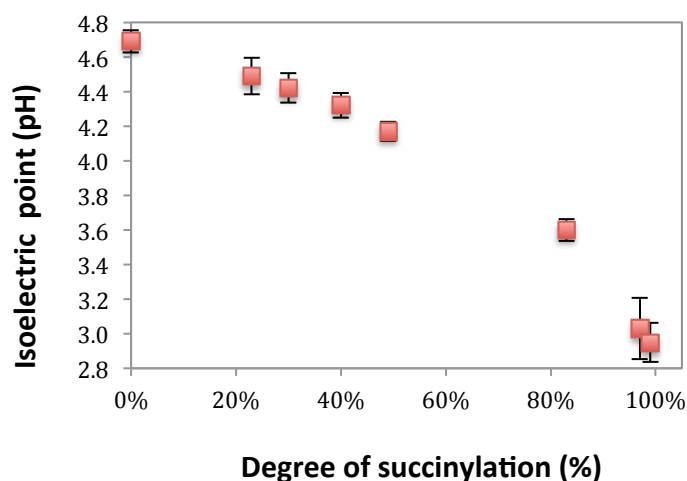


Figure 5.12 The isoelectric point of α_{s1} -casein, as determined from zeta potential measurements, for samples with different levels of succinylation. Each data point is an average of two replicates. Error bars represent the standard deviation of the mean of the replicates.

The pI of α_{s1} -casein based on the zeta potential results (Figure 5.11) was plotted against the level of succinylation (Figure 5.12). This shows that the pI of α_{s1} -casein shifted from pH 4.69 to pH 2.95 as the level of succinylation increased from 0% (standard sample - native α_{s1} -casein) to 99%. It was observed that the 99% succinylated α_{s1} -casein had an approximately 1.74 unit reduction in the pI compared to native α_{s1} -casein.

IEF-PAGE

The pI of succinylated α_{s1} -casein was also determined using IEF-PAGE (Figure 5.13), as described in Section 3.2.2.

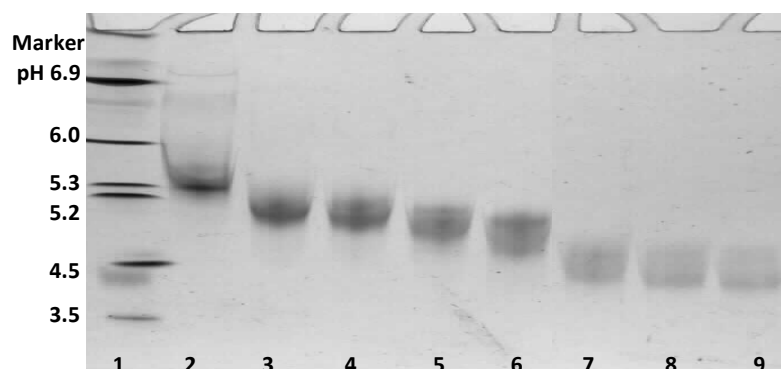


Figure 5.13 IEF-PAGE of α_{s1} -casein with different levels of succinylation. From left to right: pH marker proteins (Lane 1), standard sample (native α_{s1} -casein, Lane 2), α_{s1} -casein with different levels of succinylation: 23% (Lane 3), 30% (Lane 4), 40% (Lane 5), 49% (Lane 6), 83% (Lane 7), 97% (Lane 8), 99% (Lane 9).

The IEF protein marker used in this experiment represents a pH range of 3.0 to 7.0 (Figure 5.13, Lane 1; as described in Section 3.2.2). The bands representing the succinylated α_{s1} -casein (Lanes 3 to 9) gradually shifted to lower band positions compared to the native proteins (Lanes 2). This indicates that the succinylated caseins have a longer migration distance than the native caseins and the migration distance increased as the level of succinylation increased. Unlike dephosphorylation (see Section 3.2.2), succinylation led to an increase in the total negative charge of α_{s1} -casein, which resulted in a longer migration distance to neutralize its net charge. The negatively charged protein migrates towards the anode and the negative charge of the protein decreased as the protein migrates through a gradient of decreasing pH until the protein has a zero net charge and stops migrating (Alberts et al., 2007; Allen et al., 1984). Therefore, when compared to native α_{s1} -casein, succinylated α_{s1} -casein reached the lower pH region before the protein stops migration.

The results showed that the native α_{s1} -casein had an apparent pI around pH 5.25 (Figure 5.13, Lane 2), and the succinylated α_{s1} -casein had a lower pI compared to native casein (Lanes 2 to 9). When the level of succinylation increased to 99%, the pI of α_{s1} -casein decreased to around pH 4.00 (Lane 9). The reduction in pI between native α_{s1} -casein and 99% succinylated α_{s1} -casein was around 1.25 pH units.

Comparing pI results from charge calculation, zeta potential and IEF methods

In a previous study, 32% to 64% succinylated whey protein complexes were generated, and the zeta potential results showed a pI shift from pH 4.9 to 3.8 (Morand et al., 2011b). The pI of succinylated α_{s1} -casein also decreased as the succinylation degree increased (Figure 5.12). In this study, the IEF-PAGE and charge calculation methods showed a gradual reduction in the apparent pI of α_{s1} -casein with increasing the level of succinylation. The zeta potential measurement showed a linear reduction in the pI of α_{s1} -casein as the level of succinylation increased from 0 to 49%; however, the apparent pI of α_{s1} -casein rapidly dropped when the level of succinylation increased further to 83% and 99%.

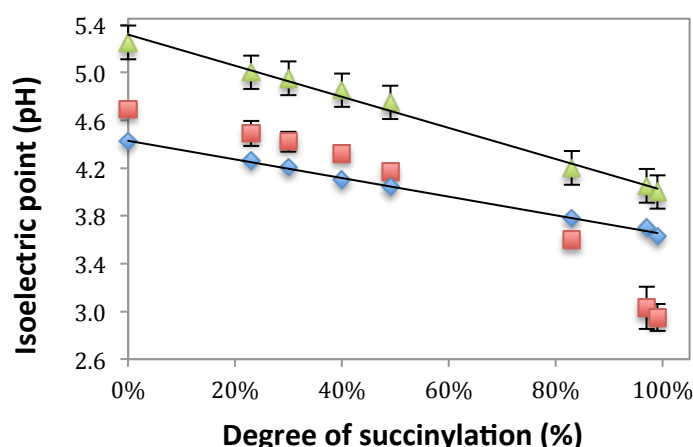


Figure 5.14 The isoelectric point of succinylated α_{s1} -casein with different level of succinylation, which were determined using IEF gel (\blacktriangle), zeta potential measurement (\blacksquare) and charge calculation (\blacklozenge). Error bars represent the standard deviation of the mean of replicate measurements.

Both IEF gel and theoretical charge calculation methods showed a linear decrease in the pI of succinylated α_{s1} -casein, even though the levels of reduction in the pI were different (Figure 5.14). The zeta potential results showed a similar reduction in the pI between the 83% succinylated α_{s1} -casein and native α_{s1} -casein compared to the IEF-PAGE and the calculation of theoretical charge versus pH methods (Figure 5.14). When the level of succinylation increased from 0% to 83%, the pI values of α_{s1} -casein obtained from the zeta potential method was very close to the pI values obtained

from the charge calculation method. However, when the level of succinylation increased from 83% to 99%, the zeta potential method showed a greater reduction in the pI of succinylated α_{s1} -casein (0.57 unit) compared with the charge calculation method that showed a 0.08 unit reduction. This could be due to the fact that the zeta potential method measures the surface charge of protein in an ionized environment, whereas the isoionic point was calculated based on the amount of charge in a deionized environment (described in Section 3.2.2). During the zeta potential measurement, the pH of protein samples was adjusted with HCl and NaOH (described in Section 2.2.9), which could affect the ionic strength of the protein samples. It has been reported that the zeta potential is sensitive to the change in ionic strength at different pH conditions (Carneiro-da-Cunha et al., 2011; Coday et al., 2015; Galisteo et al., 1990; Hsu & Huang, 2002; Pfeiffer et al., 2014). In addition, succinylation could lead to a rearrangement of α_{s1} -casein molecules due to the change in the net charge, such as monomerization of α_{s1} -casein upon succinylation (as described in Section 5.2.5). This may affect the electrophoretic mobility of α_{s1} -casein for the zeta potential measurement. A non-linear relationship was observed when the calculated pI was plotted against the pI from zeta potential method (Figure 5.15 A). This could be due to the limitation of zeta potential measurement that only surface charges of proteins were determined, whereas, the isoionic point of α_{s1} -casein was against an estimated level of succinylation based on zero to 13 succinylated lysine residues. Even so, the zeta potential and charge calculation methods showed a similar trend of changes in the apparent pI of α_{s1} -casein due to succinylation.

Figure 5.14 shows that the IEF measurement gave a higher pI value than charge calculation and zeta potential methods. This could be due to the limitation of the commercial native IEF gel for proteins that have low solubility close to their pI (as described in Section 3.2.2). However, a linear relationship was found when the calculated pI was plotted against the pI from the IEF gel (Figure 5.15 B). Figure 5.15 B confirmed that the charge calculation and IEF methods provided consistent results that succinylation contributed to a decrease in the pI of α_{s1} -casein.

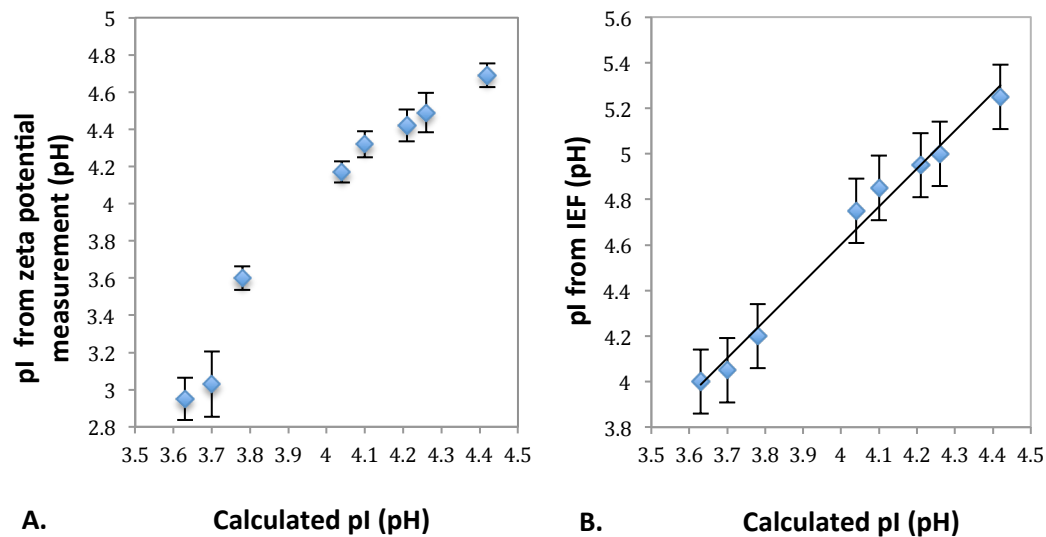


Figure 5.15 The relationship between charge calculation and zeta potential methods (A), The relationship between charge calculation and IEF gel methods for measuring the pI of native and succinylated α_{s1} -casein (B). Error bars represent the standard deviation of the mean of the replicates.

The zeta potential measurement confirms the pI shift between native and succinylated α_{s1} -casein when the α_{s1} -casein samples are at the same pH and ionic environment. By contrast to the zeta potential method, the IEF gel method showed higher pI values of native α_{s1} -casein and succinylated α_{s1} -casein (Figure 5.14). This result is in agreement with results from dephosphorylated α_{s1} -casein, which showed that the pI values of native α_{s1} -casein and dephosphorylated α_{s1} -casein obtained from IEF gel were higher compared to those from the zeta potential method. This could be due to the fact that the IEF gel measures the pI based on the total net charge of proteins, whereas the zeta potential method determines the pI based on the surface charge of proteins (described in Section 3.2.2).

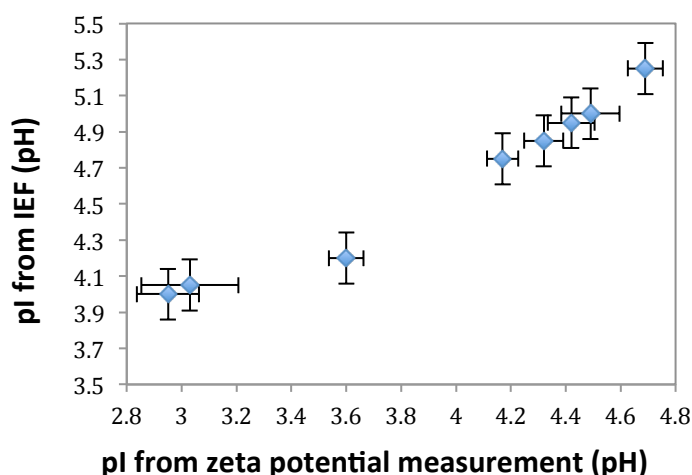


Figure 5.16 The relationship between zeta potential and IEF gel methods for measuring the pI of native and succinylated α_{s1} -casein. Error bars represent the standard deviation of the mean of the replicates.

When the pI values obtained from zeta potential were plotted against the pI values obtained from IEF gel, a non-linear relationship was found (Figure 5.16). When the level of succinylated α_{s1} -casein increased from 0% to 99%, the pI decreased from pH 4.69 to pH 2.95 when measured by the zeta potential method, and the IEF gel showed a reduction in the pI from pH 5.25 to pH 4.00. At the lower pI values from zeta potential measurement (pH 2.95 and 3.03), the pI from IEF method shifted to a higher value (pH 4.0 and 4.05), which contributed to the non-linear relationship between the IEF and zeta potential methods. This could result from the fact that the zeta potential measurement caused a lower pI value of α_{s1} -casein with the higher level succinylation (83% and 99%) due to the rearrangement of α_{s1} -casein molecules (as described previously). The IEF gel and zeta potential methods showed that the pI shift of succinylated α_{s1} -casein is in agreement, even though the different pI values were obtained from the two methods.

Overall, IEF-PAGE, zeta potential and the calculation of theoretical charge versus pH methods were performed to determine the change in pI of succinylated α_{s1} -casein. All three methods showed consistent trends with the pI of succinylated α_{s1} -casein decreasing in comparison to native α_{s1} -casein. These findings are in agreement with

a previous study by Morand et al. (2011b), who reported that the succinylation of proteins decreases the pI by converting the amino groups into carboxyl groups, thereby increasing the negative charge.

5.2.3 Hydrophobicity of succinylated α_{s1} -casein

Hydrophobic interactions play an important role in the functional properties of milk proteins such as emulsification, foaming and acid gelation (Lieske et al., 2000; Morand et al., 2012; Moro et al., 2001; Murphy & Howell, 1990). The succinylation of α_{s1} -casein resulted in the overall charge increasing at pH 7.0 when the hydrophilic lysine residues were succinylated, thereby affecting the predicted hydrophobicity of α_{s1} -casein. Thus, measurements of the surface hydrophobicity of the protein may be useful in predicting the functionality of α_{s1} -casein. The apparent hydrophobicity of both native and succinylated α_{s1} -casein was examined by an ANS fluorescence probe (as described in Sections 3.2.10).

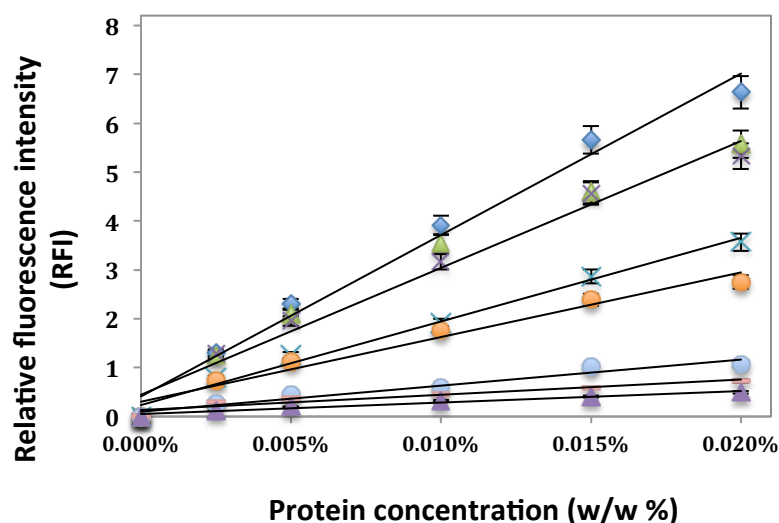


Figure 5.17 Relative fluorescence intensity of α_{s1} -casein. Standard (native α_{s1} -casein, ♦), α_{s1} -casein with different levels of succinylation: 23% (▲), 30% (×), 40% (×), 49% (●), 83% (●), 97% (-), 99% (▲). Each data point is an average of three replicates. Error bars represent the standard deviation of the mean of the replicates.

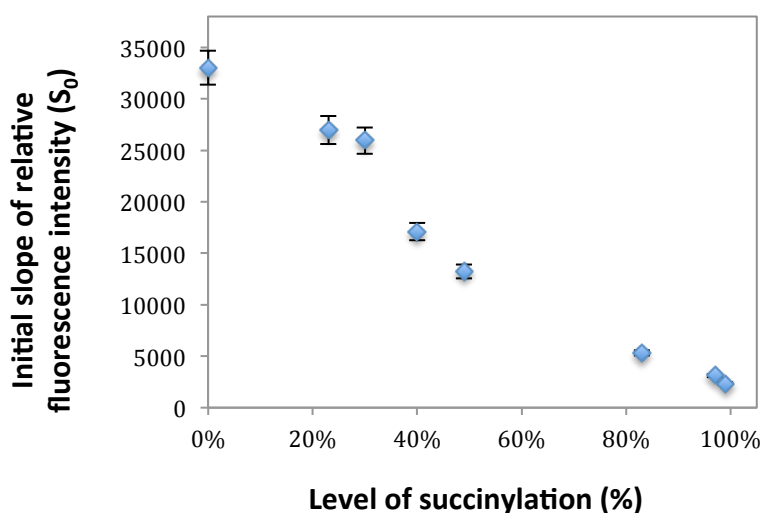


Figure 5.18 Initial slope (S_0) of the relative fluorescence intensity of the α_{s1} -caseins with different levels of succinylated lysine residues. Error bars represent the standard deviation of the mean of the replicates.

The RFI of α_{s1} -casein increased as the protein concentration increased (Figure 5.17). The plot in Figure 5.17 showed that the RFI of succinylated α_{s1} -casein diminished over the protein concentration range of 0.0025% to 0.02% in comparison to native α_{s1} -casein. Increasing the level of succinylation from 0 to 99% resulted in a 16-fold reduction in the S_0 of RFI from 33000 to 2000 (Figure 5.18).

In this study, the S_0 of the RFI results determined using the ANS fluorescence probe indicated that the hydrophobicity of succinylated α_{s1} -casein decreased as the degree of succinylation increased (Figure 5.17 and Figure 5.18). These findings are in agreement with the results from previous studies by Shilpashree et al. (2015) and Yang et al. (2015). In their studies, 82% succinylated yak casein micelles and 96% succinylated sodium caseinate at pH 7.0 showed a large decrease in the surface hydrophobicity in comparison to unmodified proteins. It also has been reported that the surface hydrophobicity of canola protein isolate at pH 7.0 decreased as the level of succinylation increased, which was also examined using the ANS fluorescence probe technique (Paulson & Tung, 1987).

However, Morand et al. (2012) have reported that for a heat-induced whey protein complex at pH 7.0, increasing the succinylation from 15% to 90% only resulted in a minor reduction of the surface hydrophobicity. This minor change in the surface hydrophobicity might be because the heat-induced whey protein complex is much more complicated than the α_{s1} -casein fraction, as it contains β -lactoglobulin, α -lactalbumin, immunoglobulin and bovine serum albumin with minor amounts of κ -, α_{s1} - and α_{s2} -caseins. Succinylation may lead to a rearrangement of the complex structure due to the increased electrostatic repulsion between protein molecules. This rearranged complex structure could potentially bury some of the hydrophobic regions of proteins that were initially exposed on the surface of the unmodified complex, resulting in the buried hydrophobic regions being unavailable to be accessed by hydrophobic probe. In addition, the non-ionic 6-propionyl-2-(N,N-dimethylamino)-naphthalene probe (PRODAN) was applied to examine the surface hydrophobicity in the study, which might have different affinity for the hydrophobic regions in comparison to the ANS probe.

Overall, the ANS fluorescence probe is well established for determining the hydrophobicity of proteins (as described in Section 3.2.3, (Koudelka et al., 2009). In this study, the results of the ANS fluorescence probe measurement showed a consistent hydrophobicity decrease between native α_{s1} -casein and succinylated α_{s1} -casein.

5.2.4 Secondary structure of succinylated α_{s1} -casein

The succinylation of α_{s1} -casein converts the amino groups of lysine residues into carboxyl groups, which results in the overall charge of α_{s1} -casein increasing. This change in the net charge of α_{s1} -casein might have an effect on its conformation (Formaggioni et al., 1999; Treweek, 2012). Therefore, the secondary structure of succinylated α_{s1} -casein was estimated using a CD spectrometer (as described in Section 2.2.13).

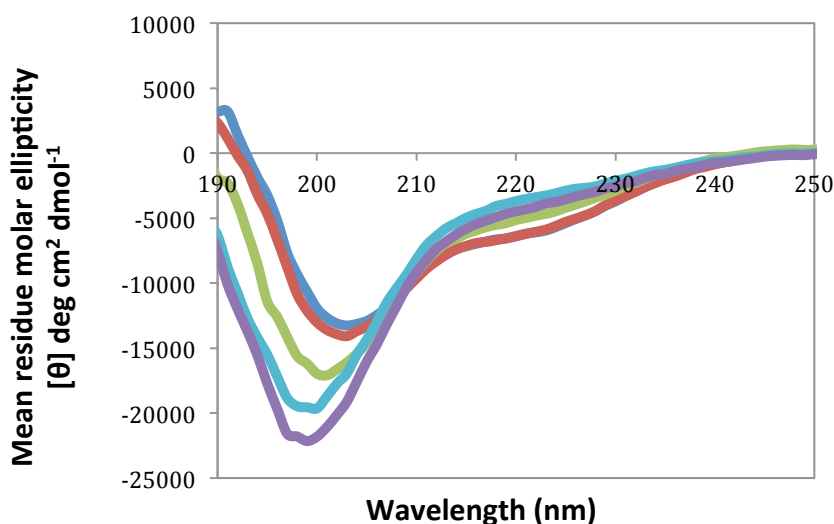


Figure 5.19 Effect of succinylation levels on the far-UV CD mean residue ellipticity $[\theta]$ of α_{s1} -casein expressed in degree cm^2/dmol . **Standard (blue)-native α_{s1} -casein; casein with 23% (red), 49% (green), 83% (light blue) and 99% succinylation (purple).**

The troughs at different wavelength correspond to the specific secondary structural features of proteins, which was described in Section 3.2.4. The far-UV CD spectra demonstrated that the absolute value of mean residue ellipticity of succinylated α_{s1} -casein increased at a wavelength between 190 and 208 nm compared with the standard sample (Figure 5.19). The absolute value of mean residue ellipticity at the wavelengths between 208 and 250 nm showed a minor reduction between succinylated α_{s1} -casein and the standard sample. The secondary structural features for each dichroic spectrum in Figure 5.19 were calculated (as described in Section 3.2.4; Raussens et al., 2003). The calculated levels of secondary structure of native and succinylated α_{s1} -casein are given in Table 5.1.

Table 5.1 shows that standard sample contained 15% helix, ~28% β -sheet and 39% random coil structure. These findings are consistent with previous studies where 8-15% α -helix, 18-40% β -sheet and 24-35% random coil structure were determined in α_{s1} -casein using CD spectroscopy or Raman spectroscopy (Horne, 2002; Kumosinski et al., 1993; Malin et al., 2005; Michael Byler et al., 1988). However, the level of random coil structure (39%) is slightly higher than reported in previous studies (24-

35%). This could be due to the impurities in the α_{s1} -casein sample (as described in Section 3.2.4).

Table 5.1 The level of secondary structure of native and succinylated α_{s1} -casein estimated by CD. (15 accumulations for one determination; standard error given for three determinations, standard errors less than 1 are not stated).

Degree of succinylation (%)	α -Helix (%)	β -Sheet (%)	Random coil (%)
0% standard	15.0	27.6	39.0
23% succinylation	13.7	28.9 \pm 1	39.2 \pm 1
49% succinylation	10.6	31.7	40.3 \pm 1
83% succinylation	5.3 \pm 1	35.3	41.6 \pm 1
99% succinylation	4.8	35.1 \pm 1	41.7

The levels of α -helix, β -sheet and random coil of succinylated α_{s1} -casein with different level of succinylation are also shown in Table 5.1. When the level of succinylation increased to 99%, the level of β -sheet in α_{s1} -casein increased to 35.1% and the level of α -helix decreased to 4.8% (Table 5.1). The level of random coil structure in 99% succinylated α_{s1} -casein only increased slightly to 41.7%.

Succinylation led to a significant change in the level of α -helix and β -sheet of α_{s1} -casein ($p < 0.05$). α -Helical regions are rich in lysine residues as lysine is normally a strong helix former, but the helix can be destabilized by repulsion (Holde, 1989). After succinylation, the overall net charge of α_{s1} -casein increased at pH 7.0, which led to a stronger electrostatic repulsion between protein chains of the α_{s1} -casein. These electrostatic repulsions may have inhibited the formation of α -helix. Moreover, succinylation introduces the succinyl groups onto the lysine residues of α_{s1} -casein, which leads to an increase in the steric repulsion. This steric repulsion could also hinder the formation of α -helix. Therefore, the change in the level of secondary structure could be due to the electrostatic repulsions alone or in combination with the steric hindrance (Batra et al., 1990).

Succinylation resulted in an increase in the level of β -sheet in α_{s1} -casein (Table 5.1). This finding is in agreement with the previous study by Yang et al. (2015) who reported that the content of β -sheet in 82% succinylated yak casein micelles increased by 10% compared to native yak casein micelles. The same effect of succinylation on the level of secondary structure was also found in other proteins. For example, Batra et al. (1990) reported that 97% succinylation of ovalbumin led to a reduction in the level of α -helix and an increase in the level of β -sheet, whereas the random coil structure was relatively unchanged.

5.2.5 Self-association behaviour of succinylated α_{s1} -casein

α_{s1} -Casein exhibits progressive self-association behaviour to form dimers, tetramers and hexamers, etc. (as described in Section 3.2.5; Ho & Waugh, 1965; Horne, 2002; Schmidt, 1970; Swaisgood, 2003). Succinylation led a significant change in the net charge and apparent hydrophobicity of α_{s1} -casein, which might consequently affect its self-association behaviour. Thus, sedimentation velocity measurements of native and succinylated α_{s1} -casein were conducted using the analytical ultracentrifugation method described in Section 2.2.14.

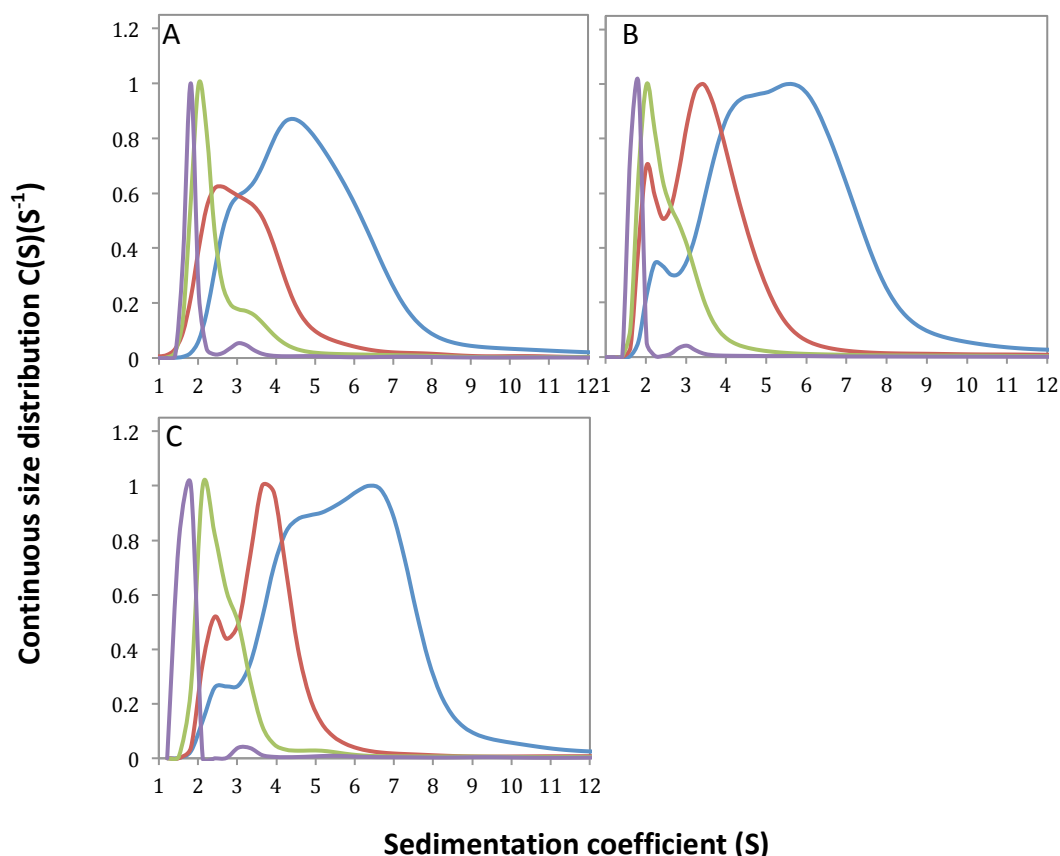


Figure 5.20 Sedimentation coefficient distribution of native and succinylated α_{s1} -casein in 10 mM phosphate buffer (containing 2.7 mM KCl and 137 mM NaCl, pH 7.4) at protein concentrations of A: 1 mg/mL, B: 2 mg/mL and C: 3 mg/mL. Standard - native α_{s1} -casein (blue); α_{s1} -casein with different level of succinylation: 23% (red), 49% (green) and 99% (purple). Confidence level in all the measurements was set to 99% for the final fits. The sedimentation coefficient distribution was determined with rmsds of 0.0049 ± 0.0002 , 0.0050 ± 0.0005 , and 0.0056 ± 0.0005 for measurement A, B and C, respectively.

The native α_{s1} -casein showed a size distribution peak at a broad range of sedimentation coefficients between 2 to 8S at all protein concentrations (Figure 5.20). At protein concentrations of 1 mg/mL, 2 mg/mL, and 3 mg/mL, succinylation resulted in a reduction in the sedimentation coefficient of the α_{s1} -casein (Figure 5.20). The 23% succinylated α_{s1} -casein showed a peak at sedimentation coefficients of 2 to 5S (Figure 5.20). When the level of succinylation increased to 49% and 99%, the size distribution peak shifted to sedimentation coefficients of about 2S and 1.5S, respectively (Figure 5.20 A, B and C).

The higher sedimentation coefficient value corresponds to larger sizes of associated species of proteins. The sedimentation coefficient distribution results indicate that the succinylated α_{s1} -casein exhibited less self-association behaviour in comparison to native α_{s1} -casein. When the level of succinylation increased from 0% to 49%, the self-associated species of α_{s1} -casein shifted to smaller sizes, indicating that the polymers dissociated and formed smaller oligomers. For the 99% succinylated α_{s1} -casein that was determined using the OPA method, there was a single species consistent with a monomeric α_{s1} -casein.

Unlike dephosphorylation (as described in Section 3.2.5), succinylation led to an increase in the electrostatic repulsion between the succinylated α_{s1} -casein molecules due to the increased overall net charge at pH 7.0. This increased electrostatic repulsion inhibits self-association, and consequently results in smaller associated species compared to native α_{s1} -casein. The self-association of the α_{s1} -casein may be driven by hydrophobic interactions but the size of the polymers and the degree of association is limited by electrostatic repulsions (as described in Section 3.2.5; Horne, 2002). Therefore, the higher level of succinylation showed a lower level of self-association due to the stronger electrostatic repulsion and lower level of hydrophobic bonding.

5.3 Conclusions

Succinylation was used to chemically modify the α_{s1} -casein to alter the charge/pI, hydrophobicity and secondary structure of the protein. The physicochemical properties of α_{s1} -casein were successfully manipulated by controlling the level of succinylation using succinic anhydride. Several analytical methods were used for the characterization of the succinylated α_{s1} -casein, which provided consistent results for the physicochemical property measurements.

After succinylation, the net charge increased as more lysine residues were capped by

succinic anhydride at pH 7.0, which consequently led to an increase in electrostatic repulsions. Succinylation of α_{s1} -casein resulted in a progressive reduction in the isoelectric point and apparent hydrophobicity, which was a consequence of the changes to the proteins net charge. Moreover, succinylation contributed to a reduction in α -helix and an increase in β -sheet secondary structural elements. The self-association behaviour of α_{s1} -casein decreased as the level of succinylation increased, which was attributed to the modified net charges and hydrophobicity of α_{s1} -casein.

The modified physicochemical properties of α_{s1} -casein are predicted to have an effect on the functional properties of the protein. For example, the secondary structural change of succinylated α_{s1} -casein may play an important role in the emulsifying properties of the protein. Therefore, in order to understand the correlation between the physicochemical properties and functionalities of α_{s1} -casein, the functional properties of α_{s1} -casein such as water binding, foaming and emulsifying properties of α_{s1} -casein were examined and are described in Chapter 6.

Chapter 6 Functional properties of succinylated α_{s1} -casein

6.1 Introduction

Succinylation had a significant effect on the physicochemical properties of α_{s1} -casein, such as net charge, pI and hydrophobicity, as described in Chapter 5. Furthermore, these physicochemical parameters can be manipulated by controlling the degree of succinylation. It has been proposed that succinylation changes the secondary structure of whey protein and increases the solubility and emulsion properties of heat denatured acid whey proteins (Kester & Richardson, 1984; Morand et al., 2011b). However, the effect of succinylation on the functional properties of α_{s1} -casein has not been reported.

This chapter will discuss how succinylation affects the viscosity, water binding capacity and interfacial properties of α_{s1} -casein due to the change in net charge and hydrophobicity. The relationship between protein charge and emulsifying properties was also investigated.

6.2 Results and discussion

6.2.1 Viscosity of succinylated α_{s1} -casein

Previous results showed that succinylation led to a change in the overall net charge and apparent hydrophobicity of α_{s1} -casein (described in Section 5.2). The modified net charge was predicted to have an impact on the viscosity of α_{s1} -casein. Therefore, the viscosity of succinylated α_{s1} -casein was examined using a capillary viscometer (described in Section 2.2.16).

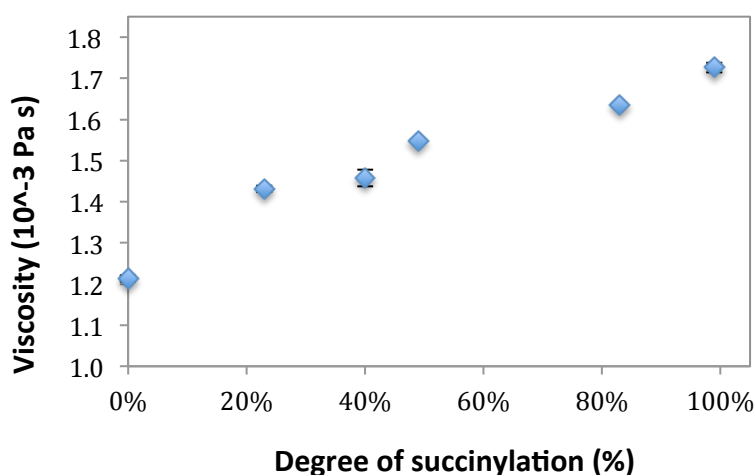


Figure 6.1 Viscosity of α_{s1} -casein with different levels of succinylation. Each data point is an average of three replicates. Error bars represent the standard deviation of the mean of the replicates.

The viscosity of succinylated α_{s1} -casein solutions significantly increased in comparison to the standard sample (Figure 6.1). The viscosity of the 99% succinylated α_{s1} -casein solution increased about 1.5 times when compared with the viscosity of the standard sample.

Succinylation resulted in the overall negative charge of α_{s1} -casein increasing, and the higher the level of succinylation the more negative charge was introduced on to the lysine residues (as described in Section 5.2.2). The increased overall net charge led to a strong electrostatic repulsion between succinylated α_{s1} -casein molecules, which contributed to the higher viscosity of succinylated α_{s1} -casein. This is consistent with the result from the viscosity of dephosphorylated α_{s1} -casein, where dephosphorylation decreased the viscosity of α_{s1} -casein due to the reduction in the net charge of α_{s1} -casein. The effect of charge on the viscosity of proteins was described in Section 4.2.2. It has been reported that the viscosity of ribonuclease increased with the overall net charge at constant ionic strength (Buzzell & Tanford, 1956). The results from our study are in agreement with a previous study by Kim and

Kinsella (1986) who showed that the viscosity of soy glycinin also increased with the level of succinylation.

In addition, the shape and size of the molecule will affect the viscosity of proteins (Viswanath et al., 2007). Succinylation reduced the self-association behaviour of α_{s1} -casein (described in Section 5.2.5), which also will have contributed to the increased viscosity of α_{s1} -casein (as described in Section 4.2.2).

6.2.2 Water binding properties of succinylated α_{s1} -casein

The impact of succinylation on the net charge and apparent hydrophobicity of α_{s1} -casein was described in Chapter 5. These changes in the net charge and availability of lysine residues were predicted to affect the water binding capacity of α_{s1} -casein. Therefore, the water binding capacity of succinylated α_{s1} -casein was determined by measuring the T2 relaxation constant using NMR (described in Section 2.2.15).

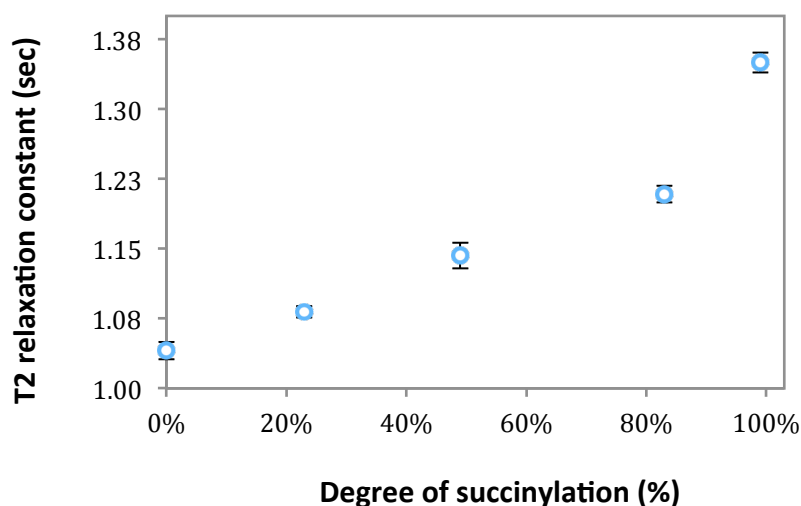


Figure 6.2 T2 relaxation constant time of succinylated α_{s1} -casein measured using NMR. Each data point is an average of two replicates. Error bars represent the standard deviation of the mean of the replicates.

The T2 relaxation constant of succinylated α_{s1} -casein was found to progressively increase as the level of succinylation increased (Figure 6.2). The T2 relaxation constant of 99% succinylated α_{s1} -casein increased about 0.3 s in comparison to the standard sample. These results indicate that the water binding capacity of succinylated α_{s1} -casein was lower than native α_{s1} -casein, and the higher level of succinylation prompted a lower water binding capacity for α_{s1} -casein.

The amount of water retained by proteins is influenced by the surface hydrophobicity and net charge. Higher net charge and lower surface hydrophobicity of proteins enhanced the amount of bound water (Kinsella & Morr, 1984; Zayas, 1997). Thus, the water binding capacity of succinylated α_{s1} -casein was predicted to be higher than native α_{s1} -casein, due to the increased net charge and decreased surface hydrophobicity. However, this study showed that succinylation led to a reduction in the water binding capacity of α_{s1} -casein. This is consistent with the suggestion that amino groups play a major role in the water binding capacity of proteins (Schnepf, 1992). Hydrophilic amino acid side chains have a specific water binding affinity and capacity that is directly affected by the type and number of these hydrophilic groups in the protein polypeptide chain (Kuntz, 1971). The lysine residues appear to be the specific sites of the protein molecules where water is bound. Lysine residues as ionic side chains can bind 4 to 7 water molecules (Kuntz, 1971; Zayas, 1997). Therefore, higher levels of succinylation led to more hydrophilic lysine residues of α_{s1} -casein being capped, and consequently resulted in fewer water molecules binding to the succinylated α_{s1} -casein in comparison to the native α_{s1} -casein.

These results are consistent with the results from the water binding capacity of dephosphorylated α_{s1} -casein. Dephosphorylated α_{s1} -casein showed an increased water binding capacity due to the introduced hydroxyl groups, though dephosphorylation led to a reduction in the net charge of α_{s1} -casein (as described in Section 4.2.3). Moreover, succinylation led to a reduction in both surface hydrophobicity and water binding capacity, and dephosphorylation resulted in an increase in both surface hydrophobicity and water binding capacity. It seems that

the change in the surface hydrophobicity is at odds with the change in the water binding capacity. This could be due to the affinity of amino groups to water molecules being affected by the ionic strength of protein solutions. The water binding capacity was determined in deionized solutions, whereas, the surface hydrophobicity was measured at higher ionic strength (as described in Section 4.2.3).

6.2.3 Surface tension of air-water interfaces of succinylated α_{s1} -casein

Surface tension as a functional parameter can play an important role in the functionality of proteins and therefore the surface tension of succinylated α_{s1} -casein was measured using the Wilhelmy plate method (as described in Section 2.2.17). In order to distinguish the change in the surface tension of succinylated α_{s1} -casein a protein concentration of 0.02% α_{s1} -casein was used for the surface tension measurement (as described in Section 4.2.4).

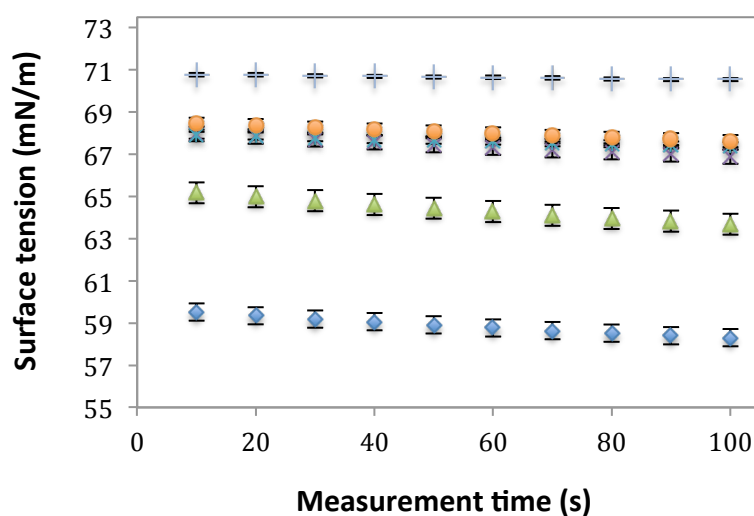


Figure 6.3 Surface tension (air-water) of succinylated α_{s1} -casein measured using the Wilhelmy plate method. Standard (native α_{s1} -casein, ◆), α_{s1} -casein with different levels of succinylation: 23% (▲), 40% (×), 49%(*), 83%(●) and 99%(+). Each data point is an average of four replicates. Error bars represent the standard deviation of the mean of the replicates.

The surface tension of succinylated α_{s1} -casein between the air and water interface increased as the level of succinylation increased (Figure 6.3). There was a major increase in the surface tension between the standard sample (~59 mN/m) and 23% succinylated α_{s1} -casein (~65 mN/m). Figure 6.3 also shows that the surface tension increased gradually between 23% and 99% succinylated α_{s1} -casein.

Succinylation led to an increase in the surface tension of the α_{s1} -casein solutions compared to native α_{s1} -casein, which is consistent with the decreased apparent hydrophobicity of succinylated α_{s1} -casein. Proteins adsorbed onto the interface due to the hydrophobic properties of the interface, and this protein adsorption was reduced with decreasing the hydrophobicity of protein (Benjamins et al., 1975; Pezennec et al., 2000; Walstra & De Roos, 1993). Therefore, the succinylated α_{s1} -casein tended to move to the hydrophobic interface more slowly than native α_{s1} -casein, and consequently led to a lower level of reduction in the surface tension than native α_{s1} -casein. This correlation is consistent with the literature (Kato & Nakai, 1980) and the results in Chapter 4 where the surface tension of dephosphorylated α_{s1} -casein decreased with increased hydrophobicity and decreased net charge of α_{s1} -casein (as described in Section 4.2.4).

The increased surface tension of succinylated α_{s1} -casein could also be influenced by the increase in the overall net charge. The repulsive force between α_{s1} -casein molecules was enhanced due to the increased negative charge, which contributed to succinylated α_{s1} -casein molecules moving away from the air-water interface (as described in Section 4.2.4). The decreased concentration of succinylated α_{s1} -casein at the air-water interface leads to the surface tension being increased.

6.2.4 Surface tension of oil-water interfaces of succinylated α_{s1} -casein

The surface tension of succinylated α_{s1} -casein between oil-water was examined using a pendant drop tension meter (described in Section 2.2.18).

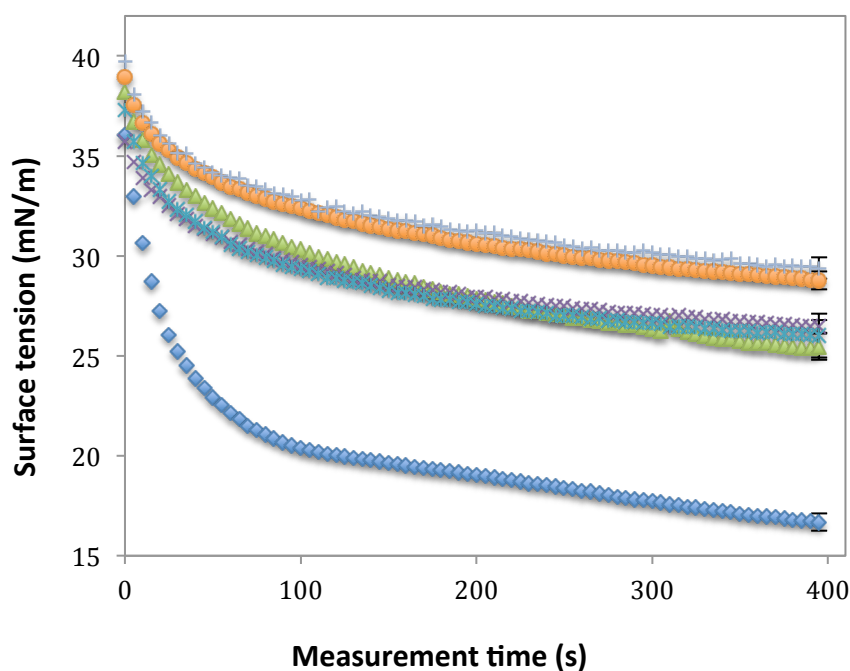


Figure 6.4 Interfacial tension (oil-water) of succinylated α_{s1} -casein measured using a pendant drop tensiometer. Standard (native α_{s1} -casein, ♦), α_{s1} -casein with different levels of succinylation: 23% (▲), 40% (×), 49%(*), 83%(●) and 99%(+). Each data point is an average of two replicates. Error bars represent the standard deviation of the mean of the replicates.

The results showed that the surface tension of succinylated α_{s1} -casein between the water and oil interface increased in comparison to the standard sample and therefore the higher level of succinylation contributed to a lower surface tension (Figure 6.4). The change in the surface tension on the oil-water interface between native and succinylated α_{s1} -casein is similar to the change on the air-water interface that was discussed in Section 6.2.3. α_{s1} -Casein is adsorbed on the oil-water interface with the hydrophobic part of the protein attaching to the oil surface and the hydrophilic part sticking out into the water phase (Beverung et al., 1999; Binks et al., 2000; Chandler, 2005; Paunov, 2003). Unlike dephosphorylation (described in Section 4.2.5), succinylation decreased the apparent hydrophobicity of α_{s1} -casein (described in Section 5.2), consequently resulting in a slow adsorption reaction of protein to the interface. Therefore, succinylated α_{s1} -casein had a higher surface tension than native α_{s1} -casein. In addition, the overall net charge of succinylated α_{s1} -

casein increased compared to native α_{s1} -casein, which contributed to an increased electrostatic repulsion between protein molecules. The proteins that are adsorbed on the interface formed a “protein-repellent surface” due to the strong intermolecular repulsion. The electrostatic repulsion between the adsorbed proteins and the proteins in the solution might retard more proteins from the solution phase adsorbing to the surface. Thus, the succinylated α_{s1} -casein had less effect on lowering surface tension than native α_{s1} -casein. This finding is in agreement with previous study by Kayitmazer (2007) who suggested that the surface tension and charge repulsion can increase with protein charge.

6.2.5 Emulsifying properties of succinylated α_{s1} -casein

In order to understand how the charge and hydrophobicity affect the functional properties of proteins, the succinylated α_{s1} -casein was used as an emulsifier. The particles sizes of a canola oil droplet in an emulsion were determined by static light scattering using a Malvern Mastersizer 2000 (described in Section 2.2.20).

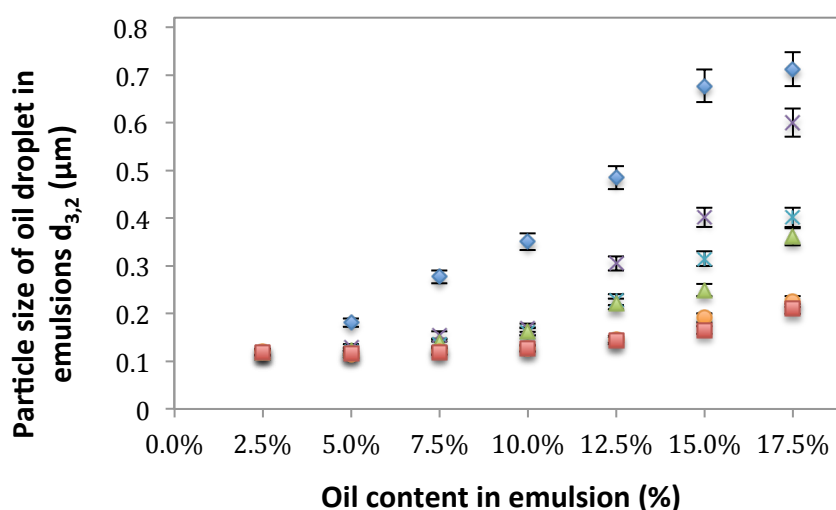


Figure 6.5 Particle size $d_{(3,2)}$ of canola oil droplet in emulsions made with α_{s1} -casein. Standard (native α_{s1} -casein, \blacklozenge), α_{s1} -casein with different levels of succinylation: 23% (\times), 40% ($*$), 49% (\blacktriangle), 83% (\bullet) and 99% (\blacksquare). Each data point is an average of two replicates. Error bars represent the standard deviation of the mean of the replicates.

In all the emulsions containing 2.5% oil, there was no noticeable difference in particle sizes between emulsions made from native α_{s1} -casein and the succinylated α_{s1} -casein (Figure 6.5). However, when the oil content of the emulsions increased above 2.5%, the particle sizes in the emulsions with native α_{s1} -casein dramatically increased compared to the succinylated α_{s1} -casein (Figure 6.5). When the oil content of the emulsions increased from 2.5 to 17.5%, the particle size of emulsions with native α_{s1} -casein increased about 6 times, whereas the particle size of emulsions with 99% succinylated α_{s1} -casein only doubled. In general the higher the level of succinylation the smaller the particle sizes that were formed in the emulsions containing above 10% oil.

The improved emulsifying properties of succinylated α_{s1} -casein could result from the increased overall net charge of succinylated α_{s1} -casein. This is consistent with the result from the emulsifying properties of dephosphorylated α_{s1} -casein where dephosphorylation resulted in poor emulsifying properties of α_{s1} -casein due to the decreased net charge (described in Section 4.2.6), as the emulsions are stabilized by the electrostatic repulsions between proteins (Dagorn-Scaviner et al., 1987; Graham & Phillips, 1976; Moro et al., 2001; Nagasawa et al., 1996; Urrutia, 2006). On the other hand, the improved emulsifying properties of succinylated α_{s1} -casein could also result from increased steric repulsion. (Chandler, 2005; Dalgleish, 1990; Kato et al., 1993; Nakamura et al., 1993; Sánchez & Patino, 2005). Succinylation of α_{s1} -casein is predicted to create a stronger steric repulsion due to the increased thickness of the adsorbed protein layer, which inhibits the oil droplets from coalescing (described in Section 4.2.6 and 9.2). Therefore, the succinylated α_{s1} -casein had better emulsifying properties than native α_{s1} -casein, even though its adsorption was slower than native α_{s1} -casein. This suggests that the enhanced emulsifying properties of succinylated α_{s1} -casein are mainly due to the charge effect. The apparent hydrophobicity of succinylated α_{s1} -casein had an impact on the protein adsorption rate rather than the stabilization capacity.

6.2.6 Foaming properties of succinylated α_{s1} -casein

The apparent hydrophobicity of the succinylated α_{s1} -casein, as one of the modified physicochemical properties, seems to have less effect on the emulsifying properties than the charge, but might play a role in the protein foam system. Therefore, the foaming properties of succinylated α_{s1} -casein were investigated by measuring the volume of protein foam and the serum separation time (described in Section 2.2.19). The mechanisms of foam formation and the foam stability were described in Section 4.2.7 (Koehler et al., 2000; Pugh, 1996).

Table 6.1 The volumes of native and succinylated α_{s1} -casein foam.

Level of succinylation (%)	Standard	23%	40%	49%	83%	99%
Volume of foam (mL)	20 \pm 1.5	19 \pm 1.5	18 \pm 1.5	18 \pm 1.5	18 \pm 1.5	18 \pm 1.5

The volumes of protein foam were very similar between the native α_{s1} -casein and succinylated α_{s1} -casein (Table 6.1). After whipping the protein solutions around 18 ~ 20 mL of foam was formed.

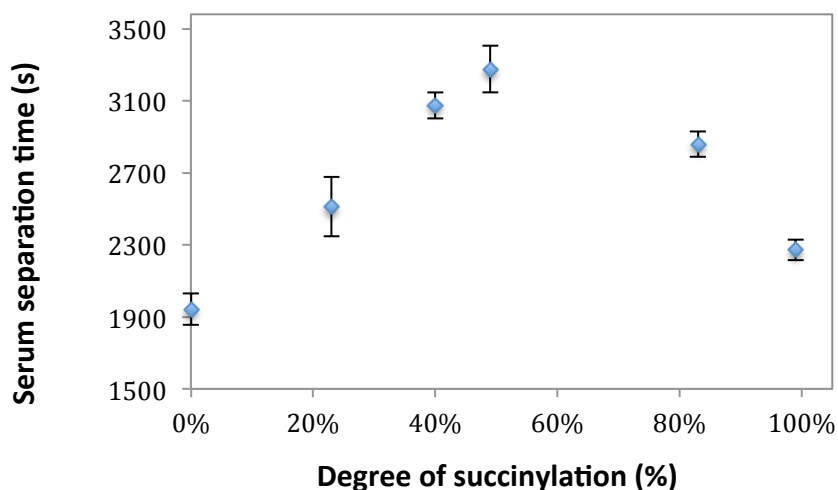


Figure 6.6 Protein serum separation time. α_{s1} -Casein with different levels of succinylation. Each data point is an average of four replicates. Error bars represent the standard deviation of the mean of the replicates.

The time of serum separation from the protein foam increased to a peak value (~ 3200 s) when the level of succinylation increased from 0% to 49% (Figure 1.6), then the separation time diminished as the level of succinylation further increased to 99% (Figure 6.6). The time of serum separation of 99% succinylated α_{s1} -casein (~ 2270 s) was still longer than native α_{s1} -casein (~ 1940 s, $P=0.0001$).

The results for the serum separation from protein foam (Figure 6.6) indicated that the foam of succinylated α_{s1} -casein collapsed more slowly than native α_{s1} -casein, and the maximum foam stability of α_{s1} -casein was achieved at the level of 49% succinylation. Succinylation led to a reduction in the hydrophobicity, which contributed to a slow adsorption of protein onto the interface. On the other hand, the electrostatic repulsions of intermolecular protein increased as the level of succinylation increased. These two factors might work together to affect the foam stability of α_{s1} -casein: when the level of succinylation was increased from 0% to 49%, the adsorption rate of α_{s1} -casein on the interface decreased due to the reduced hydrophobicity, but the overall charge on the interface increased as the charge of single succinylated protein molecules increased and sufficient α_{s1} -casein was adsorbed onto the surface, which enhanced the electrostatic repulsions at the interface. The resulting electrostatic repulsions maintained the thickness of the protein enriched laminar film that slowed down the drainage of protein serum, and consequently stabilized the protein foam (described in Section 4.2.7). However, when the level of succinylation was increased from 49% to 99%, this further decreased the hydrophobicity of the succinylated α_{s1} -casein resulting in a very poor protein adsorption rate on the interface, which led to a reduction in the overall charge on the surface, even though the net charge of single succinylated protein molecules increased. The electrostatic repulsion between the interfaces consequently decreased. The resulting electrostatic repulsion was not able to maintain the thickness of the laminar film and a faster drainage of protein serum occurred before more protein adsorbed onto the interface as the protein adsorption rate was low. Thus, the foam generated from 99% succinylated α_{s1} -casein collapsed faster than 49% succinylated α_{s1} -casein. Previous studies have reported that electrostatic forces can significantly influence the foam stability of whey proteins

(Foegeding et al., 2006; Roth et al., 2000). Moreover, when the level of succinylation was increased from 49% to 99%, the increased net charge on the single protein molecules might also slow down the protein adsorption onto the interface due to intermolecular electrostatic repulsion. Electrostatic repulsion is expected to be more prominent during adsorption and the reduction in electrostatic repulsion facilitates adsorption to the air-water interface (Davis et al., 2004; Dickinson, 1999b).

Dephosphorylation resulted in an increase in the foaming stability of α_{s1} -casein due to the reduced net charge and increased hydrophobicity (as described in Section 4.2.7). Unlike dephosphorylation, the foam stability of succinylated α_{s1} -casein did not change as it was predicted to decrease with the increased net charge and decreased surface hydrophobicity. In order to understand the relationship between charges, surface hydrophobicity and foam stability of α_{s1} -casein, the change in the net charge, surface hydrophobicity and foam stability of α_{s1} -casein due to dephosphorylation and succinylation were plotted in Figure 6.7. The net charge and hydrophobicity play a dominant role in the foaming stability of α_{s1} -casein, but the foam stability is not simply dependent on a single parameter. Figure 6.7 shows that the optimum foam stability appears to be associated with a net charge lower than 15 and hydrophobicity values lower than 20. This suggests that an optimum balance between hydrophobic force and electrostatic force contributed to the greater foaming stability of α_{s1} -casein.

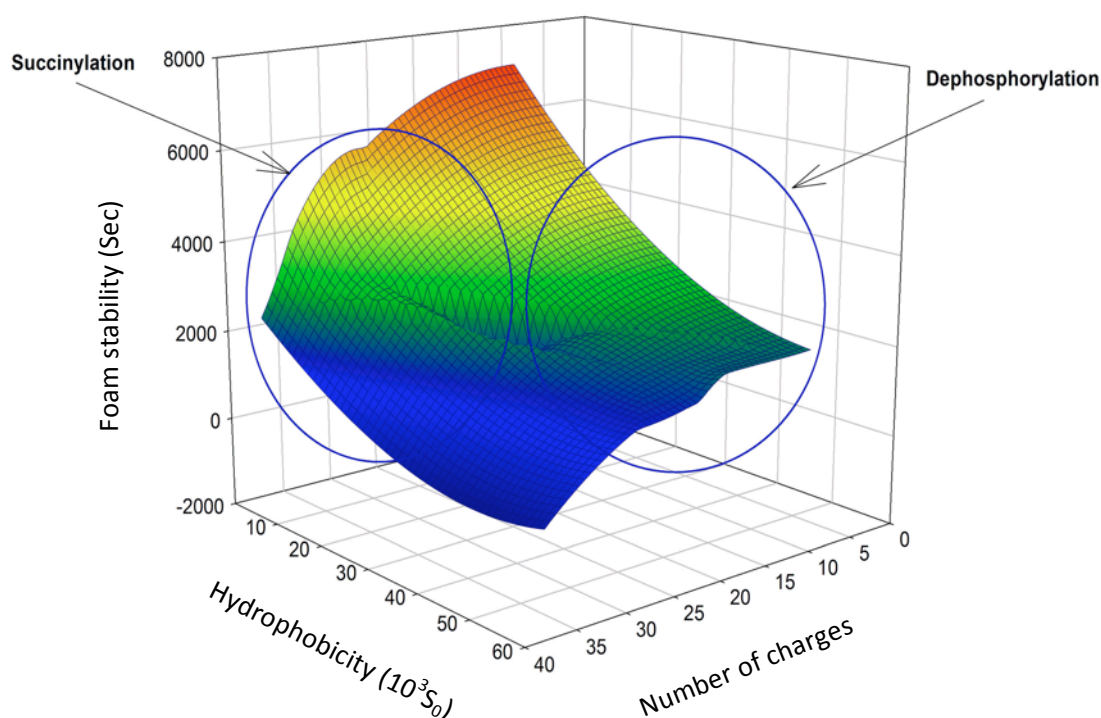


Figure 6.7 The proposed correlation model of hydrophobicity and net charge vs foam stability of α_{s1} -casein. The values of foam stability were taken from the serum separation time of dephosphorylated and succinylated α_{s1} -casein solutions. The values of surface hydrophobicity were obtained by combining of the surface hydrophobicity of dephosphorylated and succinylated α_{s1} -casein. The number of net charges was obtained from the charge calculation results of dephosphorylated and succinylated α_{s1} -casein at pH 7 (as described in Section 3.2.2 and 5.2.2).

In addition, the viscosity, interfacial viscoelasticity, the size of bubbles and air fluctuation in the room can affect the stability of protein foam (Hill, 1996; Klitzing & Müller, 2002; Monsalve & Schechter, 1984; Sánchez & Patino, 2005; Wilde, 2000b; Yu & Damodaran, 1991), but they might have less impact than the charge and hydrophobicity.

6.3 Conclusions

Succinylation modified the physicochemical properties of α_{s1} -casein and these changes significantly affected the functionality of the protein. The results from the

experimental work indicated that the net charge of the protein plays a dominant role in the emulsifying capacity of α_{s1} -casein rather than the hydrophobicity. The foaming stability of α_{s1} -casein was not dependent on a single parameter e.g. charge or hydrophobicity. The optimum balance between hydrophobic force and electrostatic force contributed to the greater foaming stability of α_{s1} -casein.

The viscosity increased with the net charge of α_{s1} -casein. But the change in charge did not affect the water binding capacity; the water binding capacity of α_{s1} -casein was more reliant on functional amino acid residues such as lysine.

Overall, the succinylated α_{s1} -casein exhibited an enhanced emulsifying capacity, even though it resulted in a poor water binding capacity. The optimum foam stability of α_{s1} -casein can be achieved by controlling the level of succinylation. Therefore, the functional properties of α_{s1} -casein can be manipulated by controlling the degree of protein modification.

Chapter 7 Characterization of transglutaminase-modified α_{s1} -casein

7.1 Introduction

Transglutaminase (TGA) can induce protein modification by deamidation, amine incorporation and enzymatic cross-linking of the protein side chains. The TGA-catalysed reactions are summarized in Figure 7.1. TGA catalyses an acyl-transfer reaction between the γ -carboxyamide group of a protein-bound glutamine (acyl donor) and various primary amines (acyl acceptors) to form both inter- and intramolecular isopeptide bonds (Boenisch et al., 2008; Czernicka et al., 2009). Intermolecular cross-link is formed between proteins, while intramolecular cross-link is formed within a protein (Gerrard, 2002). ϵ -N-(γ -Glutamyl)lysine crosslinks are formed by the TGA-catalysed reaction between a γ -carboxyamide group and the ϵ -amino group of a lysine residue (Jaros et al., 2010; Singh, 1991). However, when amine groups are absent, water molecules can act as the acyl acceptors, resulting in the deamidation of glutamine residues (Ikura et al., 1992; Motoki & Seguro, 1998).

TGA-induced cross-linking and acyl-transfer reactions can affect the physicochemical properties of caseins by increasing the molecular weight of proteins. The aim of this chapter is to understand how the physicochemical properties of α_{s1} -casein are affected by the molecular weight. In addition, the impact of TGA-induced cross-linking and non-cross-linking on the physicochemical properties of α_{s1} -casein is distinguished in this study. To do this, different levels of cross-linked α_{s1} -casein solutions were prepared by controlling the incubation time of α_{s1} -casein with TGA (described in Section 2.2.3). The physicochemical properties of cross-linked α_{s1} -casein at different incubation times were analysed using a variety of methods.

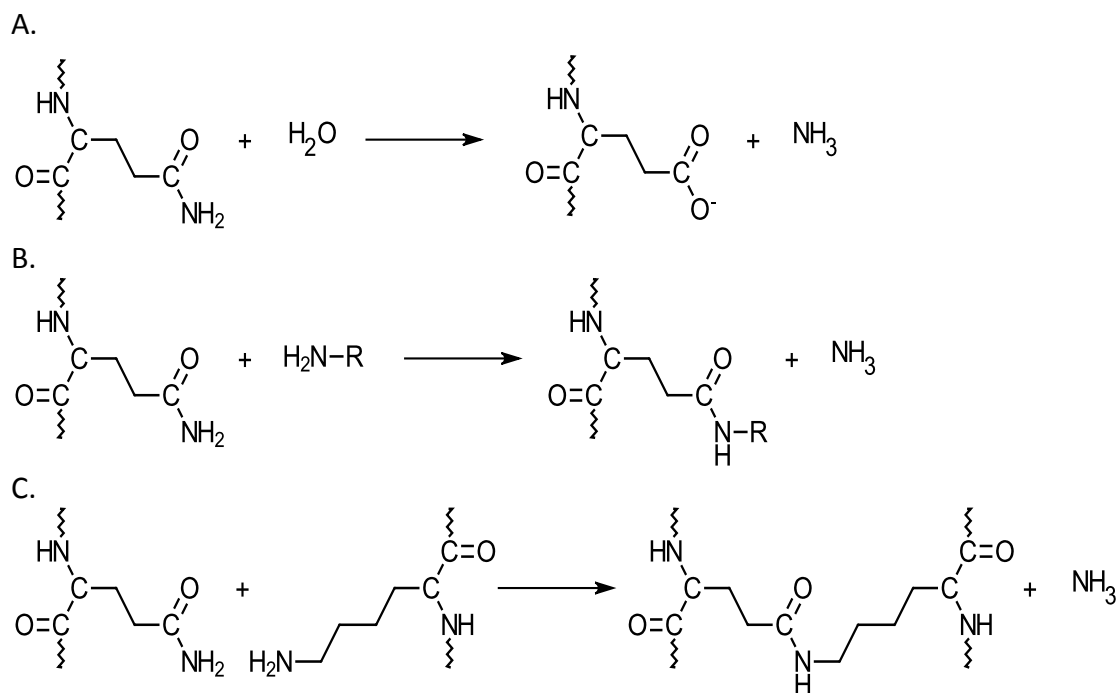


Figure 7.1 The transglutaminase induced reactions: A. deamidation B. amino incorporation C. cross-linking (Sharma et al., 2001).

7.2 Results and discussion

7.2.1 Determination of cross-linking for α_{s1} -casein

Reduced SDS – PAGE

The degree of cross-linked α_{s1} -casein was monitored using reduced SDS-PAGE (as described in Section 2.2.5). Based on both literature precedent (Jaros et al., 2006; Jaros et al., 2010) and preliminary experiments, the degree of cross-linking of α_{s1} -casein was manipulated by controlling the incubation time at a constant temperature and pH (as described in Section 2.2.3). SDS-PAGE has been used to detect the formation of TGA-catalysed protein cross-linking under reducing conditions (Faergemand et al., 1997; Faergemand et al., 1998; Hiller & Lorenzen, 2009; Lauber et al., 2003; Sharma et al., 2001). Under reducing conditions, the covalent cross-linking remains intact and therefore the protein runs as an oligomer or remains at the top of the gel. SDS-PAGE is therefore an effective and efficient way to detect intermolecular protein cross-linking.

Figure 7.2 shows the SDS-PAGE pattern for α_{s1} -casein incubated with TGA. The band intensities and protein band positions in the standard sample (Lane 2) show the total amount and the type of proteins in the native α_{s1} -casein without heat treatment. The band intensities and positions in the control sample (Lane 3) show the impact of heat treatment in the absence of enzyme. The shift in band intensities and band positions of the other samples (Lanes 4 to 10) correspond to increasing levels of cross-linking at increasing incubation times.

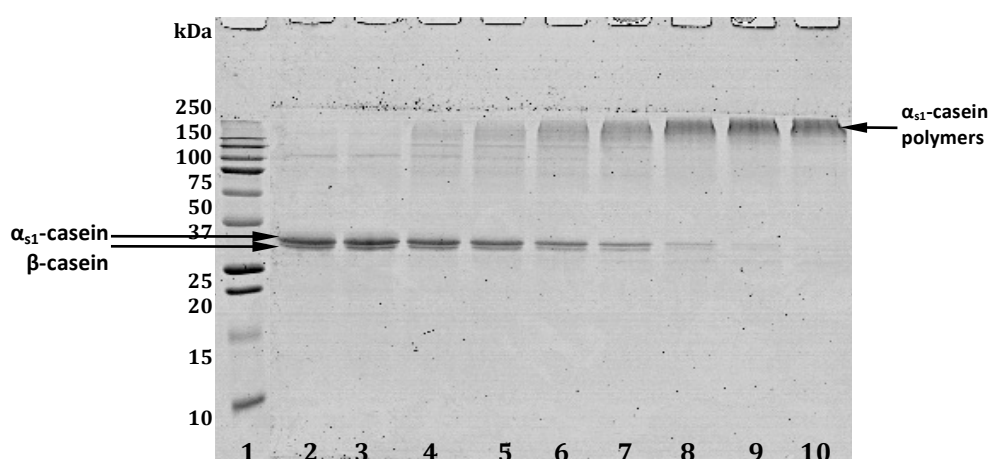


Figure 7.2 SDS-PAGE of cross-linked α_{s1} -casein at different incubation times. From left to right: molecular weight markers (Lane 1) standard sample (native α_{s1} -casein without heat treatment, Lane 2); control sample (native α_{s1} -casein with heat treatment at 85°C for 5 min, Lane 3); α_{s1} -casein incubated with TGA at incubation times: 5 min (Lane 4), 10 min (Lane 5), 20 min (Lane 6), 30 min (Lane 7), 60 min (Lane 8), 90 min (Lane 9), 120 min (Lane 10).

The SDS-PAGE shows that there was no difference in the band intensity and positions between the standard and control samples (Figure 7.2, Lane 2 and 3), which confirms that the difference in the incubated samples is due to the enzyme and not the heat treatments. Figure 7.2 also shows that the native α_{s1} -casein sample contains a minor amount of β -casein. The native α_{s1} -casein and β -casein had the highest band intensity (Lane 2 and Lane 3), and these band intensities between 25 and 37 kDa gradually diminished when the incubation time increased from 5 min to

120 min (Lanes 4 - 10). Concomitantly, the band intensities of protein at positions (between 150 and 250 kDa) increased as the incubation time increased from 0 to 120 min (Lane 2 to 10).

The SDS-PAGE results indicate that the polymerization occurred when the α_{s1} -casein was incubated with TGA (Figure 7.2, Lane 4 to 10). The level of polymerization increased with increased incubation time. These polymers of α_{s1} -casein suggest intermolecular cross-linking between glutamine and lysine residues of proteins (Hiller & Lorenzen, 2009; Jaros et al., 2010).

At incubation times of 90 min and 120 min, the α_{s1} -casein and β -casein fractions were fully polymerized (Figure 7.2, Lane 10). This indicated that the α_{s1} -casein and β -casein are both substrates for TGA. Tang et al. (2005a) have reported that when sodium caseinate was dissolved in 0.05 M Tris-HCl buffer (pH 7.5), the accessibility of sodium caseinate protein fractions to TGA decreased in the following order: κ -casein > α -casein > β -casein, which was determined using reduced SDS-PAGE. The capacity of substrates for cross-linking is also dependent on the environment of the substrate solutions. Native casein micelles showed a higher capacity for cross-linking in distilled water, but had lower activity in a milk serum system than sodium caseinate (Bonisch et al., 2004; Huppertz & de Kruif, 2007a; Huppertz & de Kruif, 2007b; Jaros et al., 2010; Vasbinder et al., 2003).

Mass spectrometry of TGA-treated α_{s1} -casein

The deamidated glutamine residues were identified by mass spectrometry (as described in Section 2.2.8). In general, peptide bonds can be hydrolysed by proteases, and the resulting hydrolysis products can be quantified by mass spectrometry. However, the ϵ -N-(γ -glutamyl)lysine isopeptide is not cleaved by all proteases (Miller & Johnson, 1999). The most common technique for the quantification of ϵ -N-(γ -glutamyl)lysine isopeptide is an ion-exchange chromatography method (Otterburn et al., 1977; Schmidt et al., 2008). In previous studies, the TGA-induced cross-linking was successfully detected by amino acid analysis, which requires a standard reference H- γ -Glu- ϵ -Lys-OH (Jaros et al., 2014;

Schmid et al., 2011; Sharma et al., 2001). After extensive proteolysis of peptide bonds with selective peptidases, the ϵ -N-(γ -glutamyl)lysine content can be measured by ion-exchange chromatography method (Mautner et al., 1999; Miller & Johnson, 1999). α_{s1} -Casein contains 4 lysine residues that are adjacent to glutamine residues (Figure 7.3). In this study, in order to hydrolyse the α_{s1} -casein samples into individual amino acids, 4 different types of protease (pepsin, pronase E, aminopeptidase M and prolidase) were used. This method of enzyme treatment was adapted from Sharma et al. (2001). However, the proteases did not fully hydrolyse the α_{s1} -caseins into individual amino acids. Thus, in the hydrolysed TGA-treated α_{s1} -casein, the sequenced peptide fractions of lysine-glutamine could be either the ϵ -N-(γ -glutamyl)lysine isopeptide or the adjacent lysine-glutamine fraction.

The TGA-induced cross-linking of α_{s1} -casein was not able to be identified by mass spectrometry, but SDS-PAGE provided a quick and simple method to assess the level of cross-linked α_{s1} -casein. Reversed-phase HPLC coupled with the mass spectrometer system has a limit of detection and quantification of some amino acids (Bartolomeo & Maisano, 2006; Fabiani et al., 2002), but is reliable for the determination of protein modifications such as deamidation (Craig & Beavis, 2003; Jedrzejewski et al., 1998), as it can efficiently separate proteins and peptides based on their hydrophobicity.

-RPKHP IKHQG LPQEV LNENL LRFFV APFPQ VFGKE KVNEL SKDIG SESTE DQAME
 DIKQM EAESI SSSEE IVPNS VEQKH IQKED VPSEY YLGYL EQLLR LKKYK VPQLE IVPNS
 AEERL HSMKE GIHAQ QKEPM IGVNQ ELAYF YPELF RQFYQ LDAYP SGAWY YVPLG
 TQYTD APSFS DIPNP IGEN SEKTT MPLW-

Figure 7.3 Full sequence of native α_{s1} -casein, highlighting the potential residues for cross linking (green and blue) and deamidation (red and blue) in the sequence (Fox, 1989).

TGA-induced cross-linking of proteins has been extensively studied (Bönisch et al., 2007; Faergemand et al., 1998; Gerrard et al., 2001; Hiller & Lorenzen, 2009; Huppertz, 2014; Yasir et al., 2007); however, TGA-induced deamidation was not

examined in these studies. Mass spectrometry was used to ascertain whether non-cross-linking modifications had occurred during incubation with TGA.

The deamidated glutamine residues of TGA-modified α_{s1} -casein were monitored using mass spectrometry (as described in Section 2.2.8 and Appendix C). The mass spectrometry chromatograph of trypsin-digested native and TGA-treated α_{s1} -casein is shown in Figure 7.4. All the peaks were labelled with a mass to charge ratio and sequenced using Xcalibur software (Liu et al., 2007).

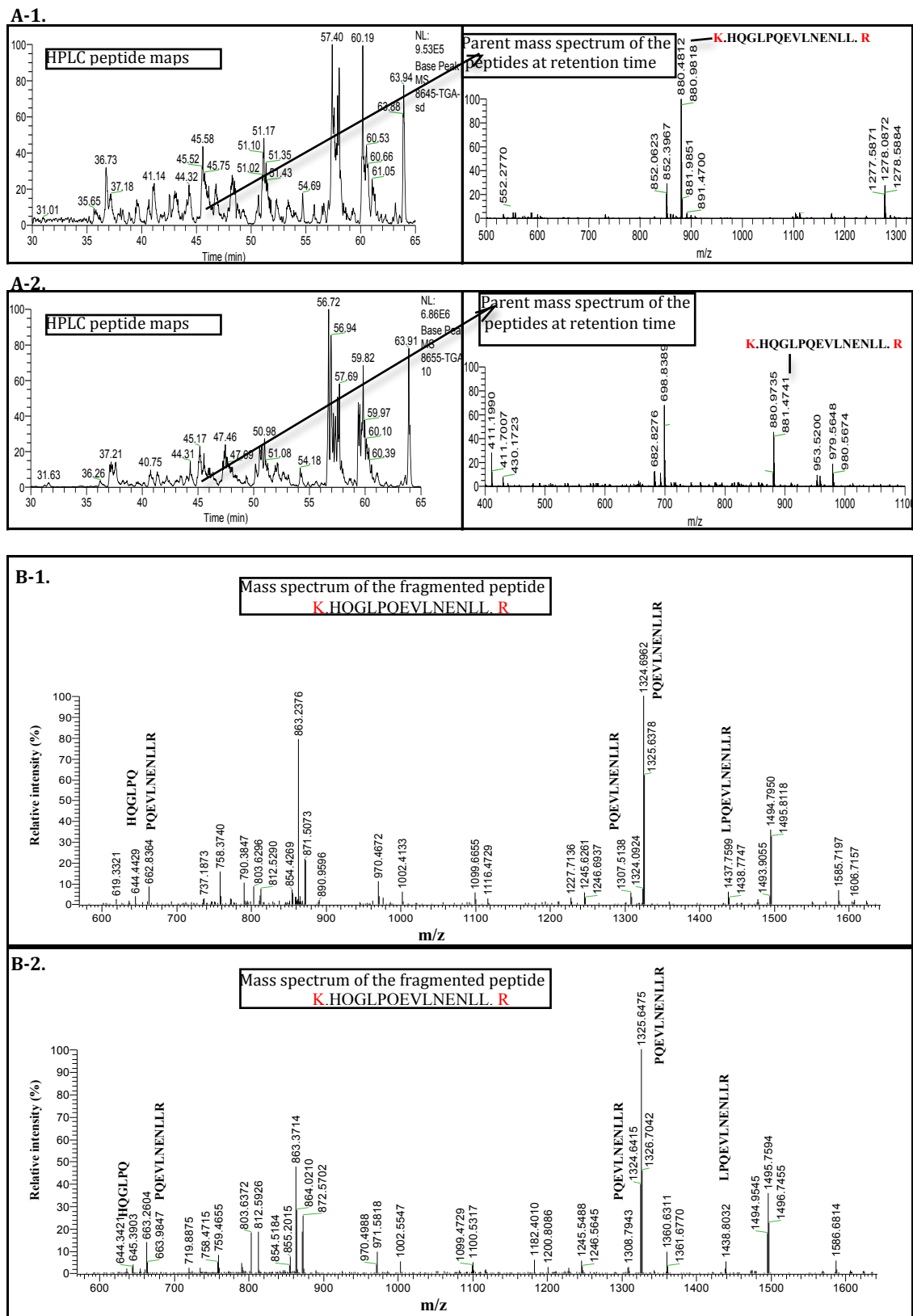


Figure 7.4 HPLC peptide maps, parent mass spectrum (A) and mass spectrum of fragmented peptide Lys₇-Arg₂₂ (B) from the trypsin-digested native α_{s1} -casein (1) and α_{s1} -casein incubated with TGA at 120 min (2). Peak assignments corresponding to the native and deamidated glutamine residues are indicated.

The difference in the patterns of HPLC peptide maps between native and TGA-treated α_{s1} -casein is due to TGA-induced cross-linking and deamidation (Figure 7.4 A). The parent mass spectrum of trypsin-digested native and TGA-treated α_{s1} -casein is shown in Figure 7.4 A. In order to determine the change in the mass due to deamidation, the peptide Lys₇-Arg₂₂ was selected as a representative mass spectrum. Figure 7.4 A shows that the peptide Lys₇-Arg₂₂ generated from TGA-treated α_{s1} -casein had a slightly shorter retention time in comparison to native α_{s1} -casein. This indicated that deamidation increased the hydrophilicity of peptide Lys₇-Arg₂₂, which is due to the increase in the net charge of deamidated glutamine residues at pH 7.

The parent mass spectrum of Lys₇-Arg₂₂ showed the trypsin cleavage sites, which are highlighted in red (Figure 7.4 A), and the fragmented peptides spectrum is shown in Figure 7.4 B. The fragmentation patterns of native α_{s1} -casein were similar to TGA-treated α_{s1} -casein. This indicated that there was no noticeable change in the mass due to deamidation. All the peaks in the fragmented peptides spectrum were used in a database search to map the deamidated glutamine residues (as described in Section 2.2.8). The peptide fractions labelled in Figure 7.4 B were identified to carry one positive charge. Thus the difference in the mass to charge ratio between native and TGA-modified α_{s1} -casein (Figure 7.4 B) indicated the increase in mass is due to the deamidation, which is summarized in Table 7.1. The change in the mass represents that the glutamine side chain was converted to the glutamate side chain due to deamidation reaction (Figure 7.1, A). At pH 7, the mass of glutamine side chain and glutamate side chain is 128.31 Da and 129.16 Da, respectively (Puri, 2002).

The mass accuracy for this measurement was ~2 ppm, as the Orbitrap mass spectrometry has mass accuracy of less than 2 ppm. However, the mass accuracy can be up to 5-10 ppm because of the fluctuations of ambient temperature. At mass accuracy of 2 ppm, the error of the mass would be ± 0.002 Da. Thus, the Orbitrap is able to determine a mass difference of < 1 Da, even with the minimum mass accuracy of 10 ppm (± 0.01 Da).

Table 7.1 The mass to charge ratio of peptide Lys₇-Arg₂₂ from native α_{s1} -casein and TGA-modified α_{s1} -casein at incubation time 120 min. All the peptide fractions carried one positive charge, with a mass accuracy of 0.01 Da.

Peptide fractions	Native α_{s1} -casein	TGA incubated α_{s1} -casein 120 min		
	Mass (m/z)	Mass (m/z)	Δ mass	No. Deamidated glutamine residues
HQGLPQ	644.4429	645.3903	0.95	1
PQEVLNENLLR	1324.6962	1325.6475	0.95	1
LPQEVLNENLLR	1437.7599	1438.8032	1.04	1
HQGLPQEVLNENLLR	1585.7197	1586.6814	0.96	1

Table 7.1 shows that the peptide fractions from TGA-incubated α_{s1} -casein had a higher molecular mass of 1 Da compared to native α_{s1} -casein, which was attributed to the deamidation of one glutamine residue. However, the peptide Lys₇-Arg₂₂ in α_{s1} -casein contains two glutamine residues. Thus, the increase of 1 Da in the molecular mass indicated that only partially deamidation occurred in the α_{s1} -casein incubated with TGA at 120 min. It has been reported that glutamine residues 2, 9, 10 and 12 of α_{s1} -casein are accessible for modification by the TGA from Guinea pig liver (Christensen et al., 1996). Microbial TGA has been reported to have different accessibility to milk proteins compared with the TGA from Guinea pig liver (Aeschlimann et al., 1992; Coussons et al., 1992; Ohtsuka et al., 2000a; Pastor et al., 1999). For whey proteins, the glutamine residues need to be more exposed to the solvent to be accessible for TGA from Guinea pig liver than the microbial TGA (Kashiwagi et al., 2002; Lee & Park, 2002; Ohtsuka et al., 2000b). However, the specificity of microbial TGA toward the glutamine residues of α_{s1} -casein has not been reported. In order to monitor the specific glutamine residues deamidated at different incubation times, the identified deamidated glutamine residues of α_{s1} -casein are summarised in Figure 7.5.

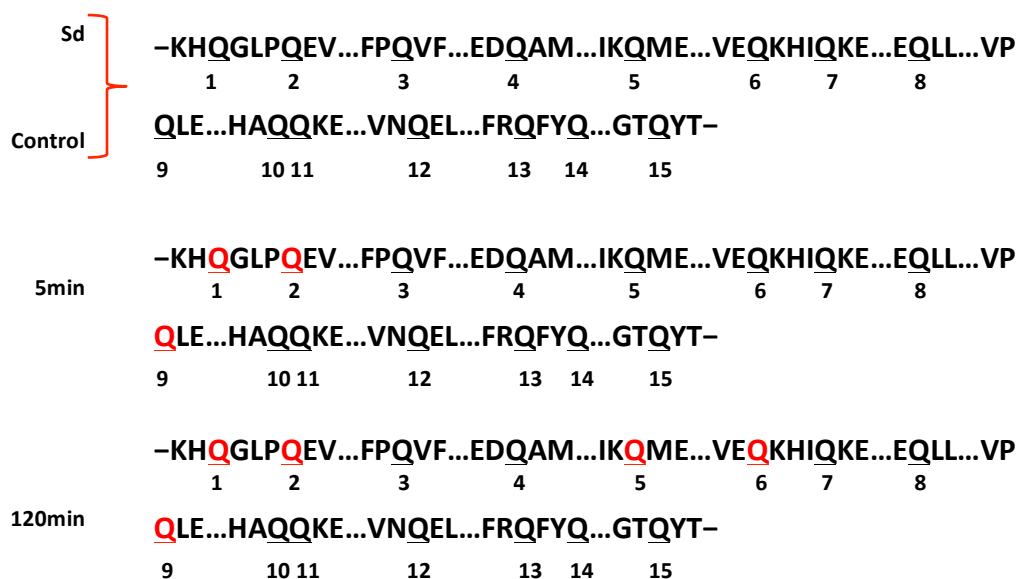


Figure 7.5 α_{s1} -Casein incubated with TGA at incubation time: 0 min (Sd = standard – native α_{s1} -casein and control – native α_{s1} -casein with heat treatment of 85°C for 5 min), 5 min and 120 min, monitored by mass spectrometry. Q (black): glutamine residues, Q (red): partially deamidated glutamine residues, which were identified by the database mapping.

α_{s1} -Casein contains fifteen glutamine residues, and these are labelled in Figure 7.5. When the α_{s1} -casein was incubated with TGA for 5 min, glutamine residues 1, 2 and 9 were partially deamidated (Figure 7.5). By the time the incubation reached 120 min glutamine residues 5 and 6 were partially deamidated. The mass spectrometry results indicate that more glutamine residues were deamidated as the incubation time of α_{s1} -casein with TGA increased, but only partial deamidation occurred. At the longest TGA incubation time (120 min), only 5 out of 15 glutamine residues were partially deamidated. This is consistent with TGA-induced cross-linking being more favourable than deamidation, and deamidation occurring only when the amine group is not available (Ikura et al., 1992; Motoki & Seguro, 1998).

This study shows that the degree of cross-linking can be successfully manipulated by controlling the incubation time whilst keeping the temperature constant. The results obtained from the reduced SDS-PAGE are in agreement with a study by Jaros et al. (2010) who reported that the polymerization of α_{s1} -casein was favoured at longer

incubation times (120 min). This change in the level of polymerization was also observed by Tang et al. (2005a) who reported that the polymerization of caseins increased as the incubation time increased. In addition, the partial deamidation of glutamine residues was observed in the TGA-treated α_{s1} -casein, although cross-linking plays a dominant role in the TGA-induced reactions.

7.2.2 Isoelectric point of TGA-treated α_{s1} -casein

TGA-catalysed cross-linking of proteins decreases the positive charge of proteins at pH 7.0, as the cross-links are formed due to the reaction between glutamine and positively charged lysine residues. In addition, TGA-induced deamidation increases the number of negatively charged carboxylate groups in the protein (Hamada & Swanson, 1994a; Schwenke, 1997). Consequently, the pI of α_{s1} -casein is predicted to be affected by protein deamidation and cross-linking due to the change in net charge. In this section, the pI of TGA-modified α_{s1} -casein was determined by measuring the zeta potential using laser Doppler electrophoresis and IEF (as described in Section 2.2.9 and 2.2.6).

Zeta potential

The zeta potential of both native and TGA-modified α_{s1} -casein samples was measured under different pH conditions to examine the effect of the treatment on the apparent pI of α_{s1} -casein.

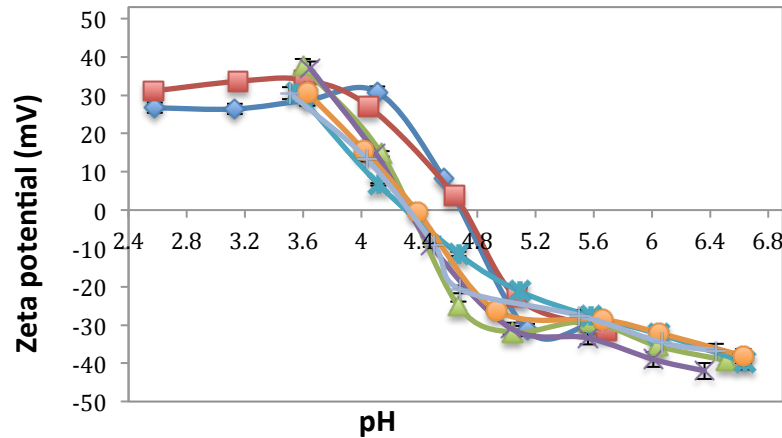


Figure 7.6 The zeta potentials of native and TGA-treated α_{s1} -casein at different pH values: standard sample (native α_{s1} -casein without heat treatment, \blacklozenge); control sample (native α_{s1} -casein with heat treatment at 85°C for 5 min, \blacksquare); α_{s1} -casein incubated with TGA at incubation time: 5 min (\blacktriangle), 20 min (\times), 30 min ($*$), 60 min (\bullet), 120 min ($+$). Each data point is an average of two replicates. Error bars represent the standard deviation of the mean of the replicates.

Figure 7.6 shows that the pH where the standard sample had zero zeta potential was similar to the control sample, around pH 4.69 and pH 4.66, respectively. The pH where the α_{s1} -casein sample had zero zeta potential decreased to 4.34 ($P < 0.05$) as the incubation time was increased from 0 min to 5 min (Figure 7.6). However, when the incubation time further increased to 120 min, the cross-linked α_{s1} -casein samples reached a zeta potential of zero at very similar pH values (Figure 7.6). This indicates that native α_{s1} -casein had a greater apparent pI in comparison to TGA-treated α_{s1} -casein. Across the range of incubation times (5 min, 20 min, 30 min, 60 min, 120 min), the apparent pI value of TGA-treated α_{s1} -casein samples remained the same, which was around pH 4.34 ($p > 0.05$) (Figure 7.6 and Figure 7.7). The zeta potential result also indicates that the heat treatment of α_{s1} -casein at 85°C for 5 min did not affect the pI of the protein.

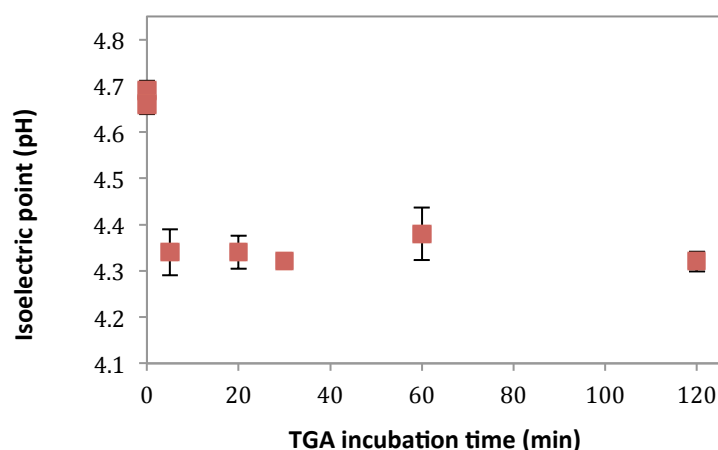


Figure 7.7 The isoelectric point of TGA-modified α_{s1} -casein at different incubation times. Each data point is an average of two replicates. Error bars represent the standard deviation of the mean of the replicates.

When the α_{s1} -casein was incubated with TGA for 5 min, three glutamine residues (residues 1, 2 and 9) were partially deamidated (as described in Section 7.3.1), and one deamidated glutamine residue resulted in a negative charge introduced onto the casein molecule. In addition, the TGA-induced cross-linking at an incubation time of 5 min led to an increase in the net charge of α_{s1} -casein. This increased the overall negative charge consequently leading to a reduction in the apparent pI of TGA-modified α_{s1} -casein compared to native α_{s1} -casein. When the TGA incubation time increased from 5 min to 120 min, glutamine residues (residues 5 and 6) were partially deamidated (as described in Section 7.3.1) and the level of cross-linking gradually increased. However, the apparent pI of TGA-incubated α_{s1} -casein did not change when the incubation time increased from 5 min to 120 min, suggesting that the change in charge due to the lower level of deamidation was not sufficient to affect the apparent pI of α_{s1} -casein. The TGA-induced cross-linking changes the net charge of α_{s1} -casein, although the cross-linked structure of α_{s1} -casein may affect the electrophoretic mobility of α_{s1} -casein for the zeta potential measurement. Moreover, the modified lysine residues could be shielded within the cross-linked α_{s1} -casein.

IEF-PAGE

The pI of TGA-modified α_{s1} -casein was determined using IEF-PAGE (Figure 7.8). The IEF-PAGE method shows the shift in apparent pI between native and TGA-modified α_{s1} -casein; however, it only provides an approximate pI value for proteins (as described in Section 3.2.2). Therefore, the pI measurement using IEF-PAGE was used to corroborate results from the zeta potential experiments.

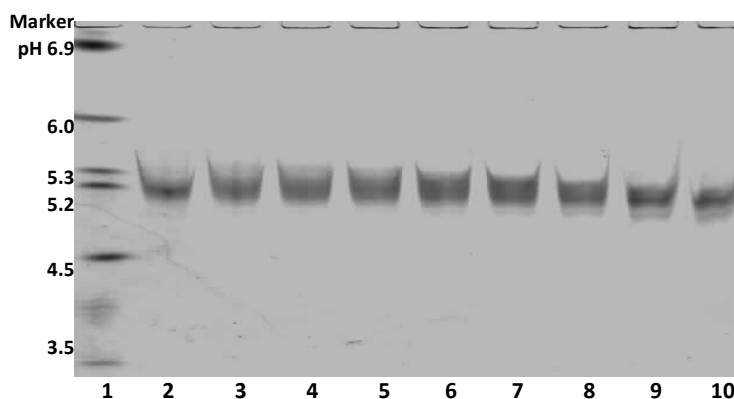


Figure 7.8 IEF-PAGE for the cross-linked α_{s1} -casein at different incubation times. From left to right: pH marker (Lane 1); standard sample (native α_{s1} -casein without heat treatment, Lane 2); control sample (native α_{s1} -casein with heat treatment at 85°C for 5 min, Lane 3); α_{s1} -casein incubated with TGA at incubation time: 5 min (Lane 4), 10 min (Lane 5), 20 min (Lane 6), 30 min (Lane 7), 60 min (Lane 8), 90 min (Lane 9) and 120 min (Lane 10).

The IEF protein marker used for the IEF-PAGE experiments represented a pH range of 3 to 7 (Figure 7.8; Lane 1; as described in Section 3.2.2). There was no difference in the band positions between the standard and control samples (Lane 2 and Lane 3). The bands representing the TGA-modified α_{s1} -casein (Lanes 4 to 10) only slightly shifted to lower band positions compared to the native proteins (Lanes 2 and 3). There is no noticeable difference in the band positions between TGA-modified α_{s1} -casein at incubation times 0 min, 5 min and 10 min (Lanes 2 to 5).

Like succinylation (see Section 5.2), TGA treatment led to an increase in the total negative charge of α_{s1} -casein at pH 7.0, which resulted in a longer migration distance to neutralize its net charge (as described in Section 3.2.2). The IEF-PAGE shows that

the native α_{s1} -casein had an apparent pI around 5.20 and the TGA-modified α_{s1} -casein after 120 min had a lower pI of around pH 4.90 (Figure 7.9). The pI values estimated from the IEF method were with an error ± 0.1 pH units.

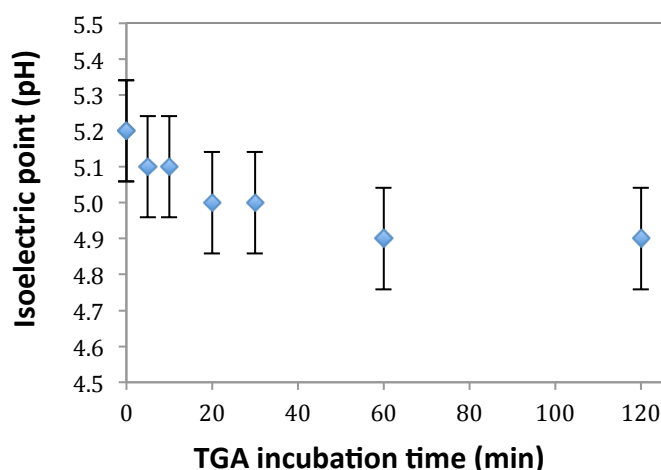


Figure 7.9 The isoelectric point of TGA-modified α_{s1} -casein at different incubation times, which were determined using an IEF gel. Each data point is an average of two replicates. Error bars represent the standard deviation of the mean of the replicates.

The IEF measurement gave a greater pI value than the zeta potential method. This could be due to the fact that the pI measurement using IEF is based on the total net charge of proteins, whereas, zeta potential measurements only determine the surface charge of proteins (as described in Section 3.2.2). However, the IEF result showed that the reduction in the pI between native α_{s1} -casein and TGA-incubated α_{s1} -casein at 120 min was only around 0.3 pH units, which is in agreement with the result from zeta potential measurement. This low level reduction in the apparent pI of TGA-treated α_{s1} -casein could be due to a low level of deamidation. In addition, the TGA-induced cross-linking had an effect on the apparent pI of α_{s1} -casein.

The IEF gel showed a gradual decrease in the apparent pI of TGA-treated α_{s1} -casein with increased incubation time. However, a high level of reduction (0.3 pH unit) in the apparent pI between native and TGA-treated α_{s1} -casein was only observed after the first 5 min of incubation time (Figure 7.7), with no further change in the pI of

TGA-treated α_{s1} -casein at prolonged incubation times. This may be due to the fact that after 5 min of TGA incubation time, a sufficient amount of cross-linked protein was formed. The cross-linked structure could shield the surface charge of α_{s1} -casein, which affects the zeta potential measurement of TGA-treated α_{s1} -casein.

TGA treatment has previously been reported to lead to a lower pI in comparison to native proteins (Nieuwenhuizen et al., 2004; Ohtsuka et al., 2001). Nieuwenhuizen et al. (2004) found that when β -lactoglobulin was incubated with microbial TGA (pH 6.0) for 24 hours, the pI of β -lactoglobulin decreased from pH 5.2 to pH 4.5, when measured using an IEF gel. The TGA treatment led to a reduction in the pI of β -lactoglobulin (0.7 unit), which is higher than the TGA-treated α_{s1} -casein (0.3 units). However, in their study, the level of cross-linking was not manipulated by controlling the incubation time, and the effect of cross-linking and deamidation on the pI of proteins was not distinguished. The slightly higher level of reduction in the pI of β -lactoglobulin could be due to the different protein substrate and different incubation conditions. In their study, more transglutaminase was added to the incubated β -lactoglobulin solution after 6 hours of incubation time. The additional enzyme could lead to more deamidated glutamine residues and cross-linked lysine residues, as the activity of the enzyme was decreased during the reaction. Thus, like TGA-treated α_{s1} -casein, the reduction in the pI of TGA-incubated β -lactoglobulin is likely to be a result of both cross-linking and deamidation.

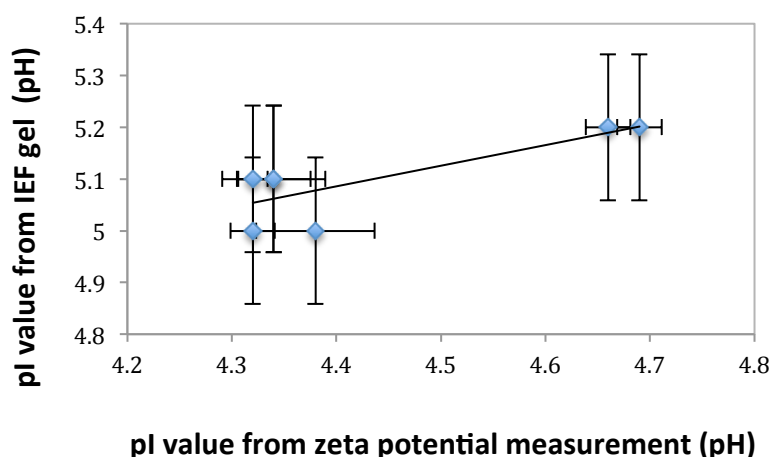


Figure 7.10 The relationship between zeta potential and IEF gel methods for measuring the pI of native and TGA-modified α_{s1} -casein. Error bars represent the standard deviation of the mean of the replicates.

The pI values of TGA-modified α_{s1} -casein obtained from the IEF gel were plotted against the zeta potential method in Figure 7.10, which shows that when the TGA incubation time of α_{s1} -casein increased from 0 min to 120 min, the pI decreased from pH 4.69 to pH 4.32 and pH 5.20 to 4.90 measured by zeta potential and IEF gel, respectively. The linear relationship between the pI values from the IEF gel and zeta potential measurement is insignificant ($r=0.82$, $p>0.05$; Figure 7.10). However, a significant linear relationship was observed between the IEF and zeta potential methods for both dephosphorylated and succinylated α_{s1} -casein (as described in Section 3.2.2 and 5.2.2). This could be because the TGA treatment led to a minor reduction in the apparent pI of α_{s1} -casein, and the IEF method is not sensitive enough to distinguish the difference. Overall, the zeta potential measurement is significant for all the dephosphorylated and TGA-treated samples, but the IEF gel seems to be insufficiently sensitive for the relatively small changes in pI observed for TGA-treated samples.

7.2.3 Hydrophobicity of TGA-treated α_{s1} -casein

The apparent hydrophobicity of TGA-modified α_{s1} -casein was measured at pH 7.8 using the ANS probe (described in Section 2.2.10). The initial slope (S_0) of the relative

fluorescence intensity (RFI) versus protein concentration plot was used as an index of the protein hydrophobicity.

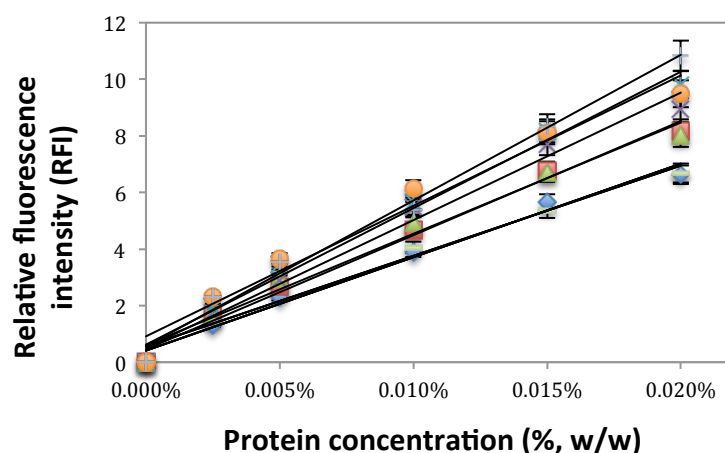


Figure 7.11 Relative fluorescence intensity of α_{s1} -casein: standard (\blacklozenge , native α_{s1} -casein without heat treatment); control (—), native α_{s1} -casein with heat treatment at 85°C for 5 min); α_{s1} -casein incubated with TGA at incubation time: 5 min (\blacksquare), 20 min (\blacktriangle), 30 min (\times), 60 min ($*$), 90 min (\bullet) and 120 min ($+$). Each data point is an average of three replicates. Error bars represent the standard deviation of the mean of the replicates.

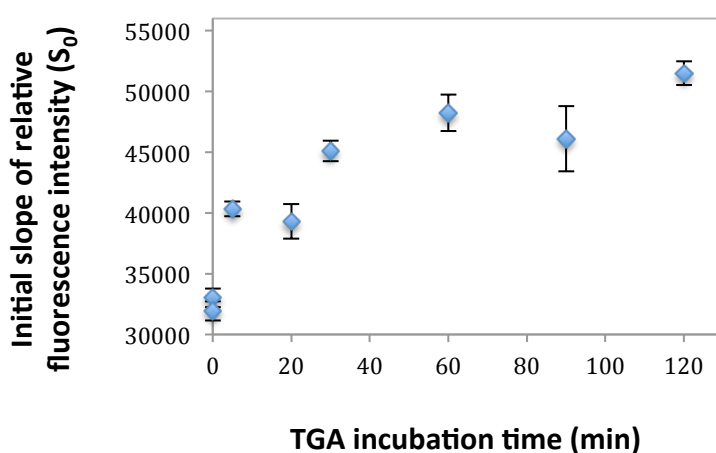


Figure 7.12 Initial slope (S_0) of the relative fluorescence intensity versus TGA incubation time of α_{s1} -casein. Error bars represent the standard deviation of the mean of the replicates.

The RFI of α_{s1} -casein increased as the protein concentration increased (Figure 7.11). The RFI of TGA-treated α_{s1} -casein over a protein concentration range of 0.0025% to 0.02% increased as the incubation time increased (Figure 7.11). There was no noticeable difference in the S_0 change between the standard and control samples (Figure 7.11). This indicates that the heat treatment (85°C, 5 min) did not affect the surface hydrophobicity of α_{s1} -casein. When the TGA incubation time increased from 0 min to 120 min, the S_0 of RFI for α_{s1} -casein gradually increased (Figure 7.11 and Figure 7.12). This indicated that the hydrophobicity of TGA-modified α_{s1} -casein increased at pH 7.0 as the TGA incubation time increased (Figure 7.11 and Figure 7.12). When the TGA incubation time increased, more glutamine residues of α_{s1} -casein were deamidated, which increased the overall net charge at pH 7.0. In theory, deamidation was predicted to reduce the surface hydrophobicity of α_{s1} -casein, which is consistent with a previous report that showed that deamidation resulted in lower surface hydrophobicity of a caseinate protein at pH 7.0 (Yao & Zhao, 2015). Thus, TGA-induced cross-linking probably increased the surface hydrophobicity of α_{s1} -casein, which is due to the fact that the hydrophilic lysine and glutamine residues were unavailable after forming the cross-link. Therefore, TGA-induced cross-linking played a dominant role in the enhanced surface hydrophobicity of α_{s1} -casein rather than deamidation.

In addition, the increase in the hydrophobicity of TGA-treated α_{s1} -casein could be the result of the reduced self-association behaviour of α_{s1} -casein (Tang et al., 2005a). It has been suggested that the surface hydrophobicity of proteins is related to the arrangement of protein molecules (De Carvalho & Grosso, 2004; Larre et al., 2000; Mariniello et al., 2003; Tang et al., 2005b; Tang & Jiang, 2007). The native α_{s1} -casein was observed to exist as a self-associated species in 10 mM phosphate buffer (pH 7.4). The self-associated species are formed by the hydrophobic associations of α_{s1} -casein (as described in Section 3.2.5). Thus, the hydrophobic groups of native α_{s1} -casein were buried in the interior of the associated species. However, it has been reported that cross-linking could lead to the disruption of the self-associated structure of the casein (Tang & Jiang, 2007). When the lysine or glutamine residues that are located on the hydrophobic regions of α_{s1} -casein were cross-linked (Horne,

1998), a rearrangement is predicted between the associated hydrophobic regions of α_{s1} -casein. This could be attributed to the exposure of the hydrophobic groups initially buried in the interior of the associated species. Thus, the higher level of TGA-induced cross-linking may result in a higher hydrophobicity of α_{s1} -casein due to the exposed hydrophobic regions. The results from the ANS probe method is in agreement with the study by Tang and Jiang (2007) who reported that treatment with TGA increased the surface hydrophobicity of both whey protein concentrate and sodium caseinate, when the samples were measured at pH 8.0 using a surface contact angle method.

7.2.4 Secondary structure of TGA-modified α_{s1} -casein

In order to understand the effect of the TGA-induced reactions on the conformation of α_{s1} -casein, the secondary structure of TGA-modified α_{s1} -casein was estimated using a CD spectrometer (as described in Section 2.2.13).

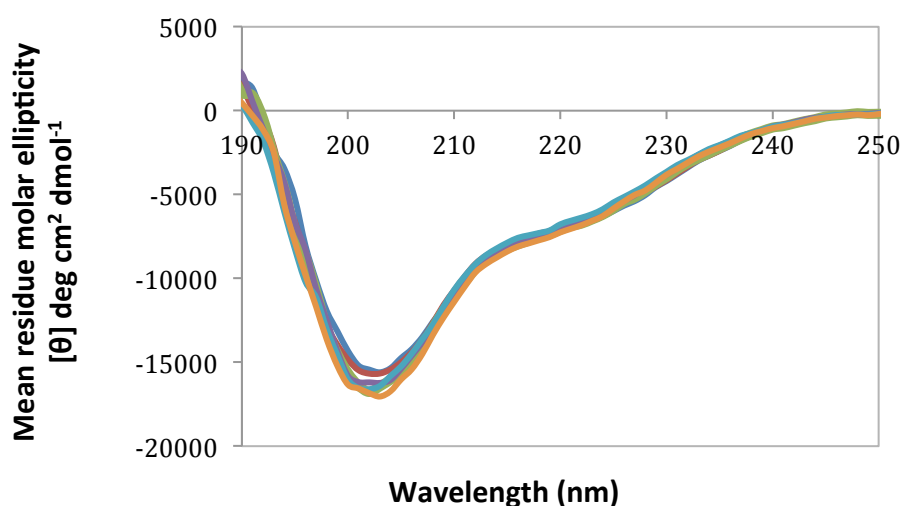


Figure 7.13 Effect of TGA incubation time on the far-UV CD mean residue ellipticity $[\theta]$ of α_{s1} -casein expressed in degree cm^2/dmol . Standard - native α_{s1} -casein (blue); control – native α_{s1} -casein with heat treatment at 85°C for 5 min (red); α_{s1} -casein incubated with TGA at incubation time: 5 min (green), 30 min (purple), 60 min (light blue) and 120 min (orange).

The far-UV CD results showed that the spectrum of α_{s1} -casein was unchanged on increasing TGA incubation time (Figure 7.13). The level of secondary structure was calculated according to the far-UV CD spectra of a α -helix, β -sheet and random coil structure that exhibited troughs at different wavelength (as described in Section 3.2.4; Kelly et al., 2005). The calculated secondary structure features for each spectrum in Figure 7.13 are given in Table 7.2 (as described in Section 3.2.4).

Table 7.2 The level of secondary structure of native and TGA-treated α_{s1} -casein estimated by CD (fifteen accumulations for one determination; standard error given for three determinations, standard errors less than 1 are not stated).

Incubation time (min)	α -Helix (%)	β -Sheet (%)	Random coil (%)
0 standard	12.8 \pm 1	29.4	39.4 \pm 1
0 control	13.5	29.4 \pm 1	39.4 \pm 1
5	13.0 \pm 1	29.3 \pm 1	39.5 \pm 1
30	12.7	29.4	39.5
60	12.0 \pm 1	30.6 \pm 1	39.7
120	13.4 \pm 1	29.8	39.4 \pm 1

As the TGA incubation time for α_{s1} -casein increased, there is no noticeable change in the calculated amount of helix, sheet or unordered structure (Table 7.2). The level of α -helix, β -sheet and random coil structure between native and TGA-treated α_{s1} -casein remains relatively invariant at about 13% ($p= 0.54$), 30% ($p= 0.45$) and 40% ($p= 0.96$), respectively (Table 7.2). The far-UV CD spectra results indicated that neither the TGA incubation nor heat treatment affected the secondary structure of α_{s1} -casein.

The formation of protein secondary structures was described in Section 5.2.4. The TGA-induced cross-linking and deamidation increased the overall net charge of α_{s1} -casein at pH 7.0, but the level of increase in the net charge was relatively low (as described in Section 7.2.2). Therefore, the increase in the electrostatic repulsion between protein chains of α_{s1} -casein due to the increased net charge was not sufficient to destabilize the secondary structure of α_{s1} -casein. The results from the

CD measurement are in agreement with a previous study by Motoki et al. (1986) who reported that only a minor increase in the level of β -sheet was found in 80% deamidated α_{s1} -casein, which was measured using a CD method. In their study, in order to control the level of deamidation without competition from cross-linking, α_{s1} -casein was citraconylated with citraconic anhydride to block the free amino groups of protein-bound lysyl side chains before TGA incubation. This is consistent with findings from the study of succinylated α_{s1} -casein that succinylation led to a significant change in the level of α -helix and β -sheet due to the high level of increase in the net charge of α_{s1} -casein (as described in Section 5.2.4). Thus, charge plays a dominant role in the secondary structure of α_{s1} -casein.

7.3 Succinylated α_{s1} -casein with TGA treatment

When the lysine residues of α_{s1} -casein were succinylated, the succinylated lysine residues are not available for cross-linking (Figure 7.1). Therefore, the level of deamidation can be manipulated by controlling the incubation time of TGA with fully succinylated α_{s1} -casein, without competition from TGA-induced cross-linking. In order to distinguish whether the effect of TGA treatment on the physicochemical properties of α_{s1} -casein is due to cross-linking or deamidation, the succinylated α_{s1} -casein samples (in Chapter 5) were incubated with TGA for up to 120 min; the treatment conditions were the same as for the TGA-modified α_{s1} -casein. The effect of deamidation could be independent of TGA-induced cross-linking, and it could be tested for the samples incubated for 120 minutes, where no crosslinking occurred (Figure 7.14).

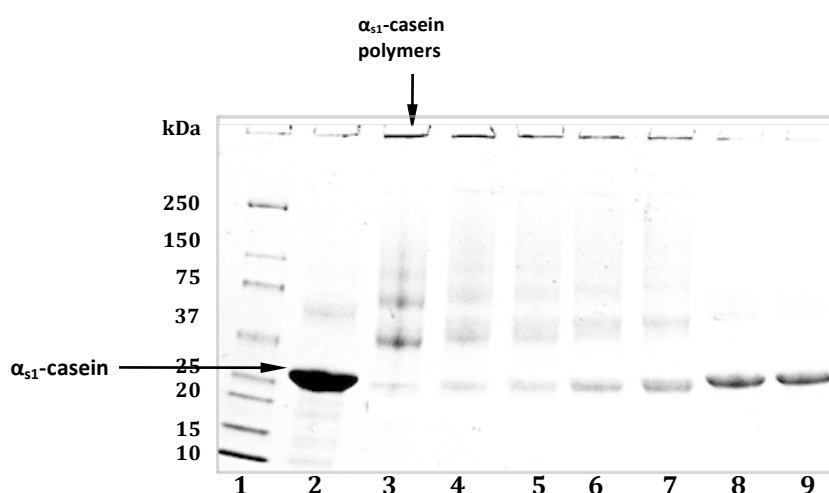


Figure 7.14 Reduced SDS-PAGE of succinylated α_{s1} -casein incubated with TGA for 120 min. From left to right: molecular weight markers (Lane 1) standard sample (native α_{s1} -casein without heat treatment, Lane 2); α_{s1} -casein with 23% (Lane 3), 30% (Lane 4), 40% (Lane 5), 49% (Lane 6), 83% (Lane 7), 97% (Lane 8), 99% (Lane 9) succinylation.

Figure 7.14 shows that the native α_{s1} -casein had the highest band intensity (Lane 2). The band intensities of proteins at positions between 25 and 37 kDa gradually increased and the band intensities of protein at positions higher than 37 kDa including the top of the gel decreased, when the level of succinylation increased (Lanes 3 to 9). This indicates that the level of cross-linked α_{s1} -casein decreased with increased level of succinylation, which is due to the increase in the amount of succinylated lysine residues. In 99% succinylated α_{s1} -casein incubated with TGA, the cross-linking was fully inhibited as no protein bands at positions higher than 37 kDa were observed (Lane 9). The 99% succinylated α_{s1} -casein showed a lower intensity than native α_{s1} -casein. This is because succinylation reduced the dye binding with proteins (as described in Section 5.2.1).

The OPA method and mass spectrometry of succinylated protein showed that 13 out of 14 lysine residues were succinylated in 99% succinylated α_{s1} -casein (as described in Section 5.2.1). Deamidation was predicted to be the dominant reaction in 99% succinylated α_{s1} -casein incubated with TGA, which could show the effect of the

deamidation on the physicochemical properties of α_{s1} -casein without the interference from cross-linking.

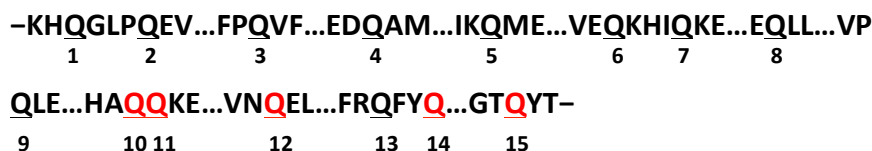


Figure 7.15 Succinylated α_{s1} -casein (99%) incubated with TGA at incubation time 120 min monitored by mass spectrometry. Q (black): glutamine residues, Q (red): partially deamidated glutamine residues, which were identified by the database mapping (more data is stated in Appendix C).

The deamidated glutamine residues of 99% succinylated α_{s1} -casein incubated with TGA were monitored using mass spectrometry (as described in Section 2.2.8). The mass spectrometry chromatograph of succinylated lysine residues was shown in Section 5.2.1, and a representative mass spectrum of the deamidated glutamine residues is shown in Section 7.2.1.

Figure 7.15 shows that glutamine residues 10, 11, 12, 14 and 15 were partially deamidated due to TGA treatment. These deamidated glutamine residues in 99% succinylated α_{s1} -casein incubated with TGA are completely different from the α_{s1} -casein with only TGA treatment, as TGA treatment resulted in the glutamine residues 1, 2, 5, 6, and 9 being deamidated. This could result because the secondary structure of α_{s1} -casein is changed due to succinylation (as described in Section 5.2.4), which could affect the specificity of the TGA toward the glutamine residues. It has been suggested that the change in the conformation of proteins could expose or bury the specific amino acid residues that are accessible for TGA modification (Kashiwagi et al., 2002; Lee & Park, 2002; Ohtsuka et al., 2000b). This confirms that deamidation is successful when the cross-linking reaction is not available.

7.4 Conclusions

The level of cross-linked α_{s1} -casein was manipulated by controlling the incubation time with TGA, with a low level of deamidation. TGA treatment led to a low level of reduction in the apparent pI of α_{s1} -casein, which is due to both cross-linking and deamidation. An increased surface hydrophobicity of α_{s1} -casein was observed after TGA treatment, as a result of the cross-linking reaction. In addition, TGA treatment did not affect the level of secondary structure of α_{s1} -casein. This indicated that the secondary structure of α_{s1} -casein is destabilized by electrostatic repulsion, and the molecular weight of α_{s1} -casein did not have an impact on the level of secondary structure. However, the increase in the electrostatic repulsion between protein chains of α_{s1} -casein due to deamidation was not sufficient to change the secondary structure of α_{s1} -casein. TGA had a higher activity for the cross-linking reaction rather than the deamidation reaction of α_{s1} -casein.

Chapter 8 Functional properties of

transglutaminase-modified α_{s1} -casein

8.1 Introduction

The relationship between charge, hydrophobicity and functional properties of α_{s1} -casein has been examined in the studies of dephosphorylation and succinylation of α_{s1} -casein. Molecular weight and shape of proteins were also reported to have an impact on the functionality of proteins (Bryant & McClements, 1998; Luyten et al., 2004; Zayas, 1997). Thus, the molecular weight of cross-linked α_{s1} -casein was manipulated by controlling the incubation time of α_{s1} -casein with transglutaminase (as described in Chapter 7). In order to understand how the molecular weight affects the functional properties of α_{s1} -casein, the interfacial properties, water binding capacity, foam stability and emulsifying properties were examined in this study.

8.2 Results and discussion

8.2.1 Viscosity of TGA-treated α_{s1} -casein

Dephosphorylation and succinylation results showed that the viscosity of α_{s1} -casein increased with increased net charge of α_{s1} -casein (described in Section 3.2.3 and 5.2.2). TGA-induced crosslinking and deamidation resulted in a low level increase in the net charge of α_{s1} -casein (as described in Section 7.2.2). In addition, the increase in the level of polymerization of α_{s1} -casein due to TGA-induced cross-linking could enhance the viscosity of α_{s1} -casein (Gharst et al., 2007). Viscosity of proteins can be affected by the shape and size of the molecules (Viswanath et al., 2007). Unlike the self-associated “spherical” polymers that were formed due to dephosphorylation (as described in Section 3.2.5), the TGA treatment resulted in cross-linked polymers. Thus, the TGA treatment was predicted to increase the viscosity of α_{s1} -casein at a

moderate level. The viscosity TGA-treated α_{s1} -casein was examined using a capillary viscometer (described in Section 2.2.16).

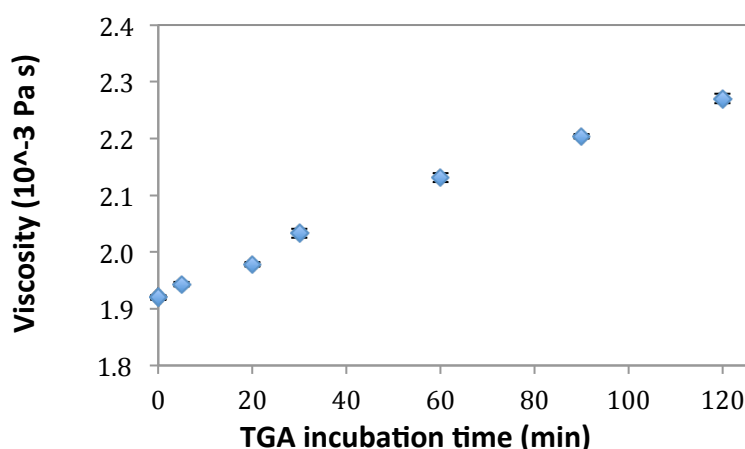


Figure 8.1 Viscosity of TGA-treated α_{s1} -casein. Each data point is an average of three replicates. Error bars represent the standard deviation of the mean of the replicates.

The viscosity of TGA-treated α_{s1} -casein solutions gradually increased with increased incubation time (Figure 8.1). The viscosity of α_{s1} -casein incubated with TGA at 120 min increased about 0.4 units when compared to the native α_{s1} -casein. The increase in the viscosity of TGA-treated α_{s1} -casein could result from both the increased overall net charge and the molecular weight of α_{s1} -casein.

The results from the viscosity of dephosphorylated and succinylated α_{s1} -casein suggested that at constant ionic strength, the viscosity of protein solutions increased with increased net charge of proteins (as described in Section 4.2.2 and 6.2.1). TGA treatment increased net charge of α_{s1} -casein at an incubation time of 5 min due to cross-linking and deamidation, but further increased incubation time did not lead to a noticeable change in the net charge (as described in Section 7.2.2). Therefore, the increase in the viscosity of TGA-treated α_{s1} -casein was affected by the increased molecular weight and net charge of proteins. But, the linear increase in the viscosity suggested that the cross-linking plays a more important role in altering the viscosity than the net charge. The results from the SDS gel showed that the molecular weight of α_{s1} -casein gradually increased with increasing incubation time due to formation of

a cross-linked polymer of α_{s1} -casein (as described in Section 7.2.1). These cross-linked polymers of α_{s1} -casein created a protein network in the solution, which are less flexible than the individual polymer chains. Thus, the cross-linking prevented α_{s1} -casein flow and consequently resulted in a higher viscosity compared to native α_{s1} -casein. This result is in agreement with previous findings that the viscosity of TGA-treated caseinate increased with the level of polymerization (Aguilera & Lillford, 2008; Faergemand et al., 1997; Kuraishi et al., 2001; Mounsey et al., 2005).

8.2.2 Water binding properties of TGA-treated α_{s1} -casein

TGA treatment increased the net charge and surface hydrophobicity of α_{s1} -casein (as described in Chapter 7); such modified physicochemical properties were predicted to have an impact on the water binding capacity of α_{s1} -casein. Therefore, the water binding capacity of TGA-modified α_{s1} -casein was determined by measuring the T2 relaxation constant using NMR (as described in Section 2.2.15 and 4.2.3).

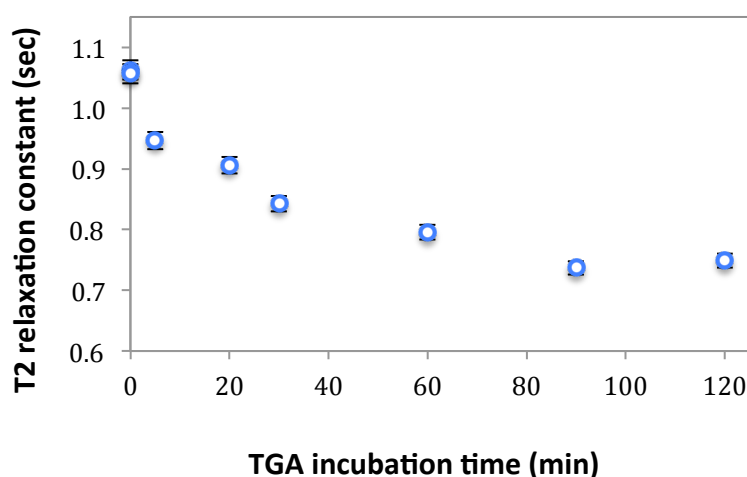


Figure 8.2 T2 relaxation constant time of TGA-treated α_{s1} -casein measured using NMR. Each data point is an average of two replicates. Error bars represent the standard deviation of the mean of the replicates.

The T2 relaxation constant of TGA-treated α_{s1} -casein gradually decreased when the incubation time increased from 0 to 90 min, and then plateaued at incubation times

between 90 and 120 min (Figure 8.2). The T2 relaxation constant of TGA-treated α_{s1} -casein at an incubation time of 120 min decreased about 0.3 s in comparison to the standard sample. These results indicate that TGA treatment increased the water binding capacity of α_{s1} -casein, and the longer the incubation time the higher the water binding capacity.

The increase in the water binding capacity of TGA-treated α_{s1} -casein could be caused by several factors. Firstly, higher net charge and lower surface hydrophobicity increase the water binding capacity of proteins (Kinsella & Morr, 1984; Zayas, 1997). TGA-treatment increased the net charge and apparent surface hydrophobicity of α_{s1} -casein. However, the increase in the surface hydrophobicity of TGA-treated α_{s1} -casein was probably due to the exposure of hydrophobic regions (as described in Section 7.2.3). These hydrophobic regions do not bind to water molecules. Therefore, the change in the net charge is likely to be responsible for the impact on the water binding capacity (as described in Section 4.2.3). Secondly, the amount of bound water could be influenced by the amino groups of proteins (Schnepf, 1992). Lysine residues have a high affinity to bind water molecules (as described in Section 6.2.2; Kuntz, 1971; Zayas, 1997), and TGA-catalysed cross-linking resulted in the lysine residues inaccessible for the water binding. However, TGA-induced deamidation introduced hydroxyl groups onto the glutamine residues that can form hydrogen bonds with water molecules (as described in Section 4.2.3). Thus, the change in the water binding capacity of TGA-treated α_{s1} -casein could be due to the overall effect of the cross-linked lysine residues and introduced hydroxyl groups.

By comparison with the results from the water binding capacity of dephosphorylated and succinylated α_{s1} -casein (as described in Section 4.2.3 and 6.2.2), the findings from the water binding capacity of TGA-treated α_{s1} -casein suggested that the specific amino groups and hydrophilic groups played a dominant role in the water binding capacity of α_{s1} -casein, and the hydroxyl groups showed a higher affinity for water molecules than the lysine residues.

In this study, the water binding capacity is defined as the number of water molecules bound to each protein molecule, whereas, the water holding capacity is defined as the amount of water entrapped in the proteins. The water binding capacity of TGA-modified casein molecules has not been reported. However, the water holding capacity of TGA-treated caseins has been extensively studied and TGA-treatment increased the amount of water in caseins and its acid-induced gels (Jaros et al., 2010; Motoki & Seguro, 1998; Ozer et al., 2007; Yokoyama et al., 2004; Zhu et al., 1995). Jaros et al. (2006) suggested that TGA treatment improved the water holding capacity of caseins, which is due to the TGA-induced polymerization of proteins. After TGA treatment, the polymerized casein molecules formed a protein network that entrapped more water molecules within the cross-linked structure than the individual casein molecules, which was proposed to result in an enhanced water holding capacity of the caseins.

8.2.3 Surface tension of air-water interfaces of TGA-treated α_{s1} -casein

The effect of charge and hydrophobicity on the surface tension of α_{s1} -casein was studied in the dephosphorylated and succinylated α_{s1} -casein (described in Section 4.2.4 and 6.2.3). In order to investigate the impact of molecular weight on the surface tension of α_{s1} -casein, the surface tension of 0.03% TGA-treated α_{s1} -casein was measured using the Wilhelmy plate method (as described in Section 2.2.17 and 4.2.4).

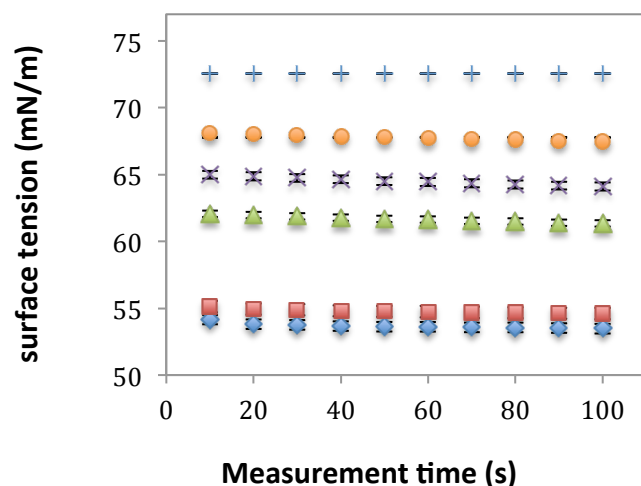


Figure 8.3 Surface tension (air-water) of TGA-treated α_{s1} -casein solutions measured using the Wilhelmy plate method. Standard-native α_{s1} -casein (incubation time – 0, \blacklozenge); control-native α_{s1} -casein with heat treatment at 85°C for 5 min (incubation time – 0, \blacksquare); α_{s1} -casein incubated with transglutaminase for 5 min (\blacktriangle), 30 min (\times), 60 min (\bullet) and 120 ($+$), respectively. Each data point is an average of four replicates. Error bars represent the standard deviation of the mean of the replicates.

The surface tension of TGA-treated α_{s1} -casein between the air and water interface gradually increased with increasing the incubation time (Figure 8.3). There was no difference in the surface tension between native α_{s1} -casein and α_{s1} -casein with heat treatment at 85°C for 5 min. When the TGA incubation time increased to 120 min, the surface tension increased about 18 mN/m in comparison to native α_{s1} -casein.

Like succinylation, TGA-induced cross-linking and deamidation increased the net charge of α_{s1} -casein, which was predicted to increase electrostatic repulsion between α_{s1} -casein molecules. This could lower the concentration of TGA-treated α_{s1} -casein on the surface and consequently result in a higher surface tension (as described in Section 4.2.4 and 6.2.3). Moreover, the surface tension of TGA-treated α_{s1} -casein could be influenced by the level of cross-linking. At constant temperature and pressure, high molecular weight polymers will lead to a higher surface tension than low molecular weight polymers (Legrand & Gaines Jr, 1969; Moreira & Demarquette, 2001; Wei et al., 2011). The relationship between the surface tension and molecular weight of polymers is $\gamma = \gamma(\infty) - c(1/M)^x$, where γ is the surface tension

(mN/m), M is the molecular weight (kDa), $\gamma(\infty)$ is the surface tension for infinite molecular weight and c is a constant (Li & Choi, 2006; Wei et al., 2011). The x value is dependent on the size of the polymers, it is 2/3 for low molecular weight polymers and 1 for high molecular weight polymers (Li & Choi, 2006; Wei et al., 2011). Therefore, the surface tension of TGA-treated α_{s1} -casein increased as the levels of cross-linking increased, which is in agreement with previous study by Partanen et al. (2009) who reported that the longer TGA incubation time led to a higher level of cross-linking and higher surface tension at the air-water interface.

The results from the studies of dephosphorylated and succinylated α_{s1} -casein showed that the surface tension of α_{s1} -casein increased with decreasing surface hydrophobicity, which is due to the hydrophobic adsorption of proteins on the interface (as described in Section 4.2.4 and 6.2.3; Benjamins et al., 1975; Pezennec et al., 2000; Walstra & De Roos, 1993). However, the surface tension of TGA-treated α_{s1} -casein increased with increasing surface hydrophobicity. TGA treatment increased the surface hydrophobicity of α_{s1} -casein due to the exposure of hydrophobic regions of α_{s1} -casein that were buried inside of the self-associated structure, but not increasing the hydrophobic properties of these exposed regions (as described in Section 7.2.3). During the adsorption process of α_{s1} -casein onto the interface, the hydrophobic adsorption on the interface was predicted to be stronger than the hydrophobic self-association of α_{s1} -casein. Therefore, the adsorption of α_{s1} -casein on the interface was not affected by exposing the hydrophobic regions that were buried inside of the self-associated structure. The change in the surface tension of TGA-treated α_{s1} -casein is likely to be affected by the effect of charge and molecular weight, but the effect of molecular weight might be more dominant than the effect of charge.

8.2.4 Surface tension of oil-water interfaces of TGA-treated α_{s1} -casein

The surface tension of TGA-treated α_{s1} -casein between oil and water was examined using a pendant drop tensiometer (described in Section 2.2.18 and 4.2.5).

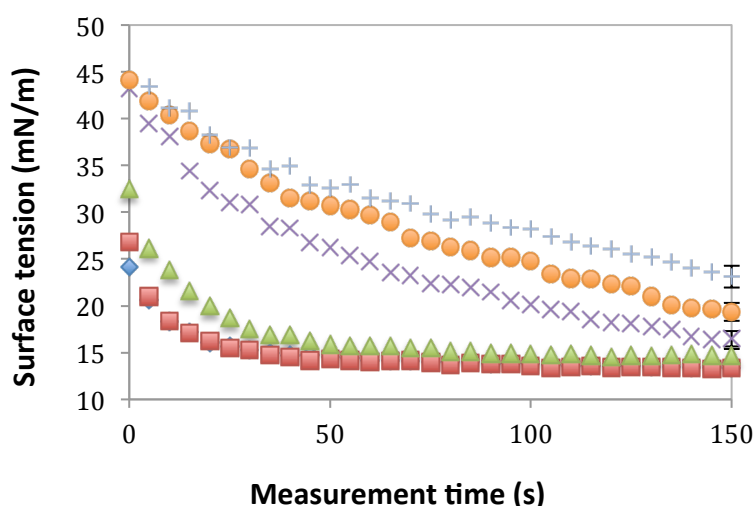


Figure 8.4 Interfacial tension (oil-water) of TGA-treated α_{s1} -casein measured using pendant drop tensiometer. Standard-native α_{s1} -casein (incubation time – 0, \blacklozenge); control-native α_{s1} -casein with heat treatment at 85°C for 5 min (incubation time – 0, \blacksquare); α_{s1} -casein incubated with transglutaminase for 5 min (\blacktriangle), 30 min (\times), 60 min (\bullet) and 120 min ($+$), respectively. Each data point is an average of three replicates. Error bars represent the standard deviation of the mean of the replicates.

The surface tension of TGA-treated α_{s1} -casein at the water and oil interface increased in comparison to native α_{s1} -casein (Figure 8.4). Figure 8.4 shows that the longer TGA incubation time led to a higher surface tension, which is similar to the change in the surface tension of TGA-treated α_{s1} -casein between the air-water interface (discussed in Section 8.2.3).

Like succinylation, the TGA-treated α_{s1} -casein had less effect on lowering surface tension than native α_{s1} -casein, which could result from the increased net charge (as described in Section 6.2.3). As a result of the increased net charge of α_{s1} -casein, a strong intermolecular repulsion could inhibit the protein adsorption on to the interface, and consequently decrease the surface tension (Kayitmazer, 2007). The results of TGA-treated α_{s1} -casein showed that the longest incubation times resulted in the highest surface tension for α_{s1} -casein (Figure 8.4). However, TGA treatment only led to an obvious increase in the net charge of α_{s1} -casein at 5 min of incubation time; and prolonged incubation times did not have a noticeable impact on the net charge of TGA-treated α_{s1} -casein (as described in Section 7.2.2). Thus, the change in

the net charge of TGA-treated α_{s1} -casein was not sufficient to account for the increase in the surface tension of TGA-treated α_{s1} -casein. On the other hand, proteins are adsorbed on to the oil-water interface by their hydrophobic regions (Beverung et al., 1999; Binks et al., 2000; Chandler, 2005; Paunov, 2003), but the change in the apparent hydrophobicity of TGA-treated α_{s1} -casein did not affect the surface tension (as described in Section 8.2.3). Therefore, the molecular weight of TGA-treated α_{s1} -casein is proposed to account for the effect on the surface tension of TGA-treated α_{s1} -casein (as described in Section 8.2.3), as the molecular weight of TGA-treated α_{s1} -casein gradually increased with increasing the incubation times. Similar to the air-water interface, the change in a single parameter was not sufficient to alter the surface tension of TGA-treated α_{s1} -casein, but the overall impact of the increased molecular weight and net charge of TGA-treated α_{s1} -casein played a major role in the increased surface tension on oil-water interface (as described in Section 8.2.3).

8.2.5 Emulsifying properties of TGA-treated α_{s1} -casein

In order to investigate how the change in the molecular weight will affect emulsifying properties of proteins, the TGA-treated α_{s1} -casein was used as an emulsifier, and the particles sizes of a canola oil droplet in an emulsion were determined by static light scattering using a Malvern Mastersizer 2000 (as described in Section 2.2.20 and 4.2.6).

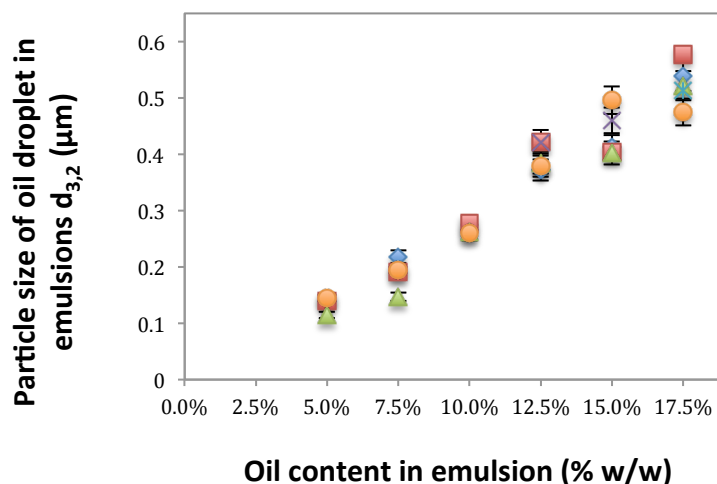


Figure 8.5 Particle size $d_{(3,2)}$ of canola oil droplet in emulsions made with α_{s1} -casein. Standard-native α_{s1} -casein (incubation time – 0, ♦); control-native α_{s1} -casein with heat treatment at 85°C for 5 min (incubation time – 0, ■); α_{s1} -casein incubated with transglutaminase for 5 min (▲), 30 min (×), 60 min (*) and 120 min (●), respectively. Each data point is an average of three replicates. Error bars represent the standard deviation of the mean of the replicates.

In all the emulsions containing different levels of oil, there was no noticeable difference in particle sizes between emulsions made from native α_{s1} -casein and the TGA-treated α_{s1} -casein (Figure 8.5). When the oil content of the emulsions increased from 2.5 to 17.5%, the particle size of emulsions with native and TGA-treated α_{s1} -casein increased at a similar level, which indicates that the amount of protein in the emulsions was not sufficient to stabilize the smaller oil droplets.

The result from the emulsifying properties of dephosphorylated and succinylated α_{s1} -casein indicated that the oil droplets were stabilized by the thickness of the protein layer, which was mainly dependent on the electrostatic repulsions between protein molecules and the interface (Dagorn-Scaviner et al., 1987; Graham & Phillips, 1976; Moro et al., 2001; Nagasawa et al., 1996; Urrutia, 2006). The thickness of the protein layer on the interface increased with increasing net charge of proteins (as described in Section 4.2.6 and 6.2.5). TGA treatment increased the net charge of α_{s1} -casein at a low level. Thus, the thickness of protein layer on the oil droplets was predicted to increase moderately, which led to a smaller size of oil droplets in the

emulsions with TGA-treated α_{s1} -casein. However, the TGA-treated α_{s1} -casein had less effect on lowering the surface tension on the oil-water interface than native α_{s1} -casein, which was presumably due to the increased molecular weight. The higher surface tension enhanced the tendency of oil droplets to coalesce (Blanchette et al., 2009) and consequently resulted in a larger sizes of oil droplets in the emulsions with TGA-treated α_{s1} -casein. Therefore, the TGA treatment did not cause a noticeable change in the size of oil droplets, which was due to the combined effect of net charge and molecular weight. The results are consistent with the suggestion that the change in the surface hydrophobicity of α_{s1} -casein only having an impact on the adsorption rate of proteins on the surface, but not the size of oil droplets (as described in Section 4.2.4 and 7.2.3).

The effect of TGA treatment on the emulsifying properties of milk proteins has been extensively studied, and it was shown that the TGA treatment increased the emulsifying properties of milk proteins (Dickinson et al., 1999; Gaspar & de Góes-Favoni, 2015; Hinz et al., 2007; Jiang & Zhao, 2011; Liu & Damodaran, 1999; Sharma et al., 2002). These studies mainly focused on the TGA treatment after emulsification, and the stabilization at a long storage time were determined using different techniques such as the emulsifying property index, turbidity measurement and microscopy analysis. However, TGA treatment showed no effect on the emulsifying properties of α_{s1} -casein in this study. The different findings from previous studies might result from the fact that the TGA treatment of α_{s1} -casein was applied before emulsification and the particle size was measured as the emulsifying property index. When the TGA treatment was applied after emulsification, the proteins at the interface were cross-linked, which locked the proteins into position. Therefore, the TGA-treated proteins covered the surface of the droplet as a monolayer. By contrast, when the TGA treatment was applied before emulsification, the cross-linked proteins covered the surface of the droplet, and a multilayer might be formed at the surface. The multilayer of proteins at the surface was predicted to have a different emulsifying capacity compared with the monolayer of proteins.

In addition, the stability of the emulsions with TGA-treated α_{s1} -casein was not monitored over storage time in this study. The TGA treatment of α_{s1} -casein may have an impact on the storage stability of emulsions. Dickinson et al. (1999) has reported that the TGA-induced cross-linking of sodium caseinate before emulsification slightly decreased the coalescence rate at long storage times. In a previous study by Færgemand et al. (1998), it was observed that the emulsions with TGA-treated sodium caseinate had a similar size distribution over 20 days of storage times in comparison to native sodium caseinate.

8.2.6 Foaming properties of TGA-treated α_{s1} -casein

The surface tension of α_{s1} -casein on the air-water interface was modified by the TGA treatment, which was predicted to have an impact on the foaming properties of α_{s1} -casein. Therefore, the foaming properties of TGA-treated α_{s1} -casein were investigated by measuring the volume of protein foam and the serum separation time (described in Section 2.2.19). The mechanisms of foam formation and the foam stability were described in Section 4.2.7 (Koehler et al., 2000; Pugh, 1996).

Table 8.1 The volumes of foam from native and TGA-treated α_{s1} -casein.

Incubation time (min)	0 Standard	0 Control	5	20	30	60	90	120
Volume of foam (mL)	25±1	25±1	25±1	25±1	25±1	25±1	25±1	25±1

The volumes of protein foam were identical between the native and TGA-treated α_{s1} -casein (Table 8.1). After whipping the protein solutions around 25 mL of foam was formed.

The time of serum separation from the α_{s1} -casein foam decreased as the TGA incubation time increased from 0 to 60 min (Figure 8.6). When the TGA incubation time further increased to 120 min, the separation time then increased again (~1310 s), but was still shorter than the time of serum separation from native α_{s1} -casein

foam (~1680 s; Figure 8.6). These results indicated that the foam of TGA treated α_{s1} -casein collapsed faster than native α_{s1} -casein, and the TGA treatment of α_{s1} -casein at incubation times between 30 to 90 min resulted in the lowest foam stability.

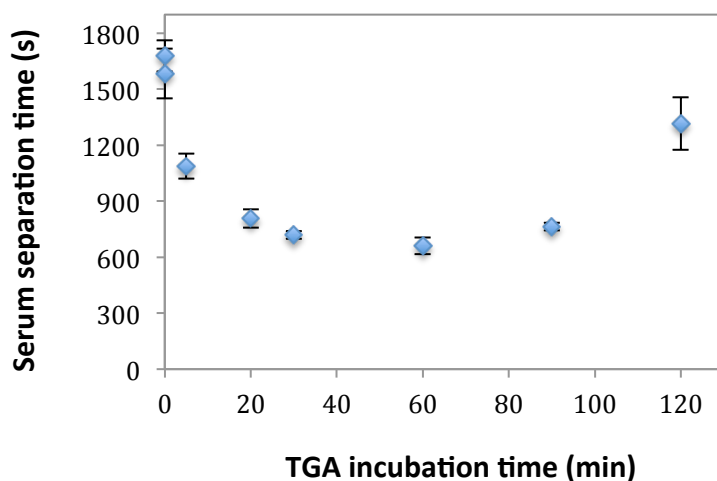


Figure 8.6 Protein serum separation time. Each data point is an average of three replicates. Error bars represent the standard deviation of the mean of the replicates.

The results from dephosphorylated and succinylated α_{s1} -casein indicated that the foam stability was affected by the net charge and hydrophobicity. It was suggested that there was an optimum balance between hydrophobic force and electrostatic force that contributed to the greater foaming stability of α_{s1} -casein (as described in Section 4.2.7 and 6.2.6). Electrostatic forces can significantly influence the foam stability of proteins (Davis et al., 2004; Dickinson, 1999b; Foegeding et al., 2006; Roth et al., 2000). Unlike succinylation, TGA-treatment led to a low level of change in the net charge (as described in Section 7.2.2), thus, the change in the electrostatic forces was predicted to have a minor effect on the foam stability of α_{s1} -casein. In addition, the change in the apparent hydrophobicity of TGA-treated α_{s1} -casein may have an impact on the foam stability. The increase in the apparent hydrophobicity of TGA-treated α_{s1} -casein was mainly due to the rearrangement of the protein network, which was predicted to have no effect on the protein adsorption on the interface (as described in Section 8.2.3).

TGA-catalysed intermolecular cross-linking led to the formation of α_{s1} -casein oligomers, which will affect protein functionality (as described in Section 7.2.1 and 8.2.1; Hiller & Lorenzen, 2009; Jaros et al., 2010). The increased molecular weight of α_{s1} -casein due to TGA-induced cross-linking was predicted to have a major impact on the foam stability. In this study, the level of oligomerization of TGA-treated α_{s1} -casein increased when the incubation time increased to 60 min. This formation of oligomers could reduce the flexibility of α_{s1} -casein molecules, which may reduce the coverage of α_{s1} -casein on the air-water interface and consequently resulted in lower foam stability in comparison to native α_{s1} -casein. It has been reported that the greater foam stability was dependent on the optimum balance between the degree of oligomerization of surfactants and the length of the space between the oligomerized monomers (Salonen et al., 2010). However, the length of the space between the cross-linked α_{s1} -casein molecules was not able to be determined in this study.

On the other hand, the surface viscosity may affect the foam stability. When the TGA incubation time further increased to 120 min, the viscosity of α_{s1} -casein on the air-water interface might be enhanced by the formation of a stable network of TGA-treated α_{s1} -casein. The increase in the surface viscosity could retard the foam collapse and foam drainage rate. It has been suggested that TGA treatment could lead to a change in the viscosity of α_{s1} -casein on the air-water interface (Færgemand et al., 1997). The modification of interfacial viscoelasticity due to TGA-induced cross-linking may play a role in the stability of protein foam, as the viscoelasticity had a significant impact on the size of air bubbles and the thickness of the protein film between bubbles (Hill, 1996; Klitzing & Müller, 2002; Monsalve & Schechter, 1984; Sánchez & Patino, 2005; Wilde, 2000a; Yu & Damodaran, 1991).

The moderate TGA treatment promoted the functionalities of milk proteins, but prolonged incubation time inhibited the enhancement of the functionalities (DeJong & Koppelman, 2006; Eissa & Khan, 2005; Jaros et al., 2010). However, the impact of extensive TGA treatment on the foam stability has not been reported. The foam stability of TGA-treated proteins can be affected by many factors that were not

investigated in the study, such as the interfacial viscoelasticity, air fluctuation and humidity of the experimental environment.

8.3 Conclusions

TGA-induced cross-linking had a significant effect on the foam stability of α_{s1} -casein, but not the volume of the foam. The optimum balance between the size and the length of space of the cross-linked α_{s1} -casein could contribute to the greater foam stability of α_{s1} -casein. However, the modified foam stability of TGA-treated α_{s1} -casein was not dependent on a single factor, it was also affected by the air-water surface tension, net charge and hydrophobicity. The change in the net charge and hydrophobicity of proteins had an impact on the foam stability, but this impact was not obvious in TGA-treated α_{s1} -casein due to the low level of change in the net charge.

A linear relationship between TGA incubation time and viscosity was found and the viscosity increased with the level of cross-linked α_{s1} -casein. The water binding capacity of TGA-treated α_{s1} -casein was reliant on the functional amino acid residues and the change in the net charge. TGA treatment led to a low level increase in the net charge of α_{s1} -casein, but significantly increased the molecular weight. However, the effect of net charge on the emulsifying capacity of α_{s1} -casein was contrary to the impact of molecular weight. As the comprehensive results of the change in the net charge and molecular weight, TGA-treatment did not alter the emulsifying capacity of α_{s1} -casein.

Chapter 9 The effect of charge on the surface structure of α_{s1} -casein-coated polystyrene latex particles

9.1 Introduction

Dephosphorylation and succinylation of α_{s1} -casein resulted in a change in the size of oil droplets in emulsions due to the change in net charge (as described in Section 4.2.7 and 6.2.6). The modified charge of α_{s1} -casein was predicted to alter the thickness of adsorbed protein layer on an oil-water interface, which could have an impact on the stability of emulsions. Therefore, in order to understand the effect of charge on the thickness of the protein layer at the interface, the thickness of a protein layer on latex particles that were coated with dephosphorylated and succinylated α_{s1} -casein was determined. The different methods for modified α_{s1} -casein coating latex particles and modification on α_{s1} -casein-coated latex particles are summarized in Figure 9.1 and described in Section 2.2.22. For comparison, some experiments with β -casein and κ -casein were also conducted.

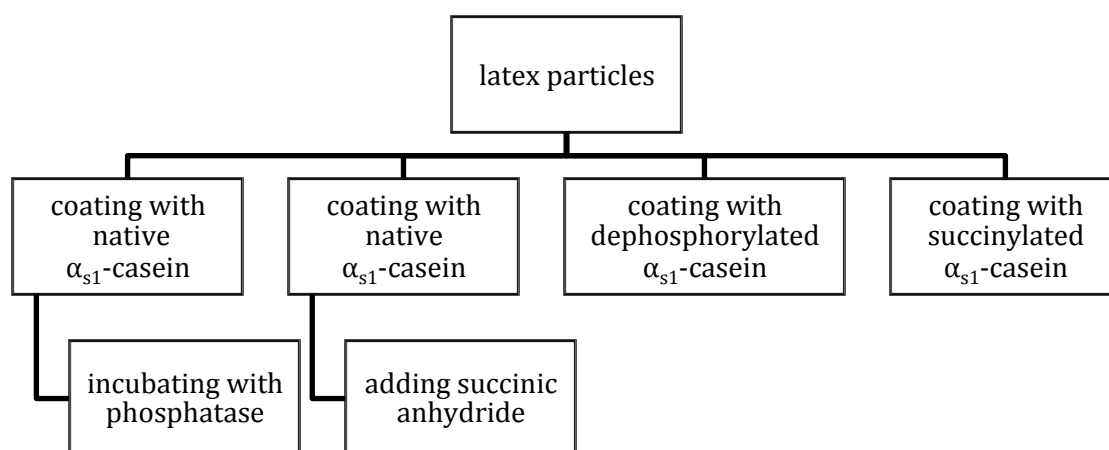


Figure 9.1 The method for coating latex particles with modified α_{s1} -casein and for modification of α_{s1} -casein-coated latex particles.

9.2 Results and discussion

9.2.1 Native casein-coated latex particles

Latex particles are negatively charged and have a hydrophobic surface. Caseins will adsorb onto the surface of latex particles by their hydrophobic regions and the hydrophilic regions remain in the serum phase (Anema, 1997; Horne & Leaver, 1995; Lee et al., 1989; Nakanishi et al., 2001; Shoemaker, 1990). It has been reported that the addition of β -casein led to an increase in the diameter of the latex particles about 26-30 nm (Dalglish, 1990; Dalglish, 1993), whereas, κ -casein and α_{s1} -casein increased the diameter of the latex particles by about 25 nm (Anema, 1997) and 21 nm (Dalglish, 1990), respectively.

The electrostatic repulsion between the negatively charged latex and proteins was predicted to lead to the hydrophilic regions of the protein stretching out from the latex surface, when the amount of negative charge of hydrophilic regions increases. In contrast, decreasing the amount of negative charge of the hydrophilic regions was predicted to result in the hydrophilic regions moving closer to the surface of the latex particles. Therefore, the thickness of protein layer on the latex particles could be altered by modifying the net charge of proteins. In order to test how the net charge changes the thickness of the protein layer, the diameters of modified protein-coated latex particles were measured. The size and zeta potential of the protein-coated latex particles were measured using a Malvern Zetasizer Nano-ZS with a method adapted from Anema (1997) (as described in Section 2.2.22). The zeta potential measurement determines the surface charge of protein-coated latex particles, which was described in Section 3.2.2.

The Malvern Zetasizer uses a dynamic light scattering technique to measure the size of particles. This technique, also known as photon correlation spectroscopy or quasi-elastic light scattering, can detect very small changes in the size of the particles (Chu, 2008; Pecora, 2013). Dynamic light scattering is ideal for the measurement of

particles or molecules with a size between 0.5 to 5000 nm in suspension (Goldburg, 1999; Pecora, 2013). During the light scattering measurement, the laser light is scattered at different intensities due to a random motion of particles in suspension (Brownian motion). Smaller particles causes the intensity to fluctuate more rapidly than large particles. The fluctuations in the intensity with time are measured, and these changes in the intensity are used for calculating diffusion coefficients. The particle diameters are then calculated from the diffusion coefficients using the Stokes-Einstein relationship (Chu, 2008; Förster et al., 1990; Pecora, 2013).

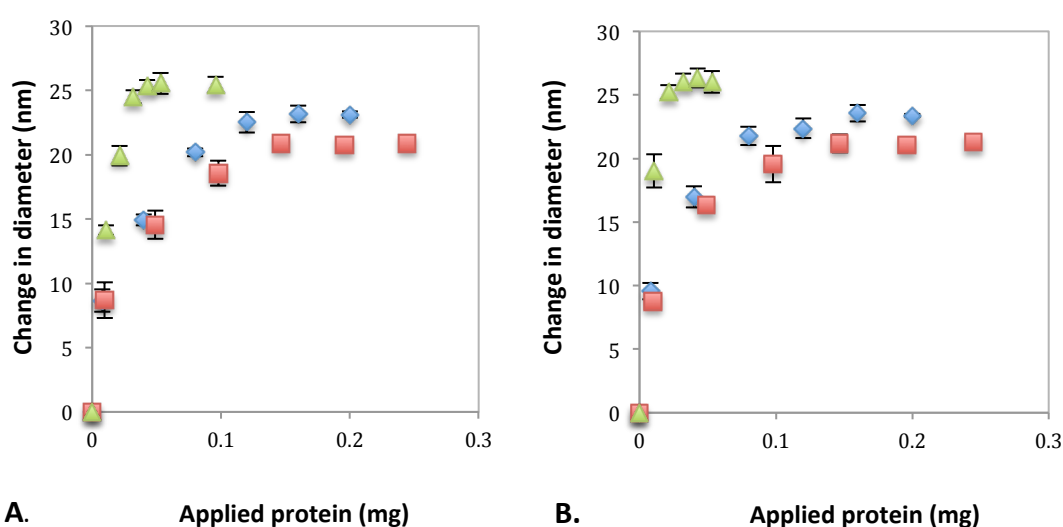


Figure 9.2 The changes in the diameters of native β -casein (\blacktriangle), κ -casein (\blacklozenge) and α_{s1} -casein (\blacksquare) -coated 60 nm (A) and 100 nm (B) latex particles.

The thickness of the protein layer on the latex surface is affected by the net charge of proteins, but also dependent on the structure of the adsorbed proteins and the length of the protein molecules (Dalgleish & Leaver, 1991a, 1991b). Figure 9.2 shows that the diameter of latex particles increased with increasing levels of added caseins, and then the change in the diameter plateaued when the amount of added caseins was sufficient to fully cover the latex surface. β -Casein required a lower level for saturation coverage than κ -casein and α_{s1} -casein in both 60 and 100 nm latex samples, whereas, κ -casein and α_{s1} -casein had similar saturation points levels (Figure 9.2). This is consistent with the fact that β -casein has a higher hydrophobicity than κ -

casein and α_{s1} -casein due to its large hydrophobic C-terminal region (as described in Chapter 1; Fox, 1982). Thus, lesser amount of β -casein was required to provide sufficient hydrophobic regions that fully cover the latex surface compared with κ -casein and α_{s1} -casein. Moreover, in both 60 and 100 nm latex samples, the addition of β -casein, κ -casein and α_{s1} -casein was found to increase the diameter of latex particles by about 26 nm, 24 nm and 21 nm, respectively (Figure 9.2). This is consistent with previous studies that showed similar level of changes in the diameter of casein-coated latex particles (Anema, 1997; Dalgleish, 1990; Dalgleish, 1993).

9.2.2 Fully dephosphorylated α_{s1} -casein-coated latex

Dephosphorylation resulted in a reduction in the net charge due to the loss of serine phosphate groups (as described in Section 3.2.2), thus, the thickness of dephosphorylated α_{s1} -casein on the latex surface was predicted to decrease.

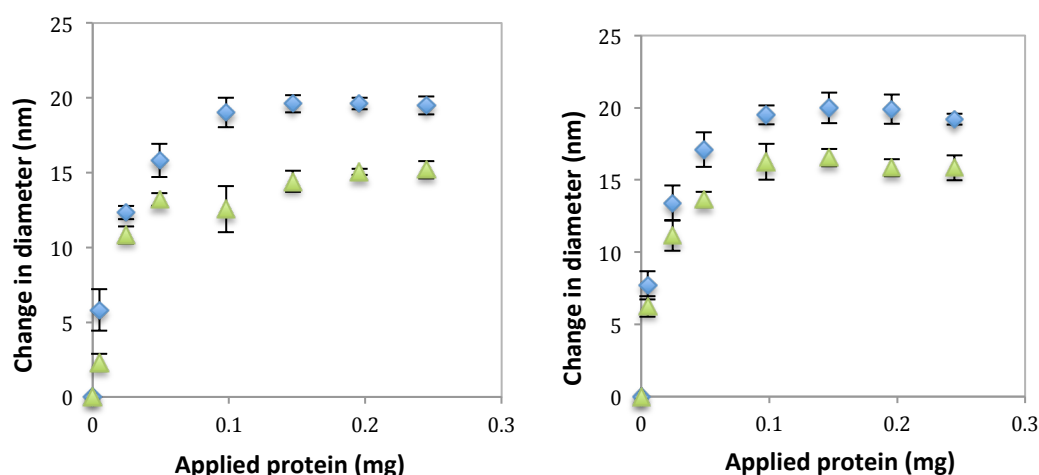


Figure 9.3 The changes in the diameters of native α_{s1} -casein (◆) and fully dephosphorylated α_{s1} -casein (▲)-coated 60 nm (A) and 100 nm (B) latex particles. Each data point is an average of two replicates. Error bars represent the standard deviation of the mean of the replicates.

In 60 and 100 nm latex samples, the addition of dephosphorylated α_{s1} -casein increased the diameter of latex particles by about 15-16 nm, which was less than the increase in the native α_{s1} -casein-coated latex (~20 nm). This indicated that dephosphorylation led to a reduction in the diameter of α_{s1} -casein-coated latex particles (by about 4-6 nm) and this was proposed to be due to the decreased net charge. The α_{s1} -casein was predicted to adsorb on the latex surface via its hydrophobic regions at the N-terminus and C-terminus (Dickinson et al., 1997a; Dickinson et al., 1997b), and the hydrophilic regions that contain the serine phosphate groups stretched out from the surface as a loop structure (Figure 9.4). When the net charge of dephosphorylated α_{s1} -casein was decreased, the electrostatic repulsion within the loop structure and between the loop structure and latex particles surface was diminished, which consequently resulted in the loop structure being closer to the surface of latex particles (Figure 9.4).

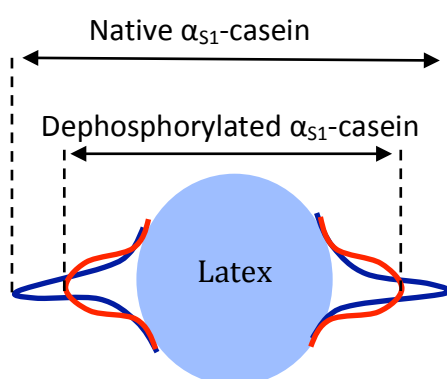


Figure 9.4 The proposed structure of native and dephosphorylated α_{s1} -casein on a latex particle.

In addition, during the titration, the native and dephosphorylated α_{s1} -casein showed a similar saturation point in 60 nm and 100 nm latex samples (Figure 9.3 A and B). Thus, the unchanged adsorption rate between native and dephosphorylated α_{s1} -casein on latex particles might be due to the overall effect of the surface of the latex particles and the hydrophobicity of native and dephosphorylated α_{s1} -casein.

Zeta potential of fully dephosphorylated α_{s1} -casein-coated latex

Dephosphorylation led to a reduction in the thickness of the α_{s1} -casein layer on latex particles due to the decreased net charge, which was predicted to alter the zeta potential of dephosphorylated α_{s1} -casein-coated latex particles. Protein adsorption on the surface of the latex particles will shield the negative charge of latex particles. When the latex particles were fully covered with protein, the zeta potential measurement determined the charge of the outer layer of the stretched hydrophilic regions.

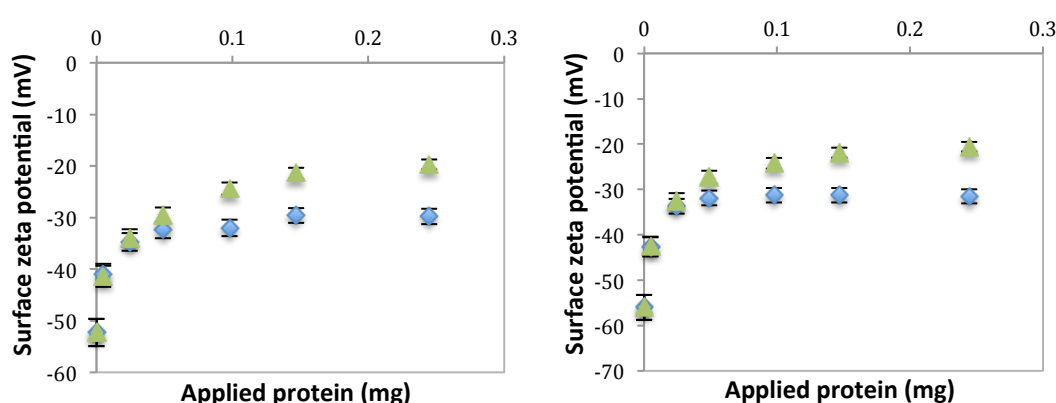


Figure 9.5 The zeta potential of native α_{s1} -casein (\blacklozenge) and fully dephosphorylated α_{s1} -casein (\blacktriangle)-coated 60 nm (A) and 100 nm (B) latex particles. Each data point is an average of two replicates. Error bars represent the standard deviation of the mean of the replicates.

The 60 and 100 nm latex particles had a zeta potential of -52 and -56 mV, respectively (Figure 9.5). When the amount of added native α_{s1} -casein increased, the absolute value of the zeta potential decreased. Figure 9.5 shows that in both 60 and 100 nm latex samples, dephosphorylation led to a reduction in the absolute value of surface zeta potential of about 9-10 mV when the latex particles were fully covered with α_{s1} -casein, which is consistent with dephosphorylation decreasing the net charge of α_{s1} -casein.

9.2.3 Dephosphorylation of casein-coated latex particles

In this experiment, latex particles were fully coated with α_{s1} -casein, and then the coated particles were washed to remove the excess casein. After this cleaning procedure, alkaline phosphate was added to the latex particles and the size of the particles during the reaction was monitored (Figure 10.1; as described in Section 2.22).

The diameters of α_{s1} -casein-coated latex particles decreased when the dephosphorylation time increased (Figure 9.6). This is due to the fact that the α_{s1} -casein gradually lost the negatively charged phosphate groups with increasing incubation time, which consequently reduced the electrostatic repulsion between the hydrophilic regions of α_{s1} -casein within the loop and between the hydrophilic regions and the latex particle surface. When the α_{s1} -casein was fully dephosphorylated, the diameters of α_{s1} -casein-coated latex particles remained unchanged with increasing incubation time. The higher level of added phosphatase (6 μL) resulted in a faster reduction of the diameters of α_{s1} -casein-coated latex particles (Figure 9.6).

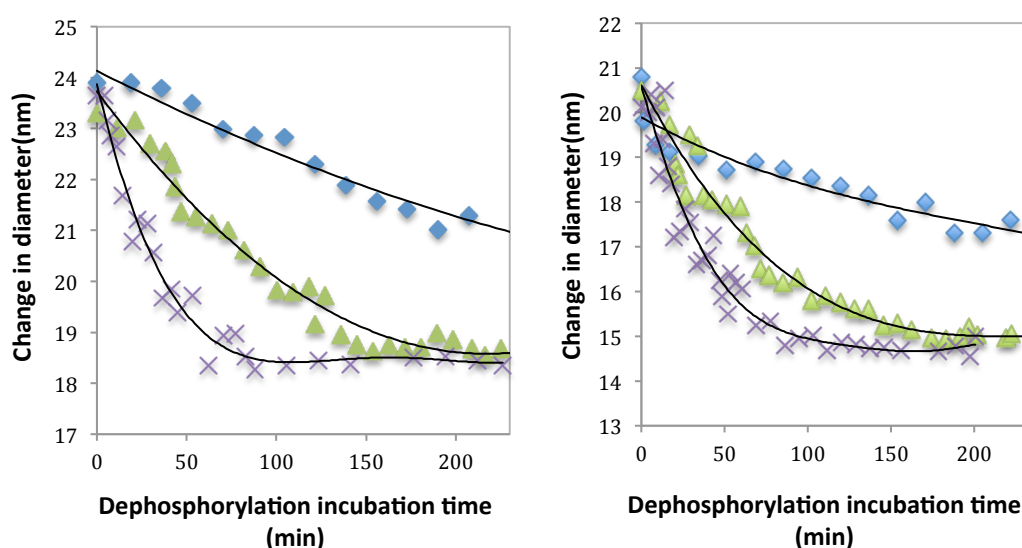


Figure 9.6 The changes in the diameters of native α_{s1} -casein-coated 60 nm (A) and 100 nm (B) latex particles incubated with 0.5 μL (\blacklozenge), 3 μL (\blacktriangle) and 6 μL (\times) of phosphatase for different times.

In both 60 and 100 nm latex samples, the addition of 3 and 6 μL of phosphatase decreased the diameter of α_{s1} -casein-coated latex particles by about 5 nm at incubation times of 200 min. This is consistent with the results from dephosphorylated α_{s1} -casein-coated latex particles. However, the addition of 0.5 μL phosphatase resulted in a reduction in the diameter of α_{s1} -casein-coated latex particles of about 3 nm. This lower level of reduction is due to the fact that a low level of addition of phosphatase contributed to a partial dephosphorylation of α_{s1} -casein at incubation times of 200 min.

In addition, at zero min of incubation time, the addition of native α_{s1} -casein increased the diameter of 60 nm latex particles by about 24 nm (Figure 9.6), which is slightly higher than the level of increased diameter of native α_{s1} -casein-coated latex particles (21 nm) at 20°C (Figure 9.2 and 10.3). This may result from the measurement error (± 2 nm), rather than the effect of temperature. Based on the results from preliminary experiments, the latex particles and protein-coated latex particles without phosphatase did not show a noticeable difference in the diameters between 20 and 37°C, even though the temperature adjustment process led to a fluctuation in the size of latex particles and protein-coated latex particles.

In order to assess the effect of dephosphorylation on the diameters of α_{s1} -casein-coated latex particles, the native κ -casein, α_{s1} -casein and β -casein-coated latex particles were incubated with the addition of a high level of phosphatase (6 μL).

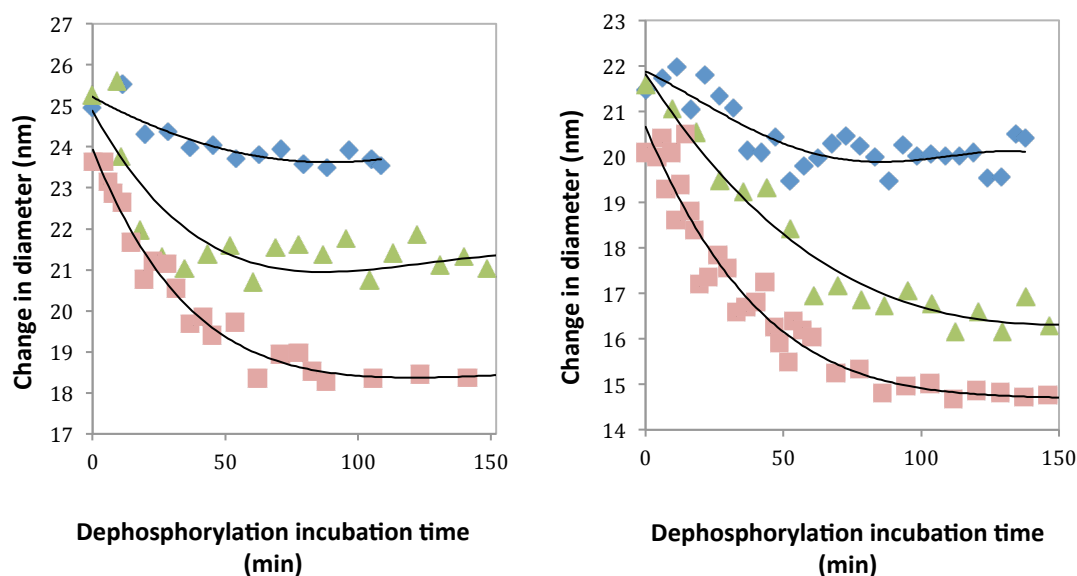


Figure 9.7 The changes in diameters of native κ -casein (\blacklozenge), β -casein (\blacktriangle) and α_{s1} -casein (\blacksquare)-coated 60 nm (A) and 100 nm (B) latex particles incubated with 6 μ L of phosphatase at different times.

Figure 9.7 shows that the level of the reduction in the diameters of different casein fractions-coated latex particles due to dephosphorylation decreased in the following order: α_{s1} -casein > β -casein > κ -casein. This is due to the fact that α_{s1} -casein and β -casein contain eight and four phosphoserine residues, respectively, whereas, κ -casein has one phosphoserine residue (as described in Chapter 1; Fox, 2009). The fewer number of serine phosphate groups the lower the level of reduction in the net charge of dephosphorylated caseins. Therefore, in both 60 and 100 nm latex samples, dephosphorylation decreased the diameters of α_{s1} -casein and β -casein-coated latex particles by about 6 and 4 nm, respectively. The diameter of dephosphorylated κ -casein-coated latex particles only decreased about 1 nm in comparison to native κ -casein. Overall these reductions in size on dephosphorylation are in proportion to the individual caseins serine phosphate contents.

9.2.4 Fully succinylated α_{s1} -casein-coated latex

Unlike dephosphorylation, succinylation increased the net charge of α_{s1} -casein (as described in Section 5.2.2). Therefore, succinylation was predicted to increase the diameters of α_{s1} -casein-coated latex particles.

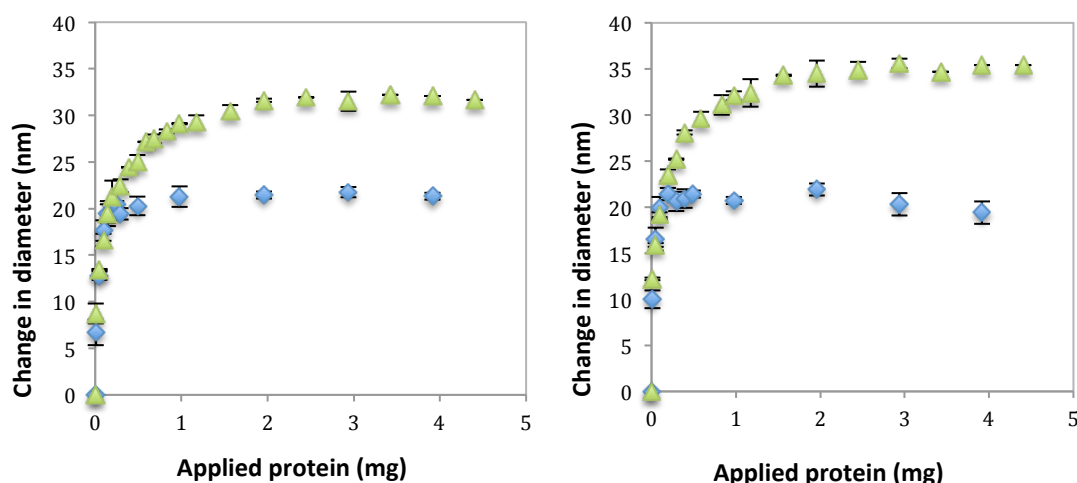


Figure 9.8 The changes in diameters of native α_{s1} -casein (◆) and fully succinylated α_{s1} -casein (▲)-coated 60 nm (A) and 100 nm (B) latex particles. Each data point is an average of two replicates. Error bars represent the standard deviation of the mean of the replicates.

The 60 and 100 nm latex particles were fully covered when about 0.1-0.2 mg of native α_{s1} -casein was added to the latex solution. However, about 2 mg of succinylated α_{s1} -casein was required to reach the saturated coverage on 60 and 100 nm latex particles (Figure 9.8). The result indicated that the succinylated α_{s1} -casein occupied less of the surface than native α_{s1} -casein, thus, more succinylated α_{s1} -casein was required to completely cover the surface. This may be due to the lower hydrophobicity of succinylated α_{s1} -casein, and possibly because that one hydrophobic region of α_{s1} -casein did not stick to the surface. Therefore, the shape of the succinylated α_{s1} -casein at the surface was different from native α_{s1} -casein, which led to a change in the coverage of proteins.

In addition to the increased level of adsorption, the increased diameter compared with native α_{s1} -casein suggests that the adsorbed structure of succinylated α_{s1} -casein on the surface of latex has changed. The native α_{s1} -casein is proposed to adsorb onto the surface via its two hydrophobic end regions that contain four and six lysine residues, respectively (Figure 9.9 A; Horne, 1998). After succinylation, the positive charges of the lysine residues were replaced by negative charges. One of the two hydrophobic regions may not bind to the latex and therefore could be stretching out from the surface of latex particles due to a strong electrostatic repulsion (Figure 9.9 B). Thus, more succinylated α_{s1} -casein was required to fully cover the surface of latex particles in comparison to native α_{s1} -casein. The stretched hydrophobic regions of succinylated α_{s1} -casein on the surface led to an increase in the diameter of the α_{s1} -casein-coated latex particles of 10 and 13 nm in 60 and 100 nm latex samples, respectively (Figure 9.8).

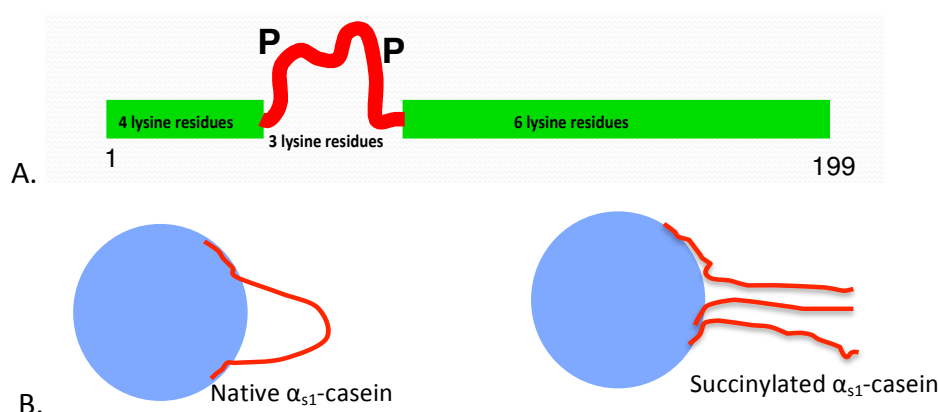


Figure 9.9 Train and loop model of primary structure of α_{s1} -casein (A) (Horne, 1998). The proposed structure of native and succinylated α_{s1} -casein on the latex surface (B).

The thickness of the protein layer is equal to half of the increased diameters of protein-coated latex particles. The thickness of the native α_{s1} -casein layer (~11 nm) and succinylated α_{s1} -casein layer (~18 nm) on latex particles is consistent with a monolayer of protein adsorption using an estimate of molecular dimensions. The protein chain length of α_{s1} -casein was estimated around 29 nm, which was

calculated with a normal length of a pure C-N bound of 1.47 Å (Vollhardt & Schore, 2011).

Zeta potential of fully succinylated α_{s1} -casein-coated latex

Succinylation led to an increase in the absolute value of zeta potential of α_{s1} -casein-coated latex particles (Table 9.1). Table 9.1 shows that the absolute value of zeta potential of succinylated α_{s1} -casein-coated 60 nm latex particles increased six mV units in comparison to native α_{s1} -casein, which is similar to the increase for succinylated α_{s1} -casein-coated 100 nm latex particles (6.6 mV). This is consistent with the change in the diameter of succinylated α_{s1} -casein-coated latex particles being due to the increased net charge of α_{s1} -casein.

Table 9.1 The surface zeta potential of native α_{s1} -casein and fully succinylated α_{s1} -casein-coated 60 nm and 100 nm latex particles.

	Zeta potential (mV)	Zeta potential (mV)
	Native α_{s1} -casein-coated latex	Succinylated α_{s1} -casein-coated latex
60 nm latex	-30.6 ± 1.5	-36.6 ± 1.9
100 nm latex	-37.1 ± 2.0	-43.7 ± 2.5

In contrast to dephosphorylation, succinylation resulted in a higher level of change in the diameter of α_{s1} -casein-coated latex particles. However, the level of the change in the surface zeta potential of α_{s1} -casein-coated latex particles due to succinylation was lower than that seen for dephosphorylation (10 mV reduction). This might be due to the fact that zeta potential measurements only determine the surface charge of proteins; it does not measure the total charge of proteins (as described in Section 3.2.2; Lopes et al., 1999; Reynolds & Wong, 1983; Sparks & Phillips, 1992). When the dephosphorylated α_{s1} -casein adsorbed on the latex surface (Figure 9.4), the zeta potential measurement determined the charges on the stretched central hydrophilic region of α_{s1} -casein that has the most of the dephosphorylated serine residues. However, when the succinylated α_{s1} -casein adsorbed on the latex surface, the zeta

potential measurement determined the charges on the outer layer of stuck out regions of α_{s1} -casein that only contains some of the succinylated lysine residues (Figure 9.9), but not the charges on the entire regions of the succinylated α_{s1} -casein.

9.2.5 Succinylation of α_{s1} -casein-coated latex

Succinylation of the native α_{s1} -casein-coated latex particles led to a 5 and 3 nm increase in the diameters of native α_{s1} -casein-coated 60 and 100 nm latex particles, respectively (Figure 9.10). The level of increase in the diameters due to succinylation on the native α_{s1} -casein-coated latex particles is much lower than succinylated α_{s1} -casein-coated latex particles (about 10 to 13 nm).

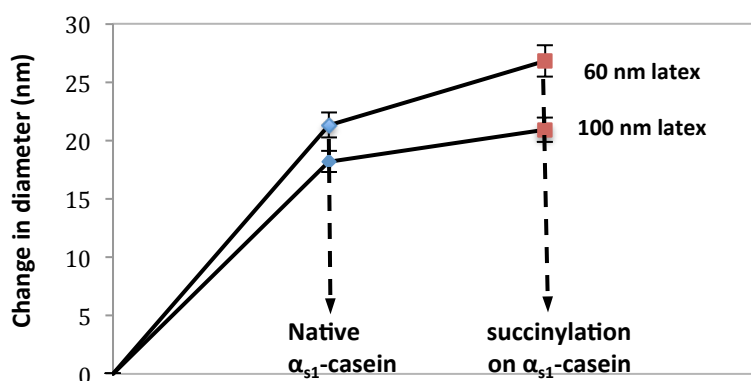


Figure 9.10 The changes in diameters of native α_{s1} -casein (◆)-coated 60 nm and 100 nm latex particles, and the effect of succinylation (■) on the changes in diameters. Each data point is an average of two replicates. Error bars represent the standard deviation of the mean of the replicates.

Unlike succinylated α_{s1} -casein-coated latex particles, the lysine residues on the hydrophobic regions might be less accessible for succinylation, as they were attached on the surface of the latex particles (Figure 9.9 A). Succinylation may only occur on the lysine residues that are located on the hydrophilic region of the α_{s1} -casein, which resulted in this hydrophilic region being more stretched from the surface of latex particles (Figure 9.11) rather than the whole protein chain stretched

out (Figure 9.9 B). Thus, succinylation on the native α_{s1} -casein-coated latex particles led to a lower increase in the diameter than succinylated α_{s1} -casein-coated latex particles. Moreover, the native α_{s1} -casein particles saturated the surface of latex particles at about 0.1 to 0.2 mg protein (Figure 9.8). This indicated that the particles required only about 0.2 mg native α_{s1} -casein to fully cover the surface. Therefore, only about 0.2 mg protein can be succinylated at the surface. Figure 9.8 showed that the addition of 0.2 mg succinylated α_{s1} -casein increased the diameter by about 5 nm within the error. This change is almost identical with the change in the diameter of native α_{s1} -casein-coated latex particles with succinylation treatment (Figure 9.10). Therefore, it is likely that the one end region of α_{s1} -casein was detached when the succinic anhydride was added into the native α_{s1} -casein-coated latex particles. However, there was not enough protein to fully cover the surface of particles, and thus the increase in the diameter is less than that when the latex particles were fully covered by the succinylated α_{s1} -casein.

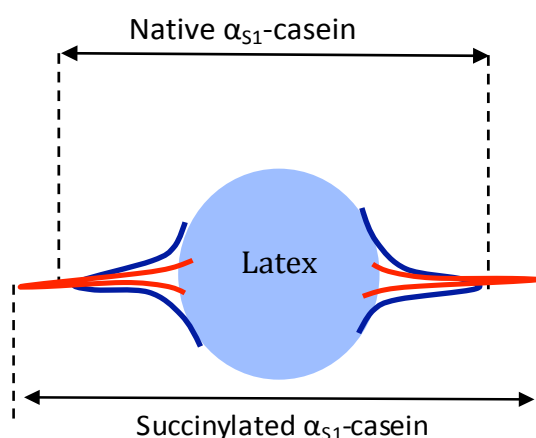


Figure 9.11 The proposed structure of succinylation on the native α_{s1} -casein-coated latex particles.

Table 9.2 The surface zeta potential of native α_{s1} -casein-coated 60 nm and 100 nm latex particles, and the effect of succinylation on the surface zeta potential.

	Zeta potential (mV)		Zeta potential (mV)
	Native latex	α_{s1} -casein-coated	Succinylation on native α_{s1} -casein-coated latex
60 nm latex	-34.7 \pm 1.8		-37.2 \pm 1.9
100 nm latex	-37.6 \pm 1.3		-39.7 \pm 1.1

Table 9.2 shows that succinylation led to an increase in the absolute value of surface zeta potential of the native α_{s1} -casein-coated 60 and 100 nm latex particles of about 2 units, which is lower than the level of increase in the absolute value of surface zeta potential of succinylated α_{s1} -casein-coated latex particles (~ 6 unit). This is consistent with the level of change in the diameters due to succinylation on the native α_{s1} -casein-coated latex particles being lower than succinylated α_{s1} -casein-coated latex particles due to the change in the net charge and conformation of α_{s1} -casein on the surface.

9.3 Conclusions

Dephosphorylation decreased the absolute value of zeta potential and the diameters of α_{s1} -casein-coated latex due to the decreased net charge. The fully dephosphorylated α_{s1} -casein was found to have a higher level of change in the diameter of α_{s1} -casein-coated latex particles than β - and κ -casein as α_{s1} -casein contains more serine phosphate groups. Unlike dephosphorylation, succinylation increased the net charge of α_{s1} -casein, and consequently led to an increase in the absolute value of zeta potential and the diameters of α_{s1} -casein-coated latex.

The change in the diameters of dephosphorylated and succinylated α_{s1} -casein-coated latex particles could provide useful information to explain the effect of dephosphorylation and succinylation on the stability of emulsions with modified α_{s1} -

casein. The results from the emulsifying capacities of modified α_{s1} -casein showed that dephosphorylation increased the particle size of emulsions with α_{s1} -casein due to the decreased net charge of α_{s1} -casein. Unlike dephosphorylation, succinylation resulted in an increase in the particle size of emulsions with α_{s1} -casein due to the increased net charge of α_{s1} -casein (as described in Section 4.2.6 and 6.2.5). These results indicated that the emulsions were stabilized by the electrostatic and steric repulsions of proteins, which is consistent with previous studies (Dickinson, 1999a, 2009; McClements, 2004; Tesch et al., 2002; Velez et al., 1996). Increasing the net charge of α_{s1} -casein increased the thickness of the protein layer on the oil droplets in the emulsions with α_{s1} -casein, which resulted in an increase in the steric repulsion and electrostatic repulsion between the α_{s1} -casein-coated oil droplets. The increased repulsions between oil droplets prevented the oil droplets from approaching each other and consequently inhibited the coalescence. In contrast, the decreased steric and electrostatic repulsions due to the reduction in the net charge of dephosphorylated α_{s1} -casein enhanced the coalescence of the oil droplets in the emulsions.

Chapter 10 General discussion and conclusions

Protein modifications have been reported to have a significant impact on the physicochemical and functional properties of milk proteins (Anderson & Kelley, 1959; Bingham et al., 1971; Clark et al., 1992; Darewicz et al., 2000; Kester & Richardson, 1984; Morand et al., 2012). However, these previous studies did not focus on the correlation between the physicochemical properties and functionalities of milk proteins. In this study, a range of modified α_{s1} -caseins has been synthesised, such as dephosphorylated, succinylated and TGA-modified α_{s1} -caseins. The physicochemical properties of these modified α_{s1} -caseins were manipulated by controlling the level of protein modifications. The physicochemical and functional properties of these modified α_{s1} -caseins were measured and summarized in Table 10.1. The correlations between these physicochemical and functional properties are discussed in this chapter.

Dephosphorylation decreased the net charge and increased the surface hydrophobicity of α_{s1} -casein by removing the negatively charged serine phosphate groups (as described in Section 3.2.3 and 3.3.4; Koudelka et al., 2009; Lorenzen & Reimerdes, 1992; Pearse et al., 1986). By contrast, succinylation increased the net charge and decreased the surface hydrophobicity of α_{s1} -casein by introducing the negatively charged succinyl groups at pH 7 (as described in Section 5.2.2 and 5.2.3; Morand et al., 2011b; Morand et al., 2012). The surface hydrophobicity decreased with increasing the net charge, and a linear relationship was observed between the net charge and surface hydrophobicity of α_{s1} -caseins ($R= 0.98$, $P<0.001$; Figure 10.1).

Table 10.1 The changes in the physicochemical and functional properties of modified α_{s1} -caseins.

	Dephosphorylation	Succinylation	TGA-treatment	Deamidation
Change of charge	-2 to -1	+1 to -2	+1 to 0	+1 to -1
Active group	9 serine residues	13 lysine residues	15 glutamine residues 13 lysine residues	15 glutamine residues
Isoionic point	4.5 to 5.0	4.5 to 3.6		
pI	4.7 to 5.3	4.7 to 3.0	4.7 to 4.4	
Hydrophobicity ANS (<i>S₀</i>)	30000→60000	30000→2500	30000→50000	
α -Helix	12% → 14%	15%→5%	13% constant	
β -Sheet	30% constant	27%→35%	29% constant	
Random coil	40% constant	39%→41%	40% constant	
Self-association	5 → 11	7→1.5		
Sedimentation coefficient (S)				
Viscosity 10^{-3} Pa s	2.2→1.8 (5 min) → constant	1.2→1.7	1.9→2.3	
Water binding T2 (sec)	1.05→0.82	1.05→1.35	1.05→0.7	
Surface tension Air-water (mN/m)	72→58	59→72	72→55	
Emulsion particle size (μ m)	0.4→1.8	0.7→0.2	0.5 constant	
Foam serum separation (Sec)	600→1150	1900→3200(50%) →2100 (100%)	1800→600 (60 min) →1200 (120 min)	

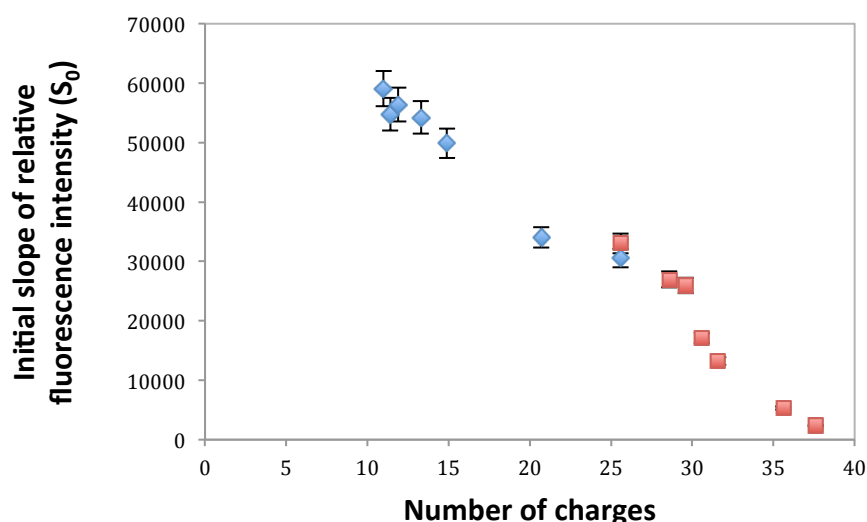


Figure 10.1 The relationship between net charge and surface hydrophobicity. Error bars represent the standard deviation of the mean of the replicates. The values of surface hydrophobicity were obtained by combining the surface hydrophobicity of dephosphorylated (◆) and succinylated (■) α_{s1} -casein. The number of net charges was obtained from the charge calculation results of dephosphorylated and succinylated α_{s1} -casein at pH 7 (as described in Section 3.2.2 and 5.2.2).

While there have been studies into the effect of succinylation and dephosphorylation on the secondary structure of other proteins such as yak casein, ovalbumin and β -casein (Batra et al., 1990; Farrell Jr et al., 2002; Holde, 1989; Yang et al., 2015), the effect of these modifications on the secondary structure of α_{s1} -casein has not been reported. In this study, the changes in the secondary structure were observed in succinylated α_{s1} -casein, but not in dephosphorylated α_{s1} -casein. α_{s1} -Casein molecules have a net negative charge above its pI, thus, the electrostatic repulsion increased when the positive charge of lysine residues was replaced by the negative charge of succinyl groups at pH 7. On the other hand, introducing succinyl groups on the lysine residues increased the steric repulsion within the α_{s1} -casein molecules. These results indicated that the secondary structure of α_{s1} -casein was dependent on the electrostatic repulsion alone or in combination with the steric repulsion within the protein molecules (Batra et al., 1990). Unlike succinylation, dephosphorylation decreased the electrostatic repulsion within the α_{s1} -casein

molecules. However, the number of reduced negative charges of dephosphorylated α_{s1} -casein was less than the number of increased negative charges of succinylated α_{s1} -casein. Therefore, the low level of change in the electrostatic repulsions within the α_{s1} -casein molecules due to dephosphorylation was not sufficient to affect the secondary structure of α_{s1} -casein when compared with succinylation.

The self-association behaviour of α_{s1} -casein has been reported to be affected by the protein concentration, pH, ionic strength and temperature of the solution (Ho & Waugh, 1965; Schmidt, 1970; Swaisgood, 2003). In this study, the AUC results showed that dephosphorylation enhanced the self-association behaviour of α_{s1} -casein, whereas, succinylation reduced the self-association behaviour of α_{s1} -casein. This confirmed that the self-association behaviour of α_{s1} -casein was influenced by both net charge and surface hydrophobicity of proteins, as the formation of the self-associated α_{s1} -casein oligomers is due to the hydrophobic interactions, but the size of the self-associated α_{s1} -casein is limited by the electrostatic repulsions (Horne, 1998; Horne, 2002; Payens et al., 1969; Schmidt, 1970). In addition, α_{s1} -casein lost calcium ion binding after dephosphorylation, consistent with the serine phosphate groups being gradually removed with increasing dephosphorylation incubation times.

The polymerization of α_{s1} -casein was increased by the TGA treatment. TGA-induced cross-linking and deamidation resulted in a lower level of change in the net charge of α_{s1} -casein in comparison to succinylation. Thus, no noticeable changes in the secondary structure were found in the TGA-treated α_{s1} -casein, which is consistent with the effect of charge on the secondary structure of α_{s1} -casein due to dephosphorylation. However, TGA treatment increased the surface hydrophobicity of α_{s1} -casein, which was the opposite of what was predicted. It is hypothesised that the increase in the surface hydrophobicity of TGA-treated α_{s1} -casein resulted from that TGA-induced cross-linking disrupting the self-associated structure of α_{s1} -casein, which exposed the hydrophobic regions initially buried inside of the self-associated structure.

10.1 Effect of physicochemical properties of α_{s1} -casein on the viscosity, water binding capacity and surface tension of α_{s1} -casein

The correlation between the physicochemical properties and functionalities of proteins was investigated by analysing food relevant functionalities of modified α_{s1} -caseins according to the type and degree of modification. Viscosity and water binding capacity are some of critical parameters that need to be controlled in the food industry. The understanding and capability to control the viscosity and water binding capacity of α_{s1} -casein has the potential to inform process parameters for dairy products and to tailor the specific functionalities of dairy products. Dephosphorylation decreased the viscosity, whereas, succinylation increased the viscosity of α_{s1} -casein. A linear relationship between the net charge and viscosity was observed for succinylated α_{s1} -casein ($R=0.97$, $P<0.001$) and dephosphorylated α_{s1} -casein ($R=0.99$, $P<0.001$; Figure 10.2). This confirmed that at a constant ionic strength and temperature, the viscosity of α_{s1} -casein solutions increased with increased net charge (as described in Section 4.2.2; Buzzell & Tanford, 1956). The dephosphorylated α_{s1} -casein at an incubation time of 5 min shows an outlier in the linear relationship (Figure 10.2). This sample might be more dephosphorylated than intended or its concentration was not quite accurate. The 5 min point was consistently giving results as it was more dephosphorylated than intended, thus, it was not included for all the correlations. Charge plays a role in the viscosity of α_{s1} -casein solutions, the viscosity for the two systems in Figure 10.2 shows that the protein concentration also had an impact on the viscosity of α_{s1} -casein solutions. Moreover, the viscosity of α_{s1} -casein solution was affected by the size and the shape of the protein molecules (Viswanath et al., 2007). TGA treatment increased the viscosity of α_{s1} -casein solutions, which was mainly dominated by the cross-linked polymers of α_{s1} -casein. This increase in the viscosity of TGA-treated α_{s1} -casein solutions was also attributed to the increased net charge of α_{s1} -casein.

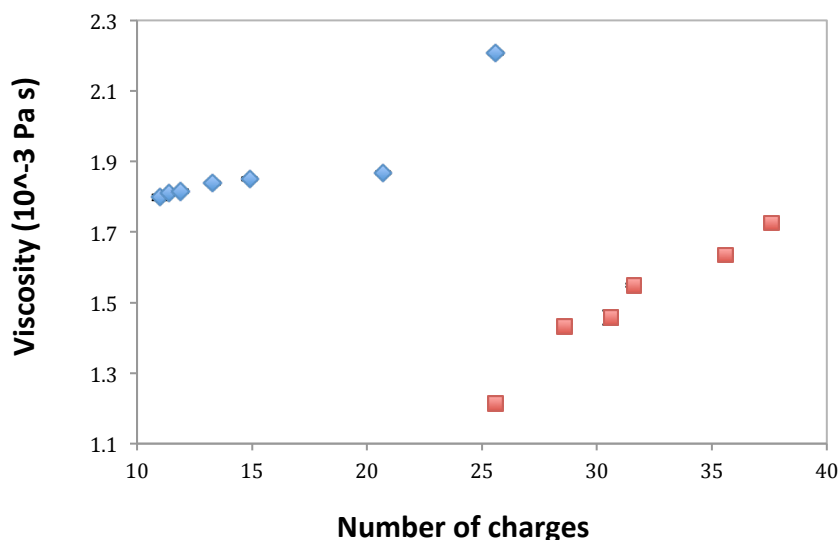


Figure 10.2 The relationship between net charge and viscosity of 3% dephosphorylated α_{s1} -casein solutions (♦), and 1% succinylated α_{s1} -casein solutions (■). Error bars represent the standard deviation of the mean of the replicates.

The water binding capacity of α_{s1} -casein was found to decrease with increasing net charge and decreasing surface hydrophobicity of proteins (Figure 10.3). However, it has been suggested that increasing net charge and decreasing surface hydrophobicity increased the amount of bound water of proteins (Kinsella & Morr, 1984; Zayas, 1997). Therefore, the water binding capacity of dephosphorylated and succinylated α_{s1} -casein was dependent on the specific hydrophilic groups or amino acid side chains, which can be altered by choosing the type and level of modification. The water binding capacity of modified α_{s1} -caseins was determined in deionized solutions. The results showed that dephosphorylation and TGA-treatment increased the water binding capacity of α_{s1} -casein. This suggested that the introduced hydrophilic groups played a dominant role in the water binding capacity of these modified α_{s1} -caseins, rather than the change in the net charge of proteins. This finding is consistent with a previous report that the hydrophilic groups or amino acid side chains such as hydroxyl groups and lysine residues had a high water binding affinity and capacity (Kuntz, 1971). Dephosphorylation and TGA-induced deamidation introduced hydroxyl groups onto the serine and glutamine residue, respectively, which consequently enhanced the amount of bound water molecules.

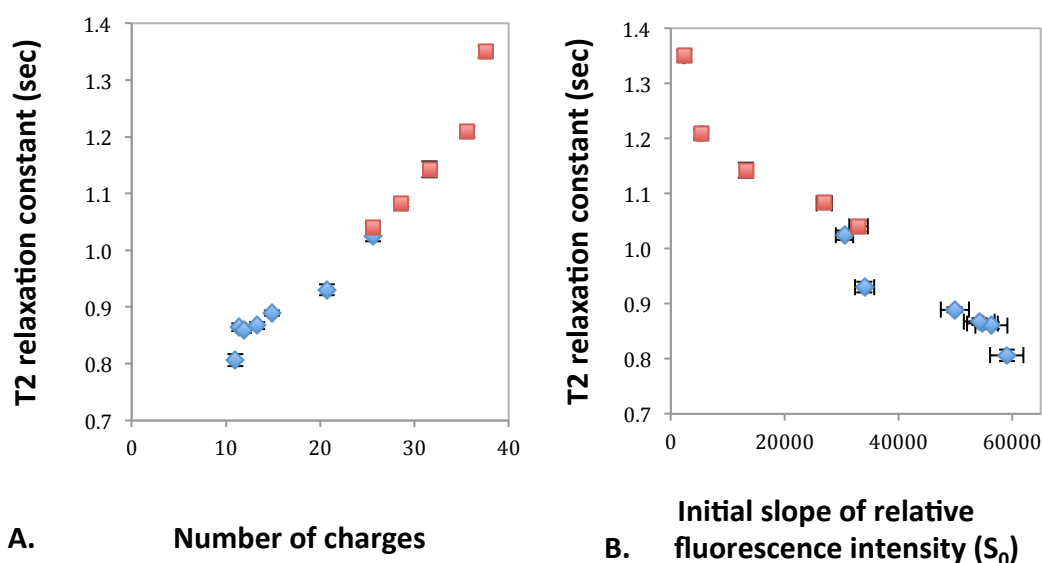


Figure 10.3 The relationship between net charge and water binding capacity (A), hydrophobicity and water binding capacity (B). The values of surface hydrophobicity, net charge and T2 relaxation constant were obtained from dephosphorylated (◆) and succinylated (■) α_{s1} -casein. Error bars represent the standard deviation of the mean of the replicates.

The surface tension of modified α_{s1} -caseins at an air and water interface were plotted against the surface tension at an oil-water interface in Figure 10.4. Protein modifications altered the surface tension of α_{s1} -casein, and a similar behaviour was observed for the surface tension at the oil-water and air-water interface. This can be seen when the two types of measurements were plotted against each other (Figure 10.4). A linear relationship between the surface tension at air-water interface and oil-water interface was observed in succinylated α_{s1} -casein ($R=0.99$, $P<0.001$), dephosphorylated α_{s1} -casein ($R=0.96$, $P=0.003$) and TGA-treated α_{s1} -casein ($R=0.96$, $P=0.009$; Figure 10.4). In the surface tension measurement, the protein concentration used for succinylated α_{s1} -casein was same as TGA-treated α_{s1} -casein, but the concentration for dephosphorylated α_{s1} -casein was lower than succinylated and TGA-treated samples (as described in Section 2.2.17 and 2.2.18). Therefore, the relationship between surface tension at air-water interface and oil-water interface was likely to be concentration dependent.

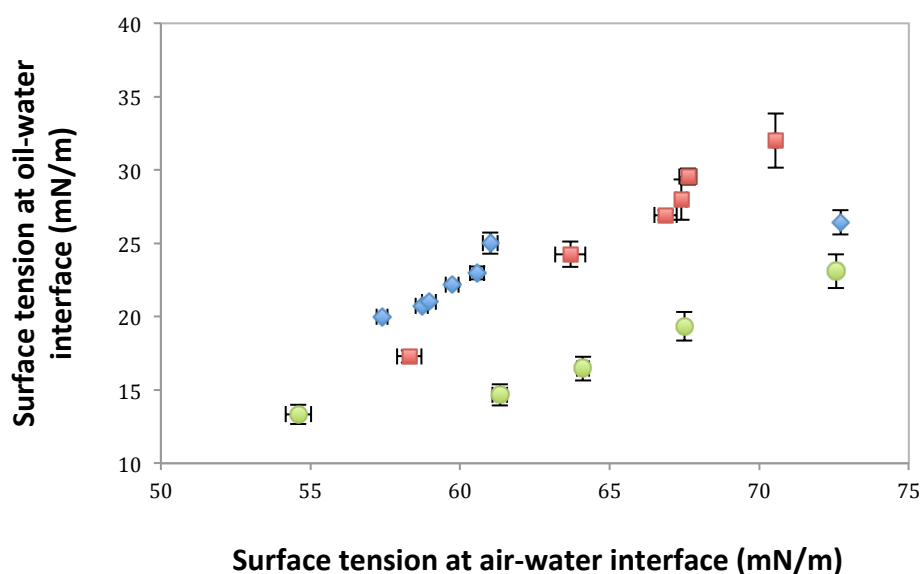


Figure 10.4 The relationship between surface tension air-water interface and oil-water interface : dephosphorylated α_{s1} -casein (◆); succinylated α_{s1} -casein (■) and TGA-treated α_{s1} -casein (●). Error bars represent the standard deviation of the mean of the replicates.

Moreover, the surface tension of α_{s1} -casein was found to increase with increased net charge and decreased hydrophobicity (as described in Section 4.2.4 and 4.2.5). A linear relationship was found between the net charge and surface tension in dephosphorylated ($R=0.99$, $P<0.001$) and succinylated samples ($R= 0.91$, $P=0.008$; Figure 10.5). The surface hydrophobicity and surface tension also showed a linear relationship in dephosphorylated ($R=0.99$, $P<0.001$) and succinylated samples ($R= 0.94$, $P=0.006$; Figure 10.6).

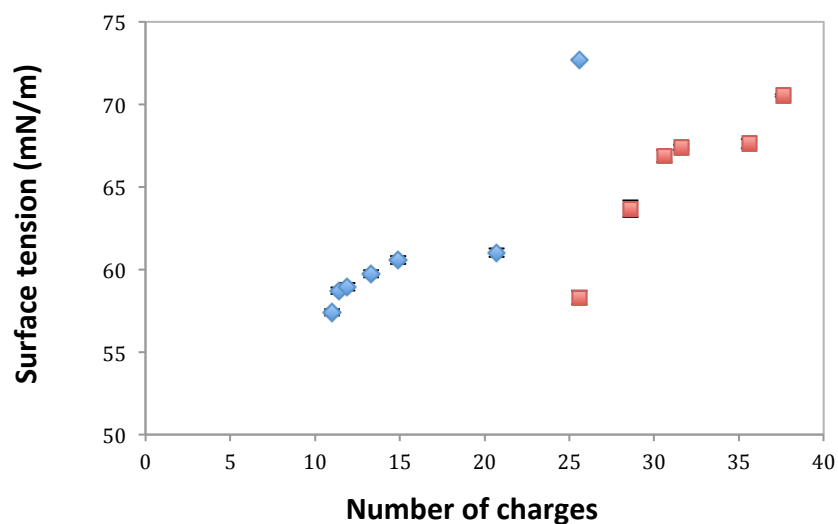


Figure 10.5 The relationship between net charge and interfacial tension (air-water) of 0.001% (w/w) dephosphorylated α_{s1} -casein solutions (◆) and 0.02% (w/w) succinylated α_{s1} -casein solutions (■). Error bars represent the standard deviation of the mean of the replicates.

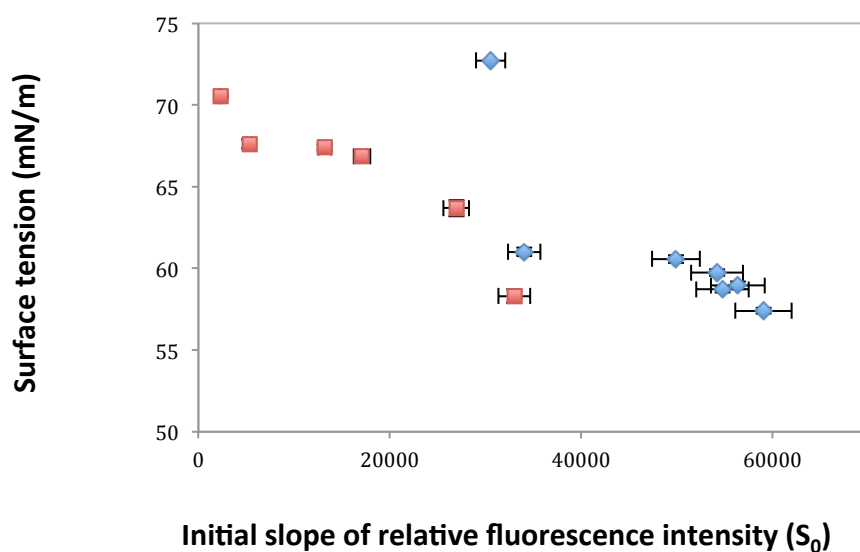


Figure 10.6 The relationship between surface hydrophobicity and interfacial tension (air-water) of 0.001% (w/w) dephosphorylated α_{s1} -casein solutions (◆) and 0.02% (w/w) succinylated α_{s1} -casein solutions (■). Error bars represent the standard deviation of the mean of the replicates.

10.2 Effect of physicochemical properties of α_{s1} -casein on the emulsifying properties

The impact of succinylation and TGA treatment on the physicochemical and emulsifying properties of milk proteins has been extensively studied (Darewicz et al., 2000; Faergemand et al., 1998; Lorenzen & Reimerdes, 1992). However, these previous studies did not focus on the correlation between the physicochemical properties and emulsifying properties of milk proteins. In this study, it was observed that dephosphorylation led to an increase in the size of oil droplets in α_{s1} -casein-stabilized emulsions, even though the surface hydrophobicity of dephosphorylated α_{s1} -casein increased. By contrast, succinylation decreased the size of the oil droplets in α_{s1} -casein-stabilized emulsions with an increased surface hydrophobicity. Figure 10.7 shows that the particle size of oil droplets decreases with increasing net charge of α_{s1} -casein, whereas, increasing surface hydrophobicity of α_{s1} -casein increased the particle size of oil droplets. The α_{s1} -caseins were adsorbed on the surface of oil droplets with the hydrophobic regions in the oil phase and the charged hydrophilic regions in the solution phase (Beverung et al., 1999; Binks et al., 2000; Chandler, 2005; Paunov, 2003). Increasing the net charge of the adsorbed α_{s1} -casein led to a stronger electrostatic repulsion between α_{s1} -casein-coated oil droplets, which inhibited the oil droplets from approaching each other and consequently stabilized the emulsions. These results suggested that the net charge of α_{s1} -casein played a dominant role in the stabilization of emulsions with modified α_{s1} -casein rather than the modified surface hydrophobicity. The surface hydrophobicity of α_{s1} -casein only played a role in the adsorption rate of protein on the surface (as described in Section 4.2.4; Kato & Nakai, 1980). The increase in the surface hydrophobicity of dephosphorylated α_{s1} -casein resulted in a faster protein adsorption on the surface of oil droplets. These results are consistent with the fact that dephosphorylation decreased the surface tension of α_{s1} -casein due to the increased surface hydrophobicity, whereas, succinylation increased the surface tension of α_{s1} -casein due to the reduction in the surface hydrophobicity.

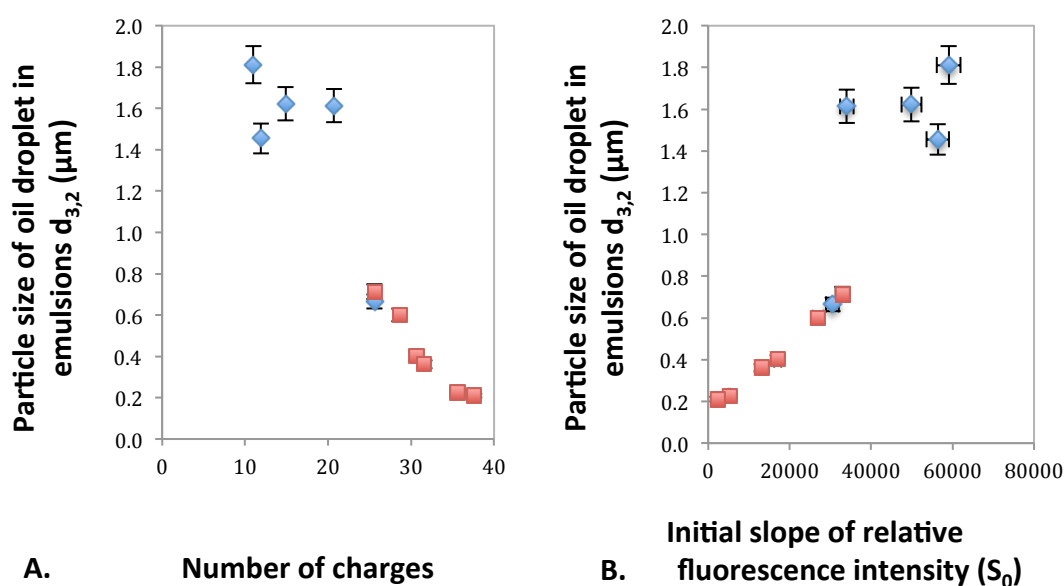


Figure 10.7 The relationship between net charge and particle size $d_{(3,2)}$ of canola oil droplet in emulsions made with α_{s1} -casein (A), and between hydrophobicity and particle size $d_{(3,2)}$ of canola oil droplet in emulsions made with α_{s1} -casein (B): dephosphorylated α_{s1} -casein (◆) and succinylated α_{s1} -casein (■). Error bars represent the standard deviation of the mean of the replicates.

The points at high particle size suggested that a large number of scatter were from unstable emulsions with oil droplets coalescence (Figure 10.7). Therefore, a linear relationship was observed for stable emulsions, the emulsions that were coalesced do not give reliable size measurements (Figure 10.7). The relationship between the emulsion stability and the net charge of α_{s1} -casein suggested a higher level of net charge of adsorbed proteins contributed to a better emulsion stability. Therefore, the emulsifying capacities of α_{s1} -casein can be manipulated by tailoring the net charge of proteins. This has an implication that the stability of dairy food emulsions can be tailored by controlling the level of protein modifications.

10.3 Effect of physicochemical properties of α_{s1} -casein on the foaming properties

The results from dephosphorylated and succinylated α_{s1} -casein indicated that the foam stability of α_{s1} -casein was governed by the combined effect of the net charge

and surface hydrophobicity. This is consistent with previous findings that surface hydrophobicity played an important role in the foaming capacity of whey proteins; however, the net charge was the most influential factor for foam stability (Nakai, 1983). Unlike emulsion stability, the protein foam is stabilized by the thickness of the protein film between the air bubbles (Belitz et al., 2008; Bergeron et al., 1996). The electrostatic repulsion between α_{s1} -casein-coated air bubbles maintained the thickness of the film before the film thinning and drainage due to gravity (Davis et al., 2004; Dickinson, 1999b).

Dephosphorylation of α_{s1} -casein increased the surface tension at an air and water interface. This indicated that dephosphorylation promoted a rapid protein adsorption on the surface, which led to more protein adsorbed on the surface. Therefore, the overall amount of net charge increased on the surface, even though the net charge of a single dephosphorylated α_{s1} -casein molecule was decreased. The foam of dephosphorylated α_{s1} -casein solution was stabilized by the increased electrostatic repulsion. Succinylation of α_{s1} -casein resulted in a slower protein adsorption, but an increase in the net charge of the α_{s1} -casein molecule. The data obtained from the foam stability of succinylated α_{s1} -casein are consistent with a model in which the key parameter controlling foaming is the total amount of charge that was adsorbed on the surface. The optimum balance between hydrophobic force and electrostatic force contributed to the greater foaming stability of α_{s1} -casein (as described in Section 4.2.7 and 6.2.6).

By contrast to succinylation and dephosphorylation, TGA treatment only led to a minor level of increase in the net charge of α_{s1} -casein (as described in Section 7.2.2), and the resulting electrostatic force was not sufficient to influence the foaming stability. The data obtained from TGA-modified α_{s1} -casein suggested that the foam stability of TGA-treated α_{s1} -casein was affected by the molecular weight, which is consistent with previous reports that TGA-catalysed intermolecular cross-linking had a significant impact on protein functionalities (Hiller & Lorenzen, 2009; Jaros et al., 2010). The optimum foam stability was dependent on the balance between the level

of oligomerized α_{s1} -casein and the space between the oligomerized monomers (Salonen et al., 2010).

The correlations between the physicochemical parameters and functionalities of α_{s1} -casein were investigated in this study. A model between the foam stability, net charge and surface hydrophobicity of α_{s1} -casein was established. This proposed model could be potentially used in dairy products, which could help to tailor desirable foam stability for certain dairy products by controlling the level of modification. The understanding and ability to control the functional properties of α_{s1} -casein supports the feasibility of improving the functionality of dairy products by incorporating the modified α_{s1} -casein into the dairy products. For example, the correlation model between emulsion stability and net charge of α_{s1} -casein is applicable in food systems, which could provide a new designed ingredient with enhanced emulsifying properties for dairy products such as protein beverages, yoghurt and cheese. On the other hand, the control of the process variables of dairy products could be informed by controlling the physicochemical and functional properties of dairy proteins. In addition, the findings in this study informed other potential options to optimise the functionalities of dairy products. In a practical dairy product process, the net charge and surface hydrophobicity of proteins can be manipulated by altering the pH, ionic strength and temperature (Badawy et al., 2010; Demetriades et al., 1997; Naidu et al., 1994; Otzen, 2002; Siegel & Firestone, 1988; Westall et al., 1985; Zaslavsky et al., 1982). The size of α_{s1} -casein was found to have a significant effect on the functional properties of proteins (as described in Section 8.2). This can also be modified by controlling the self-association behaviour of α_{s1} -casein via changing ionic strength, protein concentration and temperature (as described in Section 3.2.6; Ho & Waugh, 1965; Schmidt & Van Markwijk, 1968; Schmidt, 1970).

Several methods have been successfully developed to analyse the modified α_{s1} -caseins. In previous studies, a centrifugation method was used to access the water binding capacity by comparing the weight difference of protein sediment, which is lacking in accuracy due to proper separation of the sediment from the supernatant

(Mirmoghtadaie et al., 2009; Morand et al., 2011b). Thus, an NMR method was developed and used for the water binding capacity measurement of α_{s1} -caseins.

10.4 Recommendations

This study showed the effect of charge on the emulsion stability of α_{s1} -casein based on an estimated monolayer structure of adsorbed protein. The structure of native and modified α_{s1} -casein that adsorbed on a surface was proposed (Chapter 9). Thus, further research is necessary to investigate whether succinylation and/or dephosphorylation has an impact on the structure of adsorbed α_{s1} -casein on the surface. Neutron scattering could be a powerful technique to determine the structure of adsorbed α_{s1} -caseins on the surface. In these experiments, the lysine residues of α_{s1} -casein can be modified by reacting with deuterated succinic acid before and/or after coating on latex particles. This neutron scattering measurement could provide information on how the extent of lysine modification influences the interfacial orientation for the adsorbed α_{s1} -caseins.

In order to clarify the effect of surface rheological properties on the foam stability of α_{s1} -casein, viscoelasticity of modified α_{s1} -casein solutions should be examined. In addition, the proposed foam stability model of proteins was based on a single air bubble system. It will be useful to design and carry out an experiment that can monitor the bubble rupture between two air bubbles.

The sedimentation velocity experiment was performed on an AUC instrument to determine the self-association behaviour of modified α_{s1} -caseins. The difference in the self-association behaviour between native and modified α_{s1} -caseins was successfully identified with the sedimentation velocity experiment. A sedimentation equilibrium experiment could also be applied in any further study of milk protein self-association, which will provide detailed information on the particle size of the self-associated species (Van Holde, 1975).

Protein deamidation was obtained by incubating native α_{s1} -casein with TGA, but TGA modification also catalysed the cross-linking reaction (Chapter 7 and 8). Incubating succinylated α_{s1} -casein with TGA can block the lysine residues from cross-linking and control deamidation. However, this combined modification approach was not able to identify the effect of deamidation on α_{s1} -casein because succinylation had a significant effect on physicochemical properties of α_{s1} -casein. Therefore, it would be worthwhile to verify the effect of deamidation on the physicochemical and functional properties of α_{s1} -casein by modifying α_{s1} -casein with an available protein glutaminase.

This study focused on a low protein concentration system and investigated substantial modifications in both physicochemical and functional properties. However, the concentrations used in this study are not applicable to current formulations for dairy products. Thus, further studies should be expanded to model food systems, such as cream, yoghurts, cheese and beverages. The findings in this study suggested that an enhanced foaming property, water binding capacity and emulsion stability could be manipulated by controlling the level of modifications. Therefore, the stability and temperature sensitivity of creams could be potentially improved by incorporating modified proteins. The enhanced water binding capacity of modified proteins could optimize the texture of yoghurts by minimizing serum separation. Moreover, using an enhanced dairy protein emulsifier could promote a long shelf-life stability of protein beverages.

References

- Abercrombie-Thomas, P. L., Butrow, A. B., & Buchanan, J. H. (2010). Selected physical properties of 2-chloroethyl-3-chloropropyl sulfide (CECPRS). In: DTIC Document.
- Aeschlimann, D., Paulsson, M., & Mann, K. (1992). Identification of Gln726 in nidogen as the amine acceptor in transglutaminase-catalyzed cross-linking of laminin-nidogen complexes. *Journal of Biological Chemistry*, 267, 11316-11321.
- Aguilera, J. M., & Lillford, P. J. (2008). Structuring dairy products by means of processing and matrix design. In *Food Materials Science: Principles and Practice* (pp. 439-466). New York: Springer.
- Alberts, B., Johnson, A., Lewis, J., Raff, M., Roberts, K., & Walter, P. (2007). Manipulating proteins, DNA, and RNA. In *Molecular Biology of The Cell* (pp. 251-252). New York: Garland Science.
- Alizadeh-Pasdar, N., & Li-Chan, E. C. Y. (2000). Comparison of protein surface hydrophobicity measured at various pH values using three different fluorescent probes. *Journal of Agricultural and Food Chemistry*, 48, 328-334.
- Allen, R. C., Saravis, C. A., & Maurer, H. R. (1984). *Gel Electrophoresis and Isoelectric Focusing of Proteins*. Berlin: de Gruyter
- Anderson, L., & Kelley, J. J. (1959). The dephosphorylation of casein by alkali. *Journal of the American Chemical Society*, 81, 2275-2276.
- Andrews, A. T. (1990). Minographs on physical biochemistry. In A. R. Peacocke & W. F. Harrington (Eds.), *Electrophoresis - Theory, Techniques, and Biochemical and Clinical Applications*. Oxford: Oxford University Press.
- Anema, S. G., & Klostermeyer, H. (1996). ζ -Potentials of casein micelles from reconstituted skim milk heated at 120 °C. *International Dairy Journal*, 6, 673-687.
- Anema, S. G. (1997). The effect of chymosin on κ -casein-coated polystyrene latex particles and bovine casein micelles. *International Dairy Journal*, 7, 553-558.
- Anema, S. G., & Klostermeyer, H. (1997). Heat-induced, pH-dependent dissociation of casein micelles on heating reconstituted skim milk at temperatures below 100 °C. *Journal of Agricultural and Food Chemistry*, 45, 1108-1115.
- Anema, S. G., & Li, Y. (2003). Effect of pH on the association of denatured whey proteins with casein micelles in heated reconstituted skim milk. *Journal of Agricultural and Food Chemistry*, 51, 1640-1646.

Anema, S. G., & de Kruif, C. G. (2012). Lactoferrin binding to transglutaminase cross-linked casein micelles. *International Dairy Journal*, 26, 83-87.

Arnold, M. A., & Meyerhoff, M. E. (1984). Ion-selective electrodes. *Analytical chemistry*, 56, 20-48.

Ashok, P., Colin, W., Carlos, R. S., & Christian, L. (2008). *Enzyme Technology*. New York: Springer.

Badawy, A. M. E., Luxton, T. P., Silva, R. G., Scheckel, K. G., Suidan, M. T., & Tolaymat, T. M. (2010). Impact of environmental conditions (pH, ionic strength, and electrolyte type) on the surface charge and aggregation of silver nanoparticles suspensions. *Environmental Science & Technology*, 44, 1260-1266.

Bartolomeo, M. P., & Maisano, F. (2006). Validation of a reversed-phase HPLC method for quantitative amino acid analysis. *Journal of Biomolecular Techniques*, 17, 131-133.

Batra, P. P., Roebuck, M. A., & Uetrecht, D. (1990). Effect of lysine modification on the secondary structure of ovalbumin. *Journal of Protein Chemistry*, 9, 37-44.

Behrend, O., Ax, K., & Schubert, H. (2000). Influence of continuous phase viscosity on emulsification by ultrasound. *Ultrasonics Sonochemistry*, 7, 77-85.

Belitz, H. D., Grosch, W., & Schieberle, P. (2008). Amino acids peptides proteins. In *Food Chemistry* (pp. 62-63). New York: Springer.

Benjamins, J., De Feijter, J. A., Evans, M. T. A., Graham, D. E., & Phillips, M. C. (1975). Dynamic and static properties of proteins adsorbed at the air/water interface. *Faraday Discussion of the Chemical Society*, 59, 218-229.

Bergeron, V., Walthermo, Å., & Claesson, P. M. (1996). Disjoining pressure measurements for foam films stabilized by a nonionic sugar-based surfactant. *Langmuir*, 12, 1336-1342.

Berlin, E., Kliman, P. G., Anderson, B. A., & Pallansch, M. J. (1973). Water binding in whey protein concentrates. *Journal of Dairy Science*, 56, 984-987.

Berova, N., Nakanishi, K., & Woody, R. (2000). *Circular Dichroism: Principles and Applications*. New York: John Wiley & Sons.

Berry, S. D., Sheehy, P. A., Williamson, P., & Sharp, J. A. (2014). Significance, origin and function of bovine milk proteins: The biological implications of manipulation or modification. In M. Boland, H. Singh & A. Thompson (Eds.), *Milk Proteins* (pp. 113-140). London: Academic Press.

- Bertrand-Harb, C., Nicolas, M. G., Dalgalarrrondo, M., & Chobert, J. M. (1993). Determination of alkylation degree by three colorimetric methods and amino acid analysis. A comparative study. *Sciences des Aliments*, 13, 577-584.
- Beverung, C. J., Radke, C. J., & Blanch, H. W. (1999). Protein adsorption at the oil/water interface: characterization of adsorption kinetics by dynamic interfacial tension measurements. *Biophysical Chemistry*, 81, 59-80.
- Bingham, E. W., Farrell, H. M., & Carroll, R. J. (1971). Dephosphorylation of α_{s1} -casein - effects on solubility and casein micelle formation. *Abstracts of Papers of the American Chemical Society*, 23, 237-238.
- Binks, B. P., Cho, W. G., Fletcher, P. D. I., & Petsev, D. N. (2000). Stability of oil-in-water emulsions in a low interfacial tension system. *Langmuir*, 16, 1025-1034.
- Blanchette, F., Messio, L., & Bush, J. W. M. (2009). The influence of surface tension gradients on drop coalescence. *Physics of Fluids*, 21, 72-107.
- Boenisch, M. P., Heidebach, T. C., & Kulozik, U. (2008). Influence of transglutaminase protein cross-linking on the rennet coagulation of casein. *Food Hydrocolloids*, 22, 288-297.
- Bonfatti, V., Grigoletto, L., Cecchinato, A., Gallo, L., & Carnier, P. (2009). Erratum to Validation of a new reversed-phase high-performance liquid chromatography method for separation and quantification of bovine milk protein genetic variants [J. Chromatogr. A 1195 (2008) 101-106]. *Journal of Chromatography*, 1216.
- Bonisch, M. P., Lauber, S., & Kulozik, U. (2004). Effect of ultra-high temperature treatment on the enzymatic cross-linking of micellar casein and sodium caseinate by transglutaminase. *Journal of Food Science*, 69, 398-404.
- Bönisch, M. P., Huss, M., Weitzl, K., & Kulozik, U. (2007). Transglutaminase cross-linking of milk proteins and impact on yoghurt gel properties. *International Dairy Journal*, 17, 1360-1371.
- Boström, M., Williams, D. R. M., & Ninham, B. W. (2001). Surface tension of electrolytes: specific ion effects explained by dispersion forces. *Langmuir*, 17, 4475-4478.
- Brew, K. (2003). α -Lactalbumin. In P. F. Fox & P. L. H. McSweeney (Eds.), *Advanced Dairy Chemistry - Proteins*. New York: Kluwer academic/plenum publishers.
- Brownlow, S., Cabral, J. H. M., Cooper, R., Flower, D. R., Yewdall, S. J., Polikarpov, I., North, A. C. T., & Sawyer, L. (1997). Bovine β -lactoglobulin at 1.8 angstrom resolution - Still an enigmatic lipocalin. *Structure*, 5, 481-495.

Bryant, C. M., & McClements, D. J. (1998). Molecular basis of protein functionality with special consideration of cold-set gels derived from heat-denatured whey. *Trends in Food Science & Technology*, 9, 143-151.

Buzzell, J. G., & Tanford, C. (1956). The effect of charge and ionic strength on the viscosity of ribonuclease. *Journal of Physical Chemistry*, 60, 1204-1207.

Bylund, G. (1995). *Dairy Processing Handbook*. Lund: Tetra Pak Processing Systems AB.

Caessens, P. W. J. R., De Jongh, H. H. J., Norde, W., & Gruppen, H. (1999). The adsorption-induced secondary structure of β -casein and of distinct parts of its sequence in relation to foam and emulsion properties. *Biochimica et Biophysica Acta - Protein Structure and Molecular Enzymology*, 1430, 73-83.

Campbell, N. F., Shih, F. F., & Marshall, W. E. (1992). Enzymatic phosphorylation of soy protein isolate for improved functional-properties. *Journal of Agricultural and Food Chemistry*, 40, 403-406.

Carneiro-da-Cunha, M. G., Cerqueira, M. A., Souza, B. W. S., Teixeira, J. A., & Vicente, A. A. (2011). Influence of concentration, ionic strength and pH on zeta potential and mean hydrodynamic diameter of edible polysaccharide solutions envisaged for multilayered films production. *Carbohydrate Polymers*, 85, 522-528.

Cayot, P., & Lorient, D. (1998). *Structure and Technical Properties of Milk Proteins*. Paris: Technique et Documentation Lavoisier.

Chalikian, T. V. (2001). Structural thermodynamics of hydration. *The Journal of Physical Chemistry B*, 105, 12566-12578.

Chandler, D. (2005). Interfaces and the driving force of hydrophobic assembly. *Nature*, 437, 640-647.

Christensen, B. M., Sørensen, E. S., Højrup, P., Petersen, T. E., & Rasmussen, L. K. (1996). Localization of potential transglutaminase cross-linking sites in bovine caseins. *Journal of Agricultural and Food Chemistry*, 44, 1943-1947.

Chu, B. (2008). Dynamic light scattering. In *Soft Matter Characterization* (pp. 335-372). New York: Springer.

Church, F. C., Swaisgood, H. E., Porter, D. H., & Catignani, G. L. (1983). Spectrophotometric assay using ortho-phthaldialdehyde for determination of proteolysis in milk and isolated milk proteins. *Journal of Dairy Science*, 66, 1219-1227.

Clark, D. C., Smith, L. J., & Chaplin, L. C. (1992). The effect of dephosphorylation on the conformation of peptides from β -casein. *Collection of Czechoslovak Chemical Communications*, 57, 425-428.

Coburn, S. P., Mahuren, J. D., Jain, M., Zubovic, Y., & Wortsman, J. (1998). Alkaline Phosphatase (EC 3.1. 3.1) in Serum Is Inhibited by Physiological Concentrations of Inorganic Phosphate 1. *The Journal of Clinical Endocrinology & Metabolism*, 83, 3951-3957.

Coday, B. D., Luxbacher, T., Childress, A. E., Almaraz, N., Xu, P., & Cath, T. Y. (2015). Indirect determination of zeta potential at high ionic strength: Specific application to semipermeable polymeric membranes. *Journal of Membrane Science*, 478, 58-64.

Cohen, P. (2002). The origins of protein phosphorylation. *Nature Cell Biology*, 4, 127-130.

Connors, K. A. (1986). *Chemical Stability of Pharmaceuticals: A Handbook for Pharmacists*. New York: John Wiley & Sons.

Coussons, P. J., Price, N. C., Kelly, S. M., Smith, B., & Sawyer, L. (1992). Factors that govern the specificity of transglutaminase-catalysed modification of proteins and peptides. *Biochemical Journal*, 282, 929-930.

Craggs, A., Moody, G. J., & Thomas, J. D. R. (1974). PVC matrix membrane ion-selective electrodes. Construction and laboratory experiments. *Journal of Chemical Education*, 51, 541.

Craig, R., & Beavis, R. C. (2003). A method for reducing the time required to match protein sequences with tandem mass spectra. *Rapid Communication in Mass Spectrometry*, 17, 2310-2316.

Crowley, P., O'Brien, C., Slattery, H., Chapman, D., Arendt, E., & Stanton, C. (2002). Functional properties of casein hydrolysates in bakery applications. *European Food Research and Technology*, 215, 131-137.

Czernicka, M., Domagala, J., Sady, M., & Wieteska, I. (2009). Functional properties of milk proteins modified by transglutaminase depending on incubation conditions with the enzyme. *Biotechnology in Animal Husbandry*, 25, 737-743.

Dagorn-Scaviner, C., Gueguen, J., & Lefebvre, J. (1987). Emulsifying properties of pea globulins as related to their adsorption behaviors. *Journal of Food Science*, 52, 335-341.

Dalgleish, D. G. (1990). The conformations of proteins on solid/water interfaces — caseins and phosvitin on polystyrene latices. *Colloids and Surfaces*, 46, 141-155.

Dalgleish, D. G., & Leaver, J. (1991a). The possible conformations of milk proteins adsorbed on oilwater interfaces. *Journal of Colloid and Interface Science*, 141, 288-294.

Dalgleish, D. G., & Leaver, J. (1991b). Dimensions and possible structures of milk. *Food Polymers, Gels and Colloids*, 82, 113-115.

Dalgleish, D. G. (1993). The sizes and conformations of the proteins in adsorbed layers of individual caseins on latices and in oil-in-water emulsions. *Colloids and Surfaces B: Biointerfaces*, 1, 1-8.

Dalgleish, D. G. (1996). Conformations and structures of milk proteins adsorbed to oil-water interfaces. *Food Research International*, 29, 541-547.

Dalgleish, D. G., van Mourik, L., & Corredig, M. (1997). Heat-induced interactions of whey proteins and casein micelles with different concentrations of α -lactalbumin and β -lactoglobulin. *Journal of Agricultural and Food Chemistry*, 45, 4806-4813.

Dalgleish, D. G. (2011). On the structural models of bovine casein micelles-review and possible improvements. *Soft Matter*, 7, 2265-2272.

Dalgleish, D. G., & Corredig, M. (2012). The structure of the casein micelle of milk and its changes during processing. *Annual Review of Food Science and Technology*, 3, 449-467.

Damodaran, S. (1997). Protein-stabilized foams and emulsions. In S. Damodaran, & A. Paraf, (Ed.), *Food Proteins and Their Applications* (pp. 57-110). New York: Dekker.

Darewicz, M., Dziuba, J., Mioduszevska, H., & Minkiewicz, P. (1999). Modulation of physicochemical properties of bovine β -casein by nonenzymatic glycation associated with enzymatic dephosphorylation. *Acta Alimentaria*, 28, 339-354.

Darewicz, M., Dziuba, J., Caessens, P., & Gruppen, H. (2000). Dephosphorylation-induced structural changes in β -casein and its amphiphilic fragment in relation to emulsion properties. *Biochimie*, 82, 191-195.

Davies, J. S. (2000). *Amino Acids, Peptides and Proteins* (Vol. 31). Cambridge: Royal society of chemistry.

Davis, J. P., Foegeding, E. A., & Hansen, F. K. (2004). Electrostatic effects on the yield stress of whey protein isolate foams. *Colloids and Surfaces B: Biointerfaces*, 34, 13-23.

De Carvalho, R. A., & Grosso, C. R. F. (2004). Characterization of gelatin based films modified with transglutaminase, glyoxal and formaldehyde. *Food Hydrocolloids*, 18, 717-726.

De Jong, G. A. H., & Koppelman, S. J. (2002). Transglutaminase catalyzed reactions: impact on food applications. *Journal of Food Science*, 67, 2798-2806.

de Jongh, H. H. J., & Broersen, K. (2012). Application potential of food protein modification. In Z. Nawaz & S. naved (Eds.), *Advances in Chemical Engineering*. Croatia: InTech Publisher.

De Kruif, C., & Grinberg, V. Y. (2002). Micellisation of β -casein. *Colloids and Surfaces A: Physicochemical and Engineering Aspects*, 210, 183-190.

De Kruif, C. G., Huppertz, T., Urban, V. S., & Petukhov, A. V. (2012). Casein micelles and their internal structure. *Advances in Colloid and Interface Science*.

De Kruif, C. G. H., C. . (2003). Casein micelle structure, functions and interactions. . In P. F. Fox & P. L. H. McSweeney (Eds.), *Advanced Dairy Chemistry-Proteins* (Vol. 1, pp. 223). New York: Kluwer academic/plenum publishers.

Defay, R., Bellemans, A., Prigogine, I. (1996). *Surface Tension and Adsorption*. London: Longmans.

DeJong, G., & Koppelman, S. (2006). Transglutaminase catalyzed reactions: impact on food applications. *Journal of Food Science*, 67, 2798-2806.

Demetriades, K., Coupland, J. N., & McClements, D. J. (1997). Physicochemical properties of whey protein - stabilized emulsions as affected by heating and ionic strength. *Journal of Food Science*, 62, 462-467.

Dewettinck, K., Rombaut, R., Thienpont, N., Le, T. T., Messens, K., & Van Camp, J. (2008). Nutritional and technological aspects of milk fat globule membrane material. *International Dairy Journal*, 18, 436-457.

Dickinson, E., & Izgi, E. (1996). Foam stabilization by protein-polysaccharide complexes. *Colloids and Surfaces A: Physicochemical and Engineering Aspects*, 113, 191-201.

Dickinson, E., & McClements, D. J. (1996). *Advances in Food Colloids*. New York: Springer.

Dickinson, E., Horne, D. S., Pinfield, V., & Leermakers, F. A. M. (1997a). Self-consistent-field modelling of casein adsorption. Comparison of results for α_{s1} -casein and β -casein. *Journal of the Chemical Society, Faraday Transactions*, 93, 425-432.

Dickinson, E., Pinfield, V. J., Horne, D. S., & Leermakers, F. A. M. (1997b). Self-consistent-field modelling of adsorbed casein interaction between two protein-coated surfaces. *Journal of the Chemical Society, Faraday Transactions*, 93, 1785-1790.

- Dickinson, E. (1999a). Caseins in emulsions: interfacial properties and interactions. *International Dairy Journal*, 9, 305-312.
- Dickinson, E. (1999b). Adsorbed protein layers at fluid interfaces: interactions, structure and surface rheology. *Colloids and Surfaces B: Biointerfaces*, 15, 161-176.
- Dickinson, E., Ritzoulis, C., Yamamoto, Y., & Logan, H. (1999). Ostwald ripening of protein-stabilized emulsions: effect of transglutaminase crosslinking. *Colloids and Surfaces B: Biointerfaces*, 12, 139-146.
- Dickinson, E. (2009). Hydrocolloids as emulsifiers and emulsion stabilizers. *Food Hydrocolloids*, 23, 1473-1482.
- Dukhin, A. S., & Parlia, S. (2014). Measuring zeta potential of protein nano-particles using electroacoustics. *Colloids and Surfaces B: Biointerfaces*, 121, 257-263.
- Edwards, P., Creamer, L. K., & Jameson, G. B. (2009). Structure and Stability of Whey Proteins. . In M. Boland, H. Singh & A. Thompson (Eds.), *Milk Proteins* (pp. 163-204). London: Elsevier Inc.
- Eissa, A. S., & Khan, S. A. (2005). Acid-induced gelation of enzymatically modified, preheated whey proteins. *Journal of Agricultural and Food Chemistry*, 53, 5010-5017.
- Elofsson, U. (1996). *Protein Adsorption in Relation to Bulk Phase Properties*. Lund: Food Technology, Lund University.
- Elsasser, T. H., Capuco, A. V., Caperna, T. J., Martinez, A., Cuttitta, F., & Kahl, S. (2007). Adrenomedullin (AM) and adrenomedullin binding protein (AM-BP) in the bovine mammary gland and milk: Effects of stage of lactation and experimental intramammary E. coli infection. *Domest Anim Endocrinol*, 32, 138-154.
- Fabiani, A., Versari, A., Parpinello, G. P., Castellari, M., & Galassi, S. (2002). High-performance liquid chromatographic analysis of free amino acids in fruit juices using derivatization with 9-fluorenylmethyl-chloroformate. *Journal of Chromatographic Science*, 40, 14-18.
- Fabri, D., Williams, M. A. K., & Halstead, T. K. (2005). Water T2 relaxation in sugar solutions. *Carbohydrate Research*, 340, 889-905.
- Faergemand, M., Otte, J., & Qvist, K. B. (1997). Enzymatic cross-linking of whey proteins by a Ca²⁺-independent microbial transglutaminase from *Streptomyces lydicus*. *Food Hydrocolloids*, 11, 19-25.
- Faergemand, M., Otte, J., & Qvist, K. B. (1998). Emulsifying properties of milk proteins cross-linked with microbial transglutaminase. *International Dairy Journal*, 8, 715-723.

Færgemand, M., Murray, B. S., & Dickinson, E. (1997). Cross-linking of milk proteins with transglutaminase at the oil-water interface. *Journal of Agricultural and Food Chemistry*, 45, 2514-2519.

Færgemand, M., Otte, J., & Qvist, K. B. (1998). Emulsifying properties of milk proteins cross-linked with microbial transglutaminase. *International Dairy Journal*, 8, 715-723.

Farrell Jr, H., Jimenez-Flores, R., Bleck, G., Brown, E., Butler, J., Creamer, L., Hicks, C., Hollar, C., Ng-Kwai-Hang, K., & Swaisgood, H. (2004). Nomenclature of the proteins of cows' milk—sixth revision. *Journal of Dairy Science*, 87, 1641-1674.

Farrell Jr, H. M., Wickham, E. D., Unruh, J. J., Qi, P. X., & Hoagland, P. D. (2001). Secondary structural studies of bovine caseins: temperature dependence of β -casein structure as analyzed by circular dichroism and FTIR spectroscopy and correlation with micellization. *Food Hydrocolloids*, 15, 341-354.

Farrell Jr, H. M., Qi, P. X., Wickham, E. D., & Unruh, J. J. (2002). Secondary structural studies of bovine caseins: Structure and temperature dependence of β -casein phosphopeptide (1-25) as analyzed by circular dichroism, FTIR spectroscopy, and analytical ultracentrifugation. *Journal of Protein Chemistry*, 21, 307-321.

Fayle, S. E. (1998). *Protein crosslinking*. PhD thesis. Department of Plant and Microbial Sciences, University of Canterbury, Christchurch.

Fayle, S. E., Gerrard, J. A., Simmons, L., Meade, S. J., Reid, E. A., & Johnston, A. C. (2000). Crosslinkage of proteins by dehydroascorbic acid and its degradation products. *Food Chemistry*, 70, 193-198.

Fennema, O. R. (1996). Water and ice. In O. R. Fennema (Ed.), *Food Chemistry* (3rd ed., pp. 17-94). New York: Marcel Dekker.

Fernley, H. N., & Walker, P. G. (1967). Studies on alkaline phosphatase. Inhibition by phosphate derivatives and the substrate specificity. *Biochemical Journal*, 104, 1011-1018.

Foegeding, E. A., Luck, P. J., & Davis, J. P. (2006). Factors determining the physical properties of protein foams. *Food Hydrocolloids*, 20, 284-292.

Formaggioni, P., Summer, A., Malacarne, M., & Mariani, P. (1999). Milk protein polymorphism: Detection and diffusion of the genetic variants in Bos genus. *Annals of Tropical Medicine and Hygiene*, 19, 127-165.

Förster, S., Schmidt, M., & Antonietti, M. (1990). Static and dynamic light scattering by aqueous polyelectrolyte solutions: effect of molecular weight, charge density and added salt. *Polymer*, 31, 781-792.

Fox, P. F. (2003). Milk proteins: general and historical aspects. In P. F. Fox & P. L. H. McSweeney (Eds.), *Advanced Dairy Chemistry-Proteins* (Vol. 1). New York: Kluwer academic/plenum publishers.

Fox, P. F. (2009). Milk: an overview. In A. Thompson, M. Boland & H. Singh (Eds.), *Milk Proteins* (pp. 1-54). Boston: Academic Press.

Fox, P. F. E. (1982). *Developments in Dairy Chemistry*. London: Elsevier applied science publishers Ltd.

Fox, P. F. E. (1989). *Developments in Dairy Chemistry*. London: Elsevier applied science publishers Ltd.

Franzen, K. L., & Kinsella, J. E. (1976). Functional properties of succinylated and acetylated soy protein. *Journal of Agricultural and Food Chemistry*, 24, 788-795.

Freeman, R. (1997). *Spin Choreography: Basic Steps in High Resolution NMR*. Oxford: Spektrum Oxford.

Galisteo, F., de las Nieves López, F. J., Cabrerizo, M., & Hidalgo-Alvarez, R. (1990). Effects of particle concentration, ionic strength, pH and temperature on the microelectrophoretic mobility of cationic polystyrene latex. I. In *Surfactants and Macromolecules: Self-Assembly at Interfaces and in Bulk* (pp. 313-320). New York: Springer.

Ganai, N. A., Bovenhuis, H., van Arendonk, J. A. M., & Visker, M. (2009). Novel polymorphisms in the bovine β -lactoglobulin gene and their effects on β -lactoglobulin protein concentration in milk. *Animal Genetics*, 40, 127-133.

Gaspar, A. L. C., & de Góes-Favoni, S. P. (2015). Action of microbial transglutaminase in the modification of food proteins: A review. *Food Chemistry*, 171, 315-322.

Gerrard, J., Fayle, S., Brown, P., Sutton, K., Simmons, L., & Rasiah, I. (2001). Effects of microbial transglutaminase on the wheat proteins of bread and croissant dough. *Journal of Food Science*, 66, 782-786.

Gerrard, J., & Sutton, K. (2005). Addition of transglutaminase to cereal products may generate the epitope responsible for coeliac disease. *Trends in Food Science & Technology*, 16, 510-512.

Gerrard, J. A. (2002). Protein-protein crosslinking in food: methods, consequences, applications. *Trends in Food Science & Technology*, 13, 391-399.

Gharst, G., Clare, D. A., Davis, J. P., & Sanders, T. H. (2007). The effect of transglutaminase crosslinking on the rheological characteristics of heated peanut flour dispersions. *Journal of Food Science*, 72, 369-375.

Goldburg, W. I. (1999). Dynamic light scattering. *American Journal of Physics*, 67, 1152-1160.

Gonzalez-Tello, P., Camacho, F., Guadix, E. M., Luzong, G., & Gonzalez, P. A. (2009). Density, viscosity and surface tension of whey protein concentrate solutions. *Journal of Food Process Engineering*, 32, 235–247.

Graham, D. E., & Phillips, M. C. (1976). The conformation of proteins at interfaces and their role in stabilizing emulsions. In A. L. Smith (Ed.), *Theory and Practice of Emulsion Technology* (pp. 75-93). London: Academic Press.

Graham, D. E., & Phillips, M. C. (1979). Proteins at liquid interfaces: I. Kinetics of adsorption and surface denaturation. *Journal of Colloid and Interface Science*, 70, 403-414.

Graham, E. R. B., Malcolm, G. N., & McKenzie, H. A. (1984). On the isolation and conformation of bovine β -casein A 1. *International Journal of Biological Macromolecules*, 6, 155-161.

Gutz, I. G. R. (2012). CurTiPot–pH and acid-base titration curves: Analysis and simulation software, Version 3.6. 1. In.

Hamada, J. S., & Swanson, B. (1994a). Deamidation of food proteins to improve functionality. *Critical Reviews in Food Science & Nutrition*, 34, 283-292.

Hamada, J. S., & Swanson, P. B. (1994b). Deamidation of food proteins to improve functionality. *Critical Reviews in Food Science & Nutrition*, 34, 283-292.

Han, X., & Spradlin, J. (2000). Process for making cheese using transglutaminase and a non-rennet protease. *Patent Number US Patent: 6093424*.

Havea, P., Singh, H., Creamer, L. K., & Campanella, O. H. (1998). Electrophoretic characterization of the protein products formed during heat treatment of whey protein concentrate solutions. *Journal of Dairy Research*, 65, 79-91.

Heck, J. M. L., Schennink, A., van Valenberg, H. J. F., Bovenhuis, H., Visker, M., van Arendonk, J. A. M., & van Hooijdonk, A. C. M. (2009). Effects of milk protein variants on the protein composition of bovine milk. *Journal of Dairy Science*, 92, 1192-1202.

Hettiarachchy, N., Kalapathy, U., & Myers, D. (1995). Alkali-modified soy protein with improved adhesive and hydrophobic properties. *Journal of the American Oil Chemists' Society*, 72, 1461-1464.

Hill, S. E. (1996). Emulsions. In G. M. Hall (Ed.), *Methods of Testing Protein Functionalities*. London: Chapman and Hall.

- Hiller, B., & Lorenzen, P. C. (2009). Functional properties of milk proteins as affected by enzymatic oligomerisation. *Food Research International*, 42, 899-908.
- Hinz, K., Huppertz, T., Kulozik, U., & Kelly, A. (2007). Influence of enzymatic cross-linking on milk fat globules and emulsifying properties of milk proteins. *International Dairy Journal*, 17, 289-293.
- Ho, C., & Waugh, D. F. (1965). Interactions of bovine α_s -casein with small ions. *Journal of the American Chemical Society*, 87, 110-117.
- Hoagland, P. D., Unruh, J. J., Wickham, E. D., & Farrell Jr, H. M. (2001). Secondary structure of bovine α_{s2} -casein: Theoretical and experimental approaches. *Journal of Dairy Science*, 84, 1944-1949.
- Hoffman, R., & Ozery, Y. (2013). Hydrogen Properties NMR. *The Institute of Chemistry Hebrew University of Jerusalem*. .
- Holde, K. E. V. (1989). The protein of chromatin. In *Chromatin* (pp. 69-168). New York: Springer.
- Holland, J. W., Deeth, H. C., & Alewood, P. F. (2008). Analysis of disulphide linkages in bovine κ -casein oligomers using two-dimensional electrophoresis. *Electrophoresis*, 29, 2402-2410.
- Holland, P. T., Cargill, A., Selwood, A. I., Arnold, K., Krammer, J. L., & Pearce, K. N. (2011). Determination of soluble immunoglobulin g in bovine colostrum products by protein g affinity chromatography–turbidity correction and method validation. *Journal of Agricultural and Food Chemistry*, 59, 5248-5256.
- Holsinger, V. H. (1997). Physical and chemical properties of lactose. In P. F. Fox (Ed.), *Advanced Dairy Chemistry- Lactose, Water, Salts and Vitamins* (Vol. 3, pp. 1-31). London: Chapman & Hall.
- Holt, C. (1985). The milk salt: their secretion, concentrations and physical chemistry. In P. F. Fox (Ed.), *Lactose and Minor Constituents* (Vol. 3, pp. 143). London: Elsevier Applied Science.
- Holt, C. (1992). Structure and stability of bovine casein micelles. *Advances in Protein Chemistry*, 43, 63-151.
- Holt, C., & Horne, D. (1996). The hairy casein micelle: evolution of the concept and its implications for dairy technology. *Nederlands melk en Zuiveltijdschrift*, 50, 85-111.
- Horne, D. S., & Leaver, J. (1995). Milk proteins on surfaces. *Food Hydrocolloids*, 9, 91-95.

Horne, D. S. (1998). Casein interactions: casting light on the black boxes, the structure in dairy products. *International Dairy Journal*, 8, 171-177.

Horne, D. S. (2002). Casein structure, self-assembly and gelation. *Current Opinion in Colloid and Interface Science*, 7, 456-461.

Horne, D. S. (2006). Casein micelle structure: models and muddles. *Current Opinion in Colloid and Interface Science*, 11, 148-153.

Horne, D. S. (2009). Casein micelles structure and stability. In A. Thompson, M. Boland & H. Singh (Eds.), *Milk Proteins*. London: Elsevier Inc.

Hsu, B.-M., & Huang, C. (2002). Influence of ionic strength and pH on hydrophobicity and zeta potential of Giardia and Cryptosporidium. *Colloids and Surfaces A: Physicochemical and Engineering Aspects*, 201, 201-206.

Huppertz, T., Fox, P. F., de Kruif, K. G., & Kelly, A. L. (2006). High pressure-induced changes in bovine milk proteins: A review. *Biochimica Et Biophysica Acta-Proteins and Proteomics*, 1764, 593-598.

Huppertz, T., & de Kruif, C. G. (2007a). Ethanol stability of casein micelles cross-linked with transglutaminase. *International Dairy Journal*, 17, 436-441.

Huppertz, T., & de Kruif, C. G. (2007b). Rennet-induced coagulation of enzymatically cross-linked casein micelles. *International Dairy Journal*, 17, 442-447.

Huppertz, T., & G de Kruif, C. (2007). Rennet-induced coagulation of enzymatically cross-linked casein micelles. *International Dairy Journal*, 17, 442-447.

Huppertz, T., Smiddy, M. A., & de Kruif, C. G. (2007). Biocompatible micro-gel particles from cross-linked casein micelles. *Biomacromolecules*, 8, 1300-1305.

Huppertz, T., & de Kruif, C. G. (2008). Structure and stability of nanogel particles prepared by internal cross-linking of casein micelles. *International Dairy Journal*, 18, 556-565.

Huppertz, T. (2010). Foaming properties of milk: a review of the influence of composition and processing. *International Journal of Dairy Technology*, 63, 477-488.

Huppertz, T. (2014). Heat stability of transglutaminase-treated milk. *International Dairy Journal*, 38, 183-186.

Hwang, D. (2004). Transglutaminase cross-linked soy protein composition, fish and meat products and analogues thereof. *Patent Number EU Patent: 1459635*.

Ikura, K., Goto, M., Yoshikawa, M., Sasaki, R., & Chiba, H. (1984). Use of transglutaminase: reversible blocking of amino groups in substrate protein for a high yield of specific products. *Agricultural and Biological Chemistry*, 48, 2347-2354.

Ikura, K., Sasaki, R., & Motoki, M. (1992). Use of transglutaminase in quality-improvement and processing of food proteins. *Journal of Agricultural and Food Chemistry*, 2, 389-407.

Iqbal, J. (2011). An enzyme immobilized microassay in capillary electrophoresis for characterization and inhibition studies of alkaline phosphatases. *Analytical biochemistry*, 414, 226-231.

Jaros, D., Partschefeld, C., Henle, T., & Rohm, H. (2006). Transglutaminase in dairy products: chemistry, physics, applications. *Journal of Texture Studies*, 37, 113-155.

Jaros, D., Jacob, M., Otto, C., & Rohm, H. (2010). Excessive cross-linking of caseins by microbial transglutaminase and its impact on physical properties of acidified milk gels. *International Dairy Journal*, 20, 321-327.

Jaros, D., Schwarzenbolz, U., Raak, N., Löbner, J., Henle, T., & Rohm, H. (2014). Cross-linking with microbial transglutaminase: Relationship between polymerisation degree and stiffness of acid casein gels. *International Dairy Journal*, 38, 174-178.

Jedrzejewski, P. T., Girod, A., Tholey, A., König, N., Thullner, S., Kinzel, V., & Bossemeyer, D. (1998). A conserved deamidation site at Asn 2 in the catalytic subunit of mammalian cAMP-dependent protein kinase detected by capillary LC-MS and tandem mass spectrometry. *Protein Science*, 7, 457.

Jensen, H. B., Holland, J. W., Poulsen, N. A., & Larsen, L. B. (2012a). Milk protein genetic variants and isoforms identified in bovine milk representing extremes in coagulation properties. *Journal of Dairy Science*, 95, 2891-2903.

Jensen, H. B., Poulsen, N. A., Andersen, K. K., Hammershoj, M., Poulsen, H. D., & Larsen, L. B. (2012b). Distinct composition of bovine milk from Jersey and Holstein-Friesian cows with good, poor, or noncoagulation properties as reflected in protein genetic variants and isoforms. *Journal of Dairy Science*, 95, 6905-6917.

Jeyarajah, S., & Allen, J. C. (1994). Calcium binding and salt-induced structural changes of native and preheated. beta.-lactoglobulin. *Journal of Agricultural and Food Chemistry*, 42, 80-85.

Jiang, S.-J., & Zhao, X.-H. (2011). Transglutaminase-induced cross-linking and glucosamine conjugation of casein and some functional properties of the modified product. *International Dairy Journal*, 21, 198-205.

Jůza, J. (1997). The pendant drop method of surface tension measurement: Equation interpolating the shape factor tables for several selected planes. *Czechoslovak Journal of Physics*, 47, 351-357.

Kanaji, T., Ozaki, H., Takao, T., Kawajiri, H., Ide, H., Motoki, M., & Shimonishi, Y. (1993). Primary structure of microbial transglutaminase from *Streptovorticillium* sp. strain s-8112. *Journal of Biological Chemistry*, 268, 11565-11572.

Kashiwagi, T., Yokoyama, K., Ishikawa, K., Ono, K., Ejima, D., Matsui, H., & Suzuki, E. (2002). Crystal Structure of Microbial Transglutaminase from *Streptovorticillium mobaraense*. *Journal of Biological Chemistry*, 277, 44252-44260.

Kato, A., & Nakai, S. (1980). Hydrophobicity determined by a fluorescence probe method and its correlation with surface properties of proteins. *Biochimica et Biophysica Acta -Protein Structure*, 624, 13-20.

Kato, A., Matsuda, T., Matsudomi, N., & Kobayashi, K. (1984). Determination of protein hydrophobicity using sodium dodecyl sulfate binding method. *Journal of Agricultural and Food Chemistry*, 32, 284-288.

Kato, A., Minaki, K., & Kobayashi, K. (1993). Improvement of emulsifying properties of egg white proteins by the attachment of polysaccharide through Maillard reaction in a dry state. *Journal of Agricultural and Food Chemistry*, 41, 540-543.

Kayitmazer, A. B. (2007). *Effects of polyelectrolyte charge distribution and chain stiffness on polyelectrolyte-protein complex formation and coacervation*. PhD Thesis, Chemistry Department. University of Massachusetts Amherst, Ann Arbor.

Kelly, S. M., Jess, T. J., & Price, N. C. (2005). How to study proteins by circular dichroism. *Biochimica et Biophysica Acta-Protein Structure*, 1751, 119-139.

Kester, J., & Richardson, T. (1984). Modification of whey proteins to improve functionality. *Journal of Dairy Science*, 67, 2757-2774.

Kim, H. H. Y., & Jimenez-Flores, R. (1994). Comparison of milk proteins using preparative isoelectric focusing followed by polyacrylamide gel electrophoresis. *Journal of Dairy Science*, 77, 2177-2190.

Kim, S. H., & Kinsella, J. E. (1986). Effects of progressive succinylation on some molecular properties of soy glycinin. *Cereal Chemistry Journal*, 63, 342-345.

Kinsella, J. E., & Morr, C. V. (1984). Milk proteins: physicochemical and functional properties. *Critical Reviews in Food Science & Nutrition*, 21, 197-262.

Kiosseoglou, V., & Paraskevopoulou, A. (2011). Functional and physicochemical properties of pulse proteins. In B. K. Tiwari, A. Gowen & B. McKenna (Eds.), *Pulse Foods* (pp. 57-90). New York: Elsevier.

- Kitabatake, N. (1982). Surface tension and foaming of protein solutions. *Journal of Food Science*, 47, 1218-1221.
- Klitzing, R. V., & Müller, H. J. (2002). Film stability control. *Current Opinion in Colloid and Interface Science*, 7, 42-49.
- Koehler, S. A., Hilgenfeldt, S., & Stone, H. A. (2000). A generalized view of foam drainage: experiment and theory. *Langmuir*, 16, 6327-6341.
- Korfmacher, W. A. (2005). Foundation review: Principles and applications of LC-MS in new drug discovery. *Drug Discovery Today*, 10, 1357-1367.
- Koryta, J. (1986). Ion-selective electrodes. *Annual Review of Materials Science*, 16, 13-27.
- Koudelka, T., Hoffmann, P., & Carver, J. A. (2009). Dephosphorylation of α_s - and β -caseins and its effect on chaperone activity: a structural and functional investigation. *Journal of Agricultural and Food Chemistry*, 57, 5956-5964.
- Kumosinski, T. F., Brown, E. M., & Farrell, H. M. (1993). Three-dimensional molecular modeling of bovine caseins: an energy-minimized β -casein structure. *Journal of Dairy Science*, 76, 931-945.
- Kuntz, I. D. (1971). Hydration of macromolecules. III. Hydration of polypeptides. *Journal of the American Chemical Society*, 93, 514-516.
- Kuraishi, C., Yamazaki, K., & Susa, Y. (2001). Transglutaminase: its utilization in the food industry. *Food Reviews International*, 17, 221-246.
- Kuyama, H., Toda, C., Watanabe, M., Tanaka, K., & Nishimura, O. (2003). An efficient chemical method for dephosphorylation of phosphopeptides. *Rapid Communication in Mass Spectrometry*, 17, 1493-1496.
- Laemmli, U. K. (1970). Cleavage of structural proteins during the assembly of the head of bacteriophage T4. *Nature*, 227, 680-685.
- Larre, C., Desserre, C., Barbot, J., & Gueguen, J. (2000). Properties of deamidated gluten films enzymatically crosslinked. *Journal of Agricultural and Food Chemistry*, 48, 5444-5449.
- Latner, A. L., Parsons, M., & Skillen, A. W. (1971). Isoelectric focusing of alkaline phosphatase from human kidney and calf intestine. *Enzymologia*, 40, 1-2.
- Lauber, S., Krause, I., Klostermeyer, H., & Henle, T. (2003). Microbial transglutaminase crosslinks β -casein and β -lactoglobulin to heterologous oligomers under high pressure. *European Food Research and Technology*, 216, 15-17.

Lebowitz, J., Lewis, M. S., & Schuck, P. (2002). Modern analytical ultracentrifugation in protein science: a tutorial review. *Protein Science*, 11, 2067-2079.

Lee, E. Y., & Park, J. (2002). Pressure inactivation kinetics of microbial transglutaminase from *Streptovorticillium mobaraense*. *Journal of Food Science*, 67, 1103-1107.

Lee, J., Martic, P. A., & Tan, J. S. (1989). Protein adsorption on pluronic copolymer-coated polystyrene particles. *Journal of Colloid and Interface Science*, 131, 252-266.

Legrand, D. G., & Gaines Jr, G. L. (1969). The molecular weight dependence of polymer surface tension. *Journal of Colloid and Interface Science*, 31, 162-167.

Li, C., & Choi, P. (2006). Molecular dynamics study of the molecular weight dependence of surface tensions of normal alkanes and methyl methacrylate oligomers. *The Journal of Physical Chemistry B*, 110, 6864-6870.

Lichan, E., & Nakai, S. (1989). Enzymic dephosphorylation of bovine casein to improve acid clotting properties and digestibility for infant formula. *Journal of Dairy Research*, 56, 381-390.

Lieske, B., Konrad, G., & Faber, W. (2000). Effects of succinylation on the renneting properties of raw milk. *Milchwissenschaft*, 55, 71-74.

Lin, M. J., Lewis, M. J., & Grandison, A. S. (2006). Measurement of ionic calcium in milk. *International Journal of Dairy Technology*, 59, 192-199.

Litwinczuk, Z., Krol, J., Brodziak, A., & Barlowska, J. (2011). Changes of protein content and its fractions in bovine milk from different breeds subject to somatic cell count. *Journal of Dairy Science*, 94, 684-691.

Liu, J., Bell, A. W., Bergeron, J. J. M., Yanofsky, C. M., Carrillo, B., Beaudrie, C. E. H., & Kearney, R. E. (2007). Methods for peptide identification by spectral comparison. *Proteome Science*, 5, 3-7.

Liu, M., & Damodaran, S. (1999). Effect of transglutaminase-catalyzed polymerization of β -casein on its emulsifying properties. *Journal of Agricultural and Food Chemistry*, 47, 1514-1519.

Lopes, M. A., Monteiro, F. J., Santos, J. D., Serro, A. P., & Saramago, B. (1999). Hydrophobicity, surface tension, and zeta potential measurements of glass-reinforced hydroxyapatite composites. *Journal of Biomedical Materials Research*, 45, 370-375.

- López, E., Wang, X., Madero, L., López-Pascual, J., & Latterich, M. (2012). Functional phosphoproteomic mass spectrometry-based approaches. *Clinical and Translational Medicine*, 1, 20.
- Lorenzen, P. C., & Reimerdes, E. H. (1992). Enzymatic dephosphorylation of caseins and creaming behavior of o/w emulsions stabilized with dephosphorylated casein fractions. *Nahrung Food*, 36, 595-599.
- Lorient, D., & Linden, G. (1976). Dephosphorylation of bovine casein by milk alkaline-phosphatase. *Journal of Dairy Research*, 43, 19-26.
- Luo, Q., & Andrade, J. D. (1998). Cooperative adsorption of proteins onto hydroxyapatite. *Journal of Colloid and Interface Science*, 200, 104-113.
- Luyten, H., Vereijken, J., & Buecking, M. (2004). Using proteins as additives on foods. In R. Y. Yada (Ed.), *Proteins in Food Processing* (pp. 419-430). Boston: CRC Press.
- Makarov, A., & Scigelova, M. (2010). Coupling liquid chromatography to Orbitrap mass spectrometry. *Journal of Chromatography*, 1217, 3938-3945.
- Malin, E. L., Brown, E. M., Wickham, E. D., & Farrell Jr, H. M. (2005). Contributions of terminal peptides to the associative behavior of α_{s1} -casein. *Journal of Dairy Science*, 88, 2318-2328.
- Malvern laser light guide. (1998). Mastersizer 2000 User Manual. *Malvern Instruments Ltd., Worcestershire, UK*.
- Malvern-Instruments. (2007). *Zetasizer Nano Series - User Manual*. United Kingdom: Malvern Instrument Ltd.
- Manderson, G. A., Hardman, M. J., & Creamer, L. K. (1998). Effect of Heat Treatment on the Conformation and Aggregation of β -Lactoglobulin A, B and C. *Journal of Agricultural and Food Chemistry*, 46, 5052-5061.
- Manson, W., & Carolan, T. (1972). The alkali-induced elimination of phosphate from β -casein. *Journal of Dairy Research*, 39, 189.
- Mariniello, L., Di Pierro, P., Esposito, C., Sorrentino, A., Masi, P., & Porta, R. (2003). Preparation and mechanical properties of edible pectin-soy flour films obtained in the absence or presence of transglutaminase. *Journal of Biotechnology*, 102, 191-198.
- Martínez-Padilla, L. P., García-Mena, V., Casas-Alencáster, N. B., & Sosa-Herrera, M. G. (2014). Foaming properties of skim milk powder fortified with milk proteins. *International Dairy Journal*, 36, 21-28.

- Maste, M. C. L., Norde, W., & Visser, A. J. W. G. (1997). Adsorption-induced conformational changes in the serine proteinase savinase: a tryptophan fluorescence and circular dichroism study. *Journal of Colloid and Interface Science*, 196, 224-230.
- Matheis, G., Penner, M. H., Feeney, R. E., & Whitaker, J. R. (1983). Phosphorylation of casein and lysozyme by phosphorus oxychloride. *Journal of Agricultural and Food Chemistry*, 31, 379-387.
- Matulis, D., & Lovrien, R. (1998). 1-Anilino-8-naphthalene sulfonate anion-protein binding depends primarily on ion pair formation. *Biophysical Journal*, 74, 422-429.
- Mautner, A., Meisel, H., Lorenzen, P. C., & Schlimme, E. (1999). Bestimmung des dipeptids ϵ -(γ -glutamyl) lysin aus transglutaminase-vernetzten proteinen mittels aminosäurenanalyse. *Kieler Milchwirtschaftliche Forschungsberichte*, 51, 155-163.
- McClements, D. J. (2004). Protein-stabilized emulsions. *Current Opinion in Colloid and Interface Science*, 9, 305-313.
- McMahon, D. J., & McManus, W. R. (1998). Rethinking casein micelle structure using electron microscopy. *Journal of Dairy Science*, 81, 2985-2993.
- Medina, A., Colas, B., Meste, M., Renaudet, I., & Lorient, D. (1992). Physicochemical and dynamic properties of caseins modified by chemical phosphorylation. *Journal of Food Science*, 57, 617-621.
- Meisel, H. (2005). Biochemical properties of peptides encrypted in bovine milk proteins. *Current Medicinal Chemistry*, 12, 1905-1919.
- Mercadante, D., Melton, L. D., Norris, G. E., Loo, T. S., Williams, M. A. K., Dobson, R. C. J., & Jameson, G. B. (2012). Bovine β -lactoglobulin is dimeric under imitative physiological conditions: dissociation equilibrium and rate constants over the pH range of 2.5-7.5. *Biophysical Journal*, 103, 303-312.
- Merin, U., Bernstein, S., Bloch-Damti, A., Yagil, R., van Creveld, C., Lindner, P., & Gollop, N. (2001). A comparative study of milk serum proteins in camel (*Camelus dromedarius*) and bovine colostrum. *Livestock Production Science*, 67, 297-301.
- Meyer, M., Klostermeyer, H., & Kleyn, D. (1981). Reduced formation of lysinoalanine in enzymatically dephosphorylated casein. *Zeitschrift für Lebensmittel Untersuchung und Forschung*, 172, 446-448.
- Meyerhoff, M. E., & Opdycke, W. N. (1986). Ion-selective electrodes. *Adv. Clin. Chem*, 25, 1-47.
- Michael Byler, D., Farrell Jr, H. M., & Susi, H. (1988). Raman spectroscopic study of casein structure. *Journal of Dairy Science*, 71, 2622-2629.

Michael, C., & Rosalind, F. (2000). Changes of state and intermolecular forces. In *Advanced Chemistry* (pp. 108). New York: Oxford University Press.

Miller, M. L., & Johnson, G. V. W. (1999). Rapid, single-step procedure for the identification of transglutaminase-mediated isopeptide crosslinks in amino acid digests. *Journal of Chromatography B: Biomedical Sciences and Applications*, 732, 65-72.

Miller, R., Fainerman, V. B., Aksenenko, E. V., Leser, M. E., & Michel, M. (2004). Dynamic surface tension and adsorption kinetics of β -casein at the solution/air interface. *Langmuir*, 20, 771-777.

Mirmoghtadaie, L., Kadivar, M., & Shahedi, M. (2009). Effects of succinylation and deamidation on functional properties of oat protein isolate. *Food Chemistry*, 114, 127-131.

Mitchell, D. G., Burk Jr, D. L., Vinitski, S., & Rifkin, M. D. (1987). The biophysical basis of tissue contrast in extracranial MR imaging. *American Journal of Roentgenology*, 149, 831-837.

Modler, H. W. (1985). Functional properties of nonfat dairy ingredients-a review. Modification of products containing casein. *Journal of Dairy Science*, 68, 2195-2205.

Molina, A. C. T., Alli, I., Konishi, Y., & Kermasha, S. (2007). Effect of dephosphorylation on bovine casein. *Food Chemistry*, 101, 1263-1271.

Monsalve, A., & Schechter, R. S. (1984). The stability of foams: Dependence of observation on the bubble size distribution. *Journal of Colloid and Interface Science*, 97, 327-335.

Moon, J. H., Hong, Y. H., Huppertz, T., Fox, P. F., & Kelly, A. L. (2009). Properties of casein micelles cross - linked by transglutaminase. *International Journal of Dairy Technology*, 62, 27-32.

Morand, M., Guyomarc'h, F., & Famelart, M.-H. (2011a). How to tailor heat-induced whey protein/ κ -casein complexes as a means to investigate the acid gelation of milk—a review. *Dairy Science & Technology*, 91, 97-126.

Morand, M., Guyomarc'h, F., Legland, D., & Famelart, M. H. (2011b). Changing the isoelectric point of the heat-induced whey protein complexes affects the acid gelation of skim milk. *International Dairy Journal*, 23, 9-17.

Morand, M., Guyomarc'h, F., Pezennec, S., & Famelart, M. H. (2011c). On how κ -casein affects the interactions between the heat-induced whey protein/ κ -casein complexes and the casein micelles during the acid gelation of skim milk. *International Dairy Journal*, 21, 670-678.

Morand, M., Dekkari, A., & Famelart, M.-H. (2012). Increasing the hydrophobicity of the heat-induced whey protein complexes improves the acid gelation of skim milk. *International Dairy Journal*, 25, 103-111.

Moreira, J. C., & Demarquette, N. R. (2001). Influence of temperature, molecular weight, and molecular weight dispersity on the surface tension of PS, PP, and PE. I. Experimental. *Journal of Applied Polymer Science*, 82, 1907-1920.

Morita, A., Carastan, D., & Demarquette, N. (2002). Influence of drop volume on surface tension evaluated using the pendant drop method. *Colloid and Polymer Science*, 280, 857-864.

Moro, A., Gatti, C., & Delorenzi, N. (2001). Hydrophobicity of whey protein concentrates measured by fluorescence quenching and its relation with surface functional properties. *Journal of Agricultural and Food Chemistry*, 49, 4784-4789.

Motoki, M., Seguro, K., Nio, N., & Takinami, K. (1986). Glutamine-specific deamidation of α_{s1} -casein by transglutaminase. *Agricultural and Biological Chemistry*, 50, 3025-3030.

Motoki, M., & Seguro, K. (1998). Transglutaminase and its use for food processing. *Trends in Food Science & Technology*, 9, 204-210.

Mounsey, J. S., O'Kennedy, B. T., & Kelly, P. M. (2005). Influence of transglutaminase treatment on properties of micellar casein and products made therefrom. *Le Lait Dairy Journal*, 85, 405-418.

Muhammad, G., Saïd, B., Julien, J., Valérie, B.-B., & Thomas, C. (2013). Structural consequences of dry heating on α -lactalbumin and β -lactoglobulin at pH 6. 5. *Food Research International*, 10, 3624-3627.

Mura-Galelli, M. J., Voegel, J. C., Behr, S., Bres, E. F., & Schaaf, P. (1991). Adsorption/desorption of human serum albumin on hydroxyapatite: a critical analysis of the Langmuir model. *Proceedings of the National Academy of Sciences*, 88, 5557-5561.

Murphy, M. C., & Howell, N. K. (1990). Effect of succinylation on the functional and physicochemical properties of bovine serum albumin. *Journal of the Science of Food and Agriculture*, 51, 109-123.

Nagasawa, K., Takahashi, K., & Hattori, M. (1996). Improved emulsifying properties of β -lactoglobulin by conjugating with carboxymethyl dextran. *Food Hydrocolloids*, 10, 63-67.

Naidu, R., Bolan, N. S., Kookana, R. S., & Tiller, K. G. (1994). Ionic-strength and pH effects on the sorption of cadmium and the surface charge of soils. *European Journal of Soil Science*, 45, 419-429.

Nakai, S., Ho, L., Helbig, N., Kato, A., & Tung, M. A. (1980). Relationship between hydrophobicity and emulsifying properties of some plant proteins. *Canadian Institute of Food Science and Technology Journal*, 13, 23-27.

Nakai, S. (1983). Structure-function relationships of food proteins: with an emphasis on the importance of protein hydrophobicity. *Journal of Agricultural and Food Chemistry*, 31, 676-683.

Nakai, S., Li - Chan, E., & Hayakawa, S. (1986). Contribution of protein hydrophobicity to its functionality. *Food/Nahrung*, 30, 327-336.

Nakai, S., Li-Chan, E., & Arteaga, G. (1996). Measurement of surface hydrophobicity. In *Methods of Testing Protein Functionalities* (pp. 226). London: Chapman & Hall.

Nakamura, S., Kobayashi, K., & Kato, A. (1993). Novel surface functional properties of polymannosyl lysozyme constructed by genetic modification. *Federation of European Biochemical Societies Letters*, 328, 259-262.

Nakanishi, K., Sakiyama, T., & Imamura, K. (2001). On the adsorption of proteins on solid surfaces, a common but very complicated phenomenon. *Journal of Bioscience and Bioengineering*, 91, 233-244.

Nayak, S. K., Arora, S., Sindhu, J. S., & Sangwan, R. B. (2006). Effect of chemical phosphorylation on solubility of buffalo milk proteins. *International Dairy Journal*, 16, 268-273.

Nazmi, A. R., Schofield, L. R., Dobson, R. C. J., Jameson, G. B., & Parker, E. J. (2014). Destabilization of the homotetrameric assembly of 3-deoxy-d- arabino-heptulosonate-7-phosphate synthase from the hyperthermophile *pyrococcus furiosus* enhances enzymatic activity. *Journal of Molecular Biology*, 426, 656-673.

Nieuwenhuizen, W. F., Dekker, H. L., Gröneveld, T., de Koster, C. G., & de Jong, G. A. H. (2004). Transglutaminase-mediated modification of glutamine and lysine residues in native bovine β -lactoglobulin. *Biotechnology and Bioengineering*, 85, 248-258.

Nonaka, M., Tanaka, H., Okiyama, A., Motoki, M., Ando, H., Umeda, K., & Matsuura, A. (1989). Polymerization of several proteins by Ca^{2+} -independent transglutaminase derived from microorganisms. *Agricultural and Biological Chemistry*, 53, 2619-2623.

O'Sullivan, M., Kelly, A., & Fox, P. (2002a). Effect of transglutaminase on the heat stability of milk: a possible mechanism. *Journal of Dairy Science*, 85, 1-7.

O'Sullivan, M. M., Kelly, A. L., & Fox, P. F. (2002b). Influence of transglutaminase treatment on some physicochemical properties of milk. *Journal of Dairy Research*, 69, 433-442.

- Ohmiya, K., Sugano, S., Yun, S. E., & Shimizu, S. (1983). Immobilization of acid-phosphatase and its use for dephosphorylation of casein. *Agricultural and Biological Chemistry*, 47, 535-542.
- Ohtsuka, T., Ota, M., Nio, N., & Motoki, M. (2000a). Comparison of substrate specificities of transglutaminases using synthetic peptides as acyl donors. *Bioscience, Biotechnology, and Biochemistry*, 64, 2608-2613.
- Ohtsuka, T., Sawa, A., Kawabata, R., Nio, N., & Motoki, M. (2000b). Substrate specificities of microbial transglutaminase for primary amines. *Journal of Agricultural and Food Chemistry*, 48, 6230-6233.
- Ohtsuka, T., Umezawa, Y., Nio, N., & Kubota, K. (2001). Comparison of deamidation activity of transglutaminases. *Journal of Food Science*, 66, 25-29.
- Olson, N., Richardson, T., & Zadow, J. (1978). Reductive methylation of lysine residues in casein. *J. Dairy Res*, 45, 69.
- Ostersen, S., Foldager, J., & Hermansen, J. E. (1997). Effects of stage of lactation, milk protein genotype and body condition at calving on protein composition and renneting properties of bovine milk. *Journal of Dairy Research*, 64, 207-219.
- Otterburn, M., Healy, M., & Sinclair, W. (1977). The formation, isolation and importance of isopeptides in heated proteins. In *Protein Crosslinking* (pp. 239-262). New York: Springer.
- Otzen, D. E. (2002). Protein unfolding in detergents: effect of micelle structure, ionic strength, pH, and temperature. *Biophysical Journal*, 83, 2219-2230.
- Ozer, B., Kirmaci, H. A., Oztekin, S., Hayaloglu, A., & Atamer, M. (2007). Incorporation of microbial transglutaminase into non-fat yogurt production. *International Dairy Journal*, 17, 199-207.
- Partanen, R., Paananen, A., Forssell, P., Linder, M. B., Lille, M., Buchert, J., & Lantto, R. (2009). Effect of transglutaminase-induced cross-linking of sodium caseinate on the properties of equilibrated interfaces and foams. *Colloids and Surfaces A: Physicochemical and Engineering Aspects*, 344, 79-85.
- Partschfeld, C., Schreiner, J., Schwarzenbolz, U., & Henle, T. (2009). Studies on enzymatic crosslinking of casein micelles. *Czech Journal of Food Sciences*, 27, 99-101.
- Pastor, M. T., Diez, A., Pérez-Payá, E., & Abad, C. (1999). Addressing substrate glutamine requirements for tissue transglutaminase using substance P analogues. *Federation of European Biochemical Societies Letters*, 451, 231-234.
- Paulson, A. T., & Tung, M. A. (1987). Solubility, hydrophobicity and net charge of succinylated canola protein isolate. *Journal of Food Science*, 52, 1557-1561.

Paulsson, M. (1990). *Thermal Denaturation and Gelation of Whey Proteins and Their Adsorption at the Air/Water Interface*. Lund: Drucker.

Paunov, V. N. (2003). Novel method for determining the three-phase contact angle of colloid particles adsorbed at air-water and oil-water interfaces. *Langmuir*, 19, 7970-7976.

Payens, T. A. J., Brinkhuis, J. A., & Van Markwijk, B. W. (1969). Self-association in non-ideal systems. Combined light scattering and sedimentation measurements in β -casein solutions. *Biochimica et Biophysica Acta-Protein Structure*, 175, 434-437.

Pearse, M. J., Linklater, P. M., Hall, R. J., & Mackinlay, A. G. (1986). Effect of casein micelle composition and casein dephosphorylation on coagulation and syneresis. *Journal of Dairy Research*, 53, 381-390.

Pecora, R. (2013). *Dynamic Light Scattering: Applications of Photon Correlation Spectroscopy*. New York: Springer Science & Business Media.

Pepper, L., & Thompson, M. P. (1963). Dephosphorylation of α_s - and κ -caseins and its effect on micelle stability in κ - and α_s -casein system. *Journal of Dairy Science*, 46, 764.

Peters, F., & Arabali, D. (2013). Interfacial tension between oil and water measured with a modified contour method. *Colloids and Surfaces A: Physicochemical and Engineering Aspects*, 426, 1-5.

Pezennec, S., Gauthier, F., Alonso, C., Graner, F., Croguennec, T., Brule, G., & Renault, A. (2000). The protein net electric charge determines the surface rheological properties of ovalbumin adsorbed at the air–water interface. *Food Hydrocolloids*, 14, 463-472.

Pfeiffer, C., Rehbock, C., Hühn, D., Carrillo-Carrion, C., de Aberasturi, D. J., Merk, V., Barcikowski, S., & Parak, W. J. (2014). Interaction of colloidal nanoparticles with their local environment: the (ionic) nanoenvironment around nanoparticles is different from bulk and determines the physico-chemical properties of the nanoparticles. *Journal of The Royal Society Interface*, 11, 20130931.

Piacentini, E., Drioli, E., & Giorno, L. Membrane emulsification for cell delivery. In L. D. Bartolo (Ed.), *Biomaterials for Stem Cell Therapy* (pp. 537-568). New York: CRC Press.

Pitt-Rivers, R., & Impiombato, F. S. (1968). The binding of sodium dodecyl sulphate to various proteins. *Biochemical Journal*, 109, 825-830.

Pugh, R. J. (1996). Foaming, foam films, antifoaming and defoaming. *Advances in Colloid and Interface Science*, 64, 67-142.

Puri, D. (2002). Amino acids, peptides and proteins. In *Textbook of Medical Biochemistry* (pp. 49). India: Elsevier.

Ralston, G. B. (1993). *Introduction to Analytical Ultracentrifugation*. Fullerton: Beckman Instruments.

Raussens, V., Ruysschaert, J.-M., & Goormaghtigh, E. (2003). Protein concentration is not an absolute prerequisite for the determination of secondary structure from circular dichroism spectra: a new scaling method. *Analytical Biochemistry*, 319, 114-121.

Reginald, H. G., & Charles, M. G. (2012). Amino acids and the peptide bond. In *Biochemistry*. Stamford: Mary Finch.

Reynolds, E. C., & Wong, A. (1983). Effect of adsorbed protein on hydroxyapatite zeta potential and Streptococcus mutans adherence. *Infection and Immunity*, 39, 1285-1290.

Reynolds, J. A., & Tanford, C. (1970). The gross conformation of protein-sodium dodecyl sulfate complexes. *Journal of Biological Chemistry*, 245, 5161-5165.

Righetti, P. G. (1998). Conventional isoelectric focusing in gel slabs, in capillaries, and immobilized pH gradients. In B. D. Hames (Ed.), *Gel Electrophoresis of Proteins: A Practical Approach* (Vol. 197, pp. 127-187). New York: Oxford University Press.

Robbins, F. M., & Holmes, L. G. (1970). Circular dichroism spectra of α -lactalbumin. *Biochimica et Biophysica Acta (BBA)-Protein Structure*, 221, 234-240.

Robitaille, G., Ng-Kwai-Hang, K.-F., & Monardes, H. G. (1991). Variation in the N-acetyl neuraminic acid content of bovine κ -casein. *Journal of Dairy Research*, 58, 107-114.

Rodriguez, J., Gupta, N., Smith, R. D., & Pevzner, P. A. (2007). Does trypsin cut before proline? *Journal of Proteome Research*, 7, 300-305.

Rodríguez Niño, M. R., & Rodríguez Patino, J. M. (1998). Surface tension of protein and insoluble lipids at the air-aqueous phase interface. *Journal of the American Oil Chemists' Society*, 75, 1233-1239.

Ross, J. W. (1967). Calcium-selective electrode with liquid ion exchanger. *Science*, 156, 1378-1379.

Roth, S., Murray, B. S., & Dickinson, E. (2000). Interfacial shear rheology of aged and heat-treated β -lactoglobulin films: Displacement by nonionic surfactant. *Journal of Agricultural and Food Chemistry*, 48, 1491-1497.

Rowley, B., Lund, D., & Richardson, T. (1979). Reductive methylation of β -Lactoglobulin. *Journal of Dairy Science*, 62, 533-536.

Salonen, A., In, M., Emile, J., & Saint-Jalmes, A. (2010). Solutions of surfactant oligomers: a model system for tuning foam stability by the surfactant structure. *Soft Matter*, 6, 2271-2281.

Sánchez, C. C., & Patino, J. M. R. (2005). Interfacial, foaming and emulsifying characteristics of sodium caseinate as influenced by protein concentration in solution. *Food Hydrocolloids*, 19, 407-416.

Sánchez, C. C., Rodríguez Niño, M., Caro, A. L., & Rodríguez Patino, J. M. (2005). Biopolymers and emulsifiers at the air–water interface. Implications in food colloid formulations. *Journal of Food Engineering*, 67, 225-234.

Schägger, H., & von Jagow, G. (1991). Blue native electrophoresis for isolation of membrane protein complexes in enzymatically active form. *Analytical Biochemistry*, 199, 223-231.

Schmid, A. W., Condemi, E., Tuchscherer, G., Chiappe, D., Mutter, M., Vogel, H., Moniatte, M., & Tsybin, Y. O. (2011). Tissue transglutaminase-mediated glutamine deamidation of β -amyloid peptide increases peptide solubility, whereas enzymatic cross-linking and peptide fragmentation may serve as molecular triggers for rapid peptide aggregation. *Journal of Biological Chemistry*, 286, 12172-12188.

Schmidt, D. G., & Van Markwijk, B. W. (1968). Further studies on the associating subunit of α_{s1} -casein. *Biochimica et Biophysica Acta -Protein Structure*, 154, 613-614.

Schmidt, D. G. (1970). The association of α_{s1} -casein B at pH 6.6. *Biochimica et Biophysica Acta -Protein Structure*, 207, 130-138.

Schmidt, D. G. (1982). Association of caseins and casein micelle structure. In P. F. Fox (Ed.), *Developments in Dairy Chemistry* (pp. 61). London: Elsevier applied science publishers Ltd.

Schmidt, D. G., & Poll, J. K. (1989). Properties of artificial casein micelles .4. influence of dephosphorylation and phosphorylation of the casein. *Netherlands Milk and Dairy Journal*, 43, 53-62.

Schmidt, S., Adolf, F., & Fuchsbauer, H.-L. (2008). The transglutaminase activating metalloprotease inhibitor from *Streptomyces mobaraensis* is a glutamine and lysine donor substrate of the intrinsic transglutaminase. *Federation of European Biochemical Societies Letters*, 582, 3132-3138.

Schnepf, M. I. (1992). Protein-water interactions. In *Biochemistry of Food Proteins* (pp. 1-33). New York: Springer.

Schuster, E., Sprössler, B., & Hofemeister, J. (2002). Method for production of stay-fresh baked goods. *Patent Number EU Patent 0942654*.

Schwenke, K. D. (1997). Enzyme and chemical modification of proteins. In S. Damodaran (Ed.), *Food Proteins and Their Applications* (pp. 393-424). New York: Dekker.

Scopes, R. K. (1993). Measurement of protein and enzyme activity. In *Protein Purification: Principles and Practices* (pp. 44-68). Boston: Springer.

Sen, L. C., Lee, H. S., Feeney, R. E., & Whitaker, J. R. (1981). In vitro digestibility and functional properties of chemically modified casein. *Journal of Agricultural and Food Chemistry*, 29, 348-354.

Shahani, K. M. (1966). Milk enzymes: their role and significance. *Journal of Dairy Science*, 49, 907-920.

Sharma, R., Lorenzen, P. C., & Qvist, K. B. (2001). Influence of transglutaminase treatment of skim milk on the formation of ϵ -(γ -glutamyl)-lysine and the susceptibility of individual proteins towards crosslinking. *International Dairy Journal*, 11, 785-793.

Sharma, R., Zakora, M., & Qvist, K. B. (2002). Characteristics of oil–water emulsions stabilised by an industrial α -lactalbumin concentrate, cross-linked before and after emulsification, by a microbial transglutaminase. *Food Chemistry*, 79, 493-500.

Shilpashree, B. G., Arora, S., Chawla, P., Vakkalagadda, R., & Sharma, A. (2015). Succinylation of sodium caseinate and its effect on physicochemical and functional properties of protein. *Food Science and Technology Research*, 64, 1270-1277.

Shoemaker, C. F. (1990). Effects of the adsorption of caseins on the surface tension and rheological properties of polystyrene latex suspensions. *Food Hydrocolloids*, 4, 33-40.

Shukla, A. N. (2009). Enzymes of protein metabolism. In *Chemistry of Enzymes* (pp. 236-267). Delhi: Discovery.

Siegel, R. A., & Firestone, B. A. (1988). pH-dependent equilibrium swelling properties of hydrophobic polyelectrolyte copolymer gels. *Macromolecules*, 21, 3254-3259.

Sikorski, Z. E. (2002). Proteins. In *Chemical and Functional Properties of Food Components* (pp. 133-179). New York: CRC Press.

Silva, F. V., Lopes, G. S., Nobrega, J. A., Souza, G. B., & Nogueira, A. R. A. (2001). Study of the protein-bound fraction of calcium, iron, magnesium and zinc in bovine milk. *Spectrochimica Acta Part B-Atomic Spectroscopy*, 56, 1909-1916.

Simons Jr, S. S., & Johnson, D. F. (1976). The structure of the fluorescent adduct formed in the reaction of o-phthalaldehyde and thiols with amines. *Journal of the American Chemical Society*, 98, 7098-7099.

Simpson, R. J. (2006). Fragmentation of protein using trypsin. *Cold Spring Harbor Protocols*, 5, 45-50.

Singh, H. (1991). Modification of food proteins by covalent crosslinking. *Trends in Food Science & Technology*, 2, 196-200.

Slattery, C. W., & Evard, R. (1973). A model for the formation and structure of casein micelles from subunits of variable composition. *Biochimica et Biophysica Acta (BBA)-Protein Structure*, 317, 529-538.

Smiddy, M., Martin, J.-E., Kelly, A., De Kruif, C., & Huppertz, T. (2006). Stability of casein micelles cross-linked by transglutaminase. *Journal of Dairy Science*, 89, 1906-1914.

Smithers, G. W. (2008). Whey and whey proteins-from 'gutter-to-gold'. *International Dairy Journal*, 18, 695-704.

Sochan, A., Bieganski, A., Ryżak, M., Dobrowolski, R., & Bartmiński, P. (2012). Comparison of soil texture determined by two dispersion units of Mastersizer 2000. *International Agrophysics*, 26, 99-102.

Solomon, E. I., & Lever, A. B. P. (2006). *Inorganic Electronic Structure and Spectroscopy: Methodology*. New York: John Wiley & Sons.

Sparks, D. L., & Phillips, M. C. (1992). Quantitative measurement of lipoprotein surface charge by agarose gel electrophoresis. *Journal of Lipid Research*, 33, 123-130.

Stephan, C., Kohl, M., Turewicz, M., Podwojski, K., Meyer, H. E., & Eisenacher, M. (2010). Using laboratory information management systems as central part of a proteomics data workflow. *Proteomics*, 10, 1230-1249.

Strange, E., Hekken, D., & Thompson, M. (1991). Qualitative and quantitative determination of caseins with reverse - phase and anion - exchange HPLC. *Journal of Food Science*, 56, 1415-1420.

Sung, H. Y., Chen, H. J., Liu, T. Y., & Su, J. C. (2006). Improvement of the functionalities of soy protein isolate through chemical phosphorylation. *Journal of Food Science*, 48, 716-721.

Švedas, V.-J. K., Galaev, I. J., Borisov, I. L., & Berezin, I. V. (1980). The interaction of amino acids with o-phthalaldehyde: a kinetic study and spectrophotometric assay of the reaction product. *Analytical biochemistry*, 101, 188-195.

- Swaisgood, H. (1982). Chemistry of milk protein. In P. F. Fox (Ed.), *Developments in Dairy Chemistry- Proteins* (Vol. 1). London: Elsevier applied science.
- Swaisgood, H. (2003). Chemistry of the caseins. In P. F. Fox & P. L. H. McSweeney (Eds.), *Advanced Dairy Chemistry* (Vol. 1, pp. 139). New York: Springer.
- Szwajkowska, M., Wolanciuk, A., Barlowska, J., Krol, J., & Litwinczuk, Z. (2011). Bovine milk proteins as the source of bioactive peptides influencing the consumers' immune system - a review. *Animal Science Papers and Reports*, 29, 269-280.
- Tal, M., Silberstein, A., & Nusser, E. (1985). Why does Coomassie Brilliant Blue R interact differently with different proteins? A partial answer. *Journal of Biological Chemistry*, 260, 9976-9980.
- Tang, C., Yang, X. Q., Chen, Z., Wu, H., & Peng, Z. Y. (2005a). Physicochemical and structural characteristics of sodium caseinate biopolymers induced by microbial transglutaminase. *Journal of Food Biochemistry*, 29, 402-421.
- Tang, C. H., Jiang, Y., Wen, Q. B., & Yang, X. Q. (2005b). Effect of transglutaminase treatment on the properties of cast films of soy protein isolates. *Journal of Biotechnology*, 120, 296-307.
- Tang, C. H., & Jiang, Y. (2007). Modulation of mechanical and surface hydrophobic properties of food protein films by transglutaminase treatment. *Food Research International*, 40, 504-509.
- Tang, C. H., & Ma, C. Y. (2007). Modulation of the thermal stability of β -lactoglobulin by transglutaminase treatment. *European Food Research and Technology*, 225, 649-652.
- Tercinier, L., Ye, A., Anema, S., Singh, A., & Singh, H. (2013). Adsorption of milk proteins on to calcium phosphate particles. *Journal of Colloid and Interface Science*, 394, 458-466.
- Tesch, S., Gerhards, C., & Schubert, H. (2002). Stabilization of emulsions by OSA starches. *Journal of Food Engineering*, 54, 167-174.
- Thomason, P., & Kay, R. (2000). Eukaryotic signal transduction via histidine-aspartate phosphorelay. *Journal of Cell Science*, 113, 3141-3150.
- Townsend, A. A., & Nakai, S. (1983). Relationships between hydrophobicity and foaming characteristics of food proteins. *Journal of Food Science*, 48, 588-594.
- Traore, F., & Meunier, J. C. (1992). Crosslinking activity of placental F XIIIa on whey proteins and caseins. *Journal of Agricultural and Food Chemistry*, 40, 399-402.

Tremblay, L., Laporte, M. F., Leonil, J., Dupont, D., & Paquin, P. (2003). Quantitation of proteins in milk and milk product. In P. F. Fox & P. L. H. McSweeney (Eds.), *Advanced Dairy Chemistry-Proteins* (Vol. 1). New York: Kluwer academic/plenum publishers.

Treweek, T. M. (2012). Alpha-casein as a molecular chaperone. In W. L. Hurley (Ed.), *Milk Protein* (pp. 85-119). Rijeka, Croatia: InTech.

Tripp, B. (1993). *Dynamic surface tension of model protein solutions measured via pendant drop tensiometry*. PhD thesis. Department of Chemical Engineering. The University of Utah. Salt Lake City. United States.

Tripp, B. C., Magda, J. J., & Andrade, J. D. (1995). Adsorption of globular proteins at the air/water interface as measured via dynamic surface tension: concentration dependence, mass-transfer considerations, and adsorption kinetics. *Journal of Colloid and Interface Science*, 173, 16-27.

Urrutia, P. I. (2006). *Predicting water-in-oil emulsion coalescence from surface pressure isotherms*. University of Calgary M. Sc. Thesis.

Van Hekken, D. L., Strange, E. D., & Lu, D. P. (1996). Functional properties of chemically phosphorylated whole casein. *Journal of Dairy Science*, 79, 1942-1949.

Van Hekken, D. L., & Strange, E. D. (1997). Rheology and microstructure of chemically superphosphorylated whole casein. *Journal of Dairy Science*, 80, 2740-2750.

Van Holde, K. E. (1975). Sedimentation analysis of proteins. In H. Neurath & R. L. Hill (Eds.), *The Protein* (Vol. 1, pp. 225-291). New York: Academic Press.

Varnam, A. H. (2012). *Milk and Milk Products: Technology, Chemistry and Microbiology*. New York: Springer.

Vasbinder, A. J., Rollema, H. S., Bot, A., & de Kruif, C. G. (2003). Gelation mechanism of milk as influenced by temperature and pH; Studied by the use of transglutaminase cross-linked casein micelles. *Journal of Dairy Science*, 86, 1556-1563.

Velev, O. D., Furusawa, K., & Nagayama, K. (1996). Assembly of latex particles by using emulsion droplets as templates. 1. Microstructured hollow spheres. *Langmuir*, 12, 2374-2384.

Visker, M., Dibbitts, B. W., Kinders, S. M., van Valenberg, H. J. F., van Arendonk, J. A. M., & Bovenhuis, H. (2011). Association of bovine beta-casein protein variant I with milk production and milk protein composition. *Animal Genetics*, 42, 212-218.

- Visker, M., Heck, J. M. L., van Valenberg, H. J. F., van Arendonk, J. A. M., & Bovenhuis, H. (2012). Short communication: a new bovine milk-protein variant: α -lactalbumin variant D. *Journal of Dairy Science*, *95*, 2165-2169.
- Viswanath, D. S., Ghosh, T. K., Prasad, D. H. L., Dutt, N. V. K., & Rani, K. Y. (2007). Correlations and estimation of pure liquid viscosity. In *Viscosity of Liquids: Theory, Estimation, Experiment and Data* (pp. 135-307). Dordrecht: Springer.
- Vollhardt, K. P. C., & Schore, N. E. (2011). *Organic Chemistry: Structure and Function*. New York: WH Freeman.
- Vreeman, H., Visser, S., Slangen, C. J., & Van Riel, J. (1986). Characterization of bovine κ -casein fractions and the kinetics of chymosin-induced macropeptide release from carbohydrate-free and carbohydrate-containing fractions determined by high-performance gel-permeation chromatography. *Biochemical Journal*, *240*, 87.
- Wahlgren, M., & Arnebrant, T. (1991). Protein adsorption to solid surfaces. *Trends in biotechnology*, *9*, 201-208.
- Walstra, P., & Jenness, R. (1984). *Dairy Chemistry and Physics*. New York: John Wiley & Sons.
- Walstra, P. (1990). On the stability of casein micelles. *Journal of Dairy Science*, *73*, 1965-1979.
- Walstra, P., & De Roos, A. L. (1993). Proteins at air-water and oil-water interfaces: Static and dynamic aspects. *Food Reviews International*, *9*, 503-525.
- Walstra, P. (1999). Casein sub-micelles: do they exist? *International Dairy Journal*, *9*, 189-192.
- Walstra, P., Wouters, J. T., & Geurts, T. J. (2005). *Dairy Science and Technology* (Vol. 146). New York: CRC Press.
- Wanasundara, P., & Shahidi, F. (1997). Functional properties of acylated flax protein isolates. *Journal of Agricultural and Food Chemistry*, *45*, 2431-2441.
- Wang, J., Zhang, Q. H., Wang, Z. H., & Li, H. M. (2009). Determination of major bovine milk proteins by reversed phase high performance liquid chromatography. *Chinese Journal of Analytical Chemistry*, *37*, 1667-1670.
- Wang, Z., & Narsimhan, G. (2006). Model for Plateau border drainage of power-law fluid with mobile interface and its application to foam drainage. *Journal of Colloid and Interface Science*, *300*, 327-337.
- Wedd, M. W. (2003). Determination of particle size distributions using laser diffraction. *Educational Resources for Particle Technology*, *4*, 1-4.

Wei, H., Thompson, R. B., Park, C. B., & Chen, P. (2011). Surface tension measurement of polymer melts in supercritical fluids. In R. Miller & L. Liggieri (Eds.), *Bubble and Drop Interfaces* (pp. 293-324). Boston: CRC Press.

West, D. W., & Towers, G. E. (1976). Study of enzymic dephosphorylation of β -casein and a derived phosphopeptide. *Biochimica Et Biophysica Acta*, 453, 383-390.

Westall, J. C., Leuenberger, C., & Schwarzenbach, R. P. (1985). Influence of pH and ionic strength on the aqueous-nonaqueous distribution of chlorinated phenols. *Environmental Science & Technology*, 19, 193-198.

Wilde, P. J. (2000a). Interfaces: their role in foam and emulsion behaviour. *Current Opinion in Colloid and Interface Science*, 5, 176-181.

Wilde, P. J. (2000b). Interfaces: their role in foam and emulsion behaviour. *Current opinion in colloid & interface science*, 5, 176-181.

Woo, S. L., & Richardson, T. (1983). Functional properties of phosphorylated β -lactoglobulin. *Journal of Dairy Science*, 66, 984-987.

Wu, W. U., Hettiarachchy, N. S., & Qi, M. (1998). Hydrophobicity, solubility, and emulsifying properties of soy protein peptides prepared by papain modification and ultrafiltration. *Journal of the American Oil Chemists' Society*, 75, 845-850.

Yamauchi, K., & Yoneda, Y. (1978). Effect of dephosphorylation of casein on its coagulation and proteolysis by chymosin. *Journal of Agricultural and Biological Chemistry*, 42, 1031-1035.

Yang, M., Yang, J., Zhang, Y., & Zhang, W. (2015). Influence of succinylation on physicochemical property of yak casein micelles. *Food Chemistry*, 190, 836-842.

Yao, X. T., & Zhao, X. H. (2015). Effects of caseinate deamidation on transglutaminase-induced glucosamine conjugation and cross-linking as well as properties of the treated caseinates. *Journal of Food*, 13, 400-407.

Yasir, S. B., Sutton, K. H., Newberry, M. P., Andrews, N. R., & Gerrard, J. A. (2007). The impact of transglutaminase on soy proteins and tofu texture. *Food Chemistry*, 104, 1491-1501.

Ye, A. Q. (2011). Functional properties of milk protein concentrates: Emulsifying properties, adsorption and stability of emulsions. *International Dairy Journal*, 21, 14-20.

Yeung, A. C., Glahn, R. P., & Miller, D. D. (2001). Dephosphorylation of sodium caseinate, enzymatically hydrolyzed casein and casein phosphopeptides by intestinal

alkaline phosphatase: implications for iron availability. *Journal of Nutritional Biochemistry*, 12, 292-299.

Yokoyama, K., Nio, N., & Kikuchi, Y. (2004). Properties and applications of microbial transglutaminase. *Applied Microbiology and Biotechnology*, 64, 447-454.

Yoshikawa, M., Tamaki, M., Sugimoto, E., & Chiba, H. (1974). Effect of dephosphorylation on self-association and precipitation of β -casein. *Agricultural and Biological Chemistry*, 38, 2051-2052.

Yu, M. A., & Damodaran, S. (1991). Kinetics of protein foam destabilization: evaluation of a method using bovine serum albumin. *Journal of Agricultural and Food Chemistry*, 39, 1555-1562.

Zaslavsky, B. Y., Mestechkina, N. M., Miheeva, L. M., & Rogozhin, S. V. (1982). Measurement of relative hydrophobicity of amino acid side-chains by partition in an aqueous two-phase polymeric system: Hydrophobicity scale for non-polar and ionogenic side-chains. *Journal of Chromatography A*, 240, 21-28.

Zayas, J. F. (1997). Water holding capacity of proteins. In *Functionality of Proteins in Food* (pp. 76-133). New York: Springer.

Zhang, D. W., Mosley, A. L., Ramisetty, S. R., Rodríguez-Molina, J. B., Washburn, M. P., & Ansari, A. Z. (2012). Ssu72 phosphatase-dependent erasure of phospho-Ser7 marks on the RNA polymerase II C-terminal domain is essential for viability and transcription termination. *Journal of Biological Chemistry*, 287, 8541-8551.

Zhu, Y., Rinzema, A., Tramper, J., & Bol, J. (1995). Microbial transglutaminase—a review of its production and application in food processing. *Applied Microbiology and Biotechnology*, 44, 277-282.

Zumdahl, S. S., & Zumdahl, S. A. (2012). Properties of solutions. In *Chemistry: An Atoms First Approach* (1st ed., pp. 486). Boston: Cengage Learning.

Appendices

Appendix A: Surface tension of native α_{s1} -casein solutions

The preliminary experiments of surface tension measurement demonstrated the effect of protein concentration on the surface tension.

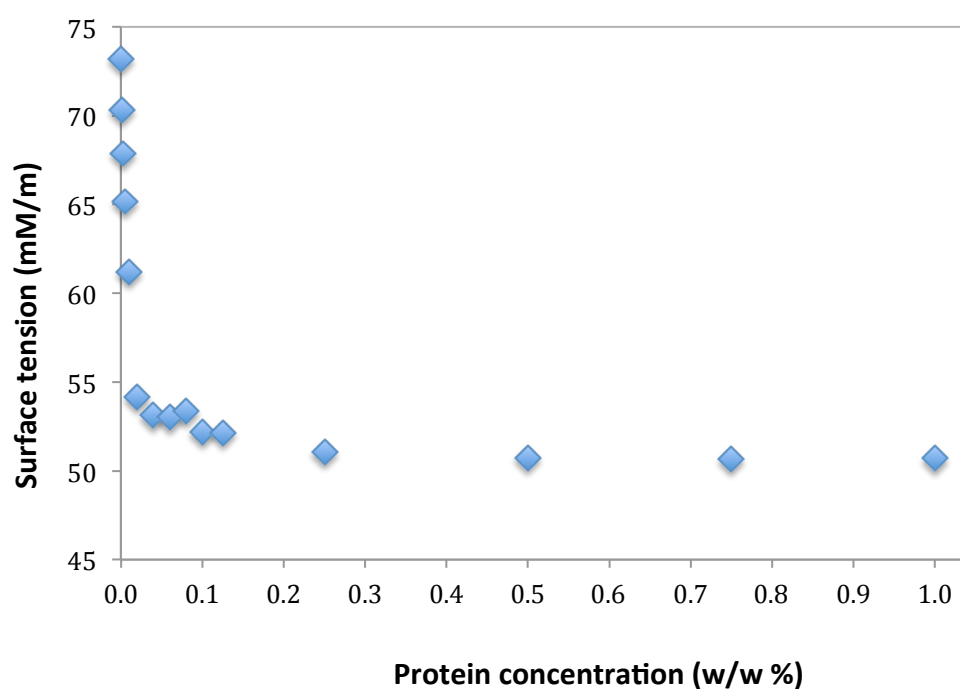


Figure A-1 The surface tension (air-water) of native α_{s1} -casein solutions at protein concentrations from 0% to 1% (w/w) measured using the Wilhelmy plate method.

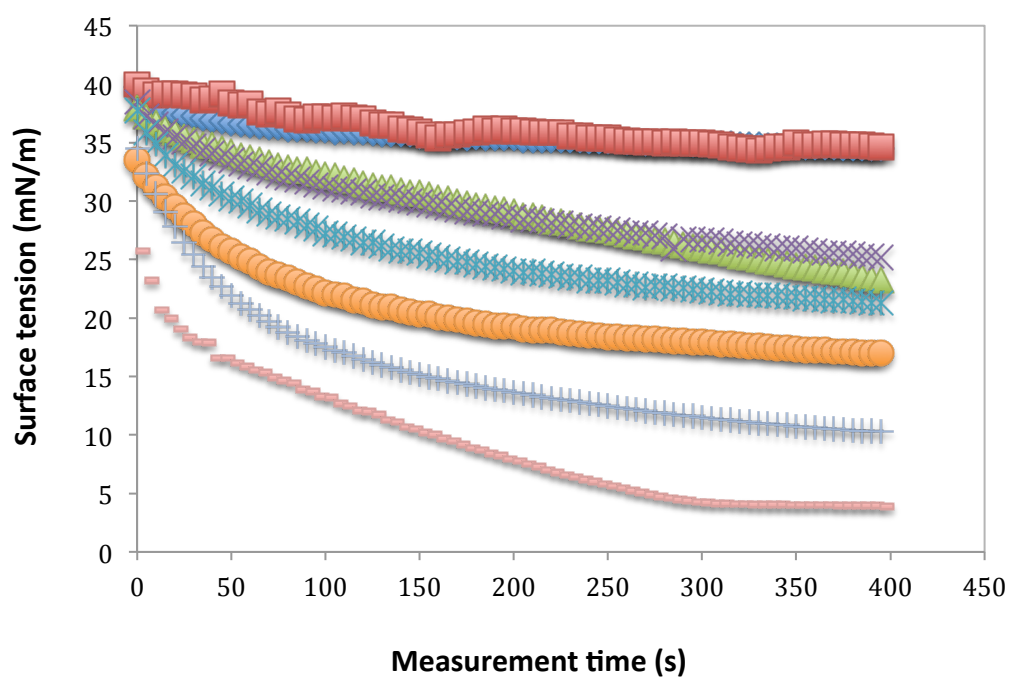


Figure A-2 Interfacial tension (oil-water) of native α_{s1} -casein solutions measured using a pendant drop tensiometer. α_{s1} -Casein solutions with protein concentration (w/w) of 0% (■), 0.001% (◆), 0.0025% (×), 0.005% (▲), 0.01% (×), 0.02% (●), 0.04% (+) and 0.08% (-).

Appendix B: T2 relaxation constant of casein solutions

The preliminary experiments of T2 relaxation constant measurement showed the relationship of water exchange with proteins, while the values are different when the T2 plots were normalised. The curves collapse onto each other in the normalized data indicated that the exchange environment of each solution is the same, thus any observed differences in the T2 value was only a property of the hydration behaviour of the protein solution.

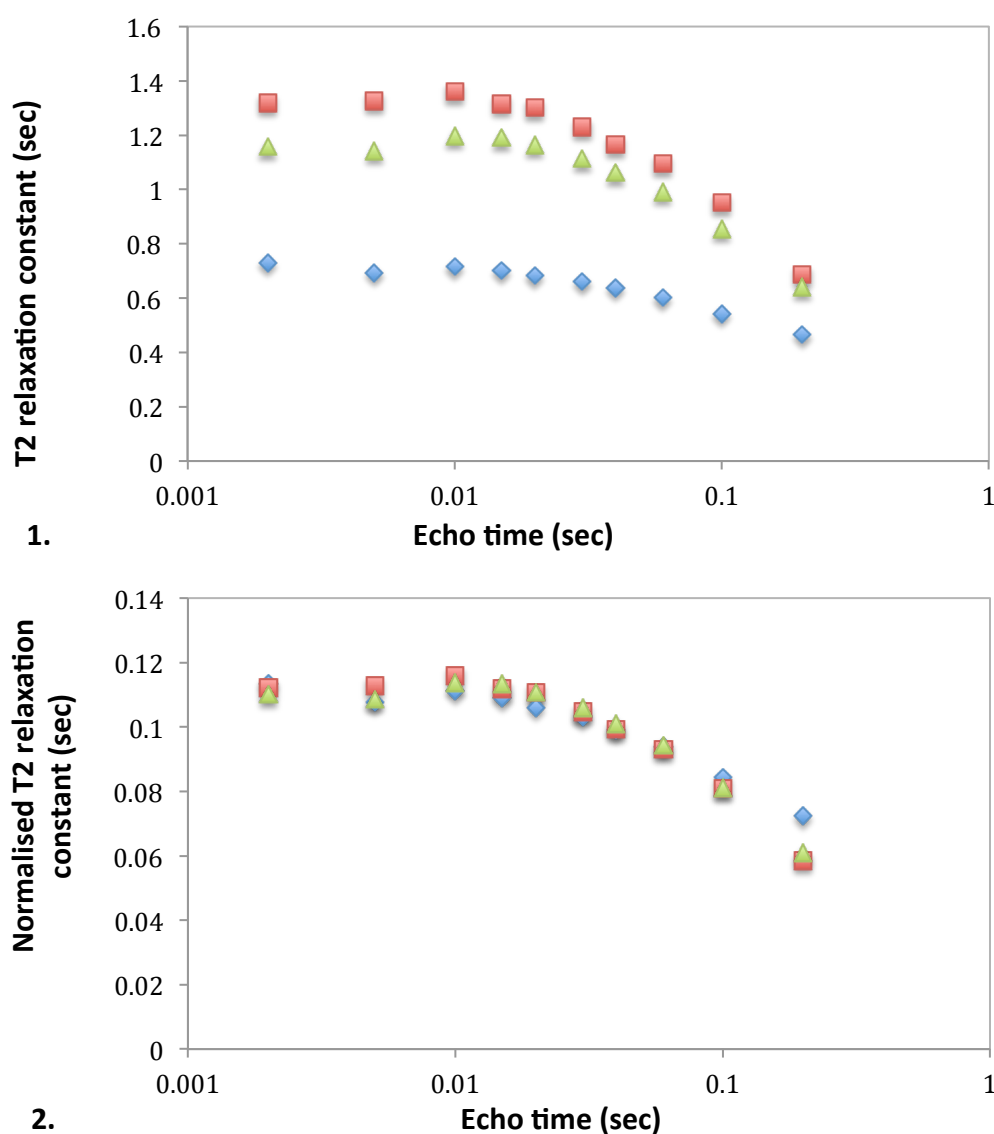


Figure B T2 relaxation constant (1) and normalised T2 constant (2) of native α_{s1} -casein solution (1% w/w, \blacklozenge), succinylated α_{s1} -casein solution (3% w/w, \blacksquare) and dephosphorylated α_{s1} -casein solution (1% w/w, \blacktriangle) at different echo times.

Appendix C: LC-MS/MS results

Appendix C1: peptides of trypsin-digested native α_{s1} -casein

[CAS1_BOVIN_B](#) Mass: 22960 Score: 2633 Queries matched: 72 emPAI: 116.03

(P02662) Alpha-S1 casein B - Bos taurus (Bovine).

Query	Observed	Mr(expt)	Mr(calc)	ppm	Score	Expect	Peptide
20	748.37	747.36	747.36	3.18	(15)	0.033	K.TTMPLW.-
21	748.37	747.37	747.36	3.51	(12)	0.059	K.TTMPLW.-
23	748.37	747.37	747.36	3.65	(9)	0.12	K.TTMPLW.-
25	748.37	747.37	747.36	4.07	(12)	0.061	K.TTMPLW.-
26	374.69	747.37	747.36	5.30	24	0.0042	K.TTMPLW.-
27	748.37	747.37	747.36	5.40	(14)	0.042	K.TTMPLW.-
289	524.26	1046.50	1046.51	-13.28	2	0.67	K.EKVNLSK.D
476	1267.70	1266.69	1266.70	-3.68	(0)	0.93	R.YLGYLEQLLR.L
477	1267.71	1266.70	1266.70	1.29	(22)	0.0065	R.YLGYLEQLLR.L
478	1267.71	1266.70	1266.70	2.24	(20)	0.01	R.YLGYLEQLLR.L
479	634.36	1266.70	1266.70	2.34	(62)	6.8e-007	R.YLGYLEQLLR.L
480	423.24	1266.70	1266.70	3.50	(40)	0.00011	R.YLGYLEQLLR.L
481	634.36	1266.70	1266.70	3.85	(63)	5.6e-007	R.YLGYLEQLLR.L
482	634.36	1266.70	1266.70	3.88	64	3.6e-007	R.YLGYLEQLLR.L
483	634.36	1266.70	1266.70	4.23	(59)	1.2e-006	R.YLGYLEQLLR.L
484	634.36	1266.70	1266.70	5.94	(62)	6.9e-007	R.YLGYLEQLLR.L
485	1267.71	1266.70	1266.70	5.95	(1)	0.87	R.YLGYLEQLLR.L
488	1268.69	1267.69	1267.68	3.65	(22)	0.0059	R.YLGYLEQLLR.L
489	634.85	1267.69	1267.68	7.61	(63)	5.2e-007	R.YLGYLEQLLR.L
612	1384.73	1383.73	1383.72	2.16	(48)	1.4e-005	R.FFVAPFPEVFGK.E
613	692.87	1383.73	1383.72	2.71	(36)	0.00023	R.FFVAPFPEVFGK.E
614	692.87	1383.73	1383.72	3.54	(35)	0.00034	R.FFVAPFPEVFGK.E
615	692.87	1383.73	1383.72	3.84	(41)	8.4e-005	R.FFVAPFPEVFGK.E
616	692.87	1383.73	1383.72	4.95	(41)	8.1e-005	R.FFVAPFPEVFGK.E
617	692.87	1383.73	1383.72	5.50	58	1.7e-006	R.FFVAPFPEVFGK.E
780	830.90	1659.79	1659.79	2.31	(63)	5.3e-007	K.VPQLEIVPNSAEER.L + Phospho (ST)
781	554.27	1659.79	1659.79	4.21	(53)	5e-006	K.VPQLEIVPNSAEER.L + Phospho (ST)
782	830.90	1659.79	1659.79	4.42	(67)	2.1e-007	K.VPQLEIVPNSAEER.L + Phospho (ST)
784	554.60	1660.78	1660.77	3.14	(68)	1.7e-007	K.VPQLEIVPNSAEER.L + Phospho (ST)
785	831.40	1660.78	1660.77	4.60	87	1.8e-009	K.VPQLEIVPNSAEER.L + Phospho (ST)
828	880.47	1758.93	1758.94	-3.02	(49)	1.2e-005	K.HQGLPQEVNLNLLR.F
829	587.32	1758.93	1758.94	-2.08	(40)	9.1e-005	K.HQGLPQEVNLNLLR.F
830	880.48	1758.94	1758.94	0.41	(66)	2.8e-007	K.HQGLPQEVNLNLLR.F
831	880.48	1758.94	1758.94	1.19	(90)	1e-009	K.HQGLPQEVNLNLLR.F
832	587.32	1758.94	1758.94	1.40	(71)	8.7e-008	K.HQGLPQEVNLNLLR.F
833	880.48	1758.94	1758.94	1.48	(72)	6.3e-008	K.HQGLPQEVNLNLLR.F
834	880.48	1758.94	1758.94	2.10	(56)	2.3e-006	K.HQGLPQEVNLNLLR.F
835	880.48	1758.94	1758.94	2.86	(35)	0.00029	K.HQGLPQEVNLNLLR.F
836	587.32	1758.94	1758.94	3.16	(50)	9.7e-006	K.HQGLPQEVNLNLLR.F
837	880.48	1758.94	1758.94	3.36	(122)	6.6e-013	K.HQGLPQEVNLNLLR.F
838	587.32	1758.94	1758.94	3.79	(73)	5e-008	K.HQGLPQEVNLNLLR.F
839	880.97	1759.93	1759.92	3.97	(119)	1.2e-012	K.HQGLPQEVNLNLLR.F
840	587.65	1759.93	1759.92	4.28	(47)	1.9e-005	K.HQGLPQEVNLNLLR.F
841	587.65	1759.93	1759.92	4.79	(66)	2.3e-007	K.HQGLPQEVNLNLLR.F

842	880.97	1759.93	1759.92	5.37	127	2e-013	K.HQGLPQEVNLNENLLR.F
888	924.37	1846.72	1846.72	2.57	92	6.4e-010	K.DIGSESTEDQAMEDIK.Q + Phospho (ST)
889	616.58	1846.72	1846.72	3.29	(6)	0.28	K.DIGSESTEDQAMEDIK.Q + Phospho (ST)
914	964.35	1926.69	1926.68	1.39	(56)	2.6e-006	K.DIGSESTEDQAMEDIK.Q + 2 Phospho (ST)
915	964.35	1926.69	1926.68	2.53	(46)	2.8e-005	K.DIGSESTEDQAMEDIK.Q + 2 Phospho (ST)
916	643.24	1926.69	1926.68	4.20	(34)	0.00039	K.DIGSESTEDQAMEDIK.Q + 2 Phospho (ST)
917	964.35	1926.69	1926.68	4.83	(70)	9.5e-008	K.DIGSESTEDQAMEDIK.Q + 2 Phospho (ST)
918	643.24	1926.69	1926.68	5.12	(53)	4.7e-006	K.DIGSESTEDQAMEDIK.Q + 2 Phospho (ST)
929	651.33	1950.96	1950.95	5.18	(58)	1.5e-006	K.YKVPQLEIVPNSAEER.L + Phospho (ST)
930	976.49	1950.96	1950.95	5.74	(77)	1.9e-008	K.YKVPQLEIVPNSAEER.L + Phospho (ST)
931	976.98	1951.94	1951.93	6.83	81	8.6e-009	K.YKVPQLEIVPNSAEER.L + Phospho (ST)
932	651.65	1951.94	1951.93	7.08	(59)	1.2e-006	K.YKVPQLEIVPNSAEER.L + Phospho (ST)
1056	746.08	2235.23	2235.21	6.43	73	5.2e-008	K.HPIKHQGLPQEVNLNENLLR.F
1147	866.69	2597.06	2597.05	2.53	(42)	6.6e-005	K.VNELSKDIGSESTEDQAMEDIK.Q + 2 Phospho (ST)
1155	1320.98	2639.94	2639.94	1.65	(26)	0.0026	K.QMEAESISSSEIIVPNSVEQK.H + 4 Phospho (ST)
1156	880.99	2639.95	2639.94	4.08	(35)	0.00035	K.QMEAESISSSEIIVPNSVEQK.H + 4 Phospho (ST)
1157	1320.98	2639.95	2639.94	4.68	47	1.9e-005	K.QMEAESISSSEIIVPNSVEQK.H + 4 Phospho (ST)
1163	893.35	2677.02	2677.02	1.05	(48)	1.5e-005	K.VNELSKDIGSESTEDQAMEDIK.Q + 3 Phospho (ST)
1164	893.35	2677.02	2677.02	2.51	(45)	3.2e-005	K.VNELSKDIGSESTEDQAMEDIK.Q + 3 Phospho (ST)
1165	1339.52	2677.02	2677.02	3.32	51	8.1e-006	K.VNELSKDIGSESTEDQAMEDIK.Q + 3 Phospho (ST)
1166	1339.53	2677.04	2677.02	9.44	(45)	3.3e-005	K.VNELSKDIGSESTEDQAMEDIK.Q + 3 Phospho (ST)
1180	907.65	2719.91	2719.91	2.92	(20)	0.011	K.QMEAESISSSEIIVPNSVEQK.H + 5 Phospho (ST)
1181	1360.96	2719.92	2719.91	3.54	(29)	0.0012	K.QMEAESISSSEIIVPNSVEQK.H + 5 Phospho (ST)
1182	907.65	2719.92	2719.91	4.64	(27)	0.0018	K.QMEAESISSSEIIVPNSVEQK.H + 5 Phospho (ST)
1183	907.98	2720.91	2720.89	8.56	(9)	0.12	K.QMEAESISSSEIIVPNSVEQK.H + 5 Phospho (ST)
1220	952.40	2854.19	2854.19	1.49	(53)	5.2e-006	K.EKVNELSKDIGSESTEDQAMEDIK.Q + 2 Phospho (ST)
1229	979.06	2934.16	2934.15	2.08	60	1.1e-006	K.EKVNELSKDIGSESTEDQAMEDIK.Q + 3 Phospho (ST)
1230	1468.09	2934.17	2934.15	4.48	(18)	0.017	K.EKVNELSKDIGSESTEDQAMEDIK.Q + 3 Phospho (ST)

Appendix C2: peptides of trypsin-digested native α_{s1} -casein with heat treatment

CAS1_BOVIN_B Mass: 22960 Score: 3140 Queries matched: 81 emPAI: 156.64

(P02662) Alpha-S1 casein B - Bos taurus (Bovine).

Query	Observed	Mr(expt)	Mr(calc)	ppm	Score	Expect	Peptide
18	748.37	747.36	747.36	2.98	(12)	0.065	K.TTMPLW.-
21	374.69	747.37	747.36	4.57	22	0.0059	K.TTMPLW.-
22	748.37	747.37	747.36	4.74	(14)	0.04	K.TTMPLW.-
23	748.37	747.37	747.36	4.92	(14)	0.042	K.TTMPLW.-
24	748.37	747.37	747.36	6.48	(8)	0.15	K.TTMPLW.-
462	1267.71	1266.70	1266.70	0.82	(45)	3.5e-005	R.YLGYLEQLLR.L
463	1267.71	1266.70	1266.70	0.90	(18)	0.015	R.YLGYLEQLLR.L
464	634.36	1266.70	1266.70	1.64	(57)	1.8e-006	R.YLGYLEQLLR.L
465	1267.71	1266.70	1266.70	3.90	(35)	0.00031	R.YLGYLEQLLR.L
466	634.36	1266.70	1266.70	4.48	(63)	5.3e-007	R.YLGYLEQLLR.L
467	634.36	1266.70	1266.70	4.81	(57)	1.9e-006	R.YLGYLEQLLR.L
468	1267.71	1266.70	1266.70	5.40	(25)	0.0031	R.YLGYLEQLLR.L
469	634.36	1266.70	1266.70	5.46	(62)	6.8e-007	R.YLGYLEQLLR.L
470	634.36	1266.70	1266.70	5.56	(64)	4.2e-007	R.YLGYLEQLLR.L
471	634.36	1266.71	1266.70	7.03	(61)	8.1e-007	R.YLGYLEQLLR.L
472	423.24	1266.71	1266.70	9.42	(43)	5.1e-005	R.YLGYLEQLLR.L
475	634.85	1267.69	1267.68	4.74	76	2.6e-008	R.YLGYLEQLLR.L
603	692.87	1383.73	1383.72	2.96	(20)	0.01	R.FFVAPFPEVFGK.E
604	1384.73	1383.73	1383.72	3.39	(36)	0.00026	R.FFVAPFPEVFGK.E
605	692.87	1383.73	1383.72	3.64	(59)	1.4e-006	R.FFVAPFPEVFGK.E
606	692.87	1383.73	1383.72	4.69	(49)	1.4e-005	R.FFVAPFPEVFGK.E
607	1384.74	1383.73	1383.72	4.91	(29)	0.0013	R.FFVAPFPEVFGK.E
608	692.87	1383.73	1383.72	5.39	(58)	1.7e-006	R.FFVAPFPEVFGK.E
609	1384.74	1383.73	1383.72	6.28	(14)	0.039	R.FFVAPFPEVFGK.E
610	692.87	1383.73	1383.72	7.24	62	6.4e-007	R.FFVAPFPEVFGK.E
761	821.44	1640.86	1640.86	1.96	61	7.2e-007	R.FFVAPFPEVFGKEK.V
768	830.90	1659.79	1659.79	2.43	(62)	6.3e-007	K.VPQLEIVPNSAEER.L + Phospho (ST)
769	830.90	1659.79	1659.79	3.61	71	7.7e-008	K.VPQLEIVPNSAEER.L + Phospho (ST)
770	554.27	1659.79	1659.79	4.09	(53)	4.9e-006	K.VPQLEIVPNSAEER.L + Phospho (ST)
772	554.60	1660.78	1660.77	6.21	(50)	9.1e-006	K.VPQLEIVPNSAEER.L + Phospho (ST)
773	831.40	1660.78	1660.77	7.65	(66)	2.5e-007	K.VPQLEIVPNSAEER.L + Phospho (ST)
814	880.48	1758.94	1758.94	0.49	(64)	4.4e-007	K.HQGLPQEVNLNLLR.F
815	880.48	1758.94	1758.94	2.19	(62)	6.8e-007	K.HQGLPQEVNLNLLR.F
816	880.48	1758.94	1758.94	2.28	(30)	0.00099	K.HQGLPQEVNLNLLR.F
817	880.48	1758.94	1758.94	3.00	(65)	3e-007	K.HQGLPQEVNLNLLR.F
818	880.48	1758.94	1758.94	3.09	(52)	6.2e-006	K.HQGLPQEVNLNLLR.F
819	880.48	1758.95	1758.94	4.18	(78)	1.5e-008	K.HQGLPQEVNLNLLR.F
820	880.48	1758.95	1758.94	4.65	(69)	1.4e-007	K.HQGLPQEVNLNLLR.F
821	880.48	1758.95	1758.94	4.88	(108)	1.6e-011	K.HQGLPQEVNLNLLR.F
822	587.32	1758.95	1758.94	4.95	(51)	7.2e-006	K.HQGLPQEVNLNLLR.F
823	587.32	1758.95	1758.94	5.39	(75)	3.2e-008	K.HQGLPQEVNLNLLR.F
824	587.65	1759.93	1759.92	3.84	(57)	1.9e-006	K.HQGLPQEVNLNLLR.F
825	587.65	1759.93	1759.92	4.31	(61)	7.9e-007	K.HQGLPQEVNLNLLR.F
826	880.97	1759.93	1759.92	6.53	(109)	1.4e-011	K.HQGLPQEVNLNLLR.F
827	880.97	1759.93	1759.92	7.12	116	2.4e-012	K.HQGLPQEVNLNLLR.F
828	881.46	1760.91	1760.91	3.12	(100)	9e-011	K.HQGLPQEVNLNLLR.F

879	924.37	1846.73	1846.72	6.06	88	1.4e-009	K.DIGSESTEDQAMEDIK.Q + Phospho (ST)
902	964.35	1926.69	1926.68	2.10	(49)	1.3e-005	K.DIGSESTEDQAMEDIK.Q + 2 Phospho (ST)
903	964.35	1926.69	1926.68	2.40	(71)	8.5e-008	K.DIGSESTEDQAMEDIK.Q + 2 Phospho (ST)
904	964.35	1926.69	1926.68	2.46	(45)	2.8e-005	K.DIGSESTEDQAMEDIK.Q + 2 Phospho (ST)
905	964.35	1926.69	1926.68	2.63	(49)	1.4e-005	K.DIGSESTEDQAMEDIK.Q + 2 Phospho (ST)
906	643.24	1926.69	1926.68	3.14	(52)	6.7e-006	K.DIGSESTEDQAMEDIK.Q + 2 Phospho (ST)
907	964.35	1926.69	1926.68	3.52	(66)	2.8e-007	K.DIGSESTEDQAMEDIK.Q + 2 Phospho (ST)
908	643.57	1927.68	1927.67	5.39	(45)	3.1e-005	K.DIGSESTEDQAMEDIK.Q + 2 Phospho (ST)
916	651.32	1950.95	1950.95	0.48	(42)	6.3e-005	K.YKVPQLEIVPN\$AEER.L + Phospho (ST)
917	976.48	1950.95	1950.95	4.32	84	3.7e-009	K.YKVPQLEIVPN\$AEER.L + Phospho (ST)
918	651.33	1950.95	1950.95	4.72	(49)	1.2e-005	K.YKVPQLEIVPN\$AEER.L + Phospho (ST)
920	651.66	1951.95	1951.93	9.66	(51)	8.7e-006	K.YKVPQLEIVPN\$AEER.L + Phospho (ST)
921	976.98	1951.95	1951.93	9.99	(72)	6e-008	K.YKVPQLEIVPN\$AEER.L + Phospho (ST)
1041	746.08	2235.22	2235.21	3.81	67	2e-007	K.HPIKHQGLPQEVLNENLLR.F
1068	772.72	2315.14	2315.13	5.36	(65)	3.5e-007	K.EPMIGVQNQLAYFYPELFR.Q
1069	1158.58	2315.14	2315.13	5.72	106	2.8e-011	K.EPMIGVQNQLAYFYPELFR.Q
1120	863.45	2587.32	2587.33	-2.65	7	0.2	K.HIQKEDVPSEYRLGYLEQLLR.L
1121	863.45	2587.32	2587.33	-2.06	(0)	0.95	K.HIQKEDVPSEYRLGYLEQLLR.L
1136	1320.98	2639.95	2639.94	2.79	(27)	0.0022	K.QMEAES\$SSSEIVPNSVEQK.H + 4 Phospho (ST)
1137	880.99	2639.95	2639.94	2.92	(33)	0.00049	K.QMEAES\$SSSEIVPNSVEQK.H + 4 Phospho (ST)
1138	1320.98	2639.95	2639.94	4.68	42	6.1e-005	K.QMEAES\$SSSEIVPNSVEQK.H + 4 Phospho (ST)
1139	880.99	2639.96	2639.94	6.72	(18)	0.015	K.QMEAES\$SSSEIVPNSVEQK.H + 4 Phospho (ST)
1144	1339.52	2677.02	2677.02	2.12	(53)	4.8e-006	K.VNEL\$KDIGSESTEDQAMEDIK.Q + 3 Phospho (ST)
1145	893.35	2677.02	2677.02	3.19	64	4.4e-007	K.VNEL\$KDIGSESTEDQAMEDIK.Q + 3 Phospho (ST)
1159	1360.96	2719.91	2719.91	1.63	(21)	0.0071	K.QMEAES\$SSSEIVPNSVEQK.H + 5 Phospho (ST)
1160	1360.96	2719.91	2719.91	2.44	(23)	0.0053	K.QMEAES\$SSSEIVPNSVEQK.H + 5 Phospho (ST)
1161	907.64	2719.91	2719.91	2.58	(23)	0.0055	K.QMEAES\$SSSEIVPNSVEQK.H + 5 Phospho (ST)
1202	952.41	2854.20	2854.19	3.93	(37)	0.00021	K.EKVNEL\$KDIGSESTEDQAMEDIK.Q + 2 Phospho (ST)
1211	979.06	2934.15	2934.15	-0.07	71	7.2e-008	K.EKVNEL\$KDIGSESTEDQAMEDIK.Q + 3 Phospho (ST)
1212	979.06	2934.16	2934.15	1.30	(47)	2.1e-005	K.EKVNEL\$KDIGSESTEDQAMEDIK.Q + 3 Phospho (ST)
1213	734.55	2934.16	2934.15	2.25	(28)	0.0015	K.EKVNEL\$KDIGSESTEDQAMEDIK.Q + 3 Phospho (ST)
1214	1468.09	2934.16	2934.15	2.37	(42)	6e-005	K.EKVNEL\$KDIGSESTEDQAMEDIK.Q + 3 Phospho (ST)
1266	1069.87	3206.60	3206.59	3.25	88	1.7e-009	K.EGIHAQQKEPMIGVQNQLAYFYPELFR.Q
1267	802.66	3206.60	3206.59	4.36	(18)	0.016	K.EGIHAQQKEPMIGVQNQLAYFYPELFR.Q
1304	1572.73	4715.18	4715.17	3.60	50	1.1e-005	R.QFYQLDAYPSGAWYYVPLGTQYTDAPSFSDIPNPIGSENSEK.T

Appendix C3: peptides of trypsin-digested dephosphorylated α_{s1} -casein at an incubation time of 20 min.

CAS1_BOVIN_B Mass: 22960 Score: 4057 Queries matched: 92 emPAI: 2037.22

(P02662) Alpha-S1 casein B - Bos taurus (Bovine).

Query	Observed	Mr(expt)	Mr(calc)	ppm	Score	Expect	Peptide
19	748.37	747.37	747.36	3.57	(13)	0.051	K.TTMPLW.-
20	748.37	747.37	747.36	5.63	(3)	0.46	K.TTMPLW.-
21	748.37	747.37	747.36	5.80	(15)	0.029	K.TTMPLW.-
22	374.69	747.37	747.36	6.18	23	0.0045	K.TTMPLW.-
23	748.37	747.37	747.36	6.39	(16)	0.024	K.TTMPLW.-
421	1267.71	1266.70	1266.70	2.55	(8)	0.17	R.YLGYLEQLLR.L
422	1267.71	1266.70	1266.70	2.79	(34)	0.00039	R.YLGYLEQLLR.L
423	1267.71	1266.70	1266.70	2.87	(4)	0.38	R.YLGYLEQLLR.L
424	1267.71	1266.70	1266.70	3.42	(30)	0.0011	R.YLGYLEQLLR.L
425	634.36	1266.70	1266.70	4.39	(49)	1.2e-005	R.YLGYLEQLLR.L
426	634.36	1266.70	1266.70	4.45	(57)	2e-006	R.YLGYLEQLLR.L
427	423.24	1266.70	1266.70	4.49	(42)	6.3e-005	R.YLGYLEQLLR.L
428	634.36	1266.70	1266.70	5.21	(60)	1.1e-006	R.YLGYLEQLLR.L
429	634.36	1266.70	1266.70	5.34	(61)	7.2e-007	R.YLGYLEQLLR.L
430	634.36	1266.71	1266.70	6.36	(61)	7.5e-007	R.YLGYLEQLLR.L
431	423.24	1266.71	1266.70	6.67	(41)	8.1e-005	R.YLGYLEQLLR.L
434	1268.69	1267.68	1267.68	2.94	(25)	0.0031	R.YLGYLEQLLR.L
435	634.85	1267.69	1267.68	6.15	68	1.4e-007	R.YLGYLEQLLR.L
551	1384.73	1383.73	1383.72	1.80	(48)	1.5e-005	R.FFVAPFPEVFGK.E
552	692.87	1383.73	1383.72	3.23	(38)	0.00018	R.FFVAPFPEVFGK.E
553	692.87	1383.73	1383.72	5.76	57	1.8e-006	R.FFVAPFPEVFGK.E
666	527.62	1579.83	1579.82	3.57	(27)	0.0022	K.VPQLEIVPNSAEER.L
667	790.92	1579.83	1579.82	3.98	(81)	7.8e-009	K.VPQLEIVPNSAEER.L
669	791.41	1580.81	1580.80	2.90	(58)	1.7e-006	K.VPQLEIVPNSAEER.L
700	830.90	1659.79	1659.79	3.99	(58)	1.8e-006	K.VPQLEIVPNSAEER.L + Phospho (ST)
701	554.27	1659.80	1659.79	6.80	(61)	7.7e-007	K.VPQLEIVPNSAEER.L + Phospho (ST)
702	831.40	1660.78	1660.77	3.44	84	4.2e-009	K.VPQLEIVPNSAEER.L Phospho (ST)
703	554.60	1660.78	1660.77	6.86	(50)	9.2e-006	K.VPQLEIVPNSAEER.L Phospho (ST)
747	880.48	1758.94	1758.94	-0.07	(61)	8.1e-007	K.HQGLPQEVNENLLR.F
748	587.32	1758.94	1758.94	0.43	(49)	1.2e-005	K.HQGLPQEVNENLLR.F
749	880.48	1758.94	1758.94	2.49	(60)	9.7e-007	K.HQGLPQEVNENLLR.F
750	880.48	1758.94	1758.94	2.86	(93)	4.9e-010	K.HQGLPQEVNENLLR.F
751	587.32	1758.94	1758.94	3.42	(54)	3.9e-006	K.HQGLPQEVNENLLR.F
752	880.48	1758.94	1758.94	4.11	(67)	1.9e-007	K.HQGLPQEVNENLLR.F
753	587.32	1758.95	1758.94	6.69	(60)	9.6e-007	K.HQGLPQEVNENLLR.F
754	880.48	1758.95	1758.94	7.08	(110)	1e-011	K.HQGLPQEVNENLLR.F
755	880.97	1759.93	1759.92	2.70	(110)	8.9e-012	K.HQGLPQEVNENLLR.F
756	587.65	1759.93	1759.92	3.68	(51)	7.3e-006	K.HQGLPQEVNENLLR.F
757	880.97	1759.93	1759.92	4.42	118	1.6e-012	K.HQGLPQEVNENLLR.F
758	587.65	1759.93	1759.92	5.23	(79)	1.1e-008	K.HQGLPQEVNENLLR.F
759	880.98	1759.94	1759.92	11.3	(82)	6e-009	K.HQGLPQEVNENLLR.F
767	884.39	1766.76	1766.75	2.39	(103)	5.3e-011	K.DIGSESTEDQAMEDIK.Q
768	884.39	1766.76	1766.75	3.30	128	1.5e-013	K.DIGSESTEDQAMEDIK.Q
769	884.39	1766.76	1766.75	3.32	(90)	1.1e-009	K.DIGSESTEDQAMEDIK.Q

770	884.39	1766.76	1766.75	3.36	(97)	1.9e-010	K.DIGSESTEDQAMEDIK.Q
771	589.93	1766.76	1766.75	4.14	(40)	9.1e-005	K.DIGSESTEDQAMEDIK.Q
772	589.93	1766.76	1766.75	5.06	(64)	3.8e-007	K.DIGSESTEDQAMEDIK.Q
773	884.88	1767.75	1767.74	5.31	(125)	3.3e-013	K.DIGSESTEDQAMEDIK.Q
829	924.37	1846.72	1846.72	2.16	(71)	8.2e-008	K.DIGSESTEDQAMEDIK.Q + Phospho (ST)
830	616.58	1846.72	1846.72	3.60	(56)	2.6e-006	K.DIGSESTEDQAMEDIK.Q + Phospho (ST)
831	924.37	1846.73	1846.72	4.63	(82)	6.9e-009	K.DIGSESTEDQAMEDIK.Q + Phospho (ST)
840	936.50	1870.99	1870.98	3.48	(69)	1.2e-007	K.YKVPQLEIVPNSAEER.L
841	624.67	1870.99	1870.98	3.66	(46)	2.6e-005	K.YKVPQLEIVPNSAEER.L
842	936.99	1871.97	1871.96	4.49	(75)	3.1e-008	K.YKVPQLEIVPNSAEER.L
843	625.00	1871.97	1871.96	4.58	(55)	3e-006	K.YKVPQLEIVPNSAEER.L
873	964.35	1926.69	1926.68	4.05	(66)	2.7e-007	K.DIGSESTEDQAMEDIK.Q + 2 Phospho (ST)
874	643.24	1926.70	1926.68	6.14	(58)	1.5e-006	K.DIGSESTEDQAMEDIK.Q + 2 Phospho (ST)
880	976.48	1950.95	1950.95	3.96	89	1.4e-009	K.YKVPQLEIVPNSAEER.L + Phospho (ST)
881	651.32	1950.95	1950.95	3.98	(50)	9.2e-006	K.YKVPQLEIVPNSAEER.L + Phospho (ST)
882	651.33	1950.95	1950.95	4.58	(65)	3.1e-007	K.YKVPQLEIVPNSAEER.L + Phospho (ST)
884	651.66	1951.95	1951.93	9.54	(49)	1.2e-005	K.YKVPQLEIVPNSAEER.L + Phospho (ST)
885	976.98	1951.95	1951.93	11.5	(85)	3.2e-009	K.YKVPQLEIVPNSAEER.L + Phospho (ST)
1040	774.37	2320.09	2320.07	4.96	(46)	2.8e-005	K.QMEAESISSSEIVPNSVEQK.H
1058	801.02	2400.05	2400.04	2.71	(40)	0.00011	K.QMEAESISSSEIVPNSVEQK.H + Phospho (ST)
1059	1201.03	2400.05	2400.04	2.89	73	4.7e-008	K.QMEAESISSSEIVPNSVEQK.H + Phospho (ST)
1060	801.03	2400.05	2400.04	5.89	(46)	2.4e-005	K.QMEAESISSSEIVPNSVEQK.H + Phospho (ST)
1061	801.35	2401.03	2401.02	2.45	(37)	0.0002	K.QMEAESISSSEIVPNSVEQK.H + Phospho (ST)
1089	1241.01	2480.01	2480.01	-0.48	(41)	7.7e-005	K.QMEAESISSSEIVPNSVEQK.H + 2 Phospho (ST)
1090	1241.01	2480.01	2480.01	1.86	(62)	6.7e-007	K.QMEAESISSSEIVPNSVEQK.H + 2 Phospho (ST)
1091	827.68	2480.01	2480.01	2.39	(39)	0.00012	K.QMEAESISSSEIVPNSVEQK.H + 2 Phospho (ST)
1092	827.68	2480.01	2480.01	2.96	(50)	9.4e-006	K.QMEAESISSSEIVPNSVEQK.H + 2 Phospho (ST)
1093	827.68	2480.01	2480.01	2.96	(47)	1.9e-005	K.QMEAESISSSEIVPNSVEQK.H + 2 Phospho (ST)
1105	1259.55	2517.09	2517.08	2.52	99	1.3e-010	K.VNELSKDIGSESTEDQAMEDIK.Q + Phospho (ST)
1106	840.04	2517.09	2517.08	3.33	(70)	9.6e-008	K.VNELSKDIGSESTEDQAMEDIK.Q + Phospho (ST)
1122	1280.99	2559.97	2559.97	-0.59	(44)	4.3e-005	K.QMEAESISSSEIVPNSVEQK.H + 3 Phospho (ST)
1123	1280.99	2559.97	2559.97	-0.20	(54)	4.2e-006	K.QMEAESISSSEIVPNSVEQK.H + 3 Phospho (ST)
1124	1281.00	2559.98	2559.97	1.36	(51)	7.4e-006	K.QMEAESISSSEIVPNSVEQK.H + 3 Phospho (ST)
1125	854.33	2559.98	2559.97	2.51	(45)	3.2e-005	K.QMEAESISSSEIVPNSVEQK.H + 3 Phospho (ST)
1126	854.33	2559.98	2559.97	3.45	(15)	0.029	K.QMEAESISSSEIVPNSVEQK.H + 3 Phospho (ST)
1127	854.34	2559.99	2559.97	5.59	(46)	2.3e-005	K.QMEAESISSSEIVPNSVEQK.H + 3 Phospho (ST)
1128	1281.49	2560.96	2560.96	1.67	(29)	0.0011	K.QMEAESISSSEIVPNSVEQK.H + 3 Phospho (ST)
1136	1299.53	2597.05	2597.05	0.93	(58)	1.8e-006	K.VNELSKDIGSESTEDQAMEDIK.Q + 2 Phospho (ST)
1137	866.69	2597.06	2597.05	4.42	(53)	4.9e-006	K.VNELSKDIGSESTEDQAMEDIK.Q + 2 Phospho (ST)
1138	867.03	2598.06	2598.03	8.37	(43)	5.4e-005	K.VNELSKDIGSESTEDQAMEDIK.Q + 2 Phospho (ST)
1144	880.99	2639.95	2639.94	2.54	(32)	0.00066	K.QMEAESISSSEIVPNSVEQK.H + 4 Phospho (ST)
1145	1320.98	2639.95	2639.94	3.62	(53)	5e-006	K.QMEAESISSSEIVPNSVEQK.H + 4 Phospho (ST)
1181	925.75	2774.23	2774.22	2.30	(67)	2.2e-007	K.EKVNELSKDIGSESTEDQAMEDIK.Q + Phospho (ST)
1182	1388.12	2774.23	2774.22	2.38	(51)	7.5e-006	K.EKVNELSKDIGSESTEDQAMEDIK.Q + Phospho (ST)
1183	694.56	2774.23	2774.22	2.93	(39)	0.00013	K.EKVNELSKDIGSESTEDQAMEDIK.Q + Phospho (ST)
1184	926.08	2775.21	2775.20	3.20	(62)	5.7e-007	K.EKVNELSKDIGSESTEDQAMEDIK.Q + Phospho (ST)
1203	952.41	2854.19	2854.19	2.27	78	1.4e-008	K.EKVNELSKDIGSESTEDQAMEDIK.Q + 2 Phospho (ST)

Appendix C4: peptides of trypsin-digested dephosphorylated α_{s1} -casein at an incubation time of 90 min.

[CAS1_BOVIN_B](#) Mass: 22960 Score: 4362 Queries matched: 93 emPAI: 524.94

(P02662) Alpha-S1 casein B - Bos taurus (Bovine).

Query	Observed	Mr(expt)	Mr(calc)	ppm	Score	Expect	Peptide
19	748.37	747.36	747.36	-0.05	(11)	0.089	K.TTMPLW.-
21	748.37	747.37	747.36	3.74	(13)	0.05	K.TTMPLW.-
22	748.37	747.37	747.36	4.40	(13)	0.048	K.TTMPLW.-
23	748.37	747.37	747.36	4.45	(13)	0.053	K.TTMPLW.-
25	374.69	747.37	747.36	5.11	27	0.0021	K.TTMPLW.-
26	748.37	747.37	747.36	5.59	(16)	0.028	K.TTMPLW.-
27	748.37	747.37	747.36	5.65	(13)	0.056	K.TTMPLW.-
440	1267.70	1266.70	1266.70	0.03	(32)	0.00059	R.YLGYLEQLLR.L
441	1267.71	1266.70	1266.70	1.29	(14)	0.044	R.YLGYLEQLLR.L
442	1267.71	1266.70	1266.70	1.53	(15)	0.034	R.YLGYLEQLLR.L
443	634.36	1266.70	1266.70	2.51	(53)	5.6e-006	R.YLGYLEQLLR.L
444	423.24	1266.70	1266.70	2.91	(35)	0.00033	R.YLGYLEQLLR.L
445	634.36	1266.70	1266.70	3.06	(55)	3e-006	R.YLGYLEQLLR.L
446	634.36	1266.70	1266.70	3.31	72	6.5e-008	R.YLGYLEQLLR.L
447	634.36	1266.70	1266.70	3.63	(60)	9e-007	R.YLGYLEQLLR.L
448	634.36	1266.70	1266.70	4.37	(58)	1.7e-006	R.YLGYLEQLLR.L
449	634.36	1266.70	1266.70	4.67	(58)	1.8e-006	R.YLGYLEQLLR.L
450	634.36	1266.70	1266.70	5.29	(61)	7.2e-007	R.YLGYLEQLLR.L
453	1268.69	1267.68	1267.68	1.12	(27)	0.0022	R.YLGYLEQLLR.L
454	634.85	1267.69	1267.68	4.19	(69)	1.2e-007	R.YLGYLEQLLR.L
562	1384.74	1383.73	1383.72	4.33	(38)	0.00018	R.FFVAPFPEVFGK.E
563	692.87	1383.73	1383.72	4.46	(25)	0.003	R.FFVAPFPEVFGK.E
564	692.87	1383.73	1383.72	4.72	57	1.9e-006	R.FFVAPFPEVFGK.E
565	692.87	1383.73	1383.72	6.49	(36)	0.00026	R.FFVAPFPEVFGK.E
679	790.92	1579.83	1579.82	3.84	(54)	4.2e-006	K.VPQLEIVPNSAEER.L
681	791.41	1580.81	1580.80	2.05	(65)	3e-007	K.VPQLEIVPNSAEER.L
682	791.41	1580.81	1580.80	3.76	72	6.4e-008	K.VPQLEIVPNSAEER.L
711	554.27	1659.79	1659.79	4.07	(49)	1.3e-005	K.VPQLEIVPNSAEER.L + Phospho (ST)
712	830.90	1659.79	1659.79	4.09	(70)	9.8e-008	K.VPQLEIVPNSAEER.L + Phospho (ST)
713	831.40	1660.78	1660.77	4.95	(71)	8.2e-008	K.VPQLEIVPNSAEER.L + Phospho (ST)
714	554.60	1660.78	1660.77	5.11	(51)	8.1e-006	K.VPQLEIVPNSAEER.L + Phospho (ST)
756	880.47	1758.93	1758.94	-4.14	(67)	1.8e-007	K.HQGLPQEVNLNLLR.F
757	880.48	1758.94	1758.94	-0.79	(89)	1.3e-009	K.HQGLPQEVNLNLLR.F
758	880.48	1758.94	1758.94	0.58	(109)	1.2e-011	K.HQGLPQEVNLNLLR.F
759	587.32	1758.94	1758.94	2.22	(40)	0.0001	K.HQGLPQEVNLNLLR.F
760	587.32	1758.94	1758.94	2.65	(54)	3.6e-006	K.HQGLPQEVNLNLLR.F
761	880.48	1758.94	1758.94	3.04	(103)	5.2e-011	K.HQGLPQEVNLNLLR.F
762	880.48	1758.94	1758.94	3.08	(53)	4.7e-006	K.HQGLPQEVNLNLLR.F
763	880.48	1758.94	1758.94	3.41	(51)	7.5e-006	K.HQGLPQEVNLNLLR.F
764	880.48	1758.95	1758.94	4.95	(115)	3.3e-012	K.HQGLPQEVNLNLLR.F
765	587.32	1758.95	1758.94	6.28	(69)	1.1e-007	K.HQGLPQEVNLNLLR.F
766	587.65	1759.93	1759.92	3.39	(45)	3.2e-005	K.HQGLPQEVNLNLLR.F
767	880.97	1759.93	1759.92	6.25	(97)	1.9e-010	K.HQGLPQEVNLNLLR.F
768	587.65	1759.93	1759.92	6.50	(67)	2.2e-007	K.HQGLPQEVNLNLLR.F

769	880.98	1759.94	1759.92	8.15	119	1.2e-012	K.HQGLPQEVLNENLLR.F
770	881.46	1760.91	1760.91	1.01	(103)	4.5e-011	K.HQGLPQEVLNENLLR.F
771	587.98	1760.91	1760.91	4.03	(64)	4.3e-007	K.HQGLPQEVLNENLLR.F
777	884.38	1766.75	1766.75	-2.45	(112)	6.1e-012	K.DIGSESTEDQAMEDIK.Q
778	884.38	1766.75	1766.75	1.66	(101)	7.9e-011	K.DIGSESTEDQAMEDIK.Q
779	884.39	1766.76	1766.75	3.44	128	1.6e-013	K.DIGSESTEDQAMEDIK.Q
780	884.39	1766.76	1766.75	3.47	(100)	9.8e-011	K.DIGSESTEDQAMEDIK.Q
781	884.39	1766.76	1766.75	4.68	(107)	1.9e-011	K.DIGSESTEDQAMEDIK.Q
782	589.93	1766.76	1766.75	6.09	(90)	1.1e-009	K.DIGSESTEDQAMEDIK.Q
783	590.26	1767.75	1767.74	7.85	(24)	0.0037	K.DIGSESTEDQAMEDIK.Q
784	884.88	1767.75	1767.74	8.00	(106)	2.4e-011	K.DIGSESTEDQAMEDIK.Q
850	924.37	1846.72	1846.72	2.54	(85)	2.9e-009	K.DIGSESTEDQAMEDIK.Q + Phospho (ST)
851	616.58	1846.73	1846.72	4.41	(54)	4e-006	K.DIGSESTEDQAMEDIK.Q + Phospho (ST)
855	625.00	1871.97	1871.96	4.05	(49)	1.4e-005	K.YKVPQLEIVPNSAEER.L
856	937.00	1871.98	1871.96	7.58	(83)	4.5e-009	K.YKVPQLEIVPNSAEER.L
857	937.00	1871.98	1871.96	10.7	(80)	1e-008	K.YKVPQLEIVPNSAEER.L
858	625.00	1871.99	1871.96	12.9	(50)	9.6e-006	K.YKVPQLEIVPNSAEER.L
859	625.33	1872.97	1872.95	14.5	(32)	0.00061	K.YKVPQLEIVPNSAEER.L
898	651.32	1950.95	1950.95	2.80	(43)	4.9e-005	K.YKVPQLEIVPNSAEER.L + Phospho (ST)
899	976.48	1950.95	1950.95	3.63	87	1.8e-009	K.YKVPQLEIVPNSAEER.L + Phospho (ST)
900	651.32	1950.95	1950.95	4.00	(52)	5.7e-006	K.YKVPQLEIVPNSAEER.L + Phospho (ST)
903	976.98	1951.94	1951.93	7.76	(77)	2.2e-008	K.YKVPQLEIVPNSAEER.L + Phospho (ST)
904	651.66	1951.94	1951.93	7.76	(49)	1.2e-005	K.YKVPQLEIVPNSAEER.L + Phospho (ST)
1065	1158.58	2315.14	2315.13	5.55	115	2.9e-012	K.EPMIGVQNQLAYFYPELFR.Q
1068	773.05	2316.14	2316.11	10.9	(47)	2.2e-005	K.EPMIGVQNQLAYFYPELFR.Q
1069	1161.05	2320.08	2320.07	4.68	(86)	2.4e-009	K.QMEAESISSSEIVPNSVEQK.H
1070	774.37	2320.09	2320.07	6.47	(70)	9e-008	K.QMEAESISSSEIVPNSVEQK.H
1072	774.70	2321.06	2321.06	2.85	(85)	3.1e-009	K.QMEAESISSSEIVPNSVEQK.H
1073	774.70	2321.07	2321.06	3.66	(44)	4.3e-005	K.QMEAESISSSEIVPNSVEQK.H
1074	1161.54	2321.07	2321.06	4.24	(93)	5.5e-010	K.QMEAESISSSEIVPNSVEQK.H
1075	1161.54	2321.07	2321.06	4.59	106	2.3e-011	K.QMEAESISSSEIVPNSVEQK.H
1101	1201.03	2400.04	2400.04	0.72	(65)	3.1e-007	K.QMEAESISSSEIVPNSVEQK.H + Phospho (ST)
1102	801.02	2400.04	2400.04	0.87	(55)	2.9e-006	K.QMEAESISSSEIVPNSVEQK.H + Phospho (ST)
1103	801.35	2401.03	2401.02	2.29	(53)	5.3e-006	K.QMEAESISSSEIVPNSVEQK.H + Phospho (ST)
1104	1201.52	2401.03	2401.02	4.30	(46)	2.6e-005	K.QMEAESISSSEIVPNSVEQK.H + Phospho (ST)
1105	1201.53	2401.04	2401.02	6.22	(60)	8.9e-007	K.QMEAESISSSEIVPNSVEQK.H + Phospho (ST)
1137	1241.00	2479.99	2480.01	-5.32	(32)	0.0007	K.QMEAESISSSEIVPNSVEQK.H + 2 Phospho (ST)
1138	1241.01	2480.00	2480.01	-0.96	(64)	4.2e-007	K.QMEAESISSSEIVPNSVEQK.H + 2 Phospho (ST)
1139	1241.01	2480.01	2480.01	2.18	(47)	1.9e-005	K.QMEAESISSSEIVPNSVEQK.H + 2 Phospho (ST)
1140	827.68	2480.01	2480.01	3.25	(48)	1.5e-005	K.QMEAESISSSEIVPNSVEQK.H + 2 Phospho (ST)
1151	1259.55	2517.09	2517.08	1.48	96	2.7e-010	K.VNELSKDIGSESTEDQAMEDIK.Q + Phospho (ST)
1152	840.04	2517.09	2517.08	3.74	(68)	1.6e-007	K.VNELSKDIGSESTEDQAMEDIK.Q + Phospho (ST)
1163	1281.00	2559.98	2559.97	2.61	(38)	0.00017	K.QMEAESISSSEIVPNSVEQK.H + 3 Phospho (ST)
1167	863.45	2587.32	2587.33	-3.03	10	0.099	K.HIQKEDVPSERYLGYLEQLLR.L
1168	863.45	2587.33	2587.33	0.04	(1)	0.86	K.HIQKEDVPSERYLGYLEQLLR.L
1204	1388.12	2774.22	2774.22	-1.30	(38)	0.00016	K.EKVNELSKDIGSESTEDQAMEDIK.Q + Phospho (ST)
1205	694.56	2774.22	2774.22	0.69	(28)	0.0017	K.EKVNELSKDIGSESTEDQAMEDIK.Q + Phospho (ST)
1206	925.75	2774.22	2774.22	1.09	74	3.7e-008	K.EKVNELSKDIGSESTEDQAMEDIK.Q + Phospho (ST)

Appendix C5: peptides of trypsin-digested dephosphorylated α_{s1} -casein at an incubation time of 180 min.

CAS1_BOVIN_B Mass: 22960 Score: 4034 Queries matched: 81 emPAI: 286.94

(P02662) Alpha-S1 casein B - Bos taurus (Bovine).

Query	Observed	Mr(expt)	Mr(calc)	ppm	Score	Expect	Peptide
15	748.37	747.36	747.36	2.48	(21)	0.0086	K.TTMPLW.-
16	374.69	747.37	747.36	3.48	28	0.0016	K.TTMPLW.-
18	748.37	747.37	747.36	4.50	(13)	0.05	K.TTMPLW.-
19	748.37	747.37	747.36	5.57	(14)	0.036	K.TTMPLW.-
21	748.37	747.37	747.36	6.23	(3)	0.52	K.TTMPLW.-
25	759.41	758.40	758.41	-10.13	2	0.63	R.LKKYK.V + Phospho (Y)
427	1267.70	1266.69	1266.70	-5.89	(8)	0.16	R.YLGYLEQLLR.L
428	1267.70	1266.69	1266.70	-4.39	(33)	0.00055	R.YLGYLEQLLR.L
429	1267.70	1266.69	1266.70	-2.89	(7)	0.2	R.YLGYLEQLLR.L
431	634.36	1266.70	1266.70	3.68	(59)	1.3e-006	R.YLGYLEQLLR.L
432	1267.71	1266.70	1266.70	3.74	(21)	0.0076	R.YLGYLEQLLR.L
433	634.36	1266.70	1266.70	4.12	(57)	1.8e-006	R.YLGYLEQLLR.L
434	634.36	1266.70	1266.70	4.14	(63)	5.4e-007	R.YLGYLEQLLR.L
435	634.36	1266.70	1266.70	4.31	(50)	1.1e-005	R.YLGYLEQLLR.L
436	634.36	1266.70	1266.70	4.40	(59)	1.2e-006	R.YLGYLEQLLR.L
437	634.36	1266.70	1266.70	4.47	(64)	3.6e-007	R.YLGYLEQLLR.L
438	1267.71	1266.70	1266.70	4.61	(2)	0.66	R.YLGYLEQLLR.L
439	634.36	1266.70	1266.70	4.78	(60)	1.1e-006	R.YLGYLEQLLR.L
440	634.36	1266.70	1266.70	5.13	(43)	4.8e-005	R.YLGYLEQLLR.L
443	1268.69	1267.69	1267.68	4.91	(34)	0.00042	R.YLGYLEQLLR.L + Deamidated (NQ)
444	634.85	1267.69	1267.68	5.17	73	5.5e-008	R.YLGYLEQLLR.L + Deamidated (NQ)
562	462.25	1383.72	1383.72	1.61	(33)	0.0005	R.FFVAPFPEVFGK.E
563	692.87	1383.73	1383.72	2.99	63	4.5e-007	R.FFVAPFPEVFGK.E
564	692.87	1383.73	1383.72	3.16	(30)	0.0011	R.FFVAPFPEVFGK.E
565	1384.74	1383.73	1383.72	8.74	(37)	0.00021	R.FFVAPFPEVFGK.E
677	790.92	1579.82	1579.82	0.51	(81)	8.4e-009	K.VPQLEIVPNSAEER.L
678	527.62	1579.83	1579.82	4.45	(33)	0.00048	K.VPQLEIVPNSAEER.L
679	791.41	1580.81	1580.80	5.34	83	5.3e-009	K.VPQLEIVPNSAEER.L
709	830.90	1659.79	1659.79	0.09	(49)	1.2e-005	K.VPQLEIVPNSAEER.L + Phospho (ST)
710	830.90	1659.79	1659.79	4.66	(72)	5.7e-008	K.VPQLEIVPNSAEER.L + Phospho (ST)
711	554.27	1659.80	1659.79	5.75	(55)	3.3e-006	K.VPQLEIVPNSAEER.L + Phospho (ST)
712	554.60	1660.78	1660.77	3.14	(42)	6.8e-005	K.VPQLEIVPNSAEER.L + Phospho (ST)
713	831.40	1660.78	1660.77	3.76	(68)	1.6e-007	K.VPQLEIVPNSAEER.L + Phospho (ST)
765	880.48	1758.94	1758.94	0.77	(68)	1.7e-007	K.HQGLPQEVNENLLR.F
766	880.48	1758.94	1758.94	1.38	(58)	1.4e-006	K.HQGLPQEVNENLLR.F
767	880.48	1758.94	1758.94	1.84	(80)	9.7e-009	K.HQGLPQEVNENLLR.F
768	880.48	1758.94	1758.94	3.02	(80)	9.3e-009	K.HQGLPQEVNENLLR.F
769	880.48	1758.94	1758.94	3.62	(89)	1.4e-009	K.HQGLPQEVNENLLR.F
770	587.32	1758.95	1758.94	4.20	(75)	3.1e-008	K.HQGLPQEVNENLLR.F
771	880.48	1758.95	1758.94	6.67	(108)	1.5e-011	K.HQGLPQEVNENLLR.F
773	587.65	1759.92	1759.92	-1.33	(58)	1.7e-006	K.HQGLPQEVNENLLR.F
774	587.65	1759.93	1759.92	2.69	(47)	1.9e-005	K.HQGLPQEVNENLLR.F
775	880.97	1759.93	1759.92	3.37	(95)	3.1e-010	K.HQGLPQEVNENLLR.F
776	587.65	1759.93	1759.92	3.60	(68)	1.6e-007	K.HQGLPQEVNENLLR.F

777	587.65	1759.93	1759.92	5.76	(43)	4.7e-005	K.HQGLPQEVLNENLLR.F
778	880.97	1759.93	1759.92	6.77	(114)	4e-012	K.HQGLPQEVLNENLLR.F
779	881.46	1760.91	1760.91	5.12	114	3.6e-012	K.HQGLPQEVLNENLLR.F
785	884.38	1766.75	1766.75	0.73	(112)	6.5e-012	K.DIGSESTEDQAMEDIK.Q
786	884.38	1766.76	1766.75	1.99	(114)	3.7e-012	K.DIGSESTEDQAMEDIK.Q
787	884.39	1766.76	1766.75	2.81	(84)	4e-009	K.DIGSESTEDQAMEDIK.Q
788	884.39	1766.76	1766.75	3.27	(84)	3.6e-009	K.DIGSESTEDQAMEDIK.Q
789	884.39	1766.76	1766.75	3.30	128	1.5e-013	K.DIGSESTEDQAMEDIK.Q
790	589.93	1766.76	1766.75	3.41	(51)	7.7e-006	K.DIGSESTEDQAMEDIK.Q
791	589.93	1766.76	1766.75	6.42	(71)	8.2e-008	K.DIGSESTEDQAMEDIK.Q
792	590.26	1767.75	1767.74	6.22	(46)	2.4e-005	K.DIGSESTEDQAMEDIK.Q
793	884.88	1767.75	1767.74	6.26	(122)	6.5e-013	K.DIGSESTEDQAMEDIK.Q
860	924.37	1846.72	1846.72	1.88	(55)	3.4e-006	K.DIGSESTEDQAMEDIK.Q + Phospho (ST)
866	624.67	1870.99	1870.98	4.11	(61)	7.4e-007	K.YKVPQLEIVPNSAEER.L
867	936.50	1870.99	1870.98	6.95	(77)	1.9e-008	K.YKVPQLEIVPNSAEER.L
868	936.99	1871.97	1871.96	3.13	(85)	3.4e-009	K.YKVPQLEIVPNSAEER.L
869	625.00	1871.97	1871.96	6.28	(55)	2.9e-006	K.YKVPQLEIVPNSAEER.L
906	651.33	1950.95	1950.95	4.26	(55)	3.1e-006	K.YKVPQLEIVPNSAEER.L + Phospho (ST)
907	976.49	1950.96	1950.95	5.33	86	2.7e-009	K.YKVPQLEIVPNSAEER.L + Phospho (ST)
910	651.65	1951.94	1951.93	3.41	(37)	0.00019	K.YKVPQLEIVPNSAEER.L + Phospho (ST)
911	976.98	1951.94	1951.93	3.53	(75)	2.9e-008	K.YKVPQLEIVPNSAEER.L + Phospho (ST)
1073	1161.05	2320.08	2320.07	2.27	(103)	4.6e-011	K.QMEAESISSSEEIVPNSVEQK.H
1074	774.37	2320.08	2320.07	2.53	(70)	9.1e-008	K.QMEAESISSSEEIVPNSVEQK.H
1076	774.70	2321.06	2321.06	2.31	(63)	5.3e-007	K.QMEAESISSSEEIVPNSVEQK.H
1077	1161.54	2321.07	2321.06	4.42	(105)	3.5e-011	K.QMEAESISSSEEIVPNSVEQK.H
1078	774.70	2321.07	2321.06	6.80	(63)	4.7e-007	K.QMEAESISSSEEIVPNSVEQK.H
1079	1161.55	2321.08	2321.06	7.86	123	4.9e-013	K.QMEAESISSSEEIVPNSVEQK.H
1099	1201.03	2400.04	2400.04	0.56	(67)	1.8e-007	K.QMEAESISSSEEIVPNSVEQK.H + Phospho (ST)
1100	801.02	2400.05	2400.04	2.53	(59)	1.3e-006	K.QMEAESISSSEEIVPNSVEQK.H + Phospho (ST)
1101	801.35	2401.03	2401.02	2.02	(57)	1.9e-006	K.QMEAESISSSEEIVPNSVEQK.H + Phospho (ST)
1102	1201.52	2401.03	2401.02	2.72	(58)	1.6e-006	K.QMEAESISSSEEIVPNSVEQK.H + Phospho (ST)
1103	801.36	2401.04	2401.02	8.33	(62)	6e-007	K.QMEAESISSSEEIVPNSVEQK.H + Phospho (ST)
1132	828.02	2481.02	2480.99	13.5	(42)	6.1e-005	K.QMEAESISSSEEIVPNSVEQK.H + 2 Phospho (ST)
1139	1259.55	2517.09	2517.08	2.75	97	1.9e-010	K.VNELSKDIGSESTEDQAMEDIK.Q + Phospho (ST)
1140	840.04	2517.09	2517.08	2.97	(72)	6.1e-008	K.VNELSKDIGSESTEDQAMEDIK.Q + Phospho (ST)
1190	925.75	2774.22	2774.22	0.12	70	1e-007	K.EKVNELSKDIGSESTEDQAMEDIK.Q + Phospho (ST)
1191	1388.12	2774.23	2774.22	3.89	(62)	6.4e-007	K.EKVNELSKDIGSESTEDQAMEDIK.Q + Phospho (ST)

Appendix C6: peptides of trypsin-digested α_{s1} -casein with 23% succinylation.

CAS1_BOVIN_B Mass: 22960 Score: 4343 Queries matched: 113 emPAI: 7448.08

(P02662) Alpha-S1 casein B - Bos taurus (Bovine).

Query	Observed	Mr(expt)	Mr(calc)	ppm	Score	Expect	Peptide
24	374.69	747.37	747.36	4.66	22	0.0058	K.TTMPLW.-
25	748.37	747.37	747.36	4.88	(14)	0.036	K.TTMPLW.-
405	1267.70	1266.70	1266.70	0.42	(22)	0.0069	R.YLGYLEQLLR.L
406	1267.71	1266.70	1266.70	1.05	(19)	0.011	R.YLGYLEQLLR.L
407	1267.71	1266.70	1266.70	2.95	(1)	0.86	R.YLGYLEQLLR.L
408	634.36	1266.70	1266.70	3.35	(57)	2e-006	R.YLGYLEQLLR.L
409	634.36	1266.70	1266.70	3.82	(42)	5.6e-005	R.YLGYLEQLLR.L
410	634.36	1266.70	1266.70	3.96	(45)	3.3e-005	R.YLGYLEQLLR.L
411	634.36	1266.70	1266.70	4.23	(49)	1.3e-005	R.YLGYLEQLLR.L
412	634.36	1266.70	1266.70	4.29	(52)	6.6e-006	R.YLGYLEQLLR.L
413	634.36	1266.70	1266.70	4.64	(39)	0.00012	R.YLGYLEQLLR.L
414	634.36	1266.70	1266.70	4.94	(64)	4e-007	R.YLGYLEQLLR.L
415	634.36	1266.70	1266.70	5.45	(62)	5.9e-007	R.YLGYLEQLLR.L
416	634.36	1266.70	1266.70	5.62	(63)	5.6e-007	R.YLGYLEQLLR.L
417	634.36	1266.71	1266.70	6.90	(67)	2.1e-007	R.YLGYLEQLLR.L
420	1268.69	1267.69	1267.68	3.81	(35)	0.00034	R.YLGYLEQLLR.L
421	634.85	1267.69	1267.68	6.19	71	7.7e-008	R.YLGYLEQLLR.L
545	462.25	1383.73	1383.72	3.11	(42)	6.9e-005	R.FFVAPFPEVFGK.E
546	692.87	1383.73	1383.72	3.16	(37)	0.00018	R.FFVAPFPEVFGK.E
547	692.87	1383.73	1383.72	4.46	70	9.9e-008	R.FFVAPFPEVFGK.E
548	692.87	1383.73	1383.72	5.07	(27)	0.0019	R.FFVAPFPEVFGK.E
549	1384.74	1383.73	1383.72	7.29	(34)	0.00038	R.FFVAPFPEVFGK.E
580	719.35	1436.69	1436.69	2.33	(44)	4.1e-005	K.HIQKEDVPSEY + Succinyl (K)
581	719.35	1436.69	1436.69	2.83	(11)	0.072	K.HIQKEDVPSEY + Succinyl (K)
582	719.35	1436.69	1436.69	3.12	66	2.5e-007	K.HIQKEDVPSEY + Succinyl (K)
583	719.35	1436.69	1436.69	3.32	(33)	0.00055	K.HIQKEDVPSEY + Succinyl (K)
585	719.84	1437.67	1437.67	-1.91	(21)	0.008	K.HIQKEDVPSEY + Succinyl (K)
697	803.91	1605.80	1605.79	1.99	59	1.2e-006	R.LHSMKEGIHAQQK.E + Succinyl (K)
698	536.27	1605.80	1605.79	2.83	(26)	0.0025	R.LHSMKEGIHAQQK.E + Succinyl (K)
699	536.27	1605.80	1605.79	3.09	(34)	0.00041	R.LHSMKEGIHAQQK.E + Succinyl (K)
700	536.27	1605.80	1605.79	3.13	(29)	0.0013	R.LHSMKEGIHAQQK.E + Succinyl (K)
701	536.27	1605.80	1605.79	3.65	(21)	0.0087	R.LHSMKEGIHAQQK.E + Succinyl (K)
702	803.91	1605.80	1605.79	4.62	(52)	7e-006	R.LHSMKEGIHAQQK.E + Succinyl (K)
703	536.28	1605.80	1605.79	6.51	(15)	0.032	R.LHSMKEGIHAQQK.E + Succinyl (K)
722	554.27	1659.80	1659.79	7.81	(50)	1.1e-005	K.VPQLEIVPNSAEER.L + Phospho (ST)
723	830.91	1659.80	1659.79	8.01	(72)	5.9e-008	K.VPQLEIVPNSAEER.L + Phospho (ST)
725	831.40	1660.78	1660.77	4.64	78	1.4e-008	K.VPQLEIVPNSAEER.L + Phospho (ST)
726	554.60	1660.78	1660.77	5.11	(40)	0.00011	K.VPQLEIVPNSAEER.L + Phospho (ST)
760	1741.89	1740.88	1740.88	2.13	(37)	0.00021	R.FFVAPFPEVFGKEK.V + Succinyl (K)
761	871.45	1740.88	1740.88	3.05	84	3.8e-009	R.FFVAPFPEVFGKEK.V + Succinyl (K)
762	581.30	1740.88	1740.88	4.65	(61)	8.6e-007	R.FFVAPFPEVFGKEK.V + Succinyl (K)
763	581.30	1740.89	1740.88	5.07	(68)	1.6e-007	R.FFVAPFPEVFGKEK.V + Succinyl (K)
776	880.48	1758.94	1758.94	2.90	(32)	0.00066	K.HQGLPQEVNLNLLR.F
777	587.32	1758.95	1758.94	4.54	(46)	2.7e-005	K.HQGLPQEVNLNLLR.F
778	880.48	1758.95	1758.94	4.73	(113)	5.4e-012	K.HQGLPQEVNLNLLR.F
779	587.32	1758.95	1758.94	4.76	(59)	1.4e-006	K.HQGLPQEVNLNLLR.F

780	587.32	1758.95	1758.94	4.90	(50)	1.1e-005	K.HQGLPQEVLNENLLR.F
781	880.97	1759.93	1759.92	2.52	(98)	1.5e-010	K.HQGLPQEVLNENLLR.F
782	587.65	1759.93	1759.92	3.67	(53)	4.6e-006	K.HQGLPQEVLNENLLR.F
783	880.97	1759.93	1759.92	6.31	(111)	8.2e-012	K.HQGLPQEVLNENLLR.F
784	587.65	1759.94	1759.92	8.22	(54)	3.7e-006	K.HQGLPQEVLNENLLR.F
785	587.98	1760.91	1760.91	0.83	(61)	7.9e-007	K.HQGLPQEVLNENLLR.F
786	881.46	1760.91	1760.91	0.92	116	2.3e-012	K.HQGLPQEVLNENLLR.F
837	924.37	1846.72	1846.72	3.05	91	8.1e-010	K.DIGSESTEDQAMEDIK.Q + Phospho (ST)
838	616.58	1846.73	1846.72	3.98	(28)	0.0015	K.DIGSESTEDQAMEDIK.Q + Phospho (ST)
867	964.35	1926.69	1926.68	1.96	(45)	2.8e-005	K.DIGSESTEDQAMEDIK.Q + 2 Phospho (ST)
868	964.35	1926.69	1926.68	2.71	(44)	4.2e-005	K.DIGSESTEDQAMEDIK.Q + 2 Phospho (ST)
869	643.24	1926.69	1926.68	3.79	(46)	2.7e-005	K.DIGSESTEDQAMEDIK.Q + 2 Phospho (ST)
870	964.35	1926.69	1926.68	4.21	(55)	3e-006	K.DIGSESTEDQAMEDIK.Q + 2 Phospho (ST)
871	964.35	1926.69	1926.68	5.31	(56)	2.6e-006	K.DIGSESTEDQAMEDIK.Q + 2 Phospho (ST)
879	651.32	1950.94	1950.95	-1.24	(43)	5.4e-005	K.YKVPQLEIVPNSAEER.L + Phospho (ST)
880	976.48	1950.95	1950.95	3.33	95	2.9e-010	K.YKVPQLEIVPNSAEER.L + Phospho (ST)
881	651.33	1950.95	1950.95	4.40	(53)	4.5e-006	K.YKVPQLEIVPNSAEER.L + Phospho (ST)
882	976.97	1951.93	1951.93	2.87	(76)	2.4e-008	K.YKVPQLEIVPNSAEER.L + Phospho (ST)
883	651.65	1951.94	1951.93	4.16	(46)	2.6e-005	K.YKVPQLEIVPNSAEER.L + Phospho (ST)
938	1026.49	2050.97	2050.96	5.49	(94)	3.5e-010	K.YKVPQLEIVPNSAEER.L + Phospho (ST); Succinyl (K)
939	684.67	2050.98	2050.96	7.13	(61)	8.2e-007	K.YKVPQLEIVPNSAEER.L + Phospho (ST); Succinyl (K)
940	1026.98	2051.95	2051.95	2.46	(94)	3.6e-010	K.YKVPQLEIVPNSAEER.L + Phospho (ST); Succinyl (K)
941	685.00	2051.97	2051.95	12.5	(30)	0.00095	K.YKVPQLEIVPNSAEER.L + Phospho (ST); Succinyl (K)
992	1090.54	2179.06	2179.06	3.26	(59)	1.2e-006	K.YKVPQLEIVPNSAEER.L + Phospho (ST); Succinyl (K)
993	727.37	2179.07	2179.06	8.28	(44)	4e-005	K.YKVPQLEIVPNSAEER.L + Phospho (ST); Succinyl (K)
1015	746.08	2235.23	2235.21	6.41	(62)	6.2e-007	K.HPIKHQGLPQEVLNENLLR.F
1027	1140.07	2278.13	2278.12	7.29	1	0.86	K.VPQLEIVPNSAEERLHSMK.E + Succinyl (K)
1028	760.70	2279.08	2279.07	2.12	(48)	1.4e-005	K.KYKVPQLEIVPNSAEER.L + Phospho (ST); 2 Succinyl (K)
1029	1140.55	2279.08	2279.07	3.89	80	1.1e-008	K.KYKVPQLEIVPNSAEER.L + Phospho (ST); 2 Succinyl (K)
1030	761.03	2280.07	2280.06	7.76	(44)	4.2e-005	K.KYKVPQLEIVPNSAEER.L + Phospho (ST); 2 Succinyl (K)
1031	1141.05	2280.09	2280.06	14.0	(74)	4.2e-008	K.KYKVPQLEIVPNSAEER.L + Phospho (ST); 2 Succinyl (K)
1052	1168.13	2334.26	2334.24	4.65	(68)	1.6e-007	K.HPIKHQGLPQEVLNENLLR.F + Succinyl (K)
1053	584.57	2334.26	2334.24	5.43	(51)	7.4e-006	K.HPIKHQGLPQEVLNENLLR.F + Succinyl (K)
1054	779.09	2334.26	2334.24	5.76	77	2.1e-008	K.HPIKHQGLPQEVLNENLLR.F + Succinyl (K)
1055	1168.14	2334.27	2334.24	12.3	(71)	7.8e-008	K.HPIKHQGLPQEVLNENLLR.F + Succinyl (K)
1056	584.82	2335.24	2335.23	3.26	(13)	0.053	K.HPIKHQGLPQEVLNENLLR.F + Succinyl (K)
1057	779.42	2335.24	2335.23	3.42	(66)	2.3e-007	K.HPIKHQGLPQEVLNENLLR.F + Succinyl (K)
1058	779.42	2335.24	2335.23	4.08	(73)	5.6e-008	K.HPIKHQGLPQEVLNENLLR.F + Succinyl (K)
1059	1168.64	2335.26	2335.23	13.4	(74)	4e-008	K.HPIKHQGLPQEVLNENLLR.F + Succinyl (K)
1095	1256.64	2511.27	2511.26	4.59	(70)	9.4e-008	R.FFVAPFPEVFGKEKVNELSK.D + 2 Succinyl (K)
1096	838.10	2511.27	2511.26	4.77	77	1.9e-008	R.FFVAPFPEVFGKEKVNELSK.D + 2 Succinyl (K)
1097	838.42	2512.25	2512.24	2.78	(42)	6.4e-005	R.FFVAPFPEVFGKEKVNELSK.D + 2 Succinyl (K)
1098	1257.14	2512.26	2512.24	8.01	(54)	4.3e-006	R.FFVAPFPEVFGKEKVNELSK.D + 2 Succinyl (K)
1115	1281.07	2560.13	2560.14	-2.96	1	0.72	K.EDVPSERYLGYLEQLRLK.K + Phospho (ST)
1123	863.45	2587.32	2587.33	-3.12	1	0.76	K.HIQKEDVPSERYLGYLEQLLR.L
1126	864.75	2591.23	2591.22	2.81	(41)	7.9e-005	R.FFVAPFPEVFGKEKVNELSK.D + Phospho (ST); 2 Succinyl (K)
1135	1320.98	2639.94	2639.94	0.52	(41)	7.3e-005	K.QMEAESISSSEIVPNSVEQK.H + 4 Phospho (ST)
1136	880.99	2639.95	2639.94	2.71	(38)	0.00017	K.QMEAESISSSEIVPNSVEQK.H + 4 Phospho (ST)
1152	1339.52	2677.02	2677.02	0.26	(57)	1.8e-006	K.VNELSKDIGSESTEDQAMEDIK.Q + 3 Phospho (ST)
1153	893.35	2677.02	2677.02	2.12	(51)	8.9e-006	K.VNELSKDIGSESTEDQAMEDIK.Q + 3 Phospho (ST)
1159	900.03	2697.07	2697.07	2.04	(56)	2.7e-006	K.VNELSKDIGSESTEDQAMEDIK.Q + 2 Phospho (ST); Succinyl (K)
1160	1349.55	2697.08	2697.07	4.74	62	6.9e-007	K.VNELSKDIGSESTEDQAMEDIK.Q + 2 Phospho (ST); Succinyl (K)
1170	1360.96	2719.91	2719.91	1.78	(22)	0.007	K.QMEAESISSSEIVPNSVEQK.H + 5 Phospho (ST)
1171	907.64	2719.91	2719.91	2.35	42	6e-005	K.QMEAESISSSEIVPNSVEQK.H + 5 Phospho (ST)

1172	907.98	2720.92	2720.89	11.0	(8)	0.17	K.QMEAESISSSEIVPNSVEQK.H + 5 Phospho (ST)
1220	1468.09	2934.16	2934.15	3.46	(36)	0.00024	K.EKVNELSKDIGSESTEDQAMEDIK.Q + 3 Phospho (ST)
1221	979.06	2934.17	2934.15	4.11	(52)	5.8e-006	K.EKVNELSKDIGSESTEDQAMEDIK.Q + 3 Phospho (ST)
1228	1478.11	2954.20	2954.20	0.42	(16)	0.024	K.EKVNELSKDIGSESTEDQAMEDIK.Q + 2 Phospho (ST); Succinyl (K)
1229	985.75	2954.21	2954.20	3.94	72	6.4e-008	K.EKVNELSKDIGSESTEDQAMEDIK.Q + 2 Phospho (ST); Succinyl (K)
1246	1012.40	3034.18	3034.17	3.87	(41)	8.3e-005	K.EKVNELSKDIGSESTEDQAMEDIK.Q + 3 Phospho (ST); Succinyl (K)
1251	1019.08	3054.23	3054.22	4.49	(70)	9.7e-008	K.EKVNELSKDIGSESTEDQAMEDIK.Q + 2 Phospho (ST); 2 Succinyl (K)
1277	1109.75	3326.22	3326.22	1.12	(65)	3.4e-007	K.QMEAESISSSEIVPNSVEQKHIQK.E + 5 Phospho (ST); Succinyl (K)
1278	1109.75	3326.23	3326.22	4.82	76	2.5e-008	K.QMEAESISSSEIVPNSVEQKHIQK.E + 5 Phospho (ST); Succinyl (K)
1338	1125.99	4499.93	4499.90	7.19	(44)	4.6e-005	R.FFVAPFPFVFGKEKVNELSKDIGSESTEDQAMEDIK.Q + 3 Phospho (ST); 2 Succinyl (K)
1339	1500.98	4499.93	4499.90	7.43	(23)	0.0057	R.FFVAPFPFVFGKEKVNELSKDIGSESTEDQAMEDIK.Q + 3 Phospho (ST); 2 Succinyl (K)
1340	1131.00	4519.97	4519.95	4.30	(29)	0.0014	R.FFVAPFPFVFGKEKVNELSKDIGSESTEDQAMEDIK.Q + 2 Phospho (ST); 3 Succinyl (K)
1341	1507.66	4519.97	4519.95	4.38	67	2.3e-007	R.FFVAPFPFVFGKEKVNELSKDIGSESTEDQAMEDIK.Q + 2 Phospho (ST); 3 Succinyl (K)

Appendix C7: peptides of trypsin-digested α_{s1} -casein with 49% succinylation.

CAS1_BOVIN_B Mass: 22960 Score: 4105 Queries matched: 119 emPAI: 9477.82

(P02662) Alpha-S1 casein B - Bos taurus (Bovine).

Query	Observed	Mr(expt)	Mr(calc)	ppm	Score	Expect	Peptide
18	748.37	747.37	747.36	5.08	(14)	0.043	K.TTMPLW.-
19	374.69	747.37	747.36	5.54	21	0.0071	K.TTMPLW.-
165	490.26	978.50	978.49	4.79	23	0.0045	R.LKKYK.V + 3 Succinyl (K)
292	573.78	1145.55	1145.55	4.17	9	0.13	K.EKVNELSK.D + 2 Succinyl (K)
386	634.36	1266.70	1266.70	2.11	(54)	4.2e-006	R.YLGYLEQLLR.L
387	1267.71	1266.70	1266.70	2.24	(37)	0.00021	R.YLGYLEQLLR.L
388	634.36	1266.70	1266.70	2.27	(46)	2.6e-005	R.YLGYLEQLLR.L
389	634.36	1266.70	1266.70	2.60	(41)	8.9e-005	R.YLGYLEQLLR.L
390	634.36	1266.70	1266.70	3.03	(46)	2.5e-005	R.YLGYLEQLLR.L
391	634.36	1266.70	1266.70	3.43	(57)	1.8e-006	R.YLGYLEQLLR.L
392	634.36	1266.70	1266.70	4.01	(39)	0.00013	R.YLGYLEQLLR.L
393	1267.71	1266.70	1266.70	4.05	(39)	0.00014	R.YLGYLEQLLR.L
394	634.36	1266.70	1266.70	4.88	(50)	1e-005	R.YLGYLEQLLR.L
395	634.36	1266.70	1266.70	4.93	(60)	9.2e-007	R.YLGYLEQLLR.L
396	634.36	1266.70	1266.70	5.24	(64)	3.9e-007	R.YLGYLEQLLR.L
397	634.36	1266.70	1266.70	5.78	(52)	6.3e-006	R.YLGYLEQLLR.L
398	634.36	1266.70	1266.70	5.86	(65)	3.1e-007	R.YLGYLEQLLR.L
399	634.36	1266.71	1266.70	6.90	(63)	5.4e-007	R.YLGYLEQLLR.L
402	1268.69	1267.68	1267.68	1.91	(34)	0.00041	R.YLGYLEQLLR.L
403	634.85	1267.69	1267.68	4.16	67	1.8e-007	R.YLGYLEQLLR.L
523	692.87	1383.73	1383.72	2.90	(21)	0.0082	R.FFVAPFPEVFGK.E
524	1384.73	1383.73	1383.72	3.17	(33)	0.00054	R.FFVAPFPEVFGK.E
525	692.87	1383.73	1383.72	6.04	61	8.4e-007	R.FFVAPFPEVFGK.E
561	719.35	1436.69	1436.69	1.60	(15)	0.034	K.HIQKEDVPSEY + Succinyl (K)
562	719.35	1436.69	1436.69	2.09	(40)	0.0001	K.HIQKEDVPSEY + Succinyl (K)
563	719.35	1436.69	1436.69	2.17	(22)	0.0058	K.HIQKEDVPSEY + Succinyl (K)
564	719.35	1436.69	1436.69	2.84	44	4.1e-005	K.HIQKEDVPSEY + Succinyl (K)
662	536.27	1605.80	1605.79	1.07	(19)	0.014	R.LHSMKEGIHAQQK.E + Succinyl (K)
663	803.91	1605.80	1605.79	2.48	22	0.0067	R.LHSMKEGIHAQQK.E + Succinyl (K)
682	830.90	1659.79	1659.79	3.07	(72)	6.7e-008	K.VPQLEIVPNSAEER.L + Phospho (ST)
683	554.27	1659.79	1659.79	4.86	(59)	1.2e-006	K.VPQLEIVPNSAEER.L + Phospho (ST)
685	554.60	1660.77	1660.77	0.99	(49)	1.2e-005	K.VPQLEIVPNSAEER.L + Phospho (ST)
686	831.40	1660.78	1660.77	4.59	80	1.1e-008	K.VPQLEIVPNSAEER.L + Phospho (ST)
698	844.87	1687.72	1687.73	-6.26	(9)	0.13	R.LHSMKEGIHAQQK.E + Phospho (ST); Succinyl (K)
727	581.30	1740.88	1740.88	2.52	(66)	2.7e-007	R.FFVAPFPEVFGKEK.V + Succinyl (K)
728	1741.89	1740.88	1740.88	2.71	(34)	0.00037	R.FFVAPFPEVFGKEK.V + Succinyl (K)
729	871.45	1740.88	1740.88	3.79	(54)	4e-006	R.FFVAPFPEVFGKEK.V + Succinyl (K)
730	871.45	1740.88	1740.88	4.09	83	5.5e-009	R.FFVAPFPEVFGKEK.V + Succinyl (K)
738	880.48	1758.95	1758.94	4.44	104	4.2e-011	K.HQGLPQEVNLNLLR.F
739	587.32	1758.95	1758.94	4.76	(46)	2.3e-005	K.HQGLPQEVNLNLLR.F
741	880.97	1759.93	1759.92	5.33	(84)	4e-009	K.HQGLPQEVNLNLLR.F
742	880.97	1759.93	1759.92	5.64	(101)	8.4e-011	K.HQGLPQEVNLNLLR.F
743	587.65	1759.93	1759.92	5.95	(25)	0.0035	K.HQGLPQEVNLNLLR.F
744	587.65	1759.93	1759.92	6.50	(42)	6.7e-005	K.HQGLPQEVNLNLLR.F
791	924.37	1846.72	1846.72	2.49	93	4.7e-010	K.DIGSESTEDQAMEDIK.Q + Phospho (ST)
825	964.35	1926.69	1926.68	0.67	(55)	3e-006	K.DIGSESTEDQAMEDIK.Q + 2 Phospho (ST)

826	964.35	1926.69	1926.68	2.23	(46)	2.3e-005	K.DIGSESTEDQAMEDIK.Q + 2 Phospho (ST)
827	964.35	1926.69	1926.68	4.86	(73)	5.1e-008	K.DIGSESTEDQAMEDIK.Q + 2 Phospho (ST)
828	643.24	1926.69	1926.68	4.98	(64)	4e-007	K.DIGSESTEDQAMEDIK.Q + 2 Phospho (ST)
840	976.48	1950.95	1950.95	2.04	(75)	2.9e-008	K.YKVPQLEIVPN S AEER.L + Phospho (ST)
841	651.32	1950.95	1950.95	3.83	(58)	1.7e-006	K.YKVPQLEIVPN S AEER.L + Phospho (ST)
890	1026.49	2050.97	2050.96	3.44	96	2.4e-010	K.YKVPQLEIVPN S AEER.L + Phospho (ST); Succinyl (K)
891	684.67	2050.97	2050.96	5.93	(51)	7.4e-006	K.YKVPQLEIVPN S AEER.L + Phospho (ST); Succinyl (K)
892	1026.98	2051.95	2051.95	3.24	(77)	2.1e-008	K.YKVPQLEIVPN S AEER.L + Phospho (ST); Succinyl (K)
1008	760.70	2279.08	2279.07	3.48	(45)	2.9e-005	K.KYKVPQLEIVPN S AEER.L + Phospho (ST); 2 Succinyl (K)
1009	1140.55	2279.08	2279.07	5.03	71	8.6e-008	K.KYKVPQLEIVPN S AEER.L + Phospho (ST); 2 Succinyl (K)
1010	761.03	2280.07	2280.06	4.45	(60)	1e-006	K.KYKVPQLEIVPN S AEER.L + Phospho (ST); 2 Succinyl (K)
1011	1141.04	2280.07	2280.06	7.92	(68)	1.7e-007	K.KYKVPQLEIVPN S AEER.L + Phospho (ST); 2 Succinyl (K)
1032	779.09	2334.25	2334.24	3.20	(63)	5.1e-007	K.HPIKHQGLPQEVNLNELLR.F + Succinyl (K)
1033	1168.13	2334.25	2334.24	4.31	71	8.8e-008	K.HPIKHQGLPQEVNLNELLR.F + Succinyl (K)
1034	584.57	2334.27	2334.24	9.68	(54)	4.5e-006	K.HPIKHQGLPQEVNLNELLR.F + Succinyl (K)
1037	779.42	2335.23	2335.23	2.50	(53)	4.5e-006	K.HPIKHQGLPQEVNLNELLR.F + Deamidated (NQ); Succinyl (K)
1059	804.76	2411.25	2411.24	4.90	(19)	0.011	R.FFVAPFPEVFGKEKVNELSK.D + Succinyl (K)
1078	1256.64	2511.26	2511.26	1.01	(37)	0.00019	R.FFVAPFPEVFGKEKVNELSK.D + 2 Succinyl (K)
1079	1256.64	2511.26	2511.26	1.56	(44)	4.1e-005	R.FFVAPFPEVFGKEKVNELSK.D + 2 Succinyl (K)
1080	838.09	2511.26	2511.26	1.93	(67)	2e-007	R.FFVAPFPEVFGKEKVNELSK.D + 2 Succinyl (K)
1081	838.10	2511.27	2511.26	3.49	(63)	5e-007	R.FFVAPFPEVFGKEKVNELSK.D + 2 Succinyl (K)
1082	838.10	2511.27	2511.26	3.63	78	1.7e-008	R.FFVAPFPEVFGKEKVNELSK.D + 2 Succinyl (K)
1083	838.10	2511.27	2511.26	5.22	(71)	8.7e-008	R.FFVAPFPEVFGKEKVNELSK.D + 2 Succinyl (K)
1084	1256.64	2511.27	2511.26	6.74	(67)	1.9e-007	R.FFVAPFPEVFGKEKVNELSK.D + 2 Succinyl (K)
1085	1257.13	2512.25	2512.24	1.56	(57)	2.2e-006	R.FFVAPFPEVFGKEKVNELSK.D + Deamidated (NQ); 2 Succinyl (K)
1086	838.42	2512.25	2512.24	3.47	(66)	2.3e-007	R.FFVAPFPEVFGKEKVNELSK.D + Deamidated (NQ); 2 Succinyl (K)
1119	1296.62	2591.23	2591.22	1.31	(47)	1.8e-005	R.FFVAPFPEVFGKEKVNELSK.D + Phospho (ST); 2 Succinyl (K)
1120	864.75	2591.23	2591.22	2.56	(69)	1.4e-007	R.FFVAPFPEVFGKEKVNELSK.D + Phospho (ST); 2 Succinyl (K)
1122	1306.65	2611.28	2611.27	1.57	(53)	5.3e-006	R.FFVAPFPEVFGKEKVNELSK.D + 3 Succinyl (K)
1123	871.44	2611.29	2611.27	4.49	(56)	2.5e-006	R.FFVAPFPEVFGKEKVNELSK.D + 3 Succinyl (K)
1126	1311.14	2620.27	2620.27	0.61	70	9.8e-008	R.LKKYKVPQLEIVPN S AEER.L + Phospho (ST); 3 Succinyl (K)
1127	874.43	2620.28	2620.27	4.21	(61)	8e-007	R.LKKYKVPQLEIVPN S AEER.L + Phospho (ST); 3 Succinyl (K)
1128	1311.64	2621.27	2621.25	6.33	(50)	9.9e-006	R.LKKYKVPQLEIVPN S AEER.L + Deamidated (NQ); Phospho (ST); 3 Succinyl (K)
1151	893.35	2677.02	2677.02	0.88	(43)	5.1e-005	K.VNELSKDIGSESTEDQAMEDIK.Q + 3 Phospho (ST)
1152	893.35	2677.02	2677.02	2.28	(51)	7.3e-006	K.VNELSKDIGSESTEDQAMEDIK.Q + 3 Phospho (ST)
1153	1339.52	2677.02	2677.02	3.32	(41)	7.1e-005	K.VNELSKDIGSESTEDQAMEDIK.Q + 3 Phospho (ST)
1157	900.03	2697.07	2697.07	3.44	(57)	1.9e-006	K.VNELSKDIGSESTEDQAMEDIK.Q + 2 Phospho (ST); Succinyl (K)
1158	1349.55	2697.08	2697.07	4.88	62	6.9e-007	K.VNELSKDIGSESTEDQAMEDIK.Q + 2 Phospho (ST); Succinyl (K)
1161	1360.96	2719.91	2719.91	0.60	(16)	0.024	K.QMEAESISSSEIVPN S VEQK.H + 5 Phospho (ST)
1162	907.64	2719.91	2719.91	0.84	(4)	0.36	K.QMEAESISSSEIVPN S VEQK.H + 5 Phospho (ST)
1163	907.64	2719.91	2719.91	2.45	(23)	0.0056	K.QMEAESISSSEIVPN S VEQK.H + 5 Phospho (ST)
1164	1360.97	2719.92	2719.91	5.16	25	0.0035	K.QMEAESISSSEIVPN S VEQK.H + 5 Phospho (ST)
1165	1360.97	2719.92	2719.91	6.19	(5)	0.32	K.QMEAESISSSEIVPN S VEQK.H + 5 Phospho (ST)
1166	1361.45	2720.89	2720.89	1.04	(13)	0.045	K.QMEAESISSSEIVPN S VEQK.H + 5 Phospho (ST)
1183	1389.53	2777.05	2777.03	6.57	(48)	1.7e-005	K.VNELSKDIGSESTEDQAMEDIK.Q + 3 Phospho (ST); Succinyl (K)
1224	973.18	2916.53	2916.53	-1.30	(2)	0.63	R.LKKYKVPQLEIVPN S AEERLHSMK.E + Phospho (ST)
1225	730.14	2916.53	2916.53	-0.51	10	0.091	R.LKKYKVPQLEIVPN S AEERLHSMK.E + Phospho (ST)
1236	979.06	2934.17	2934.15	4.56	(35)	0.00035	K.EKVNELSKDIGSESTEDQAMEDIK.Q + 3 Phospho (ST)
1241	985.74	2954.20	2954.20	0.33	(55)	3.2e-006	K.EKVNELSKDIGSESTEDQAMEDIK.Q + 2 Phospho (ST); Succinyl (K)
1249	1000.81	2999.41	2999.44	-11.43	1	0.81	K.EDVPSERYLGYLEQLRLKKYK.V + Succinyl (K)
1266	1528.12	3054.23	3054.22	4.71	(23)	0.0049	K.EKVNELSKDIGSESTEDQAMEDIK.Q + 2 Phospho (ST); 2 Succinyl (K)
1267	1019.09	3054.23	3054.22	4.79	64	4.4e-007	K.EKVNELSKDIGSESTEDQAMEDIK.Q + 2 Phospho (ST); 2 Succinyl (K)
1278	1045.74	3134.21	3134.19	6.83	(61)	7.4e-007	K.EKVNELSKDIGSESTEDQAMEDIK.Q + 3 Phospho (ST); 2 Succinyl (K)
1285	800.39	3197.53	3197.51	5.33	(2)	0.68	R.LKKYKVPQLEIVPN S AEERLHSMK.E + Phospho (ST); 2 Succinyl (K)

1286	1066.85	3197.54	3197.51	7.32	(5)	0.35	R.LKKYKVPQLEIVPNSAEERLHSMK.E + Phospho (ST); 2 Succinyl (K)
1289	1072.85	3215.54	3215.57	-8.10	2	0.65	K.HIQKEDVPSERYLGYLEQLRLKK.Y + Succinyl (K)
1304	1109.75	3326.23	3326.22	3.91	49	1.1e-005	K.QMEAESISSSEIVPNSVEQKHIQK.E + 5 Phospho (ST); Succinyl (K)
1326	1190.64	3568.89	3568.91	-4.56	1	0.87	R.YLGYLEQLRLKKYKVPQLEIVPNSAEER.L
1383	1413.87	4238.60	4238.60	-0.89	(54)	4.1e-006	K.QMEAESISSSEIVPNSVEQKHIQKEDVPSEY + 5 Phospho (ST); 2 Succinyl (K)
1384	1060.66	4238.60	4238.60	0.25	(23)	0.0054	K.QMEAESISSSEIVPNSVEQKHIQKEDVPSEY + 5 Phospho (ST); 2 Succinyl (K)
1385	1413.88	4238.61	4238.60	1.80	59	1.3e-006	K.QMEAESISSSEIVPNSVEQKHIQKEDVPSEY + 5 Phospho (ST); 2 Succinyl (K)
1393	1500.97	4499.90	4499.90	0.16	(43)	6.3e-005	R.FFVAPFPEVFGKEKVNELSKDIGSESTEDQAMEDIK.Q + 3 Phospho (ST); 2 Succinyl (K)
1394	1125.98	4499.91	4499.90	1.76	(29)	0.0018	R.FFVAPFPEVFGKEKVNELSKDIGSESTEDQAMEDIK.Q + 3 Phospho (ST); 2 Succinyl (K)
1395	900.99	4499.91	4499.90	3.90	(19)	0.018	R.FFVAPFPEVFGKEKVNELSKDIGSESTEDQAMEDIK.Q + 3 Phospho (ST); 2 Succinyl (K)
1396	1500.98	4499.92	4499.90	4.89	(47)	2.3e-005	R.FFVAPFPEVFGKEKVNELSKDIGSESTEDQAMEDIK.Q + 3 Phospho (ST); 2 Succinyl (K)
1397	1507.66	4519.96	4519.95	1.93	106	3.1e-011	R.FFVAPFPEVFGKEKVNELSKDIGSESTEDQAMEDIK.Q + 2 Phospho (ST); 3 Succinyl (K)
1398	905.00	4519.96	4519.95	1.97	(22)	0.0071	R.FFVAPFPEVFGKEKVNELSKDIGSESTEDQAMEDIK.Q + 2 Phospho (ST); 3 Succinyl (K)
1399	1131.00	4519.96	4519.95	3.68	(67)	2.7e-007	R.FFVAPFPEVFGKEKVNELSKDIGSESTEDQAMEDIK.Q + 2 Phospho (ST); 3 Succinyl (K)
1400	1507.99	4520.94	4520.93	2.85	(63)	6.9e-007	R.FFVAPFPEVFGKEKVNELSKDIGSESTEDQAMEDIK.Q + 2 Phospho (ST); 3 Succinyl (K)
1405	1514.99	4541.95	4541.96	-3.20	(11)	0.094	R.FFVAPFPEVFGKEKVNELSKDIGSESTEDQAMEDIK.Q + Phospho (ST); 4 Succinyl (K)
1407	1150.99	4599.93	4599.91	4.07	(35)	0.0004	R.FFVAPFPEVFGKEKVNELSKDIGSESTEDQAMEDIK.Q + 3 Phospho (ST); 3 Succinyl (K)
1408	1534.32	4599.94	4599.91	6.63	(49)	1.4e-005	R.FFVAPFPEVFGKEKVNELSKDIGSESTEDQAMEDIK.Q + 3 Phospho (ST); 3 Succinyl (K)

Appendix C8: peptides of trypsin-digested α_{s1} -casein with 99% succinylation.

CAS1_BOVIN_B Mass: 22960 Score: 1561 Queries matched: 49 emPAI: 18.96

(P02662) Alpha-S1 casein B - Bos taurus (Bovine).

Query	Observed	Mr(expt)	Mr(calc)	ppm	Score	Expect	Peptide
16	748.37	747.37	747.36	3.46	13	0.046	K.TTMPLW.-
176	490.26	978.50	978.49	8.69	15	0.033	R.LKKYK.V + 3 Succinyl (K)
421	1267.71	1266.70	1266.70	3.42	(40)	0.00011	R.YLGYLEQLLR.L
422	634.36	1266.70	1266.70	3.54	(40)	0.0001	R.YLGYLEQLLR.L
423	634.36	1266.70	1266.70	3.76	(57)	2.2e-006	R.YLGYLEQLLR.L
424	634.36	1266.70	1266.70	3.82	(45)	2.9e-005	R.YLGYLEQLLR.L
425	634.36	1266.70	1266.70	3.93	(43)	4.6e-005	R.YLGYLEQLLR.L
426	634.36	1266.70	1266.70	4.09	(60)	1.1e-006	R.YLGYLEQLLR.L
427	634.36	1266.70	1266.70	4.78	(56)	2.3e-006	R.YLGYLEQLLR.L
428	634.36	1266.70	1266.70	4.94	(58)	1.6e-006	R.YLGYLEQLLR.L
429	634.36	1266.70	1266.70	5.27	(60)	1.1e-006	R.YLGYLEQLLR.L
430	634.36	1266.70	1266.70	5.41	(67)	1.8e-007	R.YLGYLEQLLR.L
431	634.36	1266.70	1266.70	5.46	(53)	4.7e-006	R.YLGYLEQLLR.L
432	634.36	1266.70	1266.70	5.57	70	1e-007	R.YLGYLEQLLR.L
433	1267.71	1266.70	1266.70	5.63	(28)	0.0017	R.YLGYLEQLLR.L
434	634.36	1266.70	1266.70	5.73	(58)	1.7e-006	R.YLGYLEQLLR.L
435	634.36	1266.70	1266.70	5.89	(66)	2.5e-007	R.YLGYLEQLLR.L
436	634.36	1266.70	1266.70	6.03	(54)	3.8e-006	R.YLGYLEQLLR.L
437	634.36	1266.71	1266.70	6.65	(62)	6.2e-007	R.YLGYLEQLLR.L
438	634.36	1266.71	1266.70	7.21	(54)	3.7e-006	R.YLGYLEQLLR.L
439	423.24	1266.71	1266.70	8.17	(43)	5.5e-005	R.YLGYLEQLLR.L
442	634.85	1267.69	1267.68	5.92	(65)	3.3e-007	R.YLGYLEQLLR.L
580	692.87	1383.73	1383.72	6.83	58	1.7e-006	R.FFVAPFPEVFGK.E
720	830.90	1659.79	1659.79	2.14	57	1.9e-006	K.VPQLEIVPNSAEER.L + Phospho (ST)
754	871.45	1740.88	1740.88	3.58	74	4.2e-008	R.FFVAPFPEVFGKEK.V + Succinyl (K)
755	581.30	1740.89	1740.88	5.76	(54)	4.2e-006	R.FFVAPFPEVFGKEK.V + Succinyl (K)
844	964.35	1926.69	1926.68	3.83	49	1.2e-005	K.DIGSESTEDQAMEDIK.Q + 2 Phospho (ST)
905	1026.49	2050.96	2050.96	0.32	53	5.3e-006	K.YKVPQLEIVPNSAEER.L + Phospho (ST); Succinyl (K)
1101	838.10	2511.27	2511.26	6.83	67	2.2e-007	R.FFVAPFPEVFGKEKVNELSK.D + 2 Succinyl (K)
1102	1256.65	2511.28	2511.26	8.17	(52)	6e-006	R.FFVAPFPEVFGKEKVNELSK.D + 2 Succinyl (K)
1103	838.43	2512.27	2512.24	11.0	(40)	0.0001	R.FFVAPFPEVFGKEKVNELSK.D + Deamidated (NQ); 2 Succinyl (K)
1133	874.43	2620.28	2620.27	3.26	(61)	8e-007	R.LKKYKVPQLEIVPNSAEER.L + Phospho (ST); 3 Succinyl (K)
1134	1311.15	2620.28	2620.27	4.73	(67)	1.9e-007	R.LKKYKVPQLEIVPNSAEER.L + Phospho (ST); 3 Succinyl (K)
1135	1311.64	2621.26	2621.25	2.44	(65)	3.5e-007	R.LKKYKVPQLEIVPNSAEER.L + Phospho (ST); 3 Succinyl (K)
1136	874.77	2621.28	2621.25	9.11	68	1.5e-007	R.LKKYKVPQLEIVPNSAEER.L + Phospho (ST); 3 Succinyl (K)
1137	1311.65	2621.29	2621.25	13.3	(54)	4.4e-006	R.LKKYKVPQLEIVPNSAEER.L + Phospho (ST); 3 Succinyl (K)
1219	973.18	2916.51	2916.53	-5.89	(3)	0.54	R.LKKYKVPQLEIVPNSAEERLHSMK.E + Phospho (ST)
1222	730.14	2916.52	2916.53	-2.01	(1)	0.71	R.LKKYKVPQLEIVPNSAEERLHSMK.E + Phospho (ST)
1283	800.39	3197.52	3197.51	2.21	(1)	0.79	R.LKKYKVPQLEIVPNSAEERLHSMK.E + 2 Phospho (ST); 2 Succinyl (K)
1284	1066.85	3197.53	3197.51	4.13	(3)	0.45	R.LKKYKVPQLEIVPNSAEERLHSMK.E + 2 Phospho (ST); 2 Succinyl (K)
1286	1067.18	3198.52	3198.50	7.78	20	0.01	R.LKKYKVPQLEIVPNSAEERLHSMK.E + Phospho (ST); 2 Succinyl (K)
1292	1100.19	3297.54	3297.53	4.66	(3)	0.46	R.LKKYKVPQLEIVPNSAEERLHSMK.E + Phospho (ST); 3 Succinyl (K)
1394	1507.66	4519.96	4519.95	3.92	81	9.4e-009	R.FFVAPFPEVFGKEKVNELSKDIGSESTEDQAMEDIK.Q + 2 Phospho (ST); 3 Succinyl (K)
1395	1131.00	4519.97	4519.95	4.56	(29)	0.0013	R.FFVAPFPEVFGKEKVNELSKDIGSESTEDQAMEDIK.Q + 2 Phospho (ST); 3 Succinyl (K)

1400	1095.31	5471.52	5471.47	9.14	3	0.79		K.QMEAESISSSEEIVPNSVEQKHQKEDVPSERYLGYLEQLRLK.K + 3 Phospho (ST); Succinyl (K)
1414	1388.69	6938.43	6938.42	2.28	11	0.22	-	.RPKHPIKHQGLPQEVLENENLLRFFVAPFPEVFGKEKVNELSKDIGSESTEDQAMEDIK.Q + Phospho (ST); 2 Succinyl (K)
1415	1157.41	6938.44	6938.42	3.61	(9)	0.37	-	.RPKHPIKHQGLPQEVLENENLLRFFVAPFPEVFGKEKVNELSKDIGSESTEDQAMEDIK.Q + Phospho (ST); 2 Succinyl (K)
1416	1408.70	7038.46	7038.43	4.30	(8)	0.48	-	.RPKHPIKHQGLPQEVLENENLLRFFVAPFPEVFGKEKVNELSKDIGSESTEDQAMEDIK.Q + Phospho (ST); 3 Succinyl (K)
1417	1428.70	7138.48	7138.45	5.21	(9)	0.38	-	.RPKHPIKHQGLPQEVLENENLLRFFVAPFPEVFGKEKVNELSKDIGSESTEDQAMEDIK.Q + Phospho (ST); 4 Succinyl (K)

Appendix C9: peptides of trypsin-digested TGA-treated α_{s1} -casein at an incubation time of 5 min.

CAS1_BOVIN_B Mass: 22960 Score: 2760 Queries matched: 79 emPAI: 302.35

(P02662) Alpha-S1 casein B - Bos taurus (Bovine).

Query	Observed	Mr(expt)	Mr(calc)	ppm	Score	Expect	Peptide
14	748.37	747.37	747.36	5.17	(15)	0.03	K.TTMPLW.-
16	374.69	747.37	747.36	6.15	28	0.0016	K.TTMPLW.-
17	748.37	747.37	747.36	6.24	(14)	0.042	K.TTMPLW.-
411	1267.71	1266.70	1266.70	1.37	(21)	0.0077	R.YLGYLEQLLR.L
412	634.36	1266.70	1266.70	3.91	(52)	6.3e-006	R.YLGYLEQLLR.L
413	1267.71	1266.70	1266.70	4.13	(34)	0.00037	R.YLGYLEQLLR.L
414	634.36	1266.70	1266.70	4.63	(45)	3.5e-005	R.YLGYLEQLLR.L
415	634.36	1266.70	1266.70	4.75	(51)	8.5e-006	R.YLGYLEQLLR.L
416	634.36	1266.70	1266.70	5.41	(57)	1.8e-006	R.YLGYLEQLLR.L
417	634.36	1266.70	1266.70	5.51	(54)	4.2e-006	R.YLGYLEQLLR.L
418	634.36	1266.70	1266.70	5.75	(42)	5.8e-005	R.YLGYLEQLLR.L
419	634.36	1266.70	1266.70	5.90	(33)	0.00049	R.YLGYLEQLLR.L
420	423.24	1266.71	1266.70	6.18	(49)	1.2e-005	R.YLGYLEQLLR.L
421	634.36	1266.71	1266.70	6.61	(63)	5.5e-007	R.YLGYLEQLLR.L
425	1268.69	1267.68	1267.68	1.76	(33)	0.00055	R.YLGYLEQLLR.L + Deamidated (NQ)
426	634.85	1267.69	1267.68	6.86	65	3.5e-007	R.YLGYLEQLLR.L + Deamidated (NQ)
518	692.87	1383.73	1383.72	3.52	(18)	0.015	R.FFVAPFPEVFGK.E
519	692.87	1383.73	1383.72	3.55	(34)	0.0004	R.FFVAPFPEVFGK.E
520	692.87	1383.73	1383.72	4.14	(24)	0.004	R.FFVAPFPEVFGK.E
521	692.87	1383.73	1383.72	4.38	(29)	0.0012	R.FFVAPFPEVFGK.E
522	692.87	1383.73	1383.72	4.85	(30)	0.00091	R.FFVAPFPEVFGK.E
523	692.87	1383.73	1383.72	5.13	(39)	0.00013	R.FFVAPFPEVFGK.E
524	462.25	1383.73	1383.72	5.47	(22)	0.0069	R.FFVAPFPEVFGK.E
525	1384.74	1383.73	1383.72	5.85	(46)	2.5e-005	R.FFVAPFPEVFGK.E
526	692.87	1383.73	1383.72	6.02	77	2.1e-008	R.FFVAPFPEVFGK.E
527	692.87	1383.73	1383.72	6.54	(34)	0.00038	R.FFVAPFPEVFGK.E
670	830.90	1659.79	1659.79	4.34	(72)	6.3e-008	K.VPQLEIVPNSAEER.L + Phospho (ST)
671	554.27	1659.80	1659.79	5.01	(61)	7.3e-007	K.VPQLEIVPNSAEER.L + Phospho (ST)
672	1660.81	1659.81	1659.79	11.1	(5)	0.32	K.VPQLEIVPNSAEER.L + Phospho (ST)
676	831.40	1660.78	1660.77	4.15	79	1.2e-008	K.VPQLEIVPNSAEER.L + Deamidated (NQ); Phospho (ST)
677	554.60	1660.78	1660.77	5.51	(41)	7.6e-005	K.VPQLEIVPNSAEER.L + Deamidated (NQ); Phospho (ST)
722	880.48	1758.94	1758.94	3.04	(82)	6.1e-009	K.HQGLPQEVNLNLLR.F
723	880.48	1758.94	1758.94	3.09	(92)	6e-010	K.HQGLPQEVNLNLLR.F
724	880.48	1758.94	1758.94	3.82	(76)	2.6e-008	K.HQGLPQEVNLNLLR.F
725	880.48	1758.94	1758.94	3.94	(54)	3.6e-006	K.HQGLPQEVNLNLLR.F
726	587.32	1758.95	1758.94	4.85	(60)	9.2e-007	K.HQGLPQEVNLNLLR.F
727	880.48	1758.95	1758.94	4.85	124	3.6e-013	K.HQGLPQEVNLNLLR.F
728	880.48	1758.95	1758.94	5.25	(60)	9.8e-007	K.HQGLPQEVNLNLLR.F
729	587.32	1758.95	1758.94	5.84	(43)	5.6e-005	K.HQGLPQEVNLNLLR.F
730	587.65	1759.93	1759.92	5.11	(54)	4.2e-006	K.HQGLPQEVNLNLLR.F + Deamidated (NQ)
731	880.97	1759.93	1759.92	5.42	(109)	1.3e-011	K.HQGLPQEVNLNLLR.F + Deamidated (NQ)
732	587.65	1759.93	1759.92	5.46	(72)	7.1e-008	K.HQGLPQEVNLNLLR.F + Deamidated (NQ)
733	880.97	1759.93	1759.92	5.53	(121)	7.5e-013	K.HQGLPQEVNLNLLR.F + Deamidated (NQ)
734	881.46	1760.91	1760.91	1.87	(103)	4.8e-011	K.HQGLPQEVNLNLLR.F + 2 Deamidated (NQ)

735	587.98	1760.91	1760.91	3.51	(53)	5.5e-006	K.HQGLPQEVNLNLLR.F + 2 Deamidated (NQ)
780	924.37	1846.73	1846.72	4.56	90	9.3e-010	K.DIGSESTEDQAMEDIK.Q + Phospho (ST)
806	964.35	1926.69	1926.68	2.66	(47)	2.1e-005	K.DIGSESTEDQAMEDIK.Q + 2 Phospho (ST)
807	964.35	1926.69	1926.68	3.18	(46)	2.6e-005	K.DIGSESTEDQAMEDIK.Q + 2 Phospho (ST)
808	964.35	1926.69	1926.68	4.25	(65)	2.9e-007	K.DIGSESTEDQAMEDIK.Q + 2 Phospho (ST)
809	964.35	1926.69	1926.68	4.38	(38)	0.00016	K.DIGSESTEDQAMEDIK.Q + 2 Phospho (ST)
810	643.24	1926.69	1926.68	4.90	(62)	6.5e-007	K.DIGSESTEDQAMEDIK.Q + 2 Phospho (ST)
824	651.32	1950.95	1950.95	1.14	(29)	0.0011	K.YKVPQLEIVPNSAEER.L + Phospho (ST)
825	976.48	1950.95	1950.95	4.98	93	4.7e-010	K.YKVPQLEIVPNSAEER.L + Phospho (ST)
826	651.33	1950.96	1950.95	5.74	(61)	8.4e-007	K.YKVPQLEIVPNSAEER.L + Phospho (ST)
829	976.98	1951.95	1951.93	8.11	(78)	1.8e-008	K.YKVPQLEIVPNSAEER.L + Deamidated (NQ); Phospho (ST)
830	651.66	1951.95	1951.93	8.22	(51)	8.9e-006	K.YKVPQLEIVPNSAEER.L + Deamidated (NQ); Phospho (ST)
902	694.35	2080.03	2080.02	4.38	32	0.0006	K.KYKVPQLEIVPNSAEER.L + Deamidated (NQ); Phospho (ST)
960	746.08	2235.22	2235.21	3.92	37	0.0002	K.HPIKHQGLPQEVNLNLLR.F + Deamidated (NQ)
990	772.72	2315.14	2315.13	2.97	(66)	2.7e-007	K.EPMIGVNLQELAYFPELFR.Q
991	1158.58	2315.14	2315.13	3.30	105	2.9e-011	K.EPMIGVNLQELAYFPELFR.Q
1032	828.06	2481.14	2481.16	-6.27	1	0.82	K.EDVPSERYLGYLEQLRLK.K + Deamidated (NQ); Phospho (ST)
1058	655.13	2616.47	2616.46	4.35	33	0.00052	-.RPKHPIKHQGLPQEVNLNLLR.F + Deamidated (NQ)
1059	873.16	2616.47	2616.46	4.47	(14)	0.038	-.RPKHPIKHQGLPQEVNLNLLR.F + Deamidated (NQ)
1061	655.13	2616.47	2616.46	5.23	(9)	0.12	-.RPKHPIKHQGLPQEVNLNLLR.F + Deamidated (NQ)
1062	655.38	2617.48	2617.45	12.7	(5)	0.34	-.RPKHPIKHQGLPQEVNLNLLR.F + 2 Deamidated (NQ)
1065	1320.97	2639.94	2639.94	-1.53	(16)	0.026	K.QMEAESISSSEIVPNSVEQK.H + 4 Phospho (ST)
1066	1320.98	2639.94	2639.94	-1.15	25	0.0032	K.QMEAESISSSEIVPNSVEQK.H + 4 Phospho (ST)
1067	880.99	2639.95	2639.94	3.34	(25)	0.0033	K.QMEAESISSSEIVPNSVEQK.H + 4 Phospho (ST)
1072	1339.52	2677.02	2677.02	2.42	(50)	8.9e-006	K.VNELSKDIGSESTEDQAMEDIK.Q + 3 Phospho (ST)
1073	893.35	2677.03	2677.02	4.92	70	9.9e-008	K.VNELSKDIGSESTEDQAMEDIK.Q + 3 Phospho (ST)
1086	1360.96	2719.90	2719.91	-2.19	(14)	0.039	K.QMEAESISSSEIVPNSVEQK.H + 5 Phospho (ST)
1087	1360.96	2719.91	2719.91	2.88	(22)	0.006	K.QMEAESISSSEIVPNSVEQK.H + 5 Phospho (ST)
1088	907.65	2719.92	2719.91	3.75	(23)	0.0055	K.QMEAESISSSEIVPNSVEQK.H + 5 Phospho (ST)
1135	979.06	2934.15	2934.15	-0.57	(41)	8.6e-005	K.EKVNELSKDIGSESTEDQAMEDIK.Q + 3 Phospho (ST)
1136	979.06	2934.16	2934.15	1.39	64	4.3e-007	K.EKVNELSKDIGSESTEDQAMEDIK.Q + 3 Phospho (ST)

Appendix C10: peptides of trypsin-digested TGA-treated α_{s1} -casein at an incubation time of 120 min.

CAS1_BOVIN_B Mass: 22960 Score: 2551 Queries matched: 71 emPAI: 346.56

(P02662) Alpha-S1 casein B - Bos taurus (Bovine).

Query	Observed	Mr(expt)	Mr(calc)	ppm	Score	Expect	Peptide
14	748.37	747.37	747.36	4.21	(3)	0.52	K.TTMPLW.-
15	748.37	747.37	747.36	4.72	(15)	0.029	K.TTMPLW.-
17	374.69	747.37	747.36	5.78	27	0.0021	K.TTMPLW.-
18	748.37	747.37	747.36	6.12	(14)	0.042	K.TTMPLW.-
377	1267.71	1266.70	1266.70	1.29	(41)	8.6e-005	R.YLGYLEQLLR.L
378	634.36	1266.70	1266.70	3.43	(54)	4.4e-006	R.YLGYLEQLLR.L
379	634.36	1266.70	1266.70	4.99	(57)	1.8e-006	R.YLGYLEQLLR.L
380	634.36	1266.70	1266.70	5.43	(47)	1.9e-005	R.YLGYLEQLLR.L
381	634.36	1266.70	1266.70	5.54	(54)	4.3e-006	R.YLGYLEQLLR.L
382	634.36	1266.70	1266.70	5.75	(44)	4.4e-005	R.YLGYLEQLLR.L
383	634.36	1266.70	1266.70	5.97	(55)	2.9e-006	R.YLGYLEQLLR.L
384	634.36	1266.71	1266.70	6.19	66	2.5e-007	R.YLGYLEQLLR.L
385	634.36	1266.71	1266.70	7.03	(60)	1e-006	R.YLGYLEQLLR.L
386	423.24	1266.71	1266.70	7.05	(41)	7.6e-005	R.YLGYLEQLLR.L
389	1268.69	1267.69	1267.68	3.65	(29)	0.0012	R.YLGYLEQLLR.L + Deamidated (NQ)
390	634.85	1267.69	1267.68	5.91	(65)	3.2e-007	R.YLGYLEQLLR.L + Deamidated (NQ)
502	692.87	1383.73	1383.72	5.07	(33)	0.00049	R.FFVAPFPEVFGK.E
503	692.87	1383.73	1383.72	5.32	(54)	4.4e-006	R.FFVAPFPEVFGK.E
504	692.87	1383.73	1383.72	5.32	(48)	1.5e-005	R.FFVAPFPEVFGK.E
505	1384.74	1383.73	1383.72	6.35	(31)	0.00086	R.FFVAPFPEVFGK.E
506	692.87	1383.73	1383.72	6.65	(53)	5e-006	R.FFVAPFPEVFGK.E
507	692.87	1383.73	1383.72	6.73	68	1.5e-007	R.FFVAPFPEVFGK.E
508	462.25	1383.73	1383.72	7.62	(44)	4.2e-005	R.FFVAPFPEVFGK.E
679	554.27	1659.80	1659.79	5.84	(48)	1.5e-005	K.VPQLEIVPNSAEER.L + Phospho (ST)
680	830.91	1659.80	1659.79	7.39	(69)	1.2e-007	K.VPQLEIVPNSAEER.L + Phospho (ST)
685	831.40	1660.78	1660.77	5.25	80	1.1e-008	K.VPQLEIVPNSAEER.L + Deamidated (NQ); Phospho (ST)
686	554.60	1660.78	1660.77	6.07	(32)	0.00068	K.VPQLEIVPNSAEER.L + Deamidated (NQ); Phospho (ST)
731	587.32	1758.94	1758.94	0.16	(66)	2.8e-007	K.HQGLPQEVNLNLLR.F
732	880.48	1758.94	1758.94	0.17	(86)	2.6e-009	K.HQGLPQEVNLNLLR.F
733	880.48	1758.94	1758.94	3.69	(63)	4.8e-007	K.HQGLPQEVNLNLLR.F
734	880.48	1758.95	1758.94	4.50	(113)	5.5e-012	K.HQGLPQEVNLNLLR.F
735	587.32	1758.95	1758.94	4.92	(71)	7.6e-008	K.HQGLPQEVNLNLLR.F
736	880.97	1759.93	1759.92	5.72	132	6.8e-014	K.HQGLPQEVNLNLLR.F + Deamidated (NQ)
737	587.65	1759.93	1759.92	5.92	(61)	7.9e-007	K.HQGLPQEVNLNLLR.F + Deamidated (NQ)
738	880.97	1759.93	1759.92	6.03	(97)	1.8e-010	K.HQGLPQEVNLNLLR.F + Deamidated (NQ)
739	587.65	1759.93	1759.92	6.03	(50)	9.9e-006	K.HQGLPQEVNLNLLR.F + Deamidated (NQ)
740	587.98	1760.91	1760.91	3.13	(40)	0.0001	K.HQGLPQEVNLNLLR.F + 2 Deamidated (NQ)
786	924.37	1846.73	1846.72	7.16	89	1.4e-009	K.DIGSESTEDQAMEDIK.Q + Phospho (ST)
787	924.86	1847.71	1847.70	3.78	(59)	1.2e-006	K.DIGSESTEDQAMEDIK.Q + Deamidated (NQ); Phospho (ST)
823	964.35	1926.69	1926.68	3.31	(52)	5.7e-006	K.DIGSESTEDQAMEDIK.Q + 2 Phospho (ST)
824	964.35	1926.69	1926.68	3.50	(49)	1.3e-005	K.DIGSESTEDQAMEDIK.Q + 2 Phospho (ST)
825	964.35	1926.69	1926.68	4.02	(64)	4.1e-007	K.DIGSESTEDQAMEDIK.Q + 2 Phospho (ST)
826	964.35	1926.69	1926.68	4.49	(23)	0.0047	K.DIGSESTEDQAMEDIK.Q + 2 Phospho (ST)
827	643.24	1926.69	1926.68	5.54	(48)	1.6e-005	K.DIGSESTEDQAMEDIK.Q + 2 Phospho (ST)

838	976.49	1950.96	1950.95	6.94	93	5.6e-010	K.YKVPQLEIVPNSAEER.L + Phospho (ST)
839	651.33	1950.96	1950.95	6.95	(65)	3.4e-007	K.YKVPQLEIVPNSAEER.L + Phospho (ST)
841	976.98	1951.94	1951.93	4.42	(85)	3.2e-009	K.YKVPQLEIVPNSAEER.L + Deamidated (NQ); Phospho (ST)
842	651.65	1951.94	1951.93	5.47	(55)	3.1e-006	K.YKVPQLEIVPNSAEER.L + Deamidated (NQ); Phospho (ST)
920	694.35	2080.04	2080.02	6.36	31	0.00078	K.KYKVPQLEIVPNSAEER.L + Deamidated (NQ); Phospho (ST)
1036	1158.58	2315.14	2315.13	3.65	104	3.9e-011	K.EPMIGVQNQELAYFYPELFR.Q
1037	772.72	2315.14	2315.13	5.50	(75)	3.3e-008	K.EPMIGVQNQELAYFYPELFR.Q
1040	774.75	2321.21	2321.20	4.49	18	0.017	R.LKKYKVPQLEIVPNSAEER.L + Deamidated (NQ); Phospho (ST)
1147	873.16	2616.47	2616.46	3.92	(28)	0.0016	-.RPKHPIKHQGLPQEVLNENLLR.F + Deamidated (NQ)
1148	655.13	2616.47	2616.46	3.93	(9)	0.13	-.RPKHPIKHQGLPQEVLNENLLR.F + Deamidated (NQ)
1149	655.13	2616.47	2616.46	4.98	54	4.2e-006	-.RPKHPIKHQGLPQEVLNENLLR.F + Deamidated (NQ)
1150	873.17	2616.48	2616.46	6.11	(9)	0.14	-.RPKHPIKHQGLPQEVLNENLLR.F + Deamidated (NQ)
1151	524.30	2616.48	2616.46	7.03	(21)	0.0077	-.RPKHPIKHQGLPQEVLNENLLR.F + Deamidated (NQ)
1152	524.50	2617.48	2617.45	11.8	(16)	0.025	-.RPKHPIKHQGLPQEVLNENLLR.F + 2 Deamidated (NQ)
1168	893.35	2677.03	2677.02	5.25	(54)	4.2e-006	K.VNELSKDIGSESTEDQAMEDIK.Q + 3 Phospho (ST)
1169	1339.52	2677.04	2677.02	7.35	60	9.4e-007	K.VNELSKDIGSESTEDQAMEDIK.Q + 3 Phospho (ST)
1182	907.15	2718.43	2718.45	-6.45	(15)	0.035	-.RPKHPIKHQGLPQEVLNENLLR.F + 3 Deamidated (NQ)
1183	680.61	2718.43	2718.45	-6.25	(12)	0.057	-.RPKHPIKHQGLPQEVLNENLLR.F + 3 Deamidated (NQ)
1184	1360.96	2719.91	2719.91	-0.13	(18)	0.018	K.QMEAESISSSEIVPNSVEQK.H + 5 Phospho (ST)
1185	907.64	2719.91	2719.91	2.36	(9)	0.11	K.QMEAESISSSEIVPNSVEQK.H + 5 Phospho (ST)
1186	907.65	2719.91	2719.91	3.16	(33)	0.00046	K.QMEAESISSSEIVPNSVEQK.H + 5 Phospho (ST)
1187	1360.97	2719.92	2719.91	4.28	40	9.1e-005	K.QMEAESISSSEIVPNSVEQK.H + 5 Phospho (ST)